

# Unconditionally separating noisy $\text{QNC}^0$ from bounded polynomial threshold circuits of constant depth

Min-Hsiu Hsieh<sup>\*</sup>      Leandro Mendes<sup>†</sup>      Michael de Oliveira<sup>‡</sup>  
 Sathyawageeswar Subramanian<sup>§</sup>

## Abstract

We study classes of constant-depth circuits with gates that compute restricted polynomial threshold functions, recently introduced by [Kum23] as a family that strictly generalizes  $\text{AC}^0$ . Denoting these circuit families  $\text{bPTF}^0[k]$  for *bounded polynomial threshold circuits* parameterized by an integer-valued degree-bound  $k$ , we prove three hardness results separating these classes from constant-depth quantum circuits ( $\text{QNC}^0$ ).

- We prove that the parity halving problem [WKS<sup>+</sup>19], which  $\text{QNC}^0$  over qubits can solve with certainty, remains average-case hard for polynomial size  $\text{bPTF}^0[k]$  circuits for all  $k = \mathcal{O}(n^{1/(5d)})$ .
- We construct a new family of relation problems based on computing  $\text{mod } p$  for each prime  $p > 2$ , and prove a separation of  $\text{QNC}^0$  circuits over higher dimensional quantum systems (‘qupits’) against  $\text{bPTF}^0[k]$  circuits for the same range of the degree-bound parameter as above.
- We prove that both foregoing results are noise-robust under the local stochastic noise model, by introducing fault-tolerant implementations of non-Clifford  $\text{QNC}^0/|\overline{T^{1/p}}\rangle$  circuits, that use logical magic states as advice.

We also prove tighter lower bounds on the size of  $\text{bPTF}^0[k]$  circuits that are required to solve the relational problem with certainty, which we leverage to significantly reduce the estimated resource requirements for potential demonstrations of quantum advantage against shallow-depth classical circuits.

$\text{bPTF}^0[k]$  circuits can compute certain classes of Polynomial Threshold Functions (PTFs), which in turn serve as a natural model for neural networks and exhibit enhanced expressivity and computational capabilities. Furthermore, for large enough values of  $k$ ,  $\text{bPTF}^0[k]$  contains  $\text{TC}^0$  as a subclass. The main challenges we overcome include establishing classical average-case lower bounds, designing non-local games with quantum-classical gaps in winning probabilities and developing noise-resilient non-Clifford quantum circuits necessary to extend beyond qubits to higher dimensions. We address the first challenge by developing new, tighter multi-switching lemmas for multi-output  $\text{bPTF}^0[k]$  circuits. For the second, we analyze a new family of non-local games defined in terms of  $\text{mod } p$  computations, characterized by an exponential difference between their classical and quantum success probabilities. Lastly, we extend constant-depth error correction techniques from qubits to qupits, incorporating logical advice states. These technical tools may be of more general and independent interest.

---

<sup>\*</sup>Hon Hai (Foxconn) Quantum Computing Research Center. Email: [min-hsiu.hsieh@foxconn.com](mailto:min-hsiu.hsieh@foxconn.com).

<sup>†</sup>Hon Hai (Foxconn) Quantum Computing Research Center. Email: [leandro.rsm@foxconn.com](mailto:leandro.rsm@foxconn.com).

<sup>‡</sup>International Iberian Nanotechnology Laboratory; LIP6, Sorbonne Universite; INESC TEC. Email: [michael.oliveira@inl.int](mailto:michael.oliveira@inl.int).

<sup>§</sup>University of Cambridge. Email: [ss2310@cam.ac.uk](mailto:ss2310@cam.ac.uk)

# Contents

<b>1</b>	<b>Introduction</b>	<b>3</b>
1.1	Main results . . . . .	3
1.2	Technical contributions . . . . .	6
1.3	Related work . . . . .	8
1.4	Discussion and Outlook . . . . .	9
<b>2</b>	<b>Overview of Proofs and Techniques</b>	<b>10</b>
2.1	Proof of Theorem 1.2: Separation for the qubit case . . . . .	12
2.2	Proof of Theorem 1.3: Separations for higher dimensions (qupits) . . . . .	14
2.3	Proof of Theorem 1.4: Noise-resilient separations . . . . .	15
2.4	New switching lemma for bounded PTF circuits . . . . .	17
<b>3</b>	<b>Preliminaries and Notation</b>	<b>19</b>
3.1	Low-depth complexity classes . . . . .	19
3.2	Random restrictions and Switching lemmas . . . . .	21
3.3	Non-local games and Correlation . . . . .	22
3.4	Noise and quantum error correction in higher dimensions . . . . .	22
<b>4</b>	<b>Quantum advantage in the noiseless case</b>	<b>25</b>
4.1	Separations for qubit cases . . . . .	25
4.1.1	Exact and Average-case $\text{bPTF}^0[k]$ hardness . . . . .	26
4.1.2	Qubit upper bound . . . . .	32
4.2	Separation for qupit cases . . . . .	35
4.2.1	Quantum non-local games in higher dimensions . . . . .	37
4.2.2	Average-case $\text{bPTF}^0[k]$ lower hardness . . . . .	42
4.2.3	Qupit upper bound . . . . .	45
<b>5</b>	<b>Noise-resilient quantum advantage</b>	<b>54</b>
5.1	Noise-resilient qupit Clifford circuits with quantum advice . . . . .	55
5.1.1	Qupit error threshold . . . . .	58
5.1.2	Qupit single-shot state preparation . . . . .	61
5.2	Noise-resilient quantum advantage with magic state injection . . . . .	69
5.2.1	Non-adaptive Clifford circuits with magic state injection . . . . .	69
5.2.2	Noisy quantum circuits retain a computational advantage against $\text{bPTF}^0[k]$ . . . . .	74
<b>6</b>	<b>Discussion</b>	<b>76</b>
6.1	Resource estimation . . . . .	77
6.2	Neural networks as bounded polynomial threshold circuits . . . . .	78
<b>A</b>	<b>Proof of the tight multi-switching lemma for bounded PTF circuits</b>	<b>88</b>
A.1	Tight multi-switching lemma . . . . .	88
A.2	Depth reduction lemmas . . . . .	92

# 1 Introduction

Realizing the theoretical gains promised by landmark quantum algorithms such as integer factorisation or search is challenged by the constraints of existing quantum hardware, requiring extensive resources including qubit counts, coherence times and fault-tolerant operations for their implementation [BMT<sup>+</sup>22; GE21; SVM<sup>+</sup>17]. A series of pioneering studies showed that under plausible complexity theoretic assumptions—e.g. that the polynomial hierarchy does not collapse to the third level—certain classes of quantum circuits are exponentially hard to simulate classically while being more resource-efficient and hardware-friendly. Conditional hardness results of this kind include IQP circuits [BJS11], Boson sampling experiments [AA11], and random circuit sampling [BFN<sup>+</sup>19]. On the other hand, the need for complexity theoretic assumptions and the difficulty in accounting for the noise levels present in current quantum experiments highlights a gap between theoretical models and practical implementation.

Instead of trying to compare the capabilities of shallow-depth quantum circuits with general models of classical computation, recent work has turned towards the comparison to their classical shallow-depth counterparts. Shallow-depth circuits have been studied extensively in classical computer science [Smo87; Yao85; Bar86; Eps87], and continue to be a vibrant area of research at the frontier of complexity theory [Has14; Wil14; RST15; Has16; CSS16; MW18; Che19; Wil21; HMS23].

The seminal work of Bravyi et al. [BGK18] exhibited a relational problem that can be solved by constant-depth quantum circuits consisting only of 2-qubit Clifford gates, which no constant-depth classical circuit with bounded fan-in gates can solve. This first *unconditional* separation, i.e. without any complexity theoretic assumptions, between  $\text{QNC}^0$  and  $\text{NC}^0$  spurred renewed interest in the field, and was followed by an extension of this result to a separation of  $\text{QNC}^0$  against classical circuits of unbounded fan-in ( $\text{AC}^0$ ) [WKS<sup>+</sup>19], average-case hardness [Gal19; WKS<sup>+</sup>19; CSV21], interactive protocols separating  $\text{QNC}^0$  from classical logarithmic-depth circuits of bounded fan-in ( $\text{NC}^1$ ) [GS20], the case of noisy quantum circuits requiring fault-tolerance and quantum error correction [BGK<sup>+</sup>20; GJS21; CCK23], and sampling problems [WP23].

**Constant-depth classes beyond  $\text{AC}^0$ .** Going beyond the AND and OR gates allowed in  $\text{AC}^0$ , one can consider unbounded fan-in  $\bmod p$  gates, and the corresponding family of  $\text{AC}^0[p]$  classes which contain such gates. [WKS<sup>+</sup>19] showed a separation between  $\text{QNC}^0/\text{cat}$  and  $\text{AC}^0[2]$  where the former class has access to **cat** or GHZ advice states. [GS20] showed a separation between  $\text{QNC}^0$  and  $\text{AC}^0[p]$  for every prime  $p$  in the setting of interactive protocols. Yet, no unconditional separations are known of this kind for relational problems.

An even more general class of gates is *thresholds*  $\text{Th}_k$ , which output one if the input string has Hamming weight at least  $k$ , and zero otherwise. Constant-depth circuits of threshold gates form the class  $\text{TC}^0$  [PS88], and encompass  $\text{NC}^0$  and  $\text{AC}^0$ . They are a canonical theoretical model for neural networks [SB91; MP69; Mur71; BV19], extending even to the transformer architecture which underlies large language models such as GPT [MSS22; MS23], whose general interest has spread across all scientific fields [Kro08]. A natural question that arises is whether quantum circuits can also surpass threshold circuits in constant depth. The results of [GS20] include a separation between  $\text{QNC}^0$  and  $\text{TC}^0$ , but only in the interactive setting and furthermore conditional on the (weaker) assumption that  $\text{TC}^0 \subsetneq \text{NC}^1$ . A separation of this nature that is unconditional and in the setting of relational problems without interactivity would be desirable, but appears out of reach of current techniques;  $\text{TC}^0$ , or the subclass<sup>1</sup>  $\text{AC}^0[6]$ , lies at the very frontier of classical circuit complexity.

## 1.1 Main results

In this paper, we thus explore an intermediate family of circuit classes newly introduced in [Kum23], which we call  $\text{bPTF}^0[k]$  for constant-depth *bounded polynomial threshold circuits*. They are built from gates that compute *bounded polynomial threshold functions* (PTF), which may be non-linear but include a degree-bound parameter  $k$  that restricts their behaviour to be either AND or OR functions when the input string has Hamming weight at least  $k$ . Thus for non-zero and constant  $k$  (i.e.  $k = \mathcal{O}(1)$ ) this class equals  $\text{AC}^0$ , and for the degree-bound parameter  $k = \Theta(n)$  it contains  $\text{TC}^0$ , giving us a way to study circuits beyond  $\text{AC}^0$  in this spectrum of degree bounds parameterized by  $k$ . This family of circuit classes is well-motivated from the theoretical standpoint [Kum23], for its connections to polynomial threshold functions and the interplay between the polynomial hierarchy and the counting hierarchy (Section 1.4), and also for its relation

<sup>1</sup>For a representation of the known inclusions among some of the main circuit classes discussed, see Figure 1.

to theoretical models of neural networks (Section 6.2). It thus opens up new avenues for studying the interrelationships between quantum and classical circuits and computational models.

Following previous unconditional separation results, we focus on relational or search problems, where the inputs  $x$  are  $n$ -bit strings and the outputs  $y$  are  $m$ -bit strings such that  $(x, y) \in R \subset \{0, 1\}^n \times \{0, 1\}^m$  for some relation  $R$ . We define  $\text{QNC}^0$  to be the class of computational problems  $R : \{0, 1\}^n \rightarrow \{0, 1\}^m$  solvable by quantum circuits with a constant depth using a polynomial number of gates of bounded fan-in (i.e., every gate has a fixed constant number of input and output wires) drawn from a finite, universal quantum gateset. Similarly, we denote by  $\text{bPTF}^0[k]$  the class of constant-depth classical circuits composed of unbounded fan-in gates that compute  $k$ -bounded Polynomial Threshold Functions (PTF) [Kum23], which we define below.

**Definition 1.1** (see Definition 3.4). *A polynomial threshold function<sup>2</sup> with degree-bound  $k$  is defined as follows,*

$$f(x) = \begin{cases} P(x), & \sum_{i=1}^n x_i \leq k \\ 1, & \sum_{i=1}^n x_i > k \end{cases}; \quad \text{with } P : \mathbb{F}_2^n \rightarrow \mathbb{F}_2 \text{ a polynomial over } \mathbb{F}_2 = \{0, 1\}, \quad (1.1)$$

where  $k$  restricts the maximum degree of  $P$ .

Note that the value of  $k$  also limits the degree of the polynomial  $P$ , since the restriction on the Hamming weight means that any monomial of degree at least  $k + 1$  must be identically zero when  $|x| \leq k$ . For example, we have the  $k$ -OR ( $= 1$  iff  $> k$  bits are 1's) and  $k$ -AND ( $= 0$  iff  $< n - k$  bits are 1's). When  $k = \mathcal{O}(1)$ , we recover unbounded fan-in AND, OR gates and Not gates, and  $\text{bPTF}^0[\mathcal{O}(1)]$  corresponds to  $\text{AC}^0$ . When  $k = n$ , the polynomial  $P$  can have degree  $n$  and so  $\text{bPTF}^0[n]$  includes *all* Boolean functions, therefore trivially including  $\text{TC}^0$ . More interestingly, for  $k = o(n)$ , one can consider  $\text{bPTF}^0[k]$  as  $\text{AC}^0$  circuits with additional computational power, including access to majority gates of small fan-in.

With these definitions, we are ready to present our first main result: for the parity halving problem [WKS<sup>+</sup>19], we prove average-case correlation bounds against  $\text{bPTF}^0[k]$ , establishing a separation of  $\text{QNC}^0$  from  $\text{bPTF}^0[k]$ .

**Theorem 1.2** (Informal, see Theorem 4.2 and Theorem 4.3). *For every large enough input size  $n \in \mathbb{N}$ , there exists a relation  $R \subset \{0, 1\}^n \times \{0, 1\}^m$  with  $m = \mathcal{O}(n \log n)$  such that for any  $x \in \{0, 1\}^n$ , a  $\text{QNC}^0$  circuit consisting of  $o(n^2)$  gates can output a  $y \in \{0, 1\}^m$  such that  $(x, y) \in R$  with certainty. Conversely, the size  $s$  of any  $\text{bPTF}^0[k]/\text{rpoly}$  circuit of depth  $d$  that computes any valid  $y$  is lower bounded as shown in the table below. Here  $/\text{rpoly}$  means the circuit is randomised, i.e., has access to polynomially many random input bits.*

$\text{bPTF}^0[k]/\text{rpoly}$	$k = \mathcal{O}(1) (\equiv \text{AC}^0/\text{rpoly})$	$k = n^{1/(5d)}$
<b>Exact hardness</b>	$s = \Omega \left( \exp \left( \left( \frac{\sqrt{n}}{(\log n)^{3/2 + \mathcal{O}(1)}} \right)^{\frac{1}{d-1}} \right) \right)$	$s = \Omega \left( \exp \left( \left( \frac{n^{3/10}}{(\log n)^{3/2 + \mathcal{O}(1)}} \right)^{\frac{1}{d-1}} \right) \right)$
<b>Average-case hardness</b>	-	$\Pr[\text{Success}] \leq \frac{1}{2} + \exp \left( -\Omega \left( \frac{n^{3/5 - \mathcal{O}(1)}}{(\log s)^{2d-1}} \right) \right)$

Table 1: Size lower bounds for the circuit classes  $\text{bPTF}^0[k]$ . By “exact hardness” we mean that the classical circuit is required to produce a valid output string with certainty on all inputs.

As previously mentioned, threshold circuits serve as a useful theoretical model for neural networks, and in Section 6.2, we highlight how bounded polynomial threshold circuits of constant depth similarly exhibit a strong relationship with neural networks. Building on the later class, our results show that  $\mathcal{O}(n^{1/d})$ -bounded polynomial threshold circuits of constant-depth, which have access to polynomially many random

<sup>2</sup>We note that the common definition in the literature takes  $P : \mathbb{R}_2^n \rightarrow \mathbb{R}$ , and sets  $f(x) = \frac{1}{2} (1 + \text{sgn}(P(x)))$ . On the other hand here we are interested in polynomials of degree at most  $k$  over  $\mathbb{F}_2^n$ , with threshold behaviour determined by the degree-bound parameter  $k$ .

bits, require superpolynomial size to solve a relational problem that is solved efficiently by constant depth bounded fan-in quantum circuits. Observing that even a *single gate* of a  $\text{bPTF}^0[k]/\text{rpolynomial}$  circuit with  $k = \text{polylog}(n)$ , would also require superpolynomial (i.e.  $\Omega(n^{\text{polylog}(n)})$ ) size  $\text{AC}^0$  circuits to emulate it, and since  $\text{NC}^0 \subsetneq \text{AC}^0$ , we obtain  $\text{NC}^0 \subsetneq \text{AC}^0 \subsetneq \text{bPTF}^0[k]$  for  $k = \omega(\log n)$  [Kum23]. This is thus the separation of  $\text{QNC}^0$  against the largest classical circuit class to date, obtained unconditionally. Importantly, we achieve a super-polylogarithmic value for  $k$ , demonstrating that [Theorem 1.2](#) extends separations against  $\text{AC}^0$  from prior work to this genuinely new class. Furthermore, we remark that our bounds exhibit the largest possible degree-bound parameter value for the type of relation problems considered. This is evidenced by the fact that for any larger  $k$ ,  $\text{bPTF}^0[k]$  can compute parities, and thus *can* solve the relational problem with high probability and small circuit size. This suggests that a novel approach will be needed for future work to improve our results.

Additionally, we consider the case when classical circuits are required to solve the relation with certainty on all inputs, equivalent to what is achievable by quantum circuits. We establish a new separation against  $\text{AC}^0/\text{rpolynomial}$  for this scenario, described as ‘exact hardness’ in [Theorem 1.2](#), demonstrating the tightest bounds known to date. Using this result we present a resource estimation analysis in [Section 6.1](#), showing that a quantum advantage could be realized using quantum devices that require orders of magnitude fewer qubits than prior work for both values of  $k$  in [Table 1](#).

Our second contribution lies in constructing a new family of relation problems based on computing  $\text{mod } p$  for each prime  $p > 2$ , designated as ISMR problems (see [Definition 2.1](#)). With these, we extend all previous results from qubits to higher dimensions. Throughout this paper, we refer to qudit systems of prime dimension  $p$  as ‘qupits’.

**Theorem 1.3** (Informal, see [Theorem 4.12](#)). *For every prime  $p \in \mathbb{N}$  and large enough input lengths  $n > n_p^* \in \mathbb{N}$ , there exists a relation  $\mathcal{R}_p \subset \{0, 1\}^n \times \{0, 1\}^m$  with  $m = \mathcal{O}(n \log(n)^p)$ , such that there is a  $\text{QNC}^0$  circuit over  $(\mathbb{C}^p)^{\otimes n}$  (i.e.,  $n$  ‘qupits’) consisting of  $o(n^2)$  gates that has constant correlation with  $\mathcal{R}_p^m$ . In contrast, any polynomial size  $\text{bPTF}^0[n^{1/(5d)}]/\text{rpolynomial}$  circuit has exponentially small correlation  $\exp(-\Omega(n^{3/5 - \mathcal{O}(1)}))$  with  $\mathcal{R}_p^m$ .*

Previous studies have suggested that qudit non-local games with significant quantum-classical winning probability gaps could give rise to computational separations between classical and quantum circuit classes [Aas21]. However, such separations were not explicitly demonstrated. By proving [Theorem 1.3](#), we establish the existence of such a non-local game for each prime dimension, which might be of independent interest (see [Section 4.2.1](#)). We use these non-local games to explicitly construct relational problems and quantum circuits that solve them with high correlation. Our correlation measure (see [Definition 3.15](#)) is a generalization of the usual correlation between Boolean functions to functions mapping  $\{0, 1\}^n$  to the cyclic groups  $(\mathbb{F}_p, +)$ , taking into account ‘how wrong’ an output is: if  $f(x) = 2$ , then  $\tilde{f}(x) = 4$  should intuitively be a worse guess than  $\tilde{f}(x) = 3$  for any  $f : \{0, 1\}^n \mapsto \mathbb{F}_p$ . Thus, the result above is stated in terms of the correlation between the relation problem  $\mathcal{R}_p^m$  (defined formally in [Definition 2.1](#)) and  $\text{bPTF}^0(k)/\text{rpolynomial}$  circuits. For the  $p = 3$  case, the correlation function directly provides a lower bound on the success probability of the classical circuits. We explicitly calculate these in [Theorem 4.27](#) and [Corollary 4.22](#).

**Remark.** The new relation problems  $\mathcal{R}_p$  in [Theorem 1.3](#) are still binary problems that are natural to the  $\text{bPTF}^0[k]$  class. They do not simply enforce hardness via arithmetic operations over other prime fields, and Razborov-Smolensky type lower bounds are not directly applicable to this setting for the classical binary gate sets. We also emphasize that this separation is achieved in the average-case hardness setting with uniform input distributions over binary inputs. Technically, we prove novel bounds on the classical winning strategies for qupit non-local games under *non-uniform input distributions*, handle the qupit-to-binary encoding, and ensure the use of uniform (rather than biased) random restrictions over the binary input.

We note that if we were to consider an infinite gate set such as {all single-qubit gates, CNOT} as assumed in [WP23; BBC<sup>+</sup>24; TT16], we could realize all our qupit circuits with qubit circuits in the noise-free setting [BBC<sup>+</sup>95; RZB<sup>+</sup>94]. However, the qupit  $\text{QNC}^0$  circuits we consider are defined over a standard, minimal *finite* qupit gate set. This allows for constant-depth realizations with the gate sets available on standard quantum computing devices and fault-tolerant implementations, which are impossible if infinite gate sets are required. These explicit separations not only clarify the theoretical landscape but also hold practical relevance, as many

quantum computing platforms naturally operate in higher dimensions [RMP<sup>+</sup>22; GZC<sup>+</sup>22]. Therefore, this design choice could provide a fair and effectively demonstrable quantum advantage<sup>3</sup>.

Additionally, in this setting, any finite minimal gate set over a certain qudit dimension, if attempting to solve one of the ISMR problems of another prime dimension, would require decomposition into its own native gates. In this context, relying on Solovay-Kitaev-type decompositions, the gates would very likely necessitate log-depth decompositions for approximation. Thus, under this hardware-realistic definition of qudit  $\text{QNC}^0$  circuits, we raise the following conjecture.

**Conjecture 1.** *For each pair of distinct primes  $p$  and  $q$ , there exists a relation problem  $\mathcal{R}_p$  such that  $\mathcal{R}_p \notin \text{QNC}^0$  when  $\text{QNC}^0$  is defined over a minimal universal gate set for qudits of dimension  $q$ .*

We thus conjecture that the ISMR problems could be for the qudit  $\text{QNC}^0$  circuit classes what the Razborov-Smolensky type modular problems are for the  $\text{AC}^0[p]$  circuit classes.

Finally, quantum systems are unavoidably affected by noise, and error correction is a much more complex process in the quantum realm, bringing into question the *robustness* of a computational advantage under noise. This question is of significance to both theory and practice, especially as we navigate the NISQ era. Even for very powerful quantum computational models, the introduction of noise often dramatically diminishes computational advantages that they may offer over their classical counterparts: for instance, recent work shows that even small constant error rates result in a collapse of the power of multi-prover interactive proofs where the provers share entanglement (MIP<sup>\*</sup>) from RE to multi-prover interactive proofs without shared entanglement (MIP) [DFN<sup>+</sup>24]. Our third main result is to prove that all our separations are robust to noise: even if all steps of the quantum computation are affected by local stochastic noise, there is a family of modified relation problems that these noisy quantum circuits, when provided with logical magic states, can solve, but is hard for noiseless  $\text{bPTF}^0[k]$  circuits.

**Theorem 1.4** (Informal, see Theorem 5.2). *For every prime  $p \in \mathbb{N}$  and large enough input lengths  $n > n_p^* \in \mathbb{N}$ , there exists a relation  $\mathfrak{R}_p \subset \{0, 1\}^n \times \{0, 1\}^m$  with  $m = \mathcal{O}(n \cdot \text{poly}(\log n))$  based on  $\mathcal{R}_p$ , such that for local stochastic noise with physical error rate below a constant threshold, there is a noisy qudit  $\text{QNC}^0 / |T^{1/p}\rangle$  circuit of all-to-all connectivity that has constant correlation with  $\mathfrak{R}_p$ . In contrast, any (even noiseless) polynomial size  $\text{bPTF}^0[n^{1/(5d)}]$  circuit has exponentially small correlation  $\exp(-\Omega(n^{3/5 - \mathcal{O}_d(1)}))$  with  $\mathfrak{R}_p$ .*

This result improves upon prior work in three main ways. First, it accounts for noise while addressing non-Clifford gates, going beyond the framework for noise-robust separations introduced in [BGK<sup>+</sup>20], by including logical  $T$ -type magic states. Second, it generalizes shallow-depth computational separations and the error-correction mechanisms to show that they are robust to arbitrary prime qudit dimensions. Third, these constitute the state-of-the-art in unconditional separations between noisy  $\text{QNC}^0$  and the largest classical circuit classes to date. Complementarily, as a corollary, it establishes separations with  $\text{NC}^0$  for each prime qudit dimension, potentially enabling near-term quantum advantage experiments due to the favorable error correction properties that have been demonstrated for qudits.

We remark that the difference in the correlation bounds between Theorem 1.4 and Theorem 4.12 lies in the exponent of the  $\log s$  term, resulting from the additional overhead for error correction, which nevertheless does not undermine the exponential difference between the classical and quantum correlation achieved by the respective circuit classes with  $\mathfrak{R}_p$ . Finally, we also note that although Theorem 1.4 is stated with logical  $T$ -type magic states as advice, we also prove a new separation for qubits without advice (Corollary 5.3).

## 1.2 Technical contributions

In this section we highlight the crucial new ingredients we have used and devised for the development of our main results, some of which may also be of independent interest.

**Switching lemmas.** We prove a novel multi-switching lemma (Lemma A.1) for multi-output  $\text{bPTF}^0[k]$  circuits, using inductive methods to significantly refine the parameters beyond the prior work of [Kum23]—see Section 2.4 for a further discussion. Utilizing this lemma, we establish depth reduction (Lemma A.8) for

<sup>3</sup>Note that parallel repetition techniques [WKS<sup>+</sup>19; CSV21] could be applied to Theorems 1.2 and 1.3, to amplify the advantage, facilitating experimental demonstrations.



multi-output  $\text{bPTF}^0[k]$  circuits, aimed at addressing relation-type problems. These methods have not only enabled us to substantiate our lower bounds in [Theorem 1.2](#) and [Theorem 1.3](#) but have also facilitated a precise determination of the maximum value of the degree-bound parameter  $k$  for  $\text{bPTF}^0[k]$  while elucidating the relationship between geometrical hardware constraints and the possibility for quantum advantage. Moreover, these lemmas in principle apply to circuit models of some neural network architectures with practical string-to-string mapping applications (see [Section 6.2](#)), and we surmise that they may have applications to search problems beyond what we consider.

Note that the essence of switching lemmas has remained unchanged since their introduction in the 80s, primarily addressing separations within the  $\text{AC}^0$  class. The significance of our work is underscored by the fact although Kumar’s introduction of a class that extends  $\text{AC}^0$  offered new possibilities, a priori, it is unclear whether the multi-switching lemma in [\[Kum23\]](#) can prove strong correlation bounds for multi-output functions like the PHP.

**Decision tree depth bounds.** Our second technical contribution builds on the first. More concretely, our new multi-switching lemma enables the reduction of the initial  $\text{bPTF}^0[k]$  circuit to an object we refer to as a forest line. This is a set of decision trees, where each one is responsible for computing the outcome bit of the relation problem for the set of variables left “alive” by random restrictions applied to the input. We leverage this mathematical structure for our new exact hardness results in [Theorem 1.2](#). The novelty lies in counting the super-exponential number of valid outcome strings for the chosen relation problem, through the Algebraic Normal Forms [\[Don14\]](#) that represent the valid ‘deterministic’ solutions to the problem. Using this concept, we first establish a lower bound on the number of degree two terms in the representation of any valid solution ([Lemma 4.5](#)). Then, we upper bound the number of terms each local decision tree can contribute to our remaining forest line, thus limiting the expressiveness of these decision trees and their efficacy in solving the problem correctly ([Lemma 4.6](#)). This in turn reflects the initial circuit’s ability to solve the relation problem ([Theorem 1.2](#)). This approach captures the classical-quantum circuit separation using ideas standard in theoretical computer science, sidestepping the need for non-local or non-contextual games, which have traditionally been indispensable in prior research.

**Non-local games in higher dimensions.** Our next technical contribution is to constructively prove that, for all prime qudit dimensions, there exists a family of generalized XOR non-local games, which we have coined “Modular XOR games” (see [Definition 4.14](#)), where classical strategies, at best, achieve exponentially lower success probabilities compared to their quantum counterparts as the number of parties increases ([Lemma 4.17](#)). We build on this construction by revisiting the switching lemma, leveraging the locality of the resultant forest of decision trees therein to demonstrate a separation of quantum circuits over *qudits* from  $\text{bPTF}^0[k]$ , since we show that the former can efficiently solve a family of relational problems defined via our new family of non-local games. Our method elegantly incorporates the ability to manage biased input distributions for non-local games, handling the necessary dit-to-bit mappings to ensure that we use unbiased random restrictions for  $\text{bPTF}^0[k]$ . This approach allows us to obtain average-case  $\text{bPTF}^0[k]$  hardness with respect to the uniform distribution on binary inputs for the relation problems that demonstrate the separation. Additionally, it sidesteps the task of computing explicit success probability bounds for each game, while still achieving comparable separations. This obstacle has been emphasised in prior research, which predominantly relied on established quantum-classical distinctions in non-local games [\[BGK18; WKS<sup>+</sup>19\]](#). Also, few developments beyond the conventional qubit setting were considered or achieved previously [\[Law17\]](#).

We remark that we have also integrated into the correctness proof of the candidate quantum circuit that solves the qupit relational problem a technique to efficiently describe the support of standard measurement outcomes of local unitary (LU)-equivalent generalized GHZ states with a dependence on the phases ([Lemma 4.26](#)). This allows us to incorporate a correction function for the output string, and compute the success probability of the quantum circuits in a clean way.

**Fault tolerance.** Our final technical contribution extends the fault-tolerant regime from qubit Clifford to qupit non-Clifford constant-depth quantum circuits with logical T-type magic states (see [Figure 11](#)), which can be affected by local stochastic noise ([Lemma 5.5](#)). We show that the qupit surface code, equipped with the hard decision renormalization decoder, enables fault-tolerant implementation of these quantum circuits. This includes the extension of single-shot logical state preparation for qupits. Specifically, we extend a 3D block construction of [\[RBH05\]](#) to higher dimensions, demonstrating that a specific measurement pattern results in a reduced state that is a logical  $\text{GHZ}_2$  state, up to local Clifford corrections ([Lemma 5.13](#)).

Furthermore, previous work used the minimum weight perfect matching decoder, which performs poorly in higher dimensions. By using a different decoder, we show that we can still perform corrections and recover the desired states with exponentially high confidence (Corollary 5.11).

### 1.3 Related work

A few unconditional separations between larger classes of quantum and classical circuits have also appeared in prior work [GHM<sup>+</sup>02; TT16; BBC<sup>+</sup>24; BKM<sup>+</sup>24]. However, the majority of these involve more complex ingredients, such as the use of quantum fan-in and fanout gates in combination with gate sets that offer infinite precision, rendering them impractical for consideration as true constant-depth circuit candidates. Although [BKM<sup>+</sup>24] later dropped the requirements for quantum fanout and infinite gate sets, the proposed quantum circuits still refer to multi-qubit controlled gates, which are in early development and require further research to assess their potential for fault-tolerant implementation.

This challenge shifted the focus towards the study of shallow-depth quantum circuits that can, in principle, be implemented on near-term hardware. Various extensions of the first unconditional separation between constant-depth classical and quantum circuits, established by Bravyi et al., have been achieved in the last five years. These results are intimately related, sharing similar quantum solutions all based on non-local games, but employing different techniques to prove classical hardness. Here, we provide a brief overview of the most relevant results related to our work, summarised concisely in Table 2.

**Bounded fan-in and worst-case.** We begin by noting that the results of [BGK18] were achieved by using a non-local game previously described by [BCE<sup>+</sup>07]. However, unlike the usual definition of non-local games, this extended GHZ game allowed for some communication between the parties. This additional communication was utilized to construct a quantum circuit whose outputs are based on winning strategies for this game, while also linking the circuit’s outcome to the solution of the 2D Hidden Linear Function (2D HLF) problem. The latter is a non-oracular version of the Bernstein-Vazirani problem [BV93], with the difference that the linear function  $f(x) = \mathbf{a} \cdot \mathbf{x}$  to be learnt is not accessed directly via a quantum oracle, but is ‘hidden’ by a quadratic form. The authors use lightcone arguments that exploit bounded fan-in to show that the efficacy of classical NC-type circuits in solving the 2D HLF problem is limited by the efficacy of classical strategies in winning the incorporated non-local game. Thus, it is guaranteed that the worst-case performance of such classical circuits is unconditionally inferior to the quantum solution.

**Average-case and unbounded fan-in.** Subsequent work extended this unconditional separation in two major directions: to average-case hardness or correlation bounds [Gal19; WKS<sup>+</sup>19], and to the class  $\text{AC}^0$  of unbounded fan-in AND and OR gates [WKS<sup>+</sup>19]. The latter work achieved this through a task dubbed the Parity Halving Problem (PHP), which requires producing an outcome string with a parity equal to the result of applying the mod 4 operation to the input string. The authors applied a different lower bound technique to the PHP, namely (multi-)switching lemmas, to relate  $\text{AC}^0$  circuits back to  $\text{NC}^0$  circuits, which allowed locality arguments to be ported to the former. Switching lemmas describe how the function or relation computed by an  $\text{AC}^0$  circuit simplifies when some of its input literals are randomly set to 0 or 1. Their main result was that classical solutions to the PHP require superpolynomial size  $\text{AC}^0$  circuits. For the quantum upper bound, the authors utilized poor-man’s cat states, which are local unitary (LU)-equivalent to  $n$ -party GHZ states, to efficiently solve the PHP with certainty on all inputs. Furthermore they showed an  $\text{NC}^0$  reduction from the PHP to 2D HLF, proving that the new average-case separation applies to the HLF problem as well.

**Noise resilience.** Traditional quantum fault-tolerant schemes have a significant depth overhead, and might not be compatible with earlier quantum advantage proposals. Driven by this understanding, [BGK<sup>+</sup>20] showed that for the popular local stochastic noise model, errors occurring in a given circuit layer could be corrected with constant-depth circuits. They showed that transversal Clifford gates could be realized by a constant-depth circuit equipped with single-shot state preparation and readout, thereby proving that noise resilience could be achieved within a constant depth. For the Magic Square Problem (MSP) (inspired by the Mermin-Peres magic square [Per90; Mer90b]) they exhibited a  $\text{QNC}^0$  circuit in a 1D configuration that has a quantum advantage against  $\text{NC}^0$ , and consequently a 3D configuration error-correcting code using the previous elements that offers robustness against noise while retaining the advantage against  $\text{NC}^0$ .



[CCK23] recently proved unconditional quantum advantage of noisy  $\text{QNC}^0$  circuits over  $\text{AC}^0$ . Focusing on the task of possibilistic simulation of single-qubit Clifford gate teleportation (TELEP)—a task previously shown to be challenging for  $\text{NC}^0$  [CCK22]—the authors extended the earlier separation to  $\text{AC}^0$ , while introducing a 1D-implementable quantum circuit, enabling 3D fault-tolerant construction as shown in [BGK<sup>+</sup>20].

Finally, alternative approaches have considered different types of tasks and separations, including interactive protocols [GS20; GJS21] and sampling problems [WP23]. Some studies have also applied geometric restrictions to classical circuits [BJ23] to obtain separations on the depth.

As a closing remark, we recall that while all these separations between  $\text{QNC}^0$  and classical shallow-depth circuit classes are unconditional, the quantum circuits in question can still be simulated classically in polynomial time, reiterating that the notion of separation here is more granular.

	Problem	Advantage against	Geometry	Higher dimensions	Avg.-case hardness	Noise resilience
[BGK18]	2D HLF	$\text{NC}^0/\text{rpoly}$	2D	✗	✗	✗
[WKS <sup>+</sup> 19]	PHP	$\text{AC}^0/\text{rpoly}$	2D	✗	✓	✗
[BGK <sup>+</sup> 20]	MSP	$\text{NC}^0/\text{rpoly}$	1D	✗	✓	✓
[CCK23]	TELEP	$\text{AC}^0/\text{rpoly}$	1D	✗	✓	✓
<b>Our work</b>	ISMR	$\text{bPTF}^0[k]/\text{rpoly}$	2D, 3D, ...	✓	✓	✓

Table 2: Summary of related work on unconditional separations of quantum and classical shallow-depth circuits. Please refer to the main text of Section 1.3 for problem abbreviations.

## 1.4 Discussion and Outlook

[HMP<sup>+</sup>93] showed the first lower bounds for depth two circuits of linear threshold functions with small bias, for the *inner product modulo 2* function. Gates computing polynomial threshold functions as in Definition 1.1 may be activated not only by a linear function  $\mathbf{a} \cdot \mathbf{x} - k$  of the input  $\mathbf{x} \in \{0, 1\}^n$ , but also by higher-degree polynomials [HP15]. This increases the expressivity and the computational capabilities of such gates but renders almost all known lower-bound techniques ineffective.  $\text{TC}^0$  can compute unbounded but fixed degree PTFs we consider, and the best results known for this class are barely superlinear  $\Omega(n^{1+\epsilon_d})$  lower bounds on the number of wires [IPS97]. Even for fixed depth equal to 2, only  $\omega(n^{3/2})$  gate or  $\omega(n^{5/2})$  wire lower bounds have been proven [KW16]. While our results are related to  $\text{TC}^0$  and more general PTF circuits, and use similar higher-degree polynomials, they are distinct due to the limitations on the gates in each class  $\text{bPTF}^0[k]$  introduced via the degree-bound parameter  $k$ , rendering the classes and results incomparable.

In the context of noise tolerance, our work expands the separation to larger classical classes and provides explicit quantum circuits with corresponding bounds on the correlation for all qudit prime dimensions. Our Theorems 1.3 and 1.4 necessitate all-to-all connectivity, which may require additional SWAP gates in certain device architectures, thus increasing the circuit depth. However, qudit devices with native all-to-all quantum gates are among the leading quantum hardware devices [BEG<sup>+</sup>23]. Importantly, all classical circuit classes considered for the separations— $\text{NC}^0$ ,  $\text{AC}^0$ , and  $\text{bPTF}^0[k]$ —also inherently require all-to-all connectivity, ensuring a fair comparison. Furthermore, our lower bound techniques could potentially achieve separations with noisy geometrically local circuits when problems of a distinct nature are under consideration [CCK23].

Our work raises further intriguing questions in this active research area. Having initiated the consideration of error-corrected qudit circuits for unconditional quantum separations, we question whether previous results, shown for high-dimensional error-correcting codes with improved parameters [ABC<sup>+</sup>14], could facilitate experimental demonstrations. Additionally, we have reiterated the interest of magic states in the constant-depth fault-tolerant regimes [MGD<sup>+</sup>20; PLS<sup>+</sup>24]. Although we conjecture that magic state factories should not be parallelizable to the level of being in the  $\text{QNC}^0$  circuit class, it is of great interest to understand what the simplest circuit class capable of realizing these processes is, as well as introduce the capacity for adaptive corrections during error-corrected circuit execution. This might extend the set of unconditional separations beyond the currently known limits and lift larger conditional separations to the simplest fault-tolerant quantum circuit classes [YJS19]. In parallel to these questions, it would be important to consider more complex

and alternative noise models [HL21] to better align with specific practical quantum computing architectures. Following the same line of research, it would also be interesting to understand if there is a complexity phase transition for some values of the degree-bound parameter  $k$  and the noise strength.

On a different note, our family of relational problems could generate Razborov-Smolensky type separations between qubit  $\text{QNC}^0$  circuit classes, thereby providing a foundational understanding of qudit computations in constant depth circuit classes. Additionally, we find that  $\text{bPTF}^0[k]$  circuits for  $k = n^{1/d}$  can solve problems that  $\text{AC}^0[p]$  circuits cannot, such as  $\text{mod } p$  operations over  $n^{1/d}$  bits [Smo87]. This strengthens the potential to establish, through the family of ISMR problems related to  $\text{mod } p$ , unconditional separations between qubit  $\text{QNC}^0$  circuits and  $\text{AC}^0[p]$  for any prime  $p$ , as previously conjectured [WKS<sup>+</sup>19; GS20]. Thus, our results might simplify existing conditional results by eliminating the need for interactivity or advice in proving such separations. Additionally, our work achieves near-optimal separations concerning the circuit class under study. This suggests that to attain conceptually different and relevant separations, such as with  $\text{TC}^0$ , we must identify harder problems that are solvable in this setting since the ISMR problems are solvable by  $\text{TC}^0$  [BKM<sup>+</sup>24]. This likely will necessitate the consideration of more advanced  $\text{QNC}^0$  circuits, such as constant-depth adaptive MBQC circuits and more elaborate quantum circuit designs.

**Connections between bounded PTF circuits and other complexity classes.** As a final note, we would like to highlight some additional interest in the  $\text{bPTF}^0[k]$  class and the new multi-switching lemmas. Well-known prior work relates uniform  $\text{AC}^0$  to the polynomial hierarchy PH by associating the logical formulas that an  $\text{AC}^0$  circuit represents with the quantified polynomial-time predicates describing the polynomial hierarchy [Vol98]. In particular, computational separations against  $\text{AC}^0$  have been used to establish relativized separations against the polynomial hierarchy [Yao85], and depth hierarchy results within  $\text{AC}^0$  have been used to establish separations between the levels of PH [Hås87]. Similar studies have been conducted between threshold circuits and the counting hierarchy [AW93], albeit with less success due to the lack of strong lower-bound techniques for classes such as  $\text{TC}^0$ . Interestingly,  $\text{bPTF}^0[k]$  for  $k = \omega(\log n)$  describes a computational hierarchy that likely extends beyond the polynomial hierarchy and has non-trivial overlaps with the counting hierarchy. Thus, new lower-bound techniques might enable oracle separations between these hierarchies. Additionally, this opens avenues for the study of unconditional separations between  $\text{BQLOGTIME}$  and  $\text{bPTF}^0[k]$ , which, based on our previously raised conjectures, could enable oracle separations between BQP and computational classes beyond the PH [Aar10; RT22].

**Concurrent work** The concurrent work of Grewal and Kumar [GK24], developed independently, has some overlap with our first result, establishing a separation between  $\text{QNC}^0$  and  $\text{bPTF}^0[k]$  in the qubit case. Their work includes the development of a multi-output multi-switching lemma for  $\text{bPTF}^0[k]$  (our lemma Lemma A.8), resulting in similar average-case correlation bounds against  $\text{bPTF}^0[k]$  as we obtain in Theorem 4.3<sup>4</sup>. Additionally, as pointed out in our outlook, their work confirms the foreseen possibility for a separation between  $\text{BQLOGTIME}$  and  $\text{bPTF}^0[k]$ , allowing for an oracle separation between BQP and the class of languages decidable by uniform families of polynomial size  $\text{bPTF}^0[k]$  circuits. This overlap in techniques is a natural result of ongoing attempts to extend the prior art in unconditional separation results between shallow-depth circuit classes [WKS<sup>+</sup>19].

## 2 Overview of Proofs and Techniques

In this section, we provide a concise overview of the proofs for our main results. We aim to strike a balance between rigor and accessibility by offering an intuitive discussion of the classical and quantum techniques employed. We will also highlight the key improvements we have made over existing work in this area. We begin by introducing the family of computational problems that we will be addressing.

**Inverted Strict Modular Relation Problems (ISMRP).** In this paper, we introduce a new class of relation problems that are related to the 2D hidden linear function problem from [BGK18] and generalize the parity halving problem studied in [WKS<sup>+</sup>19]. We leverage this class of problems to establish new unconditional separations between  $\text{QNC}^0$  and the  $\text{bPTF}^0[k]$  classes of bounded polynomial threshold circuits.

<sup>4</sup>In [GK24] as in [Kum23]  $\text{bPTF}^0[k]$  is denoted as  $\text{GC}^0(k)$ .

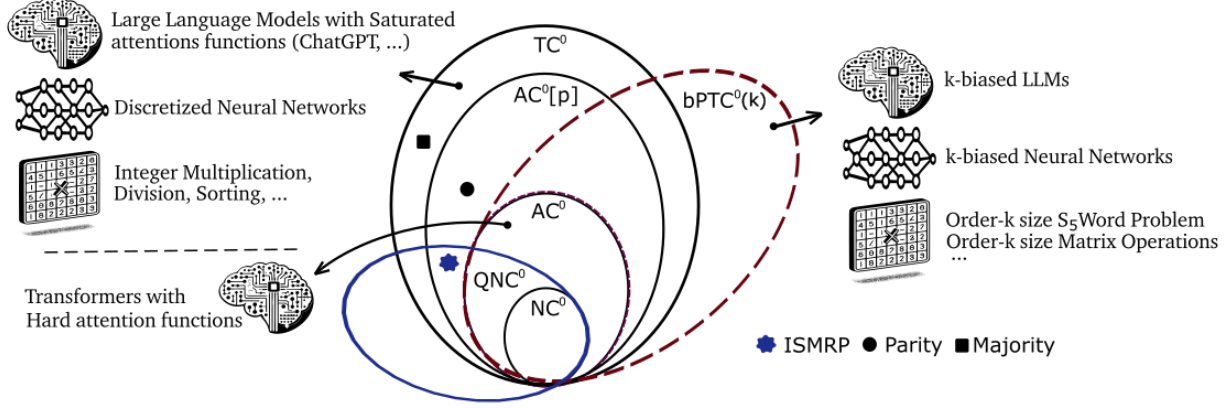


Figure 1: This illustration depicts the primary classical and quantum circuit classes analyzed in this paper, highlighting the inclusion of relevant problems that characterize the relationships and distinctions between these classes. Notably, the Parity function is computable in  $AC^0[2]$  but not in  $AC^0$ , while the Majority function is not computable in  $AC^0[p]$  but is in  $TC^0$ . We also indicate the ISMR family of problems introduced in this work (see Definition 2.1), which differentiate  $QNC^0$  from  $bPTF^0[k]$  with  $k = \omega(\log n)$ . The latter class, which strictly includes  $AC^0$ , can solve instances of  $NC^1$ -complete problems for super-logarithmic size input strings. It can also solve computational problems conjectured to be strictly beyond  $NC^1$ . This suggests a potential non-trivial overlap with  $TC^0$ . We also list more general and practically relevant computational processes known to be computable within each class, particularly neural network-type circuits.

Transformers, known for their substantial use as crucial components of modern large language models (LLMs), can be simulated by  $AC^0$  circuits when the attention mechanism in the transformer is restricted to hard attention functions [SMW<sup>+</sup>24; MSS22]. Furthermore,  $TC^0$ , recognized as the standard class for theoretically representing discretized neural networks [SB91; BP02], can simulate LLMs under realistic operational conditions [MS23], such as restricting the precision of internal variables and auto-regression or the number of time-steps the model is run for at inference. This highlights a key distinction between  $AC^0$  and  $TC^0$ , in that the latter class has enhanced expressivity for a wide range of algebraic operations, such as integer multiplications, division, and sorting [SO03; PPJ<sup>+</sup>18]. The  $bPTF^0[k]$  circuits that we study in this work are capable of simulating a variety of variants of standard neural networks. This class of circuits also supports attention functions that are likely to be beyond  $TC^0$  and may accommodate substantially different LLM architectures. We refer the reader to Section 6.2 for a more detailed discussion on these points.

**Definition 2.1.** For any positive integer  $p$ , the Inverted Strict Modular Relation Problem (ISMRP) with input and output lengths  $n$  and  $m$  respectively, denoted as  $\mathcal{R}_p^m : \mathbb{F}_2^n \mapsto \mathbb{F}_2^m$ , is defined as follows. For any  $x \in \mathbb{F}_2^n$  such that  $|x| \bmod p = 0$ ,

$$\mathcal{R}_p^m(x) := \{y \mid y \in \mathbb{F}_2^m : |y| \bmod p = -(|x|/p) \bmod p\}, \quad (2.1)$$

where  $|x| = \sum_{i=1}^n x_i$  is the Hamming weight of the  $n$ -bit string  $x$ .

The relational problem  $\mathcal{R}_p^m$  is defined only for inputs  $x$  whose Hamming weight is a multiple of  $p$ , say  $|x| = kp$  for some  $k \in \mathbb{N}$ . For any such valid input, the set of valid outputs is a set of bitstrings with length specified by the parameter  $m$  and Hamming weight equal to the additive inverse of the factor  $k$  modulo  $p$ , i.e.  $|y| = -k \bmod p$ . For  $p = 2$ ,  $\mathcal{R}_2^m$  is exactly the parity halving problem defined in [WKS<sup>+</sup>19]. By thus generalizing PHP to  $\mathcal{R}_p^m$  we will see that we can define and analyze new non-local games over qupits, allowing us to extend separation results to quantum circuits over higher dimensional systems.

For this family of problems, we provide separate analyses for quantum shallow circuits over qubits ( $p = 2$ ) and qupits ( $p > 2$  prime). In the  $p = 2$  case, we demonstrate that qubit  $QNC^0$  circuits can solve the  $\mathcal{R}_2^m$  problem exactly and with certainty, and prove both exact-case and average-case hardness results for  $bPTF^0[k]$ , in the form of lower bounds on the circuit size for a fixed depth, thereby proving Theorem 1.2. We give a sketch of our proof and an overview of the technical tools we developed for it in Section 2.1.

We will then demonstrate the average-case correlation bounds against  $\text{bPTF}^0[k]$  for all other  $\mathcal{R}_p^m$  problems for  $p > 2$ , as claimed in [Theorem 1.3](#). We complement these classical lower bounds with the respective quantum upper bounds, using the corresponding qubit  $\text{QNC}^0$  circuits for each value of  $p$ . The correlation with the ISMR problems, in this case, has a more complex interpretation than in the qubit case (see [Section 4.2.2](#) for details), and we show that our qubit  $\text{QNC}^0$  circuits achieve  $\Omega(1)$  correlation while polynomial size  $\text{bPTF}^0[k]$ , with  $k = n^{1/(5d)}$ , circuits can achieve only  $O(2^{-n})$  correlation.

## 2.1 Proof of [Theorem 1.2](#): Separation for the qubit case

This subsection is divided into two parts: average-case and exact hardness. We start with average-case hardness, to facilitate easier understanding of the proof techniques, and lead naturally into the exact case hardness. Our results for both average and exact cases rely on the quantum solution ( $\text{QNC}^0$  circuit) for the ISMRP  $\mathcal{R}_2^m$ , and diverge in how they handle the classical circuits—via upper bounds on correlation for the former, and a counting argument for the latter.

### Average-case hardness

We start by constructively proving the existence of  $\text{QNC}^0$  circuits that solve the  $\mathcal{R}_2^m$  problem with certainty, while producing output strings that are of length  $m = o(n^2)$ <sup>5</sup>. Specifically, we construct  $\text{QNC}^0$  circuits with 3D connectivity in [Lemma 4.10](#) and all-to-all connectivity in [Corollary 4.11](#). We do this using the Measurement-Based Quantum Computation (MBQC) paradigm, which allows for shallower quantum circuits and helps us improve the resource estimates as presented in [Section 6.1](#).

Given this candidate problem that  $\text{QNC}^0$  circuits can solve, the second and most challenging aspect pertains to establishing upper bounds for the probability with which  $\text{bPTF}^0[k]$  circuits of size  $s$  and depth  $d$  can solve the same problem on typical inputs of length  $n$ . This is the most technical part of the proof, as no previous lower-bound techniques exist for multi-output  $\text{bPTF}^0[k]$  circuits.

Moreover, the development of depth reduction lemmas, which sequentially reduce a  $\text{bPTF}^0[k]$  circuit to a decision forest, necessitates multi-switching lemmas. These lemmas enable the reduction of a single layer of  $\text{bPTF}^0[k]$  circuits to a decision forest. However, they require a sufficiently high probability guarantee that a layer of a  $\text{bPTF}^0[k]$  circuit will reduce to decision forests under random restrictions. It appears inconclusive as to whether the existing lemmas of this type, demonstrated in [\[Kum23\]](#), are sufficiently strong for this purpose. Consequently, we develop new tools including a new multi-switching lemma for  $\text{bPTF}^0[k]$  circuits with higher success probabilities, as follows.

**Lemma 2.2** (Informal, see [Lemma A.1](#)). *Let  $\mathcal{F} = \{F_1, F_2, F_3, \dots, F_m\}$  be a single  $\text{bPTF}^0[k]$  circuit layer with gates that have maximal fan-in of  $w$  over inputs in  $\mathbb{F}_2^n$ . Then, for sufficiently large  $l$  and small probability  $p$  it reduces under  $p$ -random restrictions to a decision forest  $\text{DT}(l)^m \gg \text{DT}(t)$ , with a global decision tree of depth  $t$  of which each leaf is a set of  $m$  decision trees of depth  $l$ . Formally,*

$$\Pr_{\rho \in R_p} [\mathcal{F} \upharpoonright_{\rho} \text{DT}(l)^m \gg \text{DT}(t)] \leq m \cdot 2^k (80wp)^t. \quad (2.2)$$

This new multi-switching lemma facilitates the creation of a depth reduction lemma, which refers to our [Lemma A.7](#). More importantly, this particular lemma enables sequential depth reductions of the circuits from depth  $d$  to a circuit of depth  $d - 1$  with high probability. It effectively allows the reduction of constant-depth  $\text{bPTF}^0[k]$  circuits to decision forests, especially in cases where there are multiple output bits as follows,

**Lemma 2.3** (Informal, see [Lemma A.9](#)). *Let  $f$  be a  $\text{bPTF}^0[k]$  circuit with  $m$  outputs and inputs in  $\mathbb{F}_2^n$ , of size  $s$  and depth  $d$ . Then, for a probability  $p$  parameterized by  $s, d, k, t$  and  $q$  and we have that*

$$\Pr_{\rho \sim R_p} [f \upharpoonright_{\rho} \text{DT}(q-1)^m \gg \text{DT}(2t-2)] \leq s \cdot 2^{-t+k}. \quad (2.3)$$

The previous lemmas enable us to reduce any initial  $\text{bPTF}^0[k]$  circuit to a decision forest. Then, a second use of random restrictions reduces this decision forest to  $m$  independent decision trees, each computing one of the outcome bits. At this point, these techniques based on random restrictions have us allowed to reduce the

<sup>5</sup>Note that solutions to the problem with outputs of length  $m = \mathcal{O}(n^2)$  would be trivially achievable even by  $\text{NC}^0$  circuits

circuits under consideration while the computational problem kept the same structure and hardness over the variables that were kept alive. From here, we explore this asymmetry using standard locality arguments, such as the lightcone techniques, we can relate the efficiency with which these decision trees solve the initial problem to the efficiency with which classical strategies solve a Mermin’s multi-player game [Mer90a] that is implicitly integrated into the  $\mathcal{R}_2^m$  problem over the variables that are preserved “alive” through the random restriction. By combining the probabilities of successful reductions with the known upper bounds for classical strategies solving this specific non-local game, we obtain our average-case hardness results for  $\text{bPTF}^0[k]$  circuits,

**Corollary 2.4** (Informal, see Corollary 4.9). *For large  $n$ , any  $\text{bPTF}^0[k]/\text{rpoly}$  circuit of depth  $d \geq 4$ , size  $s \leq \exp(n^{1/(2d-2)})$  and  $k \leq n^{1/(5d)}$  solves the  $\mathcal{R}_2^m$  with an efficiency bounded by  $\frac{1}{2} + \exp\left(-\Omega\left(\frac{n^{2-o(1)}}{m^{1+o(1)}(k \cdot \log(s))^{2d}}\right)\right)$ .*

This combination of the previous results still requires careful consideration of all parameters to prove a quantum advantage. There is an interplay between the value of the degree-bound parameter  $k$  in the  $\text{bPTF}^0[k]$  circuits and the dimensionality of the  $\text{QNC}^0$  circuits, while also optimizing all remaining degrees of freedom resulting from the proof techniques. In particular, we establish the average-case hardness, as stated in Theorem 4.3, by combining Lemma 4.10 and Corollary 4.11, which pertain to our quantum solutions, with Corollary 2.4.

### Exact-case hardness

We start by clarifying that exact-case hardness refers to the capacity of the circuit to solve the proposed problem with a probability equal to 1 for all inputs. This is different from worst-case hardness, where we choose a subset of inputs and demonstrate that computing these with a certain probability provides a certain level of hardness. In particular, from the previous average-case bound in [WKS<sup>+</sup>19], one can determine a lower bound on the size of an  $\text{AC}^0$  circuit that solves this problem in the exact-case hardness setting. Similarly, the same follows for  $\text{bPTF}^0[k]$  from our average-case hardness result referenced in Theorem 4.3. However, these bounds are not tight, as we have demonstrated with our exact hardness bound, which implies that even larger  $\text{AC}^0$  and  $\text{bPTF}^0[k]$  circuits are required to solve the problem exactly. Specifically, this allows us to ascertain that quantum-classical advantages exist with input sizes that are orders of magnitude smaller. Additionally, to the best of the authors’ knowledge, this is the first exploration of this particular hardness setting.

To achieve this result we explore some specific proprieties of the  $\mathcal{R}_2^m$  problem. The particular property is that the XOR of all the outcome bits has to equal a specific Boolean function, known as the function  $\text{LSB} : \{0,1\}^n \mapsto \{0,1\}$  which outputs the second least significant bit of the binary representation of the Hamming weight of the input  $|x\rangle$ . More precisely, each output bit produced by a  $\text{bPTF}^0[k]$  circuit can be viewed as a distinct Boolean function  $f_i : \{0,1\}^n \mapsto \{0,1\}$ , and these have to fulfill the same property. Thus, by additionally leveraging the algebraic normal form (ANF) representation we have that the XOR of respective representation of all these Boolean functions must equal the one of the  $\text{LSB}(x)$  function,

$$\underbrace{\text{ANF}(\text{bPTF}^0[k](x))}_{y_1} \oplus \underbrace{\text{ANF}(\text{bPTF}^0[k](x))}_{y_2} \oplus \dots \oplus \underbrace{\text{ANF}(\text{bPTF}^0[k](x))}_{y_m} = \text{ANF}(\text{LSB}(x)). \quad (2.4)$$

The previous setting follows from the consideration of input distribution over the entire set of inputs in  $\mathbb{F}_2^n$ . However, the input considered for the quantum solution includes only even strings; thus, the same statement must be considered for partial Boolean functions. We address the entire problem with this additional difficulty in a twofold manner. First, we demonstrate a foundational structure of the ANF for all the exponential number of Boolean functions that equal the partial evaluation of the LSB function. We do this by showing that all these functions require, in their ANF representation, a minimum number of terms of a certain degree, as outlined in Lemma 4.5. Secondly, we examine the capacity of decision trees, to which  $\text{bPTF}^0[k]$  circuits can be reduced with the random restriction, in generating terms of the previously identified degree, as detailed in our Lemma 4.6<sup>6</sup>. Finally, these two components, in conjunction with our switching lemma Lemma 2.3 that reduces  $\text{bPTF}^0[k]$  circuits to decision trees, allow us to determine a minimal depth of the decision tree’s that directly translate to the minimal size for this class of circuits,

<sup>6</sup>An illustrative example demonstrating the tree depth dependence on the ANF of Boolean functions is the parity function, which necessitates any decision tree to have a depth at least equal to the input size. This requirement ensures the tree can produce all the degree 1 terms of the parity function’s ANF.



**Lemma 2.5** (Informal, [Lemma 4.7](#)). *For sufficiently large  $n$ , any  $\text{bPTF}^0[k]/\text{rpoly}$  circuit depth  $d \geq 4$  and  $k \leq n^{1/(5d)}$  that solves the  $\mathcal{R}_2^m$  has size no smaller than  $s \geq \exp\left(\tilde{O}\left((nk^{-d}m^{-1/2})^{1/(d-1)}\right)\right)$ .*

The combination of this bound with the specific parameters of quantum upper bounds [Lemma 4.10](#) and [Corollary 4.11](#) complete our [Theorem 1.2](#). Subsequently, we will enlarge the set of average-case hardness separation between  $\text{QNC}^0$  and  $\text{bPTF}^0[k]$  with an infinite set of concretely instantiated relation problems.

## 2.2 Proof of [Theorem 1.3](#): Separations for higher dimensions (qupits)

For our second result, we consider an infinite class of instances of the ISMR problems as candidates to separate qudit  $\text{QNC}^0$  from  $\text{bPTF}^0[k]$ , beyond the  $\mathcal{R}_2^m$  problem and related problems that have been explored in previous works. These problems, however, possess some special properties, as the outcomes depend uniquely on the modular residue of their Hamming weight in  $\mathbb{F}_p$ . Therefore, we employ a correlation measure based on the nature of this problem as follows,

$$\text{Corr}_{\mathcal{D}}(f, g) = \mathbb{E}_{x \sim \mathcal{D}} \left[ \text{Re} \left( e^{i \frac{2\pi |f(x)| - |g(x)|}{p}} \right) \right]. \quad (2.5)$$

Intuitively, these correlation functions assess the distance between two relations using the natural measure of the inner product for domains that form an Abelian group [\[Don14\]](#).

Now, the proof will be divided into two parts. In the first part, we will demonstrate that polynomial-size  $\text{bPTF}^0[k]$  circuits exhibit a correlation that asymptotically approaches zero as the input size increases. In the second part, we demonstrate that quantum circuits over qupits solve all these instances of ISMR problems with a constant positive and far from zero correlation for inputs of arbitrary size.

For the first part, we will employ proof techniques used for the average-case hardness results of [Theorem 1.2](#). However, in this higher-dimensional setting, many essential technical tools have not yet been developed or defined. We begin by noting that we are defining a family of XOR non-local games ([Definition 4.14](#)) related to the respective ISMR problems ([Definition 4.1](#)) for the first time, to the best of the authors' knowledge, and we need to determine the upper bounds of the efficiencies for any classical strategy. This contrasts with previous works, which relied on known non-local games and their predetermined optimal winning strategies.

**Lemma 2.6** (Informal, see [Lemma 4.17](#)). *Any local probabilistic classical strategy  $w_{\mathcal{G}_p}$  that solves the Modular XOR non-local games, denoted as  $G_p$ , with  $n$  parties and messages over  $\mathbb{F}_p^n$ , taken from  $\mathcal{D}_p$  a uniform distribution over  $\mathbb{F}_2^{n(p-1)}$  with Hamming weight satisfying  $(\sum_{i=1}^n x_i) \bmod p = 0$  and a bit to base- $p$  encoding, the maximal correlation with  $r$  restricted bits is bounded by  $\text{Corr}_{\mathcal{D}_p}(w_{\mathcal{G}_p}, \mathcal{G}_p) \leq (c_p)^{\frac{n-r}{p-1}}$ , with  $c_p \in (0, 1)$ .*

To utilize the bounds determined for the non-local games, which are naturally defined as mappings of the type  $\mathbb{F}_p^n \mapsto \mathbb{F}_p^m$ , we need to consider encodings and decodings between binary strings in  $\mathbb{F}_2^n$  and strings in  $\mathbb{F}_p^n$ . Furthermore, we address an issue that arises in many of these encodings: they translate distributions that are uniform over one field to non-uniform distributions over another. This is particularly crucial as we aim to use uniform random restrictions in the proof process; hence, we require non-local games that correspond to uniform distributions of strings in  $\mathbb{F}_2^n$ . We resolve this problem by considering biased inputs for the non-local games that correspond to uniform distributions of strings in  $\mathbb{F}_2^n$  when mapped back using our encoding. This involves choosing a specific encoding that allows for a linear bias in the non-local games, which we could accommodate in our proof technique for the winning strategies of non-local games while still obtaining sufficiently tight upper bounds.

From this upper bound on the optimal classical strategies, and the particular case for the qutrit winning probability [Lemma 4.19](#), we have that we can now extend the lightcone arguments for  $\text{NC}^0$  circuits allowing us to take advantage of the non-local game for which we were able to bound the classical winning probability. This follows by considering blocks of bits representing the dits of the non-local game and exploring that these dits do not have any particular structure as in previous works [\[CCK23\]](#) to apply lightcone arguments as in [Lemma 4.18](#). This combination of results already determines a new  $\text{NC}^0$  separation with qupits as described in [Theorem 4.27](#), which we will further explore to obtain the separations against  $\text{bPTF}^0[k]$ .

For that last step, we resort to our multi-switching lemmas [Lemma A.8](#), to reduce an  $\text{bPTF}^0[k]$  circuit to a decision tree that can be analyzed as of bounded causal effect, reducing it therefore to  $\text{NC}^0$  type circuit. In



particular, we obtain that through our capability of using uniform distributions of inputs we do have random restriction that are taking without any bias and obtain therefore average-case hardness results. From the previous considerations and building blocks, we obtain exactly that.

**Lemma 2.7** (Informal, see [Lemma 4.21](#)). *For sufficiently large  $n$  and  $q \in \mathbb{N}_{>0}$ , any  $\text{bPTF}^0[k]/\text{rpoly}$  circuit  $C$  of depth  $d \geq 4$ , size  $s \leq \exp(n^{1/(2d-2)})$  and parameter  $k \leq n^{1/(5d)}$  solves the  $\mathcal{R}_p^m$  with correlation bounded by,*

$$\text{Corr}_{\mathcal{D}_p}(C, \mathcal{R}_p^m) = \exp\left(-\Omega\left(\frac{n^{2-o(1)}}{m^{1+2/q} \log(s)^{2d-2} k^{2d}}\right)\right), \quad (2.6)$$

with  $\mathcal{D}_p$  being the uniform distribution over string in  $\mathbb{F}_2^n$  that satisfy  $|x| \bmod p = 0$ .

For the quantum lower bound, the initial step involves the creation of a generalization of the “poor man’s cat state” introduced in [\[WKS<sup>+</sup>19\]](#), as detailed in our [Definition 4.23](#). These states serve as the resource states and we demonstrate that they can be generated using  $\text{QNC}^0$  circuits, as shown in [Lemma 4.24](#). Subsequently, employing these resource states, we illustrate that another  $\text{QNC}^0$  circuit can produce a classical outcome string related to the ISMRP. In particular, this string can classically be reduced with a  $\text{NC}^0$  circuit to a solution to each one of the  $\mathcal{R}_p^m$  problems sufficiently small outcome string  $m$  and constant and non-zero correlation.

**Lemma 2.8** (Informal, see [Lemma 4.26](#)). *There exists a  $\text{QNC}^0$  circuit, denoted as  $C_Q$ , that given a generalized poor-man’s cat state  $|\text{GPM}_p^n\rangle$ , solves the ISMRP, represented as  $\mathcal{R}_p^m$ , across a uniform distribution  $\mathcal{D}_p$  in  $\mathbb{F}_2^n$  that satisfy the condition  $\sum_{i=1}^n x_i \bmod p = 0$ , with a correlation,*

$$\text{Corr}_{\mathcal{D}_p}(C_Q, \mathcal{R}_p^m) = \frac{p-1}{p^2}. \quad (2.7)$$

Moreover, we obtain a separation for the qutrit case with respect to the probability of success in solving the respective ISMR problem. This is possible because the correlation function still has a direct relation with the success probability and thus compares to binary case [Lemma 4.25](#).

We note that the previous lemma presented the most significant technical challenge for establishing the lower bounds for quantum correlation. This arises because poor-man’s cat states in higher dimensions produce phase components that result in complex supports for standard measurement outcomes. Initially, we find a concise and clear representation for the projections of the outcome strings based on the input and the random strings  $z$  defining the specific qubit poor man’s cat state at hand (as detailed in [Equation \(4.76\)](#) based on [Table 3](#)). The second major challenge is that the resulting support depends on a larger number of inner products between strings characterising the state and the input. Moreover, we require an  $\text{NC}^0$  reduction based on these values that enhances the efficiency of solving the initial problems. Lastly, we demonstrate that at least one inner product can be evaluated within  $\text{NC}^0$  and attached to the outcome strings, such that the entire string exhibits a larger correlation. Consequently, the quantum circuit solves the problem with a constant and input-independent correlation value, which together with the preceding steps completes the proof of [Theorem 1.3](#).

Next, we extend the results of this section to the noisy setting i.e. we obtain separations between noisy quantum circuits and *noiseless*  $\text{bPTF}^0$ , taking inspiration from [\[BGK<sup>+</sup>20\]](#).

## 2.3 Proof of [Theorem 1.4](#): Noise-resilient separations

For our computational separation between qubit  $\text{QNC}^0$  circuits afflicted by noise and noiseless  $\text{bPTF}^0[k]$  circuits, we consider the qubit generalized local stochastic noise model (see [Section 3.4](#)), which is standard in quantum error correction. This model is favored due to its ability to account for gate-level noise, noisy input state preparation, and noisy measurement, while allowing for (weakly) non-local errors by requiring the probability of an error to decay exponentially with the number of qubits it affects non-trivially.

At a high level, we define a family of relation problems related to the noise-tolerant realization of the  $\text{QNC}^0$  circuits solving the ISMR problems (see [Definition 5.1](#)). These problems are tailored to proving the noise-robustness of our  $\text{QNC}^0$  Vs.  $\text{bPTF}^0[k]$  separations. We show that the ISMR problem is  $\text{AC}^0$ -reducible to a corresponding problem in the new family of problems exactly when an  $\text{AC}^0$  circuit can successfully decode

the outcome of these noise-tolerant  $\text{QNC}^0$  circuits. This reduction allows us to lift the hardness results shown for the noiseless case to the case of noisy  $\text{QNC}^0$  circuits, establishing the desired noise-robust separations with correlation bounds asymptotically equal to those in [Theorem 4.12](#).

We address two main technical challenges that go beyond the previous noise-robust separations explored in [\[BGK<sup>+</sup>20; GJS21\]](#). The first is that with qupits of dimension  $p \geq 3$  we need to consider *non-Clifford* circuits. The need for these more complex quantum circuits arises from the inability to violate Bell inequalities with stabilizer states for any qupit dimension beyond qubits, as shown in [\[Gro06; HBV13; MŠM<sup>+</sup>24\]](#), which also suggests that the same limitation extends to quantum-classical separations in circuit complexity. To overcome this, we must show that such circuits can also be implemented fault-tolerantly, which represents a novel departure from prior work on unconditional separations between quantum and classical circuit classes. The second challenge is the need to generalize the techniques used in [\[BGK<sup>+</sup>20\]](#) for quantum-error correction—such as single-shot state preparation, decoders, and transversal constant-depth gate execution—for arbitrary qupit dimensions, in addition to techniques related to fault-tolerantly implementing non-Clifford circuits.

We overcome the first challenge by introducing logical advice states over qupits, which enable the fault-tolerant realization of non-Clifford operations through a qupit magic state injection protocol. In particular, we prove in [Section 5.2.1](#) that for a specific CSS-type error correction code that fulfills a set of conditions listed in [Definition 5.4](#), we obtain fault-tolerant implementations of non-adaptive qupit Clifford circuits with advice states, for arbitrary prime dimensions.

**Lemma 2.9** (Informal, see [Lemma 5.5](#)). *Let  $\mathcal{EC}_C$  be the error-corrected version of  $C$ , a constant-depth Clifford circuit of depth  $d$  with advice state  $|A\rangle$ , using a code that meets the conditions in [Definition 5.4](#). The code has distance  $l = \mathcal{O}(\text{poly log } n)$  and the circuit is affected by local stochastic noise  $\mathcal{E} \sim \mathcal{N}(\varrho)$  and the advice by  $\mathcal{E}_A \sim \mathcal{N}(\rho)$ . Then, whenever  $\max\{\varrho, \rho\} < p_{th} = 2^{-2^{\mathcal{O}(d)}}$  for any input  $x \in \mathbb{F}^n$  we can show that*

$$\Pr[\text{DEC}^*(\mathcal{EC}_C(x)) = C(x)] > 0.99, \quad (2.8)$$

with  $\text{DEC}^*$  being the combined correction and decoding functions needed to retrieve the logical outcome from the encoded state.

We divide the proof into two parts. The first part demonstrates that the qupit surface code meets all the necessary conditions, generally implying that it supports single-shot state preparation, transversal gate implementation in constant depth, and single-shot information retrieval using the selected decoder. Making these steps precise in higher-dimensional  $\text{QNC}^0$  circuits requires new insights that extend beyond prior work, which we outline below. In parallel with verifying that the qupit surface code ensures the fault-tolerant implementation of the circuit architecture as shown in [Lemma 5.5](#) and [Figure 11](#), we must prove a second element. This refers to the existence of  $\text{QNC}^0$  circuits that are non-adaptive Clifford circuits with input-independent advice states capable of solving the ISMR problems; this requires redesigning new quantum circuits and forms the second piece of the proof.

## Noise-resilient qupit Clifford circuits with quantum advice

The first condition, concerning the transversal implementation of Clifford operations, follows from the work of [\[Mou16\]](#). However, achieving single-shot state preparation and information retrieval in the qupit surface code is more complex than implementing transversal gates. In higher dimensions, errors do not simply manifest as defects at the endpoints of the qupit lattice, as they do in the qubit case. Instead, for every error, defects are likely to be scattered throughout the lattice. This distribution of defects motivated the use of the HDRG decoder, as it has been shown to have good error-correction properties beyond the qubit case, overcoming issues with the previously considered minimum weight perfect matching decoder [\[WAB15; Anw14\]](#).

The information retrieval property necessitates that the code and decoder accurately perform logical  $\bar{Z}$  measurements even under noisy conditions. In [Lemma 5.10](#), we extend a result from [\[BH13\]](#) to the definition of local stochastic noise discussed in this text. We demonstrate that the HDRG decoder’s probability of failure decreases exponentially as the qupit lattice size increases. Consequently, the HDRG decoder reliably yields the correct outcome for logical measurements, provided the noise rate does not exceed a certain threshold. Specifically, we establish that  $\Pr[\text{Success}] \geq 1 - \exp(-\Omega(m^\eta))$ , where  $m$  is the surface code distance and  $\eta$  is a constant.

We also demonstrate that single-shot state preparation can be achieved using the qudit surface code and the HDRG decoder for qupits of dimension  $p \geq 2$ . More precisely, we show that the 3D block construction from [RBH05] preparing logical Bell pairs can be adapted for single-shot state preparation of  $\text{GHZ}_2$  qupit states, a capability not previously demonstrated. This adaptation involves defining functions necessary for the single-shot state preparation process, typically categorized as recovery and repair. The recovery function entails applying operations to retrieve the correct state from the randomness inherent in the noise-free process, while the repair function corrects the states based on the effects of noise that may occur during the described noise-free state preparation circuit and the recovery function.

The recovery function is derived directly from our generalization of the state preparation process. Regarding the repair function, we establish its feasibility up to the single-shot properties, using the alternative lifting properties proposed in [BGK<sup>+</sup>20] and considering a repair function based on the HDRG decoder (Lemma 5.12). This shows that these logical states can be prepared for errors below a certain threshold with exponentially high confidence for increasing the lattice size.

### Non-adaptive Clifford circuits with magic state injection

To redesign the quantum circuits proposed in Lemma 4.26 for the required noise-resilient architecture from Lemma 5.5, we retain all Clifford operations as they present no difficulties. However, handling the non-Clifford rotations requires a new approach. Initially, we could consider using a gate teleportation gadget that integrates the non-Clifford gate into the advice state, as illustrated in Equation (5.63). Unfortunately, while these gadgets are adaptive, we only have access to non-adaptive gadgets for a noise-resilient execution. Consequently, we implement the non-adaptive gadgets as depicted in Section 5.2.1, and in Lemma 5.15, we discuss the additional phases introduced by the lack of adaptive corrections. Due to their diagonal nature, we demonstrate that it is still possible to address the ISMR problems using a more complex reduction from the outcome of these qupit  $\text{QNC}^0$  circuits, involving a considerably more intricate  $\text{NC}^0$  reduction.

**Lemma 2.10** (Informal, see Lemma 5.16). *There exist constant-depth non-adaptive Clifford circuits with the advice state  $|T^{1/p}\rangle^{\otimes n}$ , denoted as  $\text{Cliff}_{+T}$ , that solve the ISMR problems  $\mathcal{R}_p^m$  and  $m = \mathcal{O}(n \cdot g^{p^3})$ , for a uniform distribution  $\mathcal{D}_p$  of input strings that satisfy the condition  $\sum_{i=1}^n x_i \bmod p = 0$  within  $\mathbb{F}_2^n$  with a correlation,  $\text{Corr}_{\mathcal{D}_p}(|\text{Cliff}_{+T}\rangle, |\mathcal{R}_p^m\rangle) = \frac{p-1}{p^2}$ .*

In our final step, we show that there exists a noisy quantum circuit that solves the proposed noise-resilient relation problems with large constant correlation. We consider the encoded version of the circuits proposed in Lemma 5.16 using the qupit surface code and the HDRG decoder. This does provides us with the quantum lower bound on the correlation described in Lemma 5.17. Additionally, we obtain the classical lower bound through the  $\text{AC}^0$ -reduction from the noise relation problems to the ISMR problems.

Furthermore, we demonstrate that a minimal universal gate set, which requires only the set of Clifford gates and a single magic gate, suffices. We prove that this magic gate is related to  $T$ -type qubit gates, as shown in Lemma 5.14. Thus, we recover the standard noise-resilient circuit architecture, incorporating magic state injection gadgets for all qupit dimensions, thereby extending the scope of these results.

As a corollary, we also obtain the same separation for qubits. However, since these are based on Clifford gates, we obtain a direct separation between noisy  $\text{QNC}^0$  circuits and  $\text{bPTF}^0[k]$  circuits without any advice states.

## 2.4 New switching lemma for bounded PTF circuits

As mentioned in Section 2.1, we prove a new multi-switching lemma for  $\text{bPTF}^0[k]$  circuits, which provides tighter concentration bounds compared to previous work. We then use it to establish depth reduction for  $\text{bPTF}^0[k]$  circuits with multiple output bits. Our approach parallels the strategies employed for multi-output  $\text{AC}^0$  circuits [Ros17; WKS<sup>+</sup>19], tailored specifically to  $\text{bPTF}^0[k]$  circuits. Using this tool, we analyze how  $\text{bPTF}^0[k]$  circuits reduce under random restrictions, showing that we obtain *decision forests* of low complexity with high probability. These more tractable decision forests can then be compared with quantum circuits via lightcone arguments.

### Tighter multi-switching lemma for $\text{bPTF}^0[k]$

On the technical side, our main contribution is a multi-switching lemma, which shows that a finite set of depth-2  $\text{bPTF}^0[k] \circ \text{AND}_w$  circuits reduces to a decision forest of the type  $\text{DT}(w)^m \succcurlyeq \text{DT}(t)$  with high probability converging to unity as  $1 - O(2^{-t})$ . We provide the formal statement in [Lemma 2.2](#) and the proof in [Lemma A.1](#). Note that while [Theorem 3.12](#), as proven in [\[Kum23\]](#), also functions as a multi-switching lemma, a tighter bound on the probability is necessary to reduce the initial circuit to a tree-like structure. In particular, in the success probability of the switching lemma,  $4(64(2^k m)^{1/q} pw)^t$ , the dependence on the size  $t$  of the global and  $q$  of local decision trees in the decision forest must be removed from the term  $m$ , that accounts for the number of  $\text{bPTF}^0[k]$  circuits simultaneously reduced by the lemma. Expanding on this technical limitation, the primary bottleneck arises when employing the lemma for the depth reduction step. This dependency necessitates the utilization of large fixing probabilities for the random restrictions, ultimately leading to the fixation of nearly all the free variables. Consequently, this is insufficient to prove a separation from  $\text{QNC}^0$ . In contrast, our tighter bound for the various lemmas allows for subsequent separation from  $\text{QNC}^0$  circuits via locality arguments.

Our proof of [Lemma A.1](#) for  $\text{bPTF}^0[k]$  employs an inductive approach similar to the one used by [\[Has16\]](#) for  $\text{AC}^0$  circuits. We conduct induction over the number of variables fixed by random restrictions and the circuits  $f_i$  corresponding to each output bit, aiming to lower bound the probability with which the latter reduce to decision trees of the type  $\text{DT}(l)$ . Simultaneously, when we encounter a circuit that does *not* reduce to a decision tree of the type  $\text{DT}(l)$  with a set of variables fixed by random restrictions, we query the variables that remain “alive” to forcefully simplify this circuit. These variables then become part of the global decision tree  $\text{DT}(t)$ , sequentially contributing to the construction of a decision forest. To make this approach effective, we address the issue of fixing variables and clauses that describe these circuits by combining our induction with canonical decision trees from the witness method technique (also used by [\[Kum23\]](#) to prove [Theorem 3.12](#)).

The induction technique described above necessitates the use of *downward-closed* random restrictions. This property ensures that the size of our canonical decision tree does not increase when additional variables, left alive by the initial random restriction, are further restricted. In other words, it guarantees the monotonicity of decision tree size under random restrictions, which is crucial for the inductive reasoning process. This is accomplished through [Algorithm 3](#), which constructs our canonical decision trees  $\text{DT}(l)$  corresponding to the leaves of the decision forest. We prove two ingredients that ensure downward closedness. First, [Lemma A.5](#) shows that all random restrictions reducing the circuit to a fixed decision tree  $\text{DT}(l)$  overlap in the variables that they fix. Then, [Lemma A.6](#) shows that for any arbitrary random restriction, fixing more variables does not increase the depth of the decision tree to which the initial circuit reduces.

### Depth reduction for $\text{bPTF}^0[k]$

Adopting the proof technique of [\[Ros17\]](#) for  $\text{AC}^0$  circuits, we use [Lemma A.1](#) to prove a new depth reduction lemma for  $\text{bPTF}^0[k]$  circuits.

The multi-switching lemma first reduces the depth by 1, from  $d$  to  $d - 1$ , for a computational object of the type  $\text{bPTF}[k; d; s_1, s_2, \dots, s_d] \circ \text{DT}(w)^{s_1} \succcurlyeq \text{DT}(t - 1)$ . This describes a decision forest that provides the input for a  $\text{bPTF}[k; d; s_1, s_2, \dots, s_d]$  circuit of depth  $d$ , with layers having  $s_1, \dots, s_d$  gates each, which will subsequently have its depth reduced, as demonstrated in the following lemma.

**Lemma 2.11** (Informal, see [Lemma A.7](#)). *For  $f \in \text{bPTF}[k; d; s_1, s_2, \dots, s_d] \circ \text{DT}(w)^{s_1} \succcurlyeq \text{DT}(t - 1)$  parameterized by circuit depth  $d$ , decision tree depth  $t$ , and restriction probability  $p$ , we have that*

$$\Pr_{\rho \sim R_p} \left[ f|_{\rho} \notin \text{bPTF}[k; d; s_2, \dots, s_d] \circ \text{DT}(l)^{s_2} \succcurlyeq \text{DT}(t - 1) \right] \leq s_1 \cdot 2^k (400wp)^{t/2}, \quad (2.9)$$

where  $l \geq \log s_1 + k + 2$ .

Using this result, we can reduce the depth of a  $\text{bPTF}^0[k]$  circuit while simultaneously constructing the decision forest to which it will be reduced. More precisely, iterative application of the depth reduction lemma to the more elaborate computational object considered above leads to the following lemma.

**Lemma 2.12** (Informal, see [Lemma A.8](#)). *For parameters  $d, t, k, q, m, s_1, l_1, \dots, s_{d-1}, l_{d-1} \in \mathbb{N}$  and  $p_1, \dots, p_d \in (0, 1)$ , we have for  $f \in \text{bPTF}^0[k; d; s_1, \dots, s_{d-1}, m](k)$  with  $n$  inputs and  $m$  outputs that*

$$\Pr_{\rho \sim R_p} \left[ f|_{\rho} \notin \text{DT}(q-1)^m \rhd \text{DT}(2t-2) \right] \leq \sum_{i=2}^{d-1} s_i \cdot 2^k \mathcal{O}(p_i l_i)^{t/2} + 2^k m^{1/q} \mathcal{O}(p_d \cdot l_d)^t, \quad (2.10)$$

where  $p = p_1 \cdot p_2 \cdot \dots \cdot p_d$ .

Finally, we assign values to the probabilities  $p_1, \dots, p_d$  of different random restrictions and the depths  $l_1, \dots, l_d$  of the local decision trees such that for global decision tree depth  $t$ , initial circuit size  $s$ , and circuit type parameterized by  $k$ , we determine the probability of successfully reducing the circuit to decision forests. We define these decision forests informally in [Lemma 2.3](#) and formally in [Lemma A.9](#).

### 3 Preliminaries and Notation

In this work, we expand on the set of classical circuit classes against which we can establish a separation of computational power of  $\text{QNC}^0$ , for a relational problem. Towards this goal, in [Section 3.1](#) we first set up the notation and definitions for the constant-depth classical circuit classes we study, and then in [Section 3.2](#) introduce the most important techniques we use: random restrictions and switching lemmas. We then present some background on the quantum information theory of non-local games in [Section 3.3](#), and noisy quantum circuits in [Section 3.4](#).

Throughout the text we use the notation  $[n] = \{1, 2, \dots, n\}$ ,  $\log$  denotes the logarithm to base two, and  $\exp$  denotes the exponential function, with the base  $e$  or  $2$  that will be clear from context.

#### 3.1 Low-depth complexity classes

We now explicitly introduce the circuit classes and computational models that we analyze in this work. For a detailed introduction to these topics, we refer to standard textbooks such as [\[AB09\]](#). The *depth* of a circuit is the maximum number of gates that are composed sequentially. The *width* of a circuit refers to the largest number of gates applied simultaneously in any of the its layers. In terms of standard computational resources, depth is related to time, and width is related to the space of a computation. We say that a circuit is composed of bounded fan-in gates when the number of wires feeding logical values into each gate for processing is limited by a fixed constant. Conversely, unbounded fan-in refers to gates that can accommodate a polynomial number of input wires, relative to the input size, feeding into the logical gate for processing.

We assume the standard notation and definitions for classical notions such as  $\text{NC}^0$  and  $\text{AC}^0$ .  $\text{NC}^0$  is the only circuit class that uses only bounded fan-in gates, but unbounded fan-out and arbitrary wiring. A family of circuits  $\{\mathcal{C}_n\}_{n \geq 1}$  is said to be  $\text{X}$ -uniform for a complexity class  $\text{X}$  if there is a Turing machine  $T$  in  $\text{X}$  which on input  $1^n$  outputs a description of  $\mathcal{C}_n$  for each  $n$ . All of our classical circuits will be non-uniform, and admit randomised advice strings of polynomial length in the input size (denoted by  $/\text{rpoly}$ ), while our quantum circuits will always be uniform.

**Definition 3.1** ( $\text{NC}^0$  circuits). *The class  $\text{NC}^0$  consists of classical constant-depth circuits composed of bounded fan-in AND, OR, and NOT gates, with a polynomial number of gates in the input size  $n$ .*

The subsequent two circuit classes permit unbounded fan-in, which enhances their computational capabilities. They are distinguished by their computational power and the selection of gate sets.

**Definition 3.2** ( $\text{AC}^0$  circuits). *The class  $\text{AC}^0$  consists of classical constant-depth circuits composed of unbounded fan-in AND, OR, and NOT gates, with a polynomial number of gates in the input size  $n$ .*

Note that in fact circuits with sub-logarithmic depth,  $o(\log n)$ , are considered to be of constant depth.

Our primary focus will be on  $\text{QNC}^0$ , which as defined in [Section 1.1](#) is the class of constant-depth quantum circuits constructed from a universal and finite set of gates.

**Definition 3.3.** ( $\text{QNC}^i$  class). *The  $\text{QNC}^i$  class consists of quantum circuits composed of bounded fan-in quantum gates from a universal finite set, with depth  $\mathcal{O}(\log^i(n))$ , and a polynomial number of gates concerning the size of the input string  $n$ .*



In addition to the standard classical circuit classes, our analysis will focus on a novel class featuring parameterized gates, first defined by [Kum23]. However, we will present these using a different notation, in the form commonly used in relation to polynomial threshold functions [OS03; KKL17; PP22]. We first introduce the class of polynomial threshold gates restricted by a degree-bound parameter.

**Definition 3.4** (bounded polynomial threshold gates). *We denote by  $\text{bPTF}[k]$  the set of unbounded fan-in gates that implement two types of Polynomial Threshold Functions with degree-bound  $k$ , defined as follows. The first type of gates implement OR-type PTFs, of the form*

$$f_{\text{OR}}(x) = \begin{cases} P(x), & \sum_{i=0}^n x_i \leq k \\ 1, & \sum_{i=0}^n x_i > k \end{cases}; \quad \text{with } P : \mathbb{F}_2^n \rightarrow \mathbb{F}_2 \text{ a polynomial over } \mathbb{F}_2 = \{0, 1\}. \quad (3.1)$$

*These gates permit arbitrary mappings of strings with a Hamming weight bounded by  $\leq k$  and identically equal to 1 for all inputs with a Hamming weight  $> k$ . The second type of gates includes all unbounded fan-in gates that implement the analogous AND-type PTFs:*

$$f_{\text{AND}}(x) = \begin{cases} P(x), & \sum_{i=0}^n x_i \geq n - k \\ 0, & \sum_{i=0}^n x_i < n - k \end{cases}; \quad \text{with } P : \mathbb{F}_2^n \rightarrow \mathbb{F}_2 \text{ a polynomial over } \mathbb{F}_2 = \{0, 1\}. \quad (3.2)$$

*AND-type PTFs allow for arbitrary mappings of strings with Hamming weight  $\geq n - k$  and are identically equal to 0 for all inputs with a Hamming weight  $< n - k$ .*

Note that when  $k = 0$ , we recover the usual unbounded fan-in AND and OR gates. Given this definition of bounded polynomial threshold gates, we now introduce circuit classes composed of these gates, which will be the main objects of study in this work.

**Definition 3.5** (bounded polynomial threshold circuits). *The class  $\text{bPTF}^0[k]$  consists of classical circuits composed of unbounded fan-in  $\text{bPTF}[k]$  gates with constant depth, and a polynomial number of gates in the input size  $n$ .*

Note that for  $k = \mathcal{O}(1)$ ,  $\text{bPTF}^0[k]$  is equal to  $\text{AC}^0$ . In addition to these circuit classes, we also work with decision trees, which are fundamental in the study of these classes due to their role in random restriction techniques. We denote by  $\text{DT}(t)$  the class of Boolean functions computed by depth- $t$  decision trees with a single output bit.

Furthermore, we will examine more complex decision trees, whose leaves do not just bear single binary values, but additional sets of decision trees. This structure allows for a hierarchical querying process: a global decision tree first addresses a set of variables, which in turn delineates a collection of local decision trees responsible for computing the bits of the final output string. To denote non-binary values at the leaves of a decision tree, we introduce the symbol  $\bowtie$  to signify that the entity to the left represents its leaves.

**Definition 3.6** (Decision forests). *We use  $\text{DT}(w)^m \bowtie \text{DT}(t)$  to denote the class of  $(t, m, w)$ -decision forests, defined as depth- $t$  decision trees whose leaves are labeled by  $m$ -tuples of depth- $w$  decision trees.*

Building upon these objects, we introduce a new type of decision trees whose outputs become the inputs to a  $\text{bPTF}^0[k]$  circuit. In the following, we write  $\text{bPTF}[k; d; s_1, s_2, \dots, s_d]$  to denote a  $\text{bPTF}^0[k]$  circuit with depth  $d$ , and  $s_i$  gates for each layer  $i$  for  $i \in \{1, \dots, d\}$ <sup>7</sup>.

**Definition 3.7** (bounded threshold circuits with decision tree inputs). *The object  $\text{bPTF}[k; d; s_1, s_2, \dots, s_d] \circ \text{DT}(w)$  defines the class comprised of  $\text{bPTF}^0[k]$  circuits with depth  $d$ , and  $s_i$  gates per layer whose inputs are labeled by decision trees in  $\text{DT}(w)$ .*

We also introduce a second object of this type, comprising a global decision tree whose leaves specify a collection of local decision trees; these, in turn, determine the input to a  $\text{bPTF}^0[k]$  circuit.

**Definition 3.8.**  $(\text{bPTF}[k; d; s_1, s_2, \dots, s_d] \circ \text{DT}(w) \bowtie \text{DT}(t))$ . *The object  $\text{bPTF}[k; d; s_1, s_2, \dots, s_d] \circ \text{DT}(w) \bowtie \text{DT}(t)$  defines the class comprised of depth- $t$  decision trees, whose leaves are objects in  $\text{bPTF}[k; d; s_1, s_2, \dots, s_d] \circ \text{DT}(w)$ .*

<sup>7</sup>These computational objects will be our  $\text{bPTF}^0[k]$  equivalent of those introduced in [Ros17] for  $\text{AC}^0$  and used to establish the respective depth reduction techniques.



Finally, we also introduce the Algebraic Normal Form (ANF) which refers to polynomial representation of Boolean functions over  $\mathbb{F}_2$ .

**Definition 3.9** (Algebraic Normal Form.). *Every Boolean function  $f : \{0, 1\}^n \mapsto \{0, 1\}$  can be represented uniquely as,*

$$f(x) = \bigoplus_{S \subseteq [n]} c_S \prod_{i \in S} x_i. \quad (3.3)$$

with  $c_S \in \{0, 1\}$ .

## 3.2 Random restrictions and Switching lemmas

Our analysis relies heavily on random restrictions, a technique that has been widely utilized in computational circuit complexity.

**Definition 3.10** ( $p$ -random restriction). *A  $p$ -random restriction  $\rho \in R_p$  is a function mapping from a set of literals  $\{x_i\}_{i \in I}$  to values  $\{0, 1, *\}$ . It is parameterized by the probability  $p \in (0, 1)$ : each variable is independently kept ‘alive’ using the symbol  $*$  with probability  $p$ , or assigned the value 0 or 1 with equal probability  $\frac{1-p}{2}$ .*

Incorporating the concept of random restriction, the application of such constraints to a function  $f$ , denoted by  $f[\rho]$ , results in the definition of a new function evaluated according to  $f(x \circ \rho)$ . Put simply, the restrictions imposed by  $\rho$  are applied to the inputs of  $f$ , where the surviving variables adopt the values from  $x$  that are allowed to fluctuate. Thus, a restricted function can be viewed as a new function characterized by a reduced domain of input.

A random restriction can also be described by first choosing a ground truth  $z \in \{0, 1\}^n$  and a set of indices  $\Lambda \subseteq [n]$ . The random restriction, denoted as  $\rho(z, \Lambda)$ , is then defined such that  $\Lambda$  determines the indices  $x_i$  for which the corresponding bits are set to the symbol  $*$ . The remaining bits adopt the corresponding values from  $z$ . For instance, a  $p$ -random restriction in this context corresponds to a stochastic process where each index in  $\Lambda$  is selected independently with probability  $p$ , and  $z$  is chosen uniformly at random from the set  $\{0, 1\}^n$ .

With the use of random restriction, it is possible to reduce the circuits from the classes defined previously to decision trees based on switching lemmas. In particular, we will discuss two important switching lemmas derived by [Kum23] for  $\text{bPTF}^0[k]$  circuits, along with some additional useful lemmas from the same text.

**Theorem 3.11.** [Kum23] *Let  $f$  be computable by a depth-2 circuit<sup>8</sup>  $F$  comprised of a  $\text{bPTF}[k]$  gate which has as inputs AND or OR gates with maximal fan-in  $w$ , designated as  $\text{bPTF}[k] \circ \{\text{AND}, \text{OR}\}_w$ . Then,*

$$\Pr_{\rho \in R_p} [F[\rho] \notin \text{DT}(t)] \leq (20pw)^t 2^k. \quad (3.4)$$

The previous theorem indeed provides a switching lemma for  $\text{bPTF}^0[k]$ , exactly with the same structure as Hastad’s switching lemma for  $\text{AC}^0$ . Now, we will also consider a multi-switching lemma developed in the same work.

**Theorem 3.12.** [Kum23] *Let  $\mathcal{F} = \{F_1, \dots, F_m\}$  be a list of  $\text{bPTF}[k] \circ \text{AND}_w$  circuits on  $\{0, 1\}^n$ . Then,*

$$\Pr_{\rho \in R_p} [\mathcal{F}[\rho] \not\supseteq \text{DT}(q)^m \mid \text{DT}(t)] \leq 4(64(2^k m)^{1/q} pw)^t. \quad (3.5)$$

Finally, we can leverage a useful lemma that facilitates the mapping between  $\text{AND}_w$  and  $\text{OR}_w$  clauses and decision trees.

**Lemma 3.13.** [Kum23] *Any depth-2 circuit of the form  $\text{bPTF}[k] \circ \text{DT}(w)^m$  comprised of a top (i.e., last) gate, which is a  $\text{bPTF}[k]$  gate with fan-in  $m$ , with  $\text{DT}(w)$  as inputs can be expressed as a circuit in  $\text{bPTF}[k] \circ \text{AND}, \text{OR}_w$  with a size of  $m2^w$ .*

<sup>8</sup>We will refer to a circuit that computes a certain function using upper case letters, and reserve lower case letters for the corresponding abstract function.

### 3.3 Non-local games and Correlation

Non-local games are a fundamental element of study for quantum-classical separation in foundational terms. These games involve specific rules played by participants. It is possible to demonstrate that, for certain games where entanglement is a key resource, classical players cannot achieve the same winning probabilities as quantum players. Particularly of interest are XOR and generalized XOR games in the multi-party setting, as we relate these to computational relation problems. They are defined as follows.

**Definition 3.14** (XOR and generalized XOR games). *These classes of multiparty non-local games involve  $n$  parties, denoted  $p_1, \dots, p_n$ . In these games, each party  $p_i$  receives information  $x_i$ , where  $(x_1, \dots, x_n)$  is drawn from a distribution  $\mathcal{D}$ . The parties, unable to communicate post-distribution, must each provide an individual response  $y_i$ , contributing to a collective output  $y_1 \otimes y_2 \otimes \dots \otimes y_n$ . The probability of winning the game is determined by the expression,*

$$\Pr_{(x_1, \dots, x_n) \sim \mathcal{D}} \left[ \sum_{i=1}^n y_i \bmod p = f(x_1, \dots, x_n) \right], \quad (3.6)$$

where  $f : \mathbb{F}_p^n \mapsto \mathbb{F}_p$  is a predetermined function. This function maps the input tuple from the finite field  $\mathbb{F}_p^n$  to a single element in  $\mathbb{F}_p$ , thereby dictating the winning condition based on the collective responses  $y_i$ .

These are typically associated with Bell inequalities [CGP<sup>+</sup>02; BCP<sup>+</sup>14], which define the statistics that can distinguish between local hidden variable theories (classical models) and quantum observations with quantum states. Specifically, we will utilize established definitions to determine the winning probabilities for games in this context. It is also worth mentioning that our primary interest lies in achieving the maximal classical winning probability, while aiming for quantum winning probabilities that surpass the classical limit, achievable through constant-depth quantum circuits.

Additionally, we need to establish a measure of efficiency for higher-dimensional non-local games and computational problems. Specifically, we consider that the correctness of the outcome of ISMR problems and the generalized XOR non-local games depends solely on the modular residue of their Hamming weight. We can define proximity between relations based solely on that value. Furthermore, considering  $\omega^{|C(x)|}$  again, with  $\omega$  being the roots of unity, we encounter group arithmetic over the finite fields  $\mathbb{F}_p$  with respect to the addition operation. Thus, we can assess the distance between two relations using the natural measure of the inner product for domains that form an Abelian group, defined as  $\langle f, g \rangle = \sum_{|G|} f\bar{g}$  [Don14]. More precisely, we can use a general correlation measure for any circuit attempting to approximate an ISMR problem or a generalized XOR non-local game as follows,

**Definition 3.15** ( $\text{Corr}_{\mathcal{D}}(f, g)$ ). *We define the correlation between functions  $f, g : \mathbb{F}_p^n \mapsto \mathbb{F}_p$  on a distribution  $\mathcal{D}$  over  $\mathbb{F}_p^n$  as,*

$$\text{Corr}_{\mathcal{D}}(f, g) = \mathbb{E}_{x \sim \mathcal{D}} \left[ \text{Re} \left( e^{-i \frac{2\pi |f(x)| - |g(x)|}{p}} \right) \right]. \quad (3.7)$$

More precisely, it will discount for deviation will be defined by its size and the respective real part of the roots of unity involved in each dimension (see Figure 2).

### 3.4 Noise and quantum error correction in higher dimensions

We will analyze noisy quantum circuits over qubits and qudits in Section 5. To do this, we first introduce the noise model that we adopt and identify key properties for later use. We will then introduce the topological code that we use to attain noise-resilient quantum advantage.

#### Qupit operations and local stochastic noise

We first establish preliminaries on the standard operations and gates used to characterize the impact of noise. In particular, for qupits, we need to introduce the generalized Pauli operators [Got98], which are higher-dimensional versions of the single-qubit Pauli operators. Specifically, the Pauli X and Z operators generalize to the shift and clock operators, respectively

$$X = \sum_{j=0}^{p-1} |j\rangle \langle j \oplus 1|, \quad Z = \sum_{j=0}^{p-1} \omega^j |j\rangle \langle j|. \quad (3.8)$$

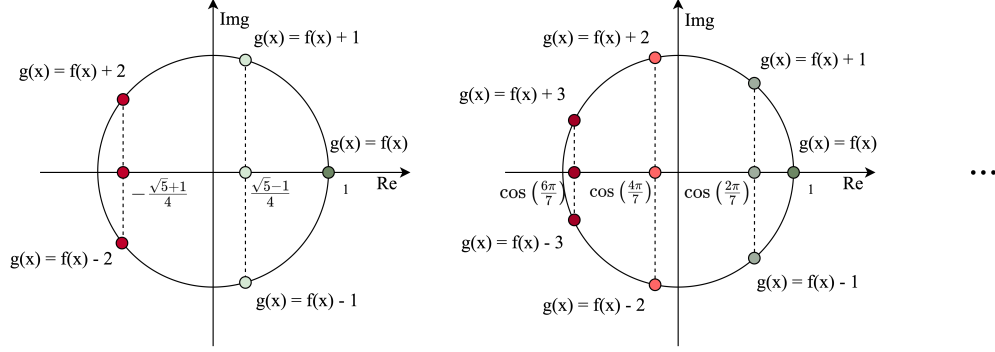


Figure 2: Illustration of the respective contributions to the correlations function based on the deviation between two arbitrary function  $f$  and  $g$  over  $\mathbb{F}_3$  and  $\mathbb{F}_5$ .

Both are non-Hermitian unitary operators, where  $j \in \mathbb{F}_p$ ,  $\omega = e^{\frac{2\pi i}{p}}$  and we will use  $\oplus$  to denote addition mod  $p$  respective to each qubit dimension under consideration. These operators have order  $p$ , and commutation relation

$$Z^p = X^p = \mathbb{1}, \quad ZX = \omega XZ. \quad (3.9)$$

For a system of  $n$ -qubits, we use the notation  $\omega(a), X(a), Z(a)$  with  $Z(a) = Z^{a_1} \otimes \dots \otimes Z^{a_n}$  for  $a \in \mathbb{F}_p^n$ .

**Definition 3.16** (Generalized Pauli group). *The generalized Pauli group  $\mathcal{P}_p$  is generated by the single qubit operators  $X$  and  $Z$ . The elements of  $\mathcal{P}_p$  are given by  $\omega^k Z^a X^b$  for  $a, b, k \in \mathbb{F}_p$ . The generalized Pauli group  $\mathcal{P}_p^{\otimes n}$  over  $n$  qubits is the  $n$ -fold tensor product of the single-qubit Pauli groups, and each operator can be expressed as  $\omega(k)Z(a)X(b)$  for  $a, b \in \mathbb{F}_p^n$  and  $k \in \mathbb{F}_p$ .*

In the rest of the paper we drop the subscript  $p$  in  $\mathcal{P}_p$  when it is clear from the context. Using the generalized Pauli operators, we can define the generalized version of the Clifford group.

**Definition 3.17** (Qubit Clifford group). *The Clifford group  $C^n$  over  $n$  qubits is the normalizer of the  $n$ -qubit Pauli group, defined as follows.*

$$C^n = \{C \in U(p^n) \mid \forall P \in \mathcal{P}^n, CPC^\dagger \in \mathcal{P}^n\}. \quad (3.10)$$

Interesting elements of the generalized Clifford group include the qubit versions of the Hadamard and CNOT gates, known as the Fourier and Sum gates respectively, as well as the involution gate INV. These can be defined as follows.

$$F = \frac{1}{\sqrt{p}} \sum_{x=0}^{p-1} \sum_{y=0}^{p-1} \omega^{xy} |x\rangle\langle y|, \quad \text{SUM} = \sum_{x=0}^{p-1} |x\rangle\langle x| \otimes |x \oplus y\rangle\langle y|, \quad \text{and} \quad \text{INV} |j\rangle = |-j\rangle. \quad (3.11)$$

We are now ready to introduce the error model we consider, along with some of its properties. In the following, for an  $n$ -qubit Pauli operator  $\mathcal{E}$  we write  $\text{Supp}(\mathcal{E})$  to denote the subset  $\mathcal{I} \subset [n]$  of indices of the qubits on which  $\mathcal{E}$  acts non-trivially. That is,  $\text{Supp}(\mathcal{E})$  is the subset of qubits that are corrupted by  $\mathcal{E}$ . The local stochastic noise model is defined as follows [Got14; FGL18].

**Definition 3.18** (Qubit local stochastic noise). *Let  $0 \leq \tau \leq 1$ . A random  $n$ -qubit Pauli error  $\mathcal{E}$  with support  $\text{Supp}(\mathcal{E}) \subseteq [n]$  is said to be  $\tau$ -local stochastic if for all  $F \subseteq [n]$ , we have*

$$\Pr[F \subseteq \text{Supp}(\mathcal{E})] \leq \tau^{|F|}. \quad (3.12)$$

We write  $\mathcal{E} \sim \mathcal{N}(\tau)$  to denote random Pauli errors that follow a  $\tau$ -local stochastic noise model.

This is a very versatile noise model, being able to account for independent, correlated, and even adversarial noise, given that the probability of an error occurring decays as its support size increases. This means that local errors are more likely to occur than non-local ones.

**Lemma 3.19.** *The qupit local stochastic noise defined in Definition 3.18, over qupit dimension  $p$ , satisfies the following properties.*

1. *Let  $\mathcal{E} \sim \mathcal{N}(\tau)$ . Then for any random error  $\mathcal{E}'$  such that  $\text{Supp}(\mathcal{E}') \subseteq \text{Supp}(\mathcal{E})$  with certainty, we have that  $\mathcal{E}' \sim \mathcal{N}(\tau)$ .*
2. *Let  $\mathcal{E} \sim \mathcal{N}(\tau)$  and  $\mathcal{E}' \sim \mathcal{N}(\varrho)$  be (possibly dependent) random Paulis. Then,  $\mathcal{E} \circ \mathcal{E}' \sim \mathcal{N}(\tau')$  where  $\tau' = p \cdot \max(\sqrt{\tau}, \sqrt{\varrho})$ .*

These properties are up to some constants equal across all qudit dimensions, and the proof for the qubit case presented in [BGK<sup>+</sup>20] extends to the qupit case with only minor differences.

When a circuit is affected by the local stochastic noise model, each layer of the circuit, defining the support of the error, will be impacted by a random Pauli operator, adhering to the local stochastic property parameterized by the respective probability.

Importantly, this noise model allows for commuting the individual error operators through Clifford circuits. This enables the overall effect of noise, represented by random Pauli errors occurring after each layer of gates, to be described as amplified local stochastic noise occurring only at the end of the entire Clifford circuit.

**Lemma 3.20.** *For any  $n$ -qupit Clifford circuit  $U_d$  of depth  $d$  composed of one- and two-qupit gates, the noisy implementation of  $U_d$  described as  $C_1\mathcal{E}_1C_2\mathcal{E}_2\dots C_d\mathcal{E}_d$  with  $\mathcal{E}_i \sim \mathcal{N}(\tau)$  when applied to  $|0\rangle$  and measured produces an outcome  $z \in \{0, 1\}^n$  with the following conditional probability.*

$$\Pr(z|\mathcal{E}) = |\langle z|U_d\mathcal{E}_t|0\rangle|^2, \quad (3.13)$$

with  $\mathcal{E}_t \sim \mathcal{N}(p^2\tau^{4-d-1})$ .

The proof in [BGK<sup>+</sup>20] for qubit systems with local stochastic noise extends straightforwardly to the qupit case.

## Qupit surface code

To address noise, we must select a quantum error correcting code with an appropriate decoder to correct the errors based on the chosen noise model. We identify the surface code over qupits as a candidate for our general purpose.

Analogously to the qubit case, we have a square lattice of qupits of size  $L \times L$ , with smooth (square tiles) and rough (tiles without all the edges) boundaries. In particular, this topological code is characterized by the stabilizer subgroup  $\mathcal{S} = \langle A_v, B_p \rangle$  defined as follows,

$$A_v = X_e \otimes X_e^\dagger \otimes X_e \otimes X_e^\dagger \quad \forall e \in V \quad (3.14)$$

$$B_p = Z_e \otimes Z_e \otimes Z_e^\dagger \otimes Z_e^\dagger \quad \forall e \in P, \quad (3.15)$$

where  $V$  defines all the edges incident to a single vertex of the lattice  $v$ , and  $P$  defines the plaquette constituted by all the edges that close a square/tile of the lattice. The entire  $L \times L$  lattice, containing  $2L^2 - 2L - 1$  qudits, defines a single logical qupit. Given this logical qupit, the logical operators  $\bar{X}$  and  $\bar{Z}$  are defined as follows

$$\prod_{e \in \text{Column}} X_e, \quad \prod_{e \in \text{Line}} Z_e, \quad (3.16)$$

which also fixes the code distance to be  $L$ . Note that throughout the entire text, we will use the notation  $|\bar{a}\rangle$  for the logical version of a state  $|a\rangle$  and  $\bar{A}$  for an operator  $A$ .

Complementary to the code, we use a hard decision renormalization decoder [BH13], which can be implemented for any stabilizer code with topological order, as is the case for the surface code that we will rely upon.

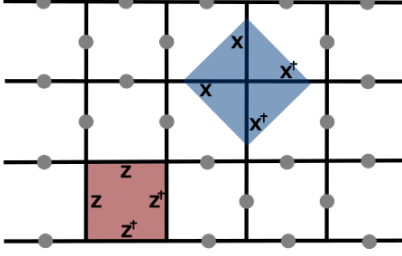


Figure 3: Illustration of  $A_v$  and  $B_p$  type surface code stabilizers on a  $3 \times 3$  lattice.

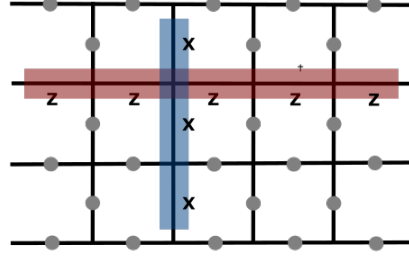


Figure 4: Representation of the logical operators  $\bar{X}$  and  $\bar{Z}$  for the surface code.

## 4 Quantum advantage in the noiseless case

We now proceed to formally state and prove our separations of noiseless shallow quantum circuits against bounded polynomial threshold circuits. We divide the analysis into two sections, the first focusing on qubit  $\text{QNC}^0$  circuits, and the second on higher dimensional qupit  $\text{QNC}^0$  circuits. In each case we deal with the respective family of ISMR problems that demonstrates the separation from  $\text{bPTF}^0[k]$ . We also highlight qualitative and quantitative differences in the results achieved in the two cases, as well as the nature of the corresponding challenges and proof methodologies.

Let us first recall the ISMR family of problems.

**Definition 4.1.** *For any positive integer  $p$ , the Inverted Strict Modular Relation Problem (ISMRP)  $\mathcal{R}_p^m : \mathbb{F}_2^n \mapsto \mathbb{F}_2^m$  with input and output lengths  $n$  and  $m$  respectively is defined as follows. For any  $x \in \mathbb{F}_2^n$  such that  $|x| \bmod p = 0$*

$$\mathcal{R}_p^m(x) := \{y \mid y \in \mathbb{F}_2^m : |y| \bmod p = -(|x|/p) \bmod p\}, \quad (4.1)$$

where  $|x| = \sum_{i=1}^n x_i$  is the Hamming weight of the  $n$ -bit string  $x$ .

Here, we use the term “strict” to denote that the problems require the outcome to be congruent modulo  $p$  to the additive *inverse* of  $|x|/p$ , rather than taking the interpretation of the Hamming weight of the input being congruent to zero modulo  $p^2$ .

As observed in [Section 2](#), for each  $p$  the ISMRP is a generalization of the Parity Halving Problem introduced and studied by [\[WKS<sup>+</sup>19\]](#). While several generalizations of PHP may be possible, ours was influenced by a specific family of non-local games for which we have derived an exponential separation between the success probabilities of the best classical and quantum winning strategies, as we shall see in [Section 4.2.3](#). Note that we consider this binary setting as it provides a fair basis for a separation between the binary  $\text{bPTF}^0[k]$  circuits and  $\text{QNC}^0$  circuits over qupits, not changing the arithmetic of the problem to dits, which could favor the quantum circuits and weaken the classical circuits class.

In the case of the qubit, we will prove that  $\text{QNC}^0$  circuits can solve the  $\mathcal{R}_2^m$  problem exactly. Additionally, we establish exact-case and average-case hardness bounds for  $\text{bPTF}^0[k]$ . We use the term “exact case” to refer to the scenario where both quantum and classical circuits are required to solve the proposed problem with probability one (i.e. with certainty) for all inputs. Although this setting was implicitly considered in previous lower bounds, such as those determined in [\[WKS<sup>+</sup>19\]](#), it was not explicitly explored. We address this gap and demonstrate that it is possible to establish stronger lower bounds on the size of the classical circuits for this scenario. Following this, we will present the average-case hardness for all other ISMR problems,  $\mathcal{R}_p^m$  where  $p > 2$  is prime, along with the respective quantum (i.e. qupit  $\text{QNC}^0$ ) upper bounds.

### 4.1 Separations for qubit cases

The qubit  $\text{QNC}^0$  case is special because it enables us to solve one of the problems in  $\mathcal{R}_2^m$  exactly, meaning it produces a correct outcome with probability 1 for all input strings. We leveraged this property to obtain larger bounds for the size of the first  $\text{AC}^0$  and then  $\text{bPTF}^0[k]$  circuits required to solve the same problems, thereby achieving greater separations with  $\text{QNC}^0$  beyond the previous results for  $\text{AC}^0$  and simultaneously

completely new bounds with  $\text{bPTF}^0[k]$ . The following theorem formally establishes this separation for  $\text{QNC}^0$  with  $3D$  and all-to-all connectivities.

**Theorem 4.2.** *There exists a  $\text{QNC}^0$  circuit that solves the  $\mathcal{R}_2^m$  exactly with a subquadratic number of gates, which an arbitrary  $\text{bPTF}^0[k]/\text{rpoly}$  circuit of depth  $d$  with access to a random string  $\text{rpoly}$  and parameter  $k$  that does require size  $s$  circuit lower bounded as follows,*

$\Omega(s)$	$3D$	$All\text{-}to\text{-}all$
$k = \mathcal{O}(1)$ ( $\text{AC}^0/\text{rpoly}$ )	$\exp\left(\left(\frac{n^{1/3}}{(\log n)^{1+\mathcal{O}(1)}}\right)^{\frac{1}{d-1}}\right)$	$\exp\left(\left(\frac{\sqrt{n}}{(\log n)^{3/2+\mathcal{O}(1)}}\right)^{\frac{1}{d-1}}\right)$
$k = n^{1/(5d)}$ ( $\text{bPTF}^0[k]/\text{rpoly}$ )	$\exp\left(\left(\frac{n^{2/15}}{(\log n)^{1+\mathcal{O}(1)}}\right)^{\frac{1}{d-1}}\right)$	$\exp\left(\left(\frac{n^{3/10}}{(\log n)^{3/2+\mathcal{O}(1)}}\right)^{\frac{1}{d-1}}\right)$

In particular, for this result, we will utilize the fact that we can reduce the  $\text{AC}^0$  and  $\text{bPTF}^0[k]$  circuits to a first decision forest using [Lemma A.9](#), and then to forest lines with a second application of random restrictions. We define a forest line as a set of individual decision trees, where each computes one of the final outcome bits. We will then demonstrate that for this object to produce exact solutions, the decision trees comprising the forest line require a minimum depth with [Lemma 4.6](#), which consequently imposes a minimum size on the initial  $\text{AC}^0$  and  $\text{bPTF}^0[k]$  circuits. More concretely, this is achieved by showing that the decision trees in this forest line require a minimum depth to produce terms of degree 2 with respect to the Algebraic Normal Form of the Boolean function they evaluate. Additionally, we establish a lower bound on the number of such degree 2 terms necessary to evaluate the relation problem exactly [Lemma 4.5](#). Therefore, by combining [Lemma A.9](#) and [Lemma 4.6](#) we obtain our classical lower bound enunciated in [Lemma 4.7](#).

In a subsequent subsection, we present quantum circuits that solve these problems exactly with  $3D$  and all-to-all connectivities in [Lemma 4.10](#) and [Corollary 4.11](#) respectively. By integrating the quantum upper bounds, from which we obtain all the parameters, with the classical lower bounds, we derive the previously stated separation.

Our second result concerning the qubit  $\text{QNC}^0$  circuits is an average-case hardness separation from the  $\text{bPTF}^0[k]$  circuits with a super-logarithmic size degree-bound parameter  $k$ , addressing the same  $\mathcal{R}_2^m$  problem, as stated in the following theorem.

**Theorem 4.3.** *There exists a  $\text{QNC}^0$  circuit that solves the  $\mathcal{R}_2^m$  over a uniform distribution of even strings exactly with a subquadratic number of gates, which an arbitrary  $\text{bPTF}^0[k]/\text{rpoly}$  circuit of depth  $d$  with access to a random string  $\text{rpoly}$  and parameter  $k$  solves the problem with probability at most,*

$\Omega(s)$	$3D$	$All\text{-}to\text{-}all$
$k = n^{1/(5d)}$	$\frac{1}{2} + \exp\left(-\Omega\left(\frac{n^{4/15-\mathcal{O}(1)}}{(\log s)^{2d-2}}\right)\right)$	$\frac{1}{2} + \exp\left(-\Omega\left(\frac{n^{3/5-\mathcal{O}(1)}}{(\log s)^{2d-1}}\right)\right)$

In this setting, we once again utilize [Lemma A.9](#) to reduce the initial  $\text{bPTF}^0[k]$  circuit to a decision forest and then, with a second application of random restrictions, to a forest line. However, in contrast to the previous case, we can directly apply [Theorem 4.8](#), which determines the maximal average-case hardness of the forest line. This can then be correlated with the hardness of the  $\text{bPTF}^0[k]$  circuits in solving the  $\mathcal{R}_2^m$  problem, a relationship we formalize in [Corollary 4.9](#).

Afterward, we once again refer to the same quantum upper bounds [Lemma 4.10](#) and [Corollary 4.11](#) to characterize all the parameters and optimize the free parameters to achieve the largest possible separation.

#### 4.1.1 Exact and Average-case $\text{bPTF}^0[k]$ hardness

To solve exactly and deterministically an ISMR problem  $\mathcal{R}_q^m$ , in the sense that to each input  $x$  a single valid output string  $y$  is created, one can demonstrate that for any of these solutions, the outcome bits  $y_i$  of  $y$  are individual Boolean functions of the type  $f_{y_i} : \{0, 1\}^n \mapsto \{0, 1\}$ . Furthermore, these individual functions do not have to fulfill any specific conditions, some of these could even be constant functions. However, the



parity of their outcomes must adhere to a property dictated by the relation problem. Specifically, the parity of these output bits computes another Boolean function.

Now we would like to specify this Boolean function specifically for the case of  $\mathcal{R}_2^m$ . In this case, for all the strings that are even we have,

$$\mathcal{D}_2(x) = \begin{cases} 1, & |x| \bmod 4 = 0 \\ 0, & |x| \bmod 4 = 2. \end{cases} \quad (4.2)$$

This, however, does not define a total Boolean functions, as it only defines the images over even input strings. Moreover, this implies that any mapping of the odd input strings while respecting the previous mapping for the even input strings creates a valid Boolean function for the parity of the outcome bits. In particular, we can now derive which is exactly the set of valid Boolean functions.

**Lemma 4.4.** *The parity of the outcome string  $y$  of a  $\text{bPTF}^0[k]$  circuit that does solve the  $\mathcal{R}_2^m$  for arbitrary input  $x \in \{0, 1\}^n$  is contained in the following set*

$$S_{\mathcal{D}_2} = \left\{ \underbrace{\bigoplus_{i_1=1}^{n-1} x_{i_1} \left( \bigoplus_{i_2=i_1+1}^n x_{i_2} \right)}_{\text{Even mapping}} \oplus \underbrace{\left( \bigoplus_{j=1}^n x_j \right) \wedge g}_{\text{Odd mapping}} \mid g \in \{0, 1\}^n \mapsto \{0, 1\} \right\}. \quad (4.3)$$

*Proof.* The correctness of the previous functions can be analyzed simply by considering two cases: one where the input strings are even, which obliges it to map the same decision version of  $\mathcal{D}_2$ , and another where the input strings are odd, necessitating consideration of all possible mappings.

**Even case.** In the case where the input strings are even, the expression  $\left( \bigoplus_{j=1}^n x_j \right) \wedge g$  contributes nothing to the outcome. This means that only the first expression has any impact on the outcome. Furthermore, the first expression is known as the “Second least significant bit” function, which computes the second bit of a binary representation of the Hamming weight of the initial bit strings [OBG24]. More precisely, it has the following definition:

$$\text{LSB}(x) = \begin{cases} 1, & |x| \bmod 4 \in \{0, 1\} \\ 0, & |x| \bmod 4 \in \{2, 3\}. \end{cases} \quad (4.4)$$

It immediately follows that for even input strings, all the elements of this set map the function to the same outcome as the parity of  $\mathcal{R}_2^m$ .

**Odd case.** For the odd case, we can be assured that the set contains all possible mappings of odd input strings. This is deduced by recognizing that the contribution of the second term is now equivalent to an arbitrary Boolean function  $g$ . Additionally, this allows for the mapping of any function such that it can be decomposed as  $\bigoplus_{i_1=1}^{n-1} x_{i_1} \left( \bigoplus_{i_2=i_1+1}^n x_{i_2} \right) \oplus h$ , with  $h$  being another arbitrary Boolean function. Thus, through this decomposition, we can cancel out the effect of the first term and obtain any arbitrary mapping for odd input strings.  $\square$

We now focus on a specific representation of these Boolean functions: their Algebraic Normal Form (ANF), which we previously used in Lemma 4.4. This representation is crucial for capturing some common structure shared by all elements in the set of valid Boolean functions. In particular, the subsequent lemma formalizes a key aspect of this structure - the number of degree-two terms present in the ANF.

**Lemma 4.5.** *Every Boolean function belonging to the set  $S_{\mathcal{D}_2}$  contains at least  $\Omega(n^2)$  degree-two terms in its Algebraic Normal Form (ANF).*

*Proof.* First, we will demonstrate that any function of the set  $S_{\mathcal{D}_2}$  does have a  $\Omega(n^2)$  term of degree two. We can conduct this analysis using the expression for  $S_{\mathcal{D}_2}$  in Equation (4.3).

Consider the left-hand side, where the number of such terms is given by  $\binom{n}{2}$ . Now, let’s examine how terms of degree-two can arise from the second part of the expression. Specifically, we consider terms generated by the operation  $\bigoplus_{j=1}^n x_j \wedge g$ , where  $g$  represents a function of degree-one terms, as higher degree terms do not generate any degree-two terms. Note that degree-three terms either maintain or increase the degree, and

any degree-two terms either increase the degree further or occur twice, cancelling each other out. It's crucial to note that if a degree-three term is generated in this process, it is subsequently cancelled out in the final ANF. Given this setup, we can generate the parity function from the first part of the expression. However, the degree-two terms that emerge from the  $k$  degree-one terms in  $f$  are bounded above by,

$$h(k) = \sum_{i=0}^k (n-i) - \binom{k}{2} = k(n-1) - \frac{k(k-1)}{2}. \quad (4.5)$$

This expression accounts for the number of terms that are generated in total minus the ones that repeat and are immediately canceled out. Taking the derivative with respect to  $k$ , we find  $\frac{dh}{dk} = n - 2k$ . This derivative indicates that  $h(k)$  reaches its maximum when  $k = \frac{n}{2}$ . At this point, the maximum number of degree 2 terms generated by  $f$  can be computed. By examining the limit as  $n$  approaches infinity, we find  $\lim_{n \rightarrow \infty} \frac{g(n/2)}{\binom{n}{2}} = \frac{1}{2}$ . This implies that for large  $n$ , approximately half of the potential degree 2 terms are effectively generated and not canceled out by the expression. Consequently, we conclude that any valid Algebraic Normal Form (ANF) must contain  $\Omega(n^2)$  degree 2 terms, as intended.  $\square$

Simultaneously, we obtain that the ANF of the various  $\text{bPTF}^0[k]$  circuits have to equal one element of the set  $S_{\mathcal{D}_2}$  if the circuit does compute correctly the  $\mathcal{R}_2^m$  problem. We can formalize the previous property as

$$\text{ANF}(\underbrace{\text{bPTF}^0[k](x)}_{y_1}) \oplus \text{ANF}(\underbrace{\text{bPTF}^0[k](x)}_{y_2}) \oplus \dots \oplus \text{ANF}(\underbrace{\text{bPTF}^0[k](x)}_{y_m}) \in S_{\mathcal{D}_2}. \quad (\text{P1})$$

Subsequently, we will build a set of arguments to prove a lower bound on the size of these circuits to fulfill this property. However, we first solve a simpler instant, where we consider decision trees  $\text{DT}(q)^m$  in place of the  $\text{bPTF}^0[k]$  circuits. This will not be a problem because later on we will be able to reduce these circuits to the previous objects. Moreover, each decision tree  $\text{DT}(q)$  of this forest line  $\text{FL}(m, d) := \bigoplus_{i=0}^m \text{DT}(q_i)$  with  $d = \max q_i$ , has a unique description as an ANF over the variables that are part of its nodes. Obtaining with that a second property over this computational structures as follows,

$$\text{ANF}(\text{FL}(m, q)) = \text{ANF}(\underbrace{\text{DT}(q)}_{y_1}) \oplus \text{ANF}(\underbrace{\text{DT}(q)}_{y_2}) \oplus \dots \oplus \text{ANF}(\underbrace{\text{DT}(q)}_{y_m}). \quad (\text{P2})$$

We want to prove the minimum decision tree depth concerning the largest decision tree depth in the previous object so that property  $P2$  is fulfilled.

For that, we will consider that for any valid Boolean function, the number of degrees two terms in its ANF is lower bounded by a quadratic term, as shown in [Lemma 4.5](#). Simultaneously, we will consider [Algorithm 1](#) which translates an arbitrary decision tree to its ANF. Here, again one can bind the number of terms of finite degree that a certain decision tree can have in its ANF. Combining these two ideas we obtain that there exists a minimum decision tree depth such that one can compute exactly one of the Boolean functions at hand.

**Lemma 4.6.** *For any forest line  $\text{FL}(m, q)$  that computes a Boolean function from the set  $S_{\mathcal{D}_2}$  does have a depth bounded by  $q = \Omega(\frac{n}{m^{1/2}})$ .*

*Proof.* This involves establishing an upper bound on the number of degree-2 terms generated by a decision tree, we examine the algorithm described in [Algorithm 1](#) for converting a binary decision tree into its Algebraic Normal Form (ANF). Initially, the algorithm identifies paths that culminate in a Boolean true value, each represented as a clause. These clauses are subsequently merged using the logical OR operation, thereby formulating a polynomial in  $\mathbb{F}_2$  that encapsulates the decision tree's Boolean function.

Focusing on the clauses formed with the logical AND operation during ANF creation. We note that these can be described by the path they follow in the tree that can be decomposed by the various left ( $L$ ) and right ( $R$ ) turns at each node assigned with a variable  $x_i$ .

**Left Turn ( $L$ ).** Incorporates the variable  $x_i$  directly as

$$\text{path}_{\text{new}} = \text{path}_{\text{old}} \wedge x_i \quad (4.6)$$

$$= \dots \wedge x_{i-1} \wedge x_i \text{ OR } = \dots \wedge (x_{i-1} \oplus 1) \wedge x_i \quad (4.7)$$

$$= \dots x_{i-1} x_i \text{ OR } = \dots x_{i-1} x_i \oplus x_i. \quad (4.8)$$

This case increases the degree of the new clause designated as  $path_{new}$  by 1.

**Right Turn (R).** Incorporates the complement of  $x_i$  as

$$path_{new} = path_{old} \wedge (x_i \oplus 1) \quad (4.9)$$

$$= (path_{old} \wedge x_i) \oplus path_{old}. \quad (4.10)$$

While the second case does not alter the degree of the new clause designated as  $path_{new}$ .

Given these transformations, degree-2 terms arise from paths with specific sequences of turns. A single left turn surrounded by right turns  $R \dots RLR \dots R$  can contribute to a degree-2 term. Furthermore, a path with two left turns, each potentially followed by right turns  $R \dots RLR \dots RLR \dots R$ , also contributes to degree-2 terms, as each left turn increases the degree by 1. The OR operations, which combine these paths, preserve the degrees of the terms in the resulting expression or increase it. Consequently, to enumerate the maximum number of degree-2 terms, it suffices to count the paths that can yield such terms. For a decision tree of depth  $q$ , the relevant paths are those with one or two left turns. The total count of such paths is given by the sum of paths with one left turn and those with two left turns  $\binom{q}{2} + \binom{q}{1}$ . This formulation provides a definitive upper bound on the number of degree-2 terms in the ANF representation of a Boolean function derived from a decision tree, predicated on the tree's depth.

In the end, we consider that in forest line  $FL(m, d)$ , there are  $m$  decision trees generating degree two terms and each can generate at most  $\binom{q}{2} + \binom{q}{1}$  such terms<sup>9</sup>. Finally, combining the previous bound with the minimum number of degree two terms necessary to prove in Lemma 4.5 we obtain that the minimum depth will depend on the size of the forest line and the size of the input strings as follows  $q \geq \frac{n}{m^{1/2}}$ .  $\square$

Now we will be able to prove a lower bound for the size of any  $bPTF^0[k]$  circuit that does compute the  $\mathcal{R}_2^m$  exactly. This will be followed by applying our new switching lemmas created in Section 2.4 to reduce the initial circuits to a decision tree of the type  $DT(w)^m \succcurlyeq DT(t)$ . Subsequently, we will apply a second set of random restrictions, that reduce the same object to a forest line  $FL(m, q)$  for which we will be able to prove a minimum depth, and consequently link this depth to the minimum size of the initial circuit.

**Lemma 4.7.** *For sufficiently large  $n$ , any  $bPTF^0[k]/rpoly$  circuit depth  $d \geq 4$  and  $k \leq n^{1/(5d)}$  that solves the  $\mathcal{R}_2^m$  has size no smaller then  $s \geq 2^{\left(\frac{n}{k^d \cdot q \cdot m^{1/2+1/q}}\right)^{1/(d-1)}}$ , with  $q \in \mathbb{N}_{>0}$ .*

*Proof.* This proof will be decomposed first into the application of a random restriction  $\rho$  with a probability equal to  $p = \frac{1}{m^{1/q} \cdot \mathcal{O}(\log(s)^{d-1} \cdot k^d)}$ . Notice that this is the largest probability one can use without disrespecting the various switching lemmas, which have the minimal conditional of generating probabilities below 1. We additionally choose  $t = pn/8$  and that  $s \leq \exp(n^{1/(2d-2)})$ , which will not interfere with our result given that this value will be asymptotically larger than the lower bounds of  $s$  derived with this assumption. With that, we first show that  $s \leq 2^{t/2}$ , this results from the following comparison and the previously defined values for the parameters,

$$2^{t/2} = \exp(\Omega(pn)) = \exp\left(\Omega\left(\frac{n^{(d-1)/(2d-2)-\frac{1}{5}}}{m^{o(1)}}\right)\right). \quad (4.11)$$

Also, we have that for any  $d \geq 4$  then  $s = \exp(n^{1/(2d-2)}) \leq \exp\left(\Omega\left(\frac{n^{(d-1)/(2d-2)-\frac{1}{5}}}{m^{o(1)}}\right)\right)$ . This ensures, as established by Lemma A.9, that with a probability exceeding  $1 - s^2 \cdot 2^{-t}$ , which is greater than  $1 - 2^{-t/2}$  and consequently surpasses  $\exp(-\Omega(pn))$ , the initial  $bPTF^0[k]$  circuit simplifies to a tree of the type  $DT(q-1)^m \succcurlyeq DT(2t-2)$ .

The second element is that at least  $pn/2$  variables remain active with very high probability. This conclusion is reached directly through the application of the Chernoff bound, given that the probability of a variable staying active is  $\Omega(pn)$ . In conjunction with the aforementioned probability, this suggests that

$$\Pr \left[ F|_{\rho \in DT(q-1)^m \succcurlyeq DT(2t-2)}, (x \circ \rho)_{S \subseteq [n]} = * \text{ for } |S| \geq pn/2 \right] = 1 - \exp(-\Omega(pn)). \quad (4.12)$$

<sup>9</sup>Notice, that we assume the existence of an efficient method to distribute the  $n$  variables across  $m$  decision trees in a way that generates all the corresponding degree-two terms. Specifically, this task aligns with the Steiner system problem, where we seek solutions for the  $S(2, m/n, n)$  system. However, the existence of such a solution is not guaranteed, and the determination of the minimal set size remains an unresolved problem. Consequently, we will limit our consideration to the trivial upper bound.

---

**Algorithm 1** Decision Tree to ANF Converter

---

```

1: procedure ANF(DT).
2:    $S = \emptyset$ ,  $\text{ANF}_{\text{DT}} = \text{False}$ .
3:    $S' = \text{RecCl}(\text{DT}, \text{root}, \text{True}, S)$ 
4:   for  $i = 0$  until  $|S'|$  do
5:      $S[i] \vee \text{ANF}_{\text{DT}}$ .
6:   end for
7:   return  $\text{Reduce}(\text{ANF}_{\text{DT}})$ .
8: end procedure

9: procedure RECCL(DT, node, path, set).
10:  if  $\text{DT}[\text{node}] = \text{True}$  then
11:    return  $\text{set} = \text{set} \uplus \{\text{path}\}$ .
12:  else
13:    if  $\text{DT}[\text{node}] = \text{False}$  then
14:      return  $\text{set}$ .
15:    else
16:      return  $\text{RecCl}(\text{DT}, \text{Left}(\text{DT}, \text{node}), \text{Var}(\text{node}) \wedge \text{path}, \text{set})$ 
17:         $\uplus \text{RecCl}(\text{DT}, \text{Right}(\text{DT}, \text{node}), (1 \oplus \text{Var}(\text{node})) \wedge \text{path}, \text{set})$ 
18:    end if
19:  end if
20: end procedure

21: procedure  $\wedge(\bigoplus_{i=0}^{k_i} x_i, \bigoplus_{j=0}^{k_j} y_j)$ 
22:  return  $\bigoplus_{i \in [k_i], j \in [k_j]} x_i y_j$ 
23: end procedure

24: procedure  $\vee(x, y)$ 
25:  return  $x \oplus y \oplus xy$ 
26: end procedure

```

---

A second random restriction  $\tau$  will be applied to the  $2t$  variables that are in the global decision tree of  $\text{DT}(q-1)^m \gg \text{DT}(2t-2)$  after applying the first random restriction  $\rho$ . This random restriction then reduces with high probability each one of the initial  $\text{bPTF}^0[k]$  circuits that compute the resulting outcome bits to a forest line  $\text{FL}(m, q-1)$ . Therefore, for all the variables that are kept alive, the  $m$  output bits are computed with local decision tree  $\text{DT}(q-1)$ ,

$$\Pr [F \upharpoonright_{\tau \circ \rho} \in \text{FL}(m, q-1), (x \circ (\tau \circ \rho))_{S' \subseteq [n]} = \text{ for } |S| \geq pn/4] = 1 - \exp(-\Omega(pn)). \quad (4.13)$$

Now as we have been using  $p$ -random restrictions we obtained that sampling even strings consistent with the restrictions does provide us with a uniform distribution over the even input strings. Exactly, the same argument does work over the restriction  $\tau$  given that the variables of the global decision tree are selected randomly in  $\{0, 1\}^{2t}$ . This property of  $p$ -random restrictions will now be applied to the [Lemma 4.4](#) defining the necessary outcome that these resulting forest line  $\text{FL}(m, q-1)$  has to produce. In particular, we can simply consider the effect of the random restrictions on the variables as,

$$S_{\mathcal{D}_2} \upharpoonright_{\tau \circ \rho} = \left\{ \bigoplus_{i_1, i_2 \in [n] \setminus [\tau \circ \rho]} x_{i_1} x_{i_2} \right\} \oplus \left( \bigoplus_{j \in [n] \setminus [\tau \circ \rho]} x_j \right) \wedge g \upharpoonright_{\tau \circ \rho} \mid g \in \{0, 1\}^n \mapsto \{0, 1\} \right\} \quad (4.14)$$

with  $[\tau \circ \rho]$  representing the set of indexes of the variables that are assigned values by the respective random restriction. We obtain that the reduced expression does keep exactly the same structure. This demonstrates that over the  $pn/4$  variables alive [Lemma 4.5](#) applies equally. Thus, we can apply [Lemma 4.6](#) considering the variables alive and the resulting forest line. Consequently, such that this object computes correctly our

relation problem we have that,

$$\begin{aligned} q &\geq \frac{(p \cdot n)}{m^{1/2}} = \frac{n}{m^{1/2+1/q} \log(s)^{d-1} k^d} \\ \log(s)^{d-1} &\geq \frac{n}{m^{1/2+1/q} k^d q} \\ s &\geq 2^{\left(\frac{n}{m^{1/2+1/q} k^d \cdot q}\right)^{1/(d-1)}}. \end{aligned}$$

The proof remains applicable in cases where the  $\text{bPTF}^0[k]$  circuit receives a random string as advice. This is grounded in our demonstration that no deterministic circuit can accurately compute the function. Therefore, any probabilistic strategy relying on random advice is destined to fail, as it merely selects from the available deterministic solutions. As a result,  $\text{bPTF}^0[k]/\text{rpoly}$  circuits are equally susceptible to failure under these conditions.  $\square$

After obtaining a tight lower bound for the size of the  $\text{bPTF}^0[k]$  circuits that compute exactly the modular relation problem that one can solve with  $\text{QNC}^0$  circuits on qubits. We intend to also create the average-case hardness scenario which will be of interest by itself as it does also serve to build a noise-resistance version of this quantum-classical separation. In particular, we will make use of the following theorem which will be applied to the forest line to obtain the correlation bound in contrast to our previous size bound for the exact case.

**Theorem 4.8.** *[WKS<sup>+</sup>19] Let  $C$  be an  $\text{NC}^0/\text{rpoly}$  circuit with  $n$  inputs,  $m$  outputs, and locality  $l$ . Then  $C$  solves  $\mathcal{R}_2^m$  on a random even-parity input with probability at most  $\frac{1}{2} + 2^{-\Omega(\min(n, \frac{n^2}{l^2 m}))}$*

The previous theorem does provide us with the tool to relate the resulting forest line, which we obtain from the set of random restrictions reducing the  $\text{bPTF}^0[k]$  circuits, with the probability with which it computes correctly the  $\mathcal{R}_2^m$  problem.

**Corollary 4.9.** *For sufficiently large  $n$  and  $q \in \mathbb{N}_{>0}$ , any  $\text{bPTF}^0[k]/\text{rpoly}$  circuit of depth  $d \geq 4$ , size  $s \leq \exp(n^{1/(2d-2)})$  and parameter  $k \leq n^{1/(5d)}$  has small correlation with  $\mathcal{R}_2^m$ , bounded by,*

$$\frac{1}{2} + \exp\left(-\Omega\left(\frac{n^2}{2^{2q} m^{1+2/q} (\log s)^{2d-1} k^{2d}}\right)\right). \quad (4.15)$$

*Proof.* The initial part of the proof follows equally to Lemma 4.7 with a first random restriction with  $\rho$  with a probability equal to  $p = \frac{1}{m^{1/q} \cdot \mathcal{O}(\log(s)^{d-1} \cdot k^d)}$  while choosing  $t = pn/8$ , and second random restriction  $\tau$  will be applied to the  $2t$  variables of the global decision tree of  $\text{DT}(q-1)^m$  resulting from the random restriction with probability  $1 - \exp(-\Omega(pn))$ .

Thus, using  $p$ -random restrictions, we find that sampling even strings that are consistent with the restrictions provide a uniform distribution over even input strings. Similarly, this argument applies to the restriction  $\tau$ , considering that the variables for the global decision tree are randomly selected from  $\{0, 1\}^{2t}$ . This characteristic of  $p$ -random restrictions enables the direct use of Theorem 4.8. Additionally, considering that there is a high probability that more than  $pn/4$  variables remain alive, and the circuit is required to solve the  $\mathcal{R}_2^m$  problem with local decision trees of depth  $q-1$ , it follows that these trees depend on at most  $2^{q-1}$  of the active variables. Consequently,

$$\begin{aligned} \Pr[\text{bPTF}_d^0(k) \text{ solves } \mathcal{R}_2^m(x), |x| \bmod 2 = 0] &\leq \frac{1}{2} + 2^{-\Omega\left(\frac{(pn)^2}{2^{2q} m}\right)} \\ &\leq \frac{1}{2} + 2^{-\Omega\left(\frac{n^2}{2^{2q} m^{1+2/q} \mathcal{O}(\log(s)^{2d-2}) k^{2d}}\right)}. \end{aligned}$$

The proof also holds for scenarios where the  $\text{bPTF}^0[k]$  circuit is provided with a random string as advice. This is because any  $\text{bPTF}^0[k]$  circuit is reduced to the same entity after the application of a random restriction. Furthermore, as established in Theorem 4.8, we know that any probabilistic strategy informed by random advice will fail. Consequently,  $\text{bPTF}^0[k]/\text{rpoly}$  circuits are also subject to failure under these conditions.  $\square$

Both these classical lower bounds left the parameters  $q$ ,  $m$ , and  $k$  undefined as we intend to study the optimal values after the consideration of the quantum circuit solving the problem. This is motivated not only by the optimal asymptotic bound but yes by the smallest values of the input for which the quantum circuits demonstrate an advantage over the classical circuit classes.

#### 4.1.2 Qubit upper bound

We will consider the optimal  $\text{QNC}^0$  circuit for the quantum upper bound that exactly solves the  $\mathcal{R}_2^m$  that maximizes the quantum-classical separation. For that, we rewrite the circuit in the measurement-based quantum computation description with 3D connectivity, while also considering all-to-all connectivity which is effectively a type of connectivity realizable by certain quantum hardware platforms [BEG<sup>+</sup>23].

**Lemma 4.10.** *There exists a  $\text{QNC}^0$  circuit with, 3D connectivity, of depth 4 and subquadratic size that does solve the  $\mathcal{R}_2^m$  exactly with  $m = \mathcal{O}(n^{4/3})$ .*

*Proof.* The proof will follow based on the demonstration that the subsequent circuit does compute the  $\mathcal{R}_2^m$ . More precisely, by describing and proving the correctness of the following 4 stages marked on it.

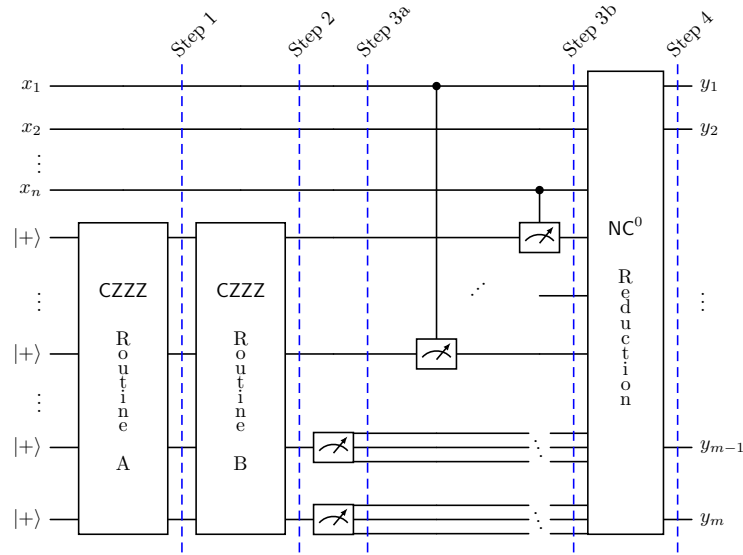


Figure 5: Illustration of the MBQC-based constant-depth quantum circuit solving an instance of the inverted strict modular relation problem. Stages 1 and 2 involve creating the graph states. In Stage 3a, the edge qubits of the graph are measured, producing the poor-man’s cat state and fanning out the measurement outcomes of the edge measurements. In Stage 3b, phase operations are applied based on the input, and the entire state is measured. Stage 4 involves the classical post-processing.

**Step 1 & 2.** The circuit begins in the Hadamard basis, and both CZZZ Routine A and CZZZ Routine B aim to generate 3D graph states without cycles. For simplicity we will first show that we can create a more densely connected 3D graph state with a simple cubic unit cell in the lattice. To achieve this structure, one needs to apply a CZ gate between each vertex (acting as the control) and its neighboring edge qubit (acting as the target). Employing single CZ gates or finite multi-control  $(C)^{\otimes t}Z$  gates would necessitate a depth at least equal to the coloring number of this 3D graph, resulting in a minimum depth of  $d = 6$ . However, from the perspective of the edges, each serves as the target for only two vertices. Hence, we suggest utilizing CZZZ gates, drawing inspiration from CZZ gates, which have been demonstrated to be native operations in certain platforms [ZGS16]. Specifically, we can leverage these gates to simultaneously target all vertices and edges. The primary challenge lies in ensuring a two-step selection of CZZZ gates, such that each vertex directs the target ZZZ gates to all adjacent edges. This can be effectively achieved using the following grid pattern in Figure 6 and afterward this using the following pattern in the second round the pattern in Figure 7.



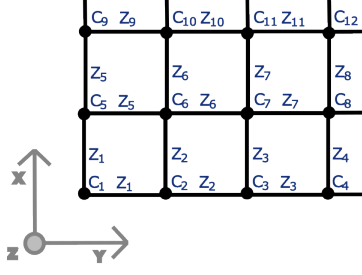


Figure 6: First horizontal entangling routine

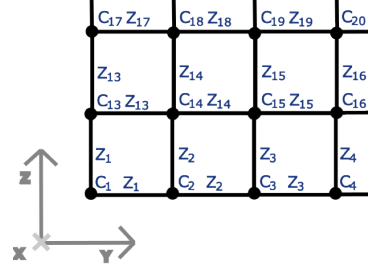


Figure 7: Second vertical entangling routine

These two sequential entangling layers effectively result in a depth-2 process that generates a larger resource state than desired. Now, one only has to remove some of the utilized gates to eliminate paths in the previously described resource state and, with that, obtaining the desired resource state, utilizing practically feasible and finite fan-in quantum gates.

**Step 3a.** This step resorts to simply measuring the Hadamard basis of all the edge qubits. This is known to create on the vertex qubits an LU equivalent to the GHZ [HEB04]. These local unitaries being all X gates do generate the state previously named poor-mans cat state, with the following description

$$|\Psi_{3a}\rangle = \frac{|v, e_1, \dots, e_{3n}\rangle + |\bar{v}, e_1, \dots, e_{3n}\rangle}{\sqrt{2}}, \text{ with } v \in \mathbb{F}_2^n. \quad (4.16)$$

while the measurement outcomes from the edges  $e_i$  do define the relations between the bits of the string  $v$  as follows,

$$v_i = v_j \oplus_{l \in \text{path}(v_i, v_j)} e_l. \quad (4.17)$$

Thus, by considering  $v_1 = 0$  one can compute the entire string  $v$  by the previous relations, which would derive that to obtain effectively a GHZ state one requires to apply a X to all the vertexes with value 1.

**Step 3b.** Although the current step does occur simultaneously with the previously described, we can analyze it as independent, given the nature of the measurement operations. Also, we will decompose the represented controlled measurement as an input-dependent controlled  $S^{x_i}$  gate based on the entire input strings  $x$ , and a set of measurements in the Hadamard computational basis.

With that, we recover that before the measurements we have the state,

$$|\Psi_{3b}\rangle = \frac{i^{\langle v, x \rangle} |v, e_1, \dots, e_{3n}\rangle + i^{\langle \bar{v}, x \rangle} |\bar{v}, e_1, \dots, e_{3n}\rangle}{\sqrt{2}} \quad (4.18)$$

$$= \frac{|v, e_1, \dots, e_{3n}\rangle + i^{\langle v, x \rangle + |x|/2} |\bar{v}, e_1, \dots, e_{3n}\rangle}{\sqrt{2}}. \quad (4.19)$$

Afterward, depending on the value of  $\langle v, x \rangle + |x|/2$  having parity either 0 or 1 does translate into a measurement of a superposition of even or odd strings respectively. Therefore, the parity of the string  $v$  directly relates to the parity of  $\langle v, x \rangle + |x|/2$ .

**Remark.** Before proceeding to the final step, it's important to note that although Steps 3a and 3b were initially considered to be sequential, they take place simultaneously. The realization that analyzing these steps as sequential yet observing that their parallel execution leads to the same outcome stems from the principle that the sequence of single-qubit measurements does not alter the outcome probabilities for any quantum state.

**Step 4.** This last  $\text{NC}^0$  reduction does the post-processing that guarantees that the outcome strings are the

result of the  $\mathcal{R}_2^m$  problem. For that we will consider that one can describe  $\langle v, x \rangle$  as follows,

$$\langle v, x \rangle = \bigoplus_{i=1}^n \text{AND}(x_i, v_i) = \bigoplus_{i=1}^n \text{AND}\left(x_i, v_c \oplus \bigoplus_{l \in \text{path}(v_i, v_c)} e_l\right) \quad (4.20)$$

$$= \bigoplus_{i=1}^n \bigoplus_{l \in \text{path}(v_i, v_c)} \text{AND}(x_i, e_l), \quad (4.21)$$

with  $v_c$  being a central vertex that we use as reference.

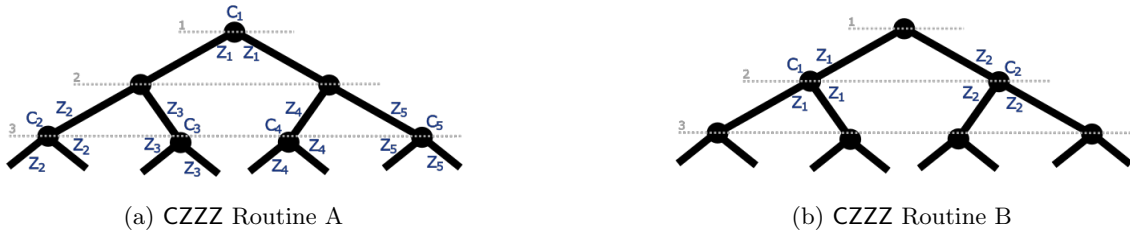
Now all the AND terms of this expression are computed in the routine, producing a single processor of depth 1. The final string provided does contain the result of all these computations and the outcome of the string  $v$  from the procedure described in stage 3b. This guarantees, as the parity of this string is equal to  $\langle x, v \rangle$ , that the outcome string has a parity equal to  $|x|/2$ . This is exactly the correct outcome for  $\mathcal{R}_2^n$ , as for even input strings  $|x|/2 = \text{LSB}(x)$ .

Finally, we have only to consider the size of the outcome string. This resorts to account for the size of the paths considered in Equation (4.21). These do depend on the distance of any vertex in the lattice to a central vertex in the 3D lattice. One can see that even for a cubic disposition this distance is upper bounded by  $n^{1/3}$ , and given that the number of paths is at most  $n$  we obtain that the number of these terms is upper bounded by  $\mathcal{O}(n^{4/3})$ , as is the final outcome string.  $\square$

Now, we do additionally consider the use of  $\text{QNC}^0$  circuit with arbitrary all-to-all connectivity which will guarantee tighter bounds.

**Corollary 4.11.** *There exists a  $\text{QNC}^0$  circuit with, all-to-all connectivity, of depth 4 and polynomial size that does solve the  $\mathcal{R}_2^m$  exactly with  $m = \mathcal{O}(n \log n)$ .*

*Proof.* The circuit for this new connectivity does not change in any manner from the circuit of figure Figure 5, except for the two CZZZ routines. The graph state intended to be created will follow that of a binary decision tree. Again, taking advantage of CZZZ gates and considering that each edge of the decision tree relates to only two vertices, we can achieve a depth of 2 in the circuit creating the resource state. In particular, this entanglement structure requires applying the CZZZ gate to all the vertices at even levels of the tree and their respective edges, and then in the second pass, performing the same procedure on the odd levels, as will be illustrated subsequently. Afterward, every other part of the circuit remains the same. Consequently, the



length of the final outcome string is solely determined by the distance from any vertex to the root node vertex of the tree, as we designate this as the central vertex. From this, we deduce that the maximum distance is at most  $\log n$ , which means the length of the outcome string is upper bounded by  $\mathcal{O}(n \log n)$ .  $\square$

This establishes two  $\text{QNC}^0$  circuits that solve the specified relational problem. We will now examine the lower bounds for  $\text{bPTF}^0[k]$  derived in the preceding section alongside this quantum upper bound and present new separations between these circuit classes. To do this, we will consider the minimum value of  $k$ , which is 0, and demonstrate a new exact-case separation between  $\text{QNC}^0$  and  $\text{AC}^0$ , with the tightest bound yet established.

Also, in this context, we consider a different scenario where the last reduction is performed by an  $\text{AC}^0$  or a  $\text{bPTF}^0[k]$  circuit, and we prove a quantum advantage for the problem being solved at step 3b of Figure 5 with a contrapositive argument against these circuit classes using a ISMR problem. This allows us to obtain even tighter quantum-classical separations. Furthermore, we find that such a separation is also feasible with

the highest value of  $k$  allowed by our classical lower bounds, indicating the existence of a problem within  $\text{QNC}^0$  that requires superpolynomial-sized  $\text{bPTF}^0[k]$  circuits, where  $k = n^{1/(5d)}$ . It is important to note that the earlier class specifies a circuit class that is strictly larger than  $\text{AC}^0$ .

**Proof of Theorem 4.2.** The determined expressions do follow from the fact that we have defined the values of  $m$  for which there exists a  $\text{QNC}^0$  solving the  $\mathcal{R}_2^m$  problem exactly in Lemma 4.10 and Corollary 4.11. This allows, us to use the exact lower bound for the size  $s$  of  $\text{bPTF}^0[k]/\text{rpoly}$  circuits of depth  $d$  derived in Lemma 4.7 with these values of  $m$  and the values selected by us for  $k$ . For instance, by considering the outcomes of the 3D  $\text{QNC}^0$  circuit with  $m = n^{4/3}$ , we obtain that the size of an  $\text{AC}^0$  circuit is larger or equal to

$$s \geq 2 \left( \frac{n^2 \left( n^{4/3} \right)^{-(1+2/q)}}{q^2} \right)^{\frac{1}{d-1}}. \quad (4.22)$$

The expression still has a non-circuit-dependent parameter  $q$  that relates only to the random restrictions used to obtain this bound. As we intend to maximize the quantum-classical separation, we would like to obtain the largest value possible for the previous expression. Therefore, we search for the value of  $q$  that archives exactly that. For that, we derive the expression in the function of  $q$  first,

$$\frac{ds}{dq} = - \frac{2^{1 + \left( \frac{n \left( n^{4/3} \right)^{-\frac{2+q}{2q}}}{q} \right)^{\frac{1}{d-1}}} \left( \frac{n \left( n^{4/3} \right)^{-\frac{2+q}{2q}}}{q} \right)^{\frac{1}{d-1}} \left( q - \log \left( n^{4/3} \right) \right)}{(d-1)q^2}. \quad (4.23)$$

Subsequently, it requires only determining for which values of the variable of  $q$ , for which the expression is equal to 0, to determine the maximums and minimums of the size depending on  $q$ . Moreover, this results in the solution  $q = \log \left( n^{4/3} \right)$  that we do requires only so substitute in our initial expression, as we know that for small integer values of  $q$  and large values close to  $n$  the expression is smaller, proving that this value a maximum as desired. Finally, we obtain that the size of an  $\text{AC}^0$  solving the  $\mathcal{R}_2^m$  problem exactly requires a size no smaller then

$$s \geq \exp \left( \left( \frac{n^{1/3}}{(\log n)^{1+\mathcal{O}(1)}} \right)^{\frac{1}{d-1}} \right). \quad (4.24)$$

All the other expressions follow equally with the respective parameters of  $m$  and  $k$ .  $\square$

The final set of separations refers to the average case hardness of solving the same problem. For these, we do focus uniquely on the case where we have the largest value of  $k$ , so we drop the case where  $k$  is zero as this was already studied previously. This again will refer to the case where we have either 3D or all-to-all connectivity in the corresponding  $\text{QNC}^0$  circuit.

**Proof of Theorem 4.3.** Again the expressions do follow from the specific values of  $m$  for which there exists a  $\text{QNC}^0$  solving the  $\mathcal{R}_2^m$  problem (Lemma 4.10 and Corollary 4.11). This is now coupled with the average-case lower bound for the efficiency with a  $\text{bPTF}^0[k]/\text{rpoly}$  circuits of depth  $d$  and size  $s$  with maximum parameter  $k$  does solve the  $\mathcal{R}_2^m$  from Corollary 4.9 does provide us the enunciates bounds up to a value for  $q$ . To determine the value of  $q$ , we employ the same methodology used in the proof of Theorem 4.2, thereby deriving the optimal values for the entire set of expressions.  $\square$

## 4.2 Separation for qupit cases

In this section, we will examine a larger set of ISMR problems, denoted as  $\mathcal{R}_p^m$ , and the correlation of our candidate circuit with the correct solutions. More concretely, we use these problems to establish distinctions between  $\text{QNC}^0$  and  $\text{bPTF}^0[k]$  circuits. For that, we demonstrate that a  $\text{QNC}^0$  circuit can solve these problems with constant and non-zero correlation while generating outcome strings of sub-quadratic size,  $m = o(n^2)$ . In contrast, we will show that a  $\text{bPTF}^0[k]$  circuit of polynomial size solves the problem with a correlation asymptotically approaching zero as the input size increases for equal-size output strings, even for large and nearly optimal parameter  $k$ , as formalized in the subsequent theorem.

**Theorem 4.12.** *For all ISMRP problems defined for a prime dimension  $p$ , denoted by  $\mathcal{R}_p^m$ , there exists a  $\text{QNC}^0$  circuit with all-to-all connectivity, considering a uniform distribution  $\mathcal{D}_p$  over  $\mathbb{F}_2^n$  of strings with a Hamming weight that satisfies  $(\sum_{i=1}^n x_i) \bmod p = 0$  as the input distribution, that solves the problem for  $m = n \cdot \log n^{p-1}$ , achieving a correlation of  $\frac{p-1}{p^2}$ . In contrast, for any  $C \in \text{bPTF}^0[k]/\text{rpoly}$  circuit with fixed depth  $d$ , size polynomial  $s$ , and parameter  $k \leq n^{1/(5d)}$  solves each one of these problems with a correlation that is bounded by,*

$\text{bPTF}^0[k]/\text{rpoly}$	$k = \mathcal{O}(1) \ (\equiv \text{AC}^0/\text{rpoly})$	$k = n^{1/(5d)}$
$\text{Corr}_{\mathcal{D}_p}(C, \mathcal{R}_p^m)$	$\exp\left(-\Omega\left(\frac{n^{1-\mathcal{O}(1)}}{(\log n)^{p-1}(\log s)^{2d-2}}\right)\right)$	$\exp\left(-\Omega\left(\frac{n^{3/5-\mathcal{O}(1)}}{(\log n)^{p-1}(\log s)^{2d-2}}\right)\right)$

The previous theorem follows in three steps, delineated in [Section 4.2.1](#), [Section 4.2.2](#), and [Section 4.2.3](#). In the first subsection, we introduce a family of non-local XOR games related to the ISMR problems and the respective mapping between bits and dits, which will later facilitate the translation between these two objects. Then, in [Lemma 4.17](#), we establish upper bounds on the efficacy of any classical strategy in solving this family of non-local XOR games.

In the second subsection, we establish the classical lower bound for  $\text{bPTF}^0[k]$  circuits that address the ISMR problems. We integrate the upper bounds determined for the non-local XOR games with light cone arguments, enabling us to constrain the maximum efficiency of  $\text{NC}^0$  circuits operating on bits in addressing the ISMR problems. Additionally, we revisit our random restriction techniques to simplify  $\text{bPTF}^0[k]$  circuits into forest lines using [Lemma A.9](#), thereby connecting with the  $\text{NC}^0$  upper bounds. This approach allows us to define upper bounds for  $\text{bPTF}^0[k]$  circuits concerning the correlation with which they resolve the problems, which equivalently translates to size lower bounds for  $\text{bPTF}^0[k]$  circuits that achieve a constant positive correlation with the ISMR problems.

Finally, in [Section 4.2.3](#), we define the quantum resource state that will be utilized for the quantum solutions. This involves a generalization of the poor man's cat state, and we also demonstrate that these states can be prepared using qubit  $\text{QNC}^0$  circuits as shown in [Lemma 4.24](#). Subsequently, in [Lemma 4.26](#), we demonstrate the existence of  $\text{QNC}^0$  circuits that address the aforementioned problems with a constant positive correlation. The synthesis of the classical lower bounds and the quantum upper bounds culminates in our previous theorem. Additionally, it is worth noting that [Theorem 4.27](#) serves as an intermediate result, delineating separations between  $\text{NC}^0$  and qubit  $\text{QNC}^0$  circuits for specific problem instances.

Simultaneously with the previous result, we establish a separation for the qutrit case that parallels the qubit case, with simple success probabilities of being correct or incorrect. This equivalence arises from the correlation measure for the qutrit case, which assesses deviations from the correct outcome by magnitudes of 0 or 1, mirroring the correlation measure in the qubit case that is translatable to the commonly used success probability. Furthermore, this problem is particularly intriguing because, while the quantum solution can address the bounded error probabilistic version of the  $\mathcal{R}_p^m$ —solving all inputs with a probability distinctly greater than  $1/2$ —the average success probability of a polynomial-size  $\text{bPTF}^0[k]$  circuit decreases asymptotically to  $1/3$  as the input size increases.

**Corollary 4.13.** *For the ISMR problems defined for a prime dimension  $p = 3$ , denoted by  $\mathcal{R}_3^m$ , there exists a  $\text{QNC}^0$  circuit with 3D connectivity, considering a uniform distribution over  $\mathbb{F}_2^n$  of strings with a Hamming weight that satisfies  $(\sum_{i=1}^n x_i) \bmod 3 = 0$  as the input distribution, that solves the problem for  $m = n^{4/3}$ , achieving a success probability strictly larger than  $\frac{1}{2}$ . In contrast, for any  $C \in \text{bPTF}^0[k]/\text{rpoly}$  circuit with fixed depth  $d$ , size polynomial  $s$ , and parameter  $k \leq n^{1/(5d)}$  solves each one of these problems with a success probability that is bounded by,*

$\text{bPTF}^0[k]/\text{rpoly}$	$k = \mathcal{O}(1) \ (\equiv \text{AC}^0/\text{rpoly})$	$k = n^{1/(5d)}$
$\Pr[\text{Success}]$	$\frac{1}{3} + \exp\left(-\Omega\left(\frac{n^{2/3-\mathcal{O}(1)}}{\log(s)^{2d-1}}\right)\right)$	$\frac{1}{3} + \exp\left(-\Omega\left(\frac{n^{4/15-\mathcal{O}(1)}}{\log(s)^{2d-1}}\right)\right)$

This corollary follows the same proof techniques as [Theorem 4.12](#), with the difference being that the correlation measure can always be directly translated into the respective success probabilities.

### 4.2.1 Quantum non-local games in higher dimensions

We will now define the precise family of XOR non-local games, enabling us to connect the correlation upper bounds of these games to the upper bounds of the ISMR problems for the previously described separations.

Recall that to define a family of non-local games of a particular type we need to describe only the function that maps the modular remainder of the responses by each player and the messages sent to the parties playing the game. In our specific game, the function will also be a modular remainder of the message sent to the parties. Additionally, we extend the XOR non-local games defined in Definition 3.14 for the correlation measure presented in Section 3.3, resulting in the following family of non-local games.

**Definition 4.14** (Modular XOR games). *The class  $\mathcal{G}_p$  of multiparty non-local XOR games involves  $n$  parties, with each party  $P_i$  receiving information  $x_i \in \mathbb{F}_p$ . After each party receives its input, without further communication, each party must provide an individual response  $y_i \in \mathbb{F}_p$ , contributing to a collective output which is the concatenation  $y = (y_1, y_2, \dots, y_n)$  of their outputs. This defines the classical strategy  $w_{\mathcal{G}}$ . The correlation with the game is determined by the following expression,*

$$\text{Corr}(w_{\mathcal{G}_p}, \mathcal{G}_p) = \mathbb{E}_{(x_1, x_2, \dots, x_n) \sim \mathcal{D}} \left[ \text{Re} \left( e^{-i \frac{2\pi (\sum_{i=1}^n y_i - \sum_{i=1}^n x_i / p)}{p}} \right) \right],$$

for an arbitrary given input distribution  $\mathcal{D}$ .

These games are naturally related to the ISMR problems (Definition 4.1) because the messages to the parties and the responses follow a similar mapping between the input and output for the inverted strict modular relation problems. However, there is a technical misalignment since the non-local games have messages to the parties in  $\mathbb{F}_p$ , while the ISMR problems involve binary strings. Furthermore, we require uniform input distributions over  $\mathbb{F}_2^n$  to achieve average-case hardness separation for the ISMR problems. This will be resolved by establishing correlation upper bounds for the Modular XOR non-local games with biased input distributions, allowing us to relate uniform binary input distributions for the ISMR problems to the corresponding biased distributions over  $\mathbb{F}_p^n$  for the non-local games.

**Encoding.** To bridge our techniques from Section 2.4 with the higher-dimensional non-local games described in Definition 4.14, we will consider a specific encoding between binary and  $p$ -ary, for prime  $p$ . Subsequently, we will demonstrate that a Hamming weight-based encoding, defined as follows, meets all the necessary criteria.

**Definition 4.15** (Hamming encoding). *We define the Hamming encoding as a mapping of the form  $H : \mathbb{F}_2^{n(p-1)} \mapsto \mathbb{F}_p^n$ , defined as follows*

$$y = \bigotimes_{j=1}^n \left( \sum_{i=1}^{p-1} x_{j \cdot p + i} \right) \quad (4.25)$$

with  $x \in \mathbb{F}_2^{n(p-1)}$  and  $y \in \mathbb{F}_p^n$ .

The previous encoding does work very well in the binary to the base- $p$ , however, the inverse from the fact that it is not injective provides a nondetermined inverse. As we will consider later, this will not be a problem to handle the ISMR problems. However, the fact that a uniform distribution over  $\mathbb{F}_2^{n(p-1)}$  generates non-uniform distributions over  $\mathbb{F}_p^n$  has to be handled. A simple demonstration of this effect can be seen with the trit case, where we have

$$00 \mapsto 0; \quad 01 \mapsto 1; \quad 10 \mapsto 1 \text{ and } 11 \mapsto 2. \quad (4.26)$$

One does see that the frequency of 1's in the resulting strings will be larger than 0 or 2. We can account for this by defining the functions that map us the precise frequency of a term in  $\mathbb{F}_p$  resulting in a binary string with the Hamming encoding, as follows,

$$\Delta_2^p(x) = \frac{\binom{x}{2}}{2^{p-1}}. \quad (4.27)$$

This allows us to account for and determine how the winning probabilities of the respective non-local games are altered by this input distribution. Additionally, we will consider the uniform distribution over  $\mathbb{F}_p$ , which

is defined simply as  $\Delta_p^p(x) = \frac{1}{p}$ . The latter distribution will allow us to prove stronger separations between  $\text{QNC}^0$  qubit circuits and  $\text{NC}^0$  circuits.

Now that we have created the necessary elements to bridge our techniques, we can start establishing the sequence of correlation upper bounds for the selected family of non-local games. However, as these demonstrations become increasingly complex when dealing with all prime dimensions  $p$ , we will first, for a better exposition, demonstrate the case for qutrits. In addition, this case is of particular interest because  $p = 3$  represents the first prime dimension where quantum circuits lack exact solutions to the ISMR problems, and the deviation of quantum-classical efficiencies captures the existing advantage.

### Ternary correlation bound

In the case of qutrits, we demonstrate that the correlation between any classical strategy, including the optimal classical strategy denoted by  $w_{\mathcal{G}_3}^*$ , and the non-local game defined by  $\mathcal{G}_3$  decreases exponentially fast as the number of participants increases. Furthermore, we aim to establish a corresponding bound for the following expression,

$$\text{Corr}_{\mathcal{D}}(w_{\mathcal{G}_3}^*, \mathcal{G}_3) = \mathbb{E}_{x \sim \mathcal{D}} \left( \text{Re} \left( e^{i \frac{2\pi(|w_{\mathcal{G}_3}^*(x)| - \sum_{i=1}^n x_i/3)}{3}} \right) \right). \quad (4.28)$$

Additionally, this correlation measure can in the trinary case be used to compute the probability with which the XOR non-local game can be solved<sup>10</sup>,

$$\Pr_{x \sim \mathcal{D}}[w_{\mathcal{G}_3}^*(x) \in \mathcal{G}_3(x)] = \frac{1 + 2 \cdot \text{Corr}_{\mathcal{D}}(w_{\mathcal{G}_3}^*, \mathcal{G}_3)}{3}. \quad (4.29)$$

Building on the previous objects, we will show that the winning probability of any classical strategy for the non-local game defined by the  $\mathcal{G}_3$  problem is bounded below  $1/2$  for sufficiently large number of participants  $n$  and asymptotically approaches  $1/3$  for uniform distributions over messages in  $\mathbb{F}_3^n$  and biased distribution over  $\mathbb{F}_3^n$  resulting from the translation from a uniform distribution over  $\mathbb{F}_2^n$  using the Hamming encoding.

**Lemma 4.16.** *Any local probabilistic classical strategy  $w_{\mathcal{G}_3}$  that solves the non-local XOR games denoted as  $\mathcal{G}_3$ , with messages over  $\mathbb{F}_3^n$ , achieves a winning probability, for uniform input distributions over  $\mathbb{F}_3^n$  with Hamming weight satisfying  $(\sum_{i=1}^n x_i) \bmod 3 = 0$  and  $r$  restricted dits, bounded by  $\frac{1}{3} + (\frac{17}{20})^{n-r}$ . Similarly, for a uniform distribution over  $\mathbb{F}_2^n$ , where the Hamming weight satisfies  $(\sum_{i=1}^n x_i) \bmod 3 = 0$  and the inputs are translated using a bit-to-ternary encoding, the winning probability with  $r$  restricted bits is bounded by  $\frac{1}{3} + (\frac{9}{10})^{\frac{n-r}{2}}$ .*

*Proof.* In this setting, classical strategies allow each participant, identified as  $i$  within a set of  $n$  parties, to generate an output of either  $x_i$  or  $x_i + b$ , with  $b$  in  $\mathbb{F}_3$ . Therefore, the efficiency of any classical strategy  $w_{\mathcal{G}_3}$  in solving the XOR non-local game  $\mathcal{G}_3$  depends on the linear function  $l_a = \sum_{i=1}^n a_i \cdot x_i$  (with  $a$  in  $\mathbb{F}_3^n$ ) resulting from the messages send to the parties and the function  $f(x) = (|x|/3)^{-1} \bmod p$  for all messages where  $|x| \bmod 3 = 0$ , which defines the non-local game.

With this defined, we would like to compute the maximal value for the correlation and consequently the probability  $\Pr[f(x) = l_a(x)]$ . In particular, we have the following expression for the correlation,

$$\text{Corr}_*(w_{\mathcal{G}_3}^*, \mathcal{G}_3) = \max_{b \in \mathbb{F}_3^n} \left( \sum_{\substack{x \in \mathbb{F}_3^n \\ |x| \bmod 3 = 0}} \frac{\text{Re} \left( e^{i \frac{2\pi 2(|x|/3)}{3}} \prod_{i=1}^n e^{i \frac{2\pi x_i b_i}{3}} \right)}{\prod_{i=1}^n \Delta_*^p(x_i)} \right). \quad (4.30)$$

without yet completely defining a distribution over the delivered messages.

The correctness of the previous expression follows from the fact that  $|x|/3 \bmod 3$  and  $\sum_{i \in \mathbb{F}_3^n} x_i b_i \bmod 3$  are up to sign changes respectively representative of the two functions  $f$  and  $l_a$  that we intended to compare.

<sup>10</sup>Note that in the case of having a maximal mismatch between the functions we obtain that  $\Pr[f(x) = g(x)] = 0$  given that will be equal to  $\text{Corr}_{\mathcal{D}}(*, *) = -0.5$ . Also, whenever  $\Pr[f(x) = g(x)] = 1$  we have that  $\text{Corr}_{\mathcal{D}}(*, *) = 1$  which is again consistent, and all the values in between do follow equally.



Also, we can simply drop the  $\text{mod } 3$  operation on  $f$  since this is inherently carried out by the arithmetic associated with the roots of unity under consideration.

With that, we will write the correlation from Equation (4.30) as,

$$\sum_{\substack{x \in \mathbb{F}_3^n \\ |x| \bmod 3 = 0}} \frac{\text{Re} \left( e^{i \frac{4\pi(|x|/3)}{3}} \prod_{i=1}^n e^{i \frac{2\pi x_i b_i}{3}} \right)}{\prod_{i=1}^n \Delta_*^p(x_i)} = \text{Re} \left( \sum_{\substack{x \in \mathbb{F}_3^n \\ |x| \bmod 3 = 0}} \left( \prod_{i=1}^n \frac{e^{i \frac{2\pi x_i (2+3b_i)}{9}}}{\Delta_*^p(x_i)} \right) \right) \quad (4.31)$$

$$= \text{Re} \left( \left( \left( \sum_{x_1 \in \mathbb{F}_3} \frac{e^{i \frac{2\pi x_1 (2+3b_1)}{9}}}{\Delta_*^p(x_1)} \right) \cdots \left( \sum_{x_{n-1} \in \mathbb{F}_3} \frac{e^{i \frac{2\pi x_{n-1} (2+3b_{n-1})}{9}}}{\Delta_*^p(x_{n-1})} \right) \right) \bullet \frac{e^{i \frac{2\pi x_n (2+3b_n)}{9}}}{\Delta_*^p(x_n)} \right) \quad (4.32)$$

with  $x_n = \left( \sum_{i=1}^{n-1} x_i \right)^{-1}$  and  $\bullet$  being a conditional multiplication operation depending on the values of  $x_1$  to  $x_{n-1}$  in the first expression, such that the total sum of the inputs fulfills the condition of being congruent with zero modulo 3.

Now that we have reduced the correlation expression to a sum over fixed and equivalent expressions, we can establish bounds for the maximum value of the entire expression to obtain an upper limit. In particular, we will now apply the method proposed for qubits in [BBT04], and use the fact that the last term  $e^{i \frac{2\pi x_n (2+3b_{n-1})}{9}}$  takes each value of  $x_n$  over  $\mathbb{F}_3^n$ ,

$$\leq \max_{b \in \mathbb{F}_3^n} \left( \text{Re} \left( \left( \sum_{x_1 \in \mathbb{F}_3} \frac{e^{i \frac{2\pi x_1 (2+3b_1)}{9}}}{\Delta_*^p(x_1)} \right) \cdots \left( \sum_{x_{n-1} \in \mathbb{F}_3} \frac{e^{i \frac{2\pi x_{n-1} (2+3b_{n-1})}{9}}}{\Delta_*^p(x_{n-1})} \right) \left( \sum_{x_n \in \mathbb{F}_3} \frac{e^{i \frac{2\pi x_n (2+3b_n)}{9}}}{\Delta_*^p(x_n) \cdot (p-1)} \right) \right) \right) \quad (4.33)$$

$$\leq \max_{b \in \mathbb{F}_3^n} \left( \text{Re} \left( \frac{\left( \frac{1}{\Delta_*^p(1)} + \frac{e^{i \frac{2\pi (2+3b_1)}{9}}}{\Delta_*^p(1)} + \frac{e^{i \frac{2\pi (4+6b_1)}{9}}}{\Delta_*^p(2)} \right)^n}{p-1} \right) \right). \quad (4.34)$$

Considering the resulting expression and  $\Delta_3^3$  fully defining the input distribution, we can show that each term in Equation (4.34) has its norm bounded for the three different assignments of  $b_i$  by the following values,

$$\left| \frac{1 + e^{i \frac{2\pi (2+3b_1)}{9}} + e^{i \frac{2\pi (4+6b_1)}{9}}}{3} \right| = \begin{cases} \frac{1}{\sqrt{3(\cos^2(\frac{\pi}{18}) + (-1 + \sin(\frac{\pi}{18}))^2)}} < 0.45, & b_i = 0 \\ \frac{1}{\sqrt{3((-1 - \cos(\frac{\pi}{9}))^2 + \sin^2(\frac{\pi}{9}))}} < 0.3, & b_i = 1 \\ \frac{1}{\sqrt{3((-1 + \cos(\frac{2\pi}{9}))^2 + \sin^2(\frac{2\pi}{9}))}} < 0.85, & b_i = 2 \end{cases}. \quad (4.35)$$

Obtaining with that the bound  $\text{Corr}_{\mathcal{D}_3'}(w_{\mathcal{G}_3}^*, \mathcal{G}_3) \leq \frac{(0.85)^n}{2}$ , with  $\mathcal{D}_3'$  being the uniform input distributions over  $\mathbb{F}_3^n$  with Hamming weight satisfying  $(\sum_{i=1}^n x_i) \bmod 3 = 0$ . Additionally, the probability  $\Pr_{x \sim \mathcal{D}_3'}[f(x) = g(x)] \leq \frac{1}{3} + \left(\frac{17}{20}\right)^n$ , which asymptotically approaches 1/3 and for  $n \geq 12$  is already strictly smaller the 1/2.

Equally, we will consider  $\Delta_2^3$  which defines the distribution  $\mathcal{D}_3$  generated by considering a uniform distribution of strings over  $\mathbb{F}_2^{2n}$  converted to strings in  $\mathbb{F}_3^n$  with the Hamming encoding. In particular, in this case, we obtain that for the three different assignments of  $b_i$ , the term in Equation (4.34) is bounded by

$$\left| \frac{1}{4} + \frac{e^{i \frac{2\pi (2+3b_1)}{9}}}{2} + \frac{e^{i \frac{2\pi (4+6b_1)}{9}}}{4} \right| = \begin{cases} \frac{1}{2} (1 + \sin(\frac{\pi}{18})) < 0.59, & b_i = 0 \\ \sin^2(\frac{\pi}{18}) < 0.04, & b_i = 1 \\ \frac{1}{2} \sqrt{\frac{1}{2} (3 + 4 \cos(\frac{2\pi}{9}) + \sin(\frac{\pi}{18}))} < 0.89, & b_i = 2 \end{cases}. \quad (4.36)$$

In this case, we obtain the following bound,  $\text{Corr}_{\mathcal{D}_3}(w_{\mathcal{G}_3}^*, \mathcal{G}_3) \leq \frac{(0.89)^n}{2}$ . Additionally, the probability  $\Pr_{x \sim \mathcal{D}_3}[f(x) = g(x)] \leq \frac{1}{3} + \left(\frac{9}{10}\right)^n$ , which asymptotically approaches 1/3 and for  $n \geq 18$  is already smaller than 1/2.

The effect of restricted dits in Equation (4.33) for the respective sum of that variables does make it have a constant normal equal to 1. Therefore, these cases do not contribute to increasing the correlation and the overall expression. Equally, the space of inputs is reduced with the same factor. This implies that restricting dits makes the overall problem equivalent to the non-restricted, non-local game with a smaller input. Also, as there is no structure of the game limiting the rearrangement of messages, we can reorganize the fixed variables such that they form a  $r/(p-1)$  dits, and the previous analysis holds equally in this case.

Finally, there is no probabilistic classical strategy that surpasses the two upper bounds determined for the correlation measures by Yao's min-max principle.  $\square$

### Higher order correlation bounds

Now, we will generalize the upper bound on the efficiency of any classical strategy, including the optimal classical strategy  $w_{\mathcal{G}_p}^*$ , for all the XOR non-local games  $\mathcal{G}_p$  defined over higher prime dimensions. Therefore, we now intend to constrain the following expression,

$$\text{Corr}_{\mathcal{D}}(w_{\mathcal{G}_p}^*, \mathcal{G}_p) = \mathbb{E}_{x \sim \mathcal{D}} \left( \text{Re} \left( e^{i \frac{2\pi \left( |w_{\mathcal{G}_p}^*(x)| - \sum_{i=1}^n x_i/p \right)}{p}} \right) \right). \quad (4.37)$$

Note that previously, for  $p$  equal to 2 and 3, due to the symmetry of the roots of unity, the correlations were still binary discriminators relating to the probability of two functions being exactly equal modulo these prime numbers. However, it is important to note that this measure no longer directly relates to the probability of the outcome being correct in binary discrimination; rather, it is a distance measure between the vectors formed by the outcome space of the two functions. Although a similar measure of distances can be created, it generates non-linear terms for which the lower bounding techniques no longer apply. Nevertheless, we can resort to this linear distance measure natural to higher dimensions and use it to prove a quantum-classical efficiency separation for the relation problems at each prime dimension.

**Lemma 4.17.** *Any local probabilistic classical strategy  $w_{\mathcal{G}_p}$  that solves one of the XOR non-local games  $\mathcal{G}_p$ , with messages over  $\mathbb{F}_p^n$ , taken from a uniform distribution  $\mathcal{D}_p$  over  $\mathbb{F}_2^{n(p-1)}$  with Hamming weight satisfying  $(\sum_{i=1}^n x_i) \bmod p = 0$  and a bit to base- $p$  encoding, the maximal correlation with  $r$  restricted bits is bounded by,*

$$\text{Corr}_{\mathcal{D}_p}(w_{\mathcal{G}_p}^*, \mathcal{G}_p) \leq \text{Re} \left( \left( \frac{2^{1-p} e^{\frac{2\pi i}{p^2}} \left( e^{-\frac{2\pi i}{p^2}} \left( 1 + e^{\frac{2\pi i}{p^2}} \right) \right)^p \right)^{\frac{n-r}{p-1}}}{1 + e^{\frac{2\pi i}{p^2}}} \right) / (p-1) \right) \leq (c_p)^{\frac{n-r}{p-1}} \quad (4.38)$$

with  $c_p \in (0, 1)$ . Simultaneously, for uniform input distribution  $\mathcal{D}'_p$  over  $\mathbb{F}_p^n$  with their Hamming weight satisfying  $(\sum_{i=1}^n x_i) \bmod p = 0$  and  $r$  restricted dits, we have

$$\text{Corr}_{\mathcal{D}'_p}(w_{\mathcal{G}_p}^*, \mathcal{G}_p) \leq \frac{1}{p^{n-1}(p-1)} \text{Re} \left( - \frac{e^{2\pi i/p^2} \left( -1 + e^{2\pi i \frac{-1+p^2}{p}} \right)}{-1 + e^{i \frac{2\pi}{p^2}}} \right)^{n-r} \leq \frac{p}{p-1} \left( \text{Re} \left( e^{\frac{2\pi i}{p^2}} \right) \right)^{n-r}. \quad (4.39)$$

*Proof.* To obtain this bound on the correlation, we again consider that classical strategies  $w_{\mathcal{G}_p}$  allow each participant, identified as  $i$  within a set of  $n$  parties, to generate an output of either  $x_i$  or  $x_i + b$ , with  $b$  in  $\mathbb{F}_p$  as defined by the generalized XOR non-local games. Thus, the capability of approximating the ideal outcome will depend on the distance of the closest linear function  $l_a = \sum_{i=1}^n a_i \cdot x_i$  with  $a$  in  $\mathbb{F}_p^n$ , and the function defined by the respective non-local game  $\mathcal{G}_p$  over  $\mathbb{F}_p$ , taking the form of a function of the type  $f : \mathbb{F}_p^n \mapsto \mathbb{F}_p$ , and specifically defined as  $f(x) = (|x|/p)^{-1} \bmod p$ .

Our generalized correlation measure will then be defined as follows for arbitrary  $p$  and distribution  $\Delta_p^*$ ,

$$\text{Corr}_*(w_{\mathcal{G}_p}^*, \mathcal{G}_p) = \max_{b \in \mathbb{F}_p^n} \left( \sum_{\substack{x \in \mathbb{F}_p^n \\ |x| \bmod p = 0}} \text{Re} \left( \frac{e^{i \frac{2\pi(p-1)(|x|/p)}{p}} \prod_{i=1}^n e^{i \frac{2\pi x_i b_i}{p}}}{\Delta_p^*(x)} \right) \right). \quad (4.40)$$

The previous expression is algebraically equivalent to the one in Equation (4.32), and the terms in the exponents are linear, in the sense that all have a degree of 1. Therefore, we can bound the previous expression similarly as follows,

$$\leq \max_{b \in \mathbb{F}_p^n} \left( \operatorname{Re} \left( \sum_{x_1 \in \mathbb{F}_p} \left( \frac{e^{i \frac{2\pi x_1 ((p-1)+pb_1)}{p^2}}}{\Delta_*^p(x_1)} \right) \cdots \sum_{x_{n-1} \in \mathbb{F}_p} \left( \frac{e^{i \frac{2\pi x_{n-1} ((p-1)+pb_{n-1})}{p^2}}}{\Delta_*^p(x_{n-1})} \right) \sum_{x_n \in \mathbb{F}_p} \left( \frac{e^{i \frac{2\pi x_n ((p-1)+pb_n)}{p^2}}}{\Delta_*^p(x_n) \cdot (p-1)} \right) \right) \right) \quad (4.41)$$

$$\leq \max_{b \in \mathbb{F}_p^n} \left( \operatorname{Re} \left( \left( \sum_{x_j \in \mathbb{F}_p} \frac{e^{i \frac{2\pi x_j ((p-1)+pb_j)}{p^2}}}{\Delta_*^p(x_j)} \right)^n / (p-1) \right) \right). \quad (4.42)$$

Unfortunately, at this point, it is no longer feasible to compute all the values for  $b$  in  $\mathbb{F}_p$  to bind the expression for a general proof, as previously done for the qutrit case. Nevertheless, there is a simple geometric intuition for the values of the expression  $\sum_{x_j \in \mathbb{F}_p} e^{i \frac{2\pi x_j ((p-1)+pb_j)}{p^2}}$ . For any value of  $b_j$  selected, the sequential product with the values of  $x_j$  moves the angle of each term involved in the sum by a step equivalent to a multiple of  $2\pi i/p^2$ , equal to  $(p-1) + pb_j$ . Ideally, the maximum for the expression would be reached with a step equal to zero, so we always have the maximum value of 1 and perfect correlation. Since this case with optimal correlation is not possible, as  $(p-1) + pb_j$  is never zero for any value of  $b_j$ , we have that the subsequent best option is to have that expression equal to either 1 or  $p^2 - 1$  to maximize either the real or the absolute values.

In addition, the same analysis holds equally for any of the distributions of the inputs  $\Delta_*^p(x)$ , as the same arguments apply for the selection of the value  $b_j$ . Therefore, by considering  $b_j = p-1$  and  $\Delta_p^p$ , we obtain the distribution  $\mathcal{D}'_p$  and define the optimal correlation as follows,

$$\operatorname{Corr}_{\mathcal{D}'_p} (w_{\mathcal{G}_p}^*, \mathcal{G}_p) \leq \frac{1}{p^{n-1} (p-1)} \operatorname{Re} \left( - \frac{e^{2\pi i/p^2} \left( -1 + e^{2\pi i \frac{-1+p^2}{p}} \right)}{-1 + e^{i \frac{2\pi}{p^2}}} \right)^n. \quad (4.43)$$

To obtain the exact value, one is only required to obtain a numerical bound for the previous expression depending on  $p$ . From an analytical point of view, we know that all the terms in the sum contained in Equation (4.42), except for the first term, are smaller than 1, even when we use the best possible value for  $b_i$ . Thus, we have that,

$$\operatorname{Corr}_{\mathcal{D}'_p} (w_{\mathcal{G}_p}^*, \mathcal{G}_p) \leq \frac{p}{p-1} (c_p)^n, \text{ with } c_p \in (0, 1). \quad (4.44)$$

Also, as  $c_p$  is no larger than  $1 - \operatorname{Re} \left( e^{\frac{2\pi i}{p^2}} \right)$ , we have that it is guaranteed that it is infinitely close to 1. Thus, the correlation of any classical strategy goes exponentially fast close to zero with increasing input size.

Now we need to consider the case where we have  $\mathcal{D}_p$  the uniform distribution over  $\mathbb{F}_2$ , whose distribution over  $\mathbb{F}_p$  we capture with  $\Delta_p^p$ . This case then defines the following bound on the correlation,

$$\operatorname{Corr}_{\mathcal{D}_p} (w_{\mathcal{G}_p}^*, \mathcal{G}_p) \leq \operatorname{Re} \left( \left( \frac{2^{1-p} e^{\frac{2\pi i}{p^2}} \left( e^{-\frac{2\pi i}{p^2}} \left( 1 + e^{\frac{2\pi i}{p^2}} \right) \right)^p}{1 + e^{\frac{2\pi i}{p^2}}} \right)^n / (p-1) \right). \quad (4.45)$$

The previous expression should asymptotically approach zero with increasing input size  $n$  for arbitrary  $p$ . To verify that this holds, we need to show that the expression

$$\varkappa_p = \left| \frac{2^{1-p} e^{\frac{2\pi i}{p^2}} \left( e^{-\frac{2\pi i}{p^2}} \left( 1 + e^{\frac{2\pi i}{p^2}} \right) \right)^p}{1 + e^{\frac{2\pi i}{p^2}}} \right|, \quad (4.46)$$

is smaller than 1 for arbitrary  $p$ . We will prove this inductively, informed by the limit of the expression  $\varkappa_p$  with an increasing value of  $p$  being 1, given that

$$\lim_{p \rightarrow \infty} \left( \frac{2^{1-p} e^{\frac{2\pi i}{p^2}} \left( e^{-\frac{2\pi i}{p^2}} \left( 1 + e^{\frac{2\pi i}{p^2}} \right) \right)^p}{1 + e^{\frac{2\pi i}{p^2}}} \right) = 1. \quad (4.47)$$

Combining this limit with the fact that for  $p = 3$ , the expression  $\varkappa_3$  is smaller than 1, it is enough to prove that the same expression  $\varkappa_p$  reaches from below its asymptotic bound. More precisely, we need to prove that this expression is monotonically increasing. For that, we only need to prove that for two values  $k$  and  $k + 1$ , the following expression is negative,

$$\varkappa_k - \varkappa_{k+1} \propto \left( \frac{2e^{\frac{2\pi i}{k^2}} \left(1 + e^{-\frac{2\pi i}{k^2}}\right)^k}{1 + e^{\frac{2\pi i}{k^2}}} - \left(1 + e^{-\frac{2\pi i}{(k+1)^2}}\right)^k \right). \quad (4.48)$$

With respect to this expression, we can show that the real part of  $\left(1 + e^{-\frac{2\pi i}{(k+1)^2}}\right)^k$  is larger than  $\left(1 + e^{-\frac{2\pi i}{k^2}}\right)^k$ . For that, we consider the norms of these values without the exponent  $k$ , and as for the first expression, the corresponding angle  $\theta_1 = \frac{-2\pi i}{(k+1)^2}$  is larger than  $\theta_2 = \frac{-2\pi i}{k^2}$ , the angle of the second expression, while both being in the fourth quadrant. Hence, the norm of the first term  $r_1$  is larger than that of the second term  $r_2$ . Then, with the exponent  $k$ , we look into their respective polar representations and observe that the respective real parts of these are equal to  $(r_1)^k \cos(k\theta_1)$  and  $(r_2)^k \cos(k\theta_2)$ . Now, as mentioned previously,  $r_1$  is larger than  $r_2$ , and also both the angles  $k\theta_1$  and  $k\theta_2$  are in the fourth quadrant, with  $k\theta_1$  being larger. Thus, having a larger value of  $\cos(k\theta_1)$  than  $\cos(k\theta_2)$ , obtaining our initial assertion.

The final step is simply to consider that the real part of  $\left(1 + e^{-\frac{2\pi i}{k^2}}\right)^k$  does not get larger than  $\left(1 + e^{-\frac{2\pi i}{(k+1)^2}}\right)^k$  with the multiplication with  $\frac{2e^{\frac{2\pi i}{k^2}}}{1 + e^{\frac{2\pi i}{k^2}}}$ . In particular, this value can be simplified to  $1 + i \tan\left(\frac{\pi}{k^2}\right)$ , which, when multiplied with the previous value, makes the real part of  $\left(1 + e^{-\frac{2\pi i}{k^2}}\right)^k$  equal to  $(r_2)^k \cos(k\theta_2)(1 - \tan\left(\frac{\pi}{k^2}\right))$ , which is bounded by  $2(r_2)^k \cos(k\theta_2)$  for  $k \geq 2$ . Also, the absolute value of the first term is smaller than the second for  $k \geq 2$ . Thus, for  $k \geq 2$ , this expression in Equation (4.48) is negative as we intended. Thus, we obtain that the value of  $\text{Corr}_{\mathcal{D}_p}(w_{\mathcal{G}_p}^*, \mathcal{G}_p)$  with the distributed messages being sampled from a uniform distribution over  $\mathbb{F}_2^{n(p-1)}$  and encoded with the Hamming encoding to strings in  $\mathbb{F}_p^n$  is bounded by  $(c_p)^n$ , with  $c_p$  being a constant strictly smaller than 1.

Finally, the effect of restricting bits or dits simply results in a version of the same XOR non-local game with fewer variables, analogous to the case in Lemma 4.16. Additionally, no probabilistic classical strategy can surpass the two upper bounds established for the correlation measures according to Yao's min-max principle.  $\square$

#### 4.2.2 Average-case $\text{bPTF}^0[k]$ lower hardness

Here, we will demonstrate that the classical circuit class  $\text{bPTF}^0[k]$  cannot solve the ISMR problems with a sufficiently significant correlation. In other words, exponentially large circuits will be required to achieve constant positive correlations with these problems. To accomplish this, we will utilize the classical correlations identified for the Modular XOR non-local games, along with the novel tools developed in Section 2.4.

#### $\text{NC}^0$ lower bounds

In the first step, we will use the previously determined correlation bounds for the XOR non-local games and lightcone arguments to demonstrate lower bounds on the efficiency of  $\text{NC}^0$  circuits solving the class of ISMR problems. This can be done given that through the Hamming encoding, we can consider each set of  $p - 1$  bits as a representation of a base- $p$  value in the non-local game for both the messages to the parties and their responses. Consequently, any valid solution to the  $\mathcal{R}_p^{m(p-1)}$  problem would equally represent a valid solution to the respective XOR non-local game played over messages of the type  $\mathbb{F}_p^n$ , and vice versa.

In addition to the previous connection, we will also show that  $\text{NC}^0$  circuits exhibit bounded locality in terms of their causal influence. This implies that each outcome depends on a fixed number of inputs that can never exceed  $n$ . More precisely, through some combinatorial arguments, it is possible to demonstrate that producing a correct outcome string with these circuits is equivalent to solving the aforementioned non-local games on a subset of the inputs with the same capacity as any of the optimal classical strategies considered before. This will allow us to show that unless the circuits have sufficient depth, they will fail with the same probability as the best classical strategies for the specific non-local games in question determined

in [Lemma 4.16](#) and [Lemma 4.17](#), and this directly defines the efficiency with which they solve the ISMR problems on binary inputs and outputs.

**Lemma 4.18.** *Let  $C$  be a circuit with  $n(p-1)$  binary inputs, arranged in  $n$  blocks of size  $p-1$ , and  $m(p-1)$  binary outputs, arranged in  $m$  blocks of size  $p-1$ , with locality  $l$  for each outcome bit. Then, for any arrangement of the blocks, there exists a subset of input blocks  $S$  of size  $\Omega(\min(n, \frac{n^2}{l^2 m (p-1)^4}))$  such that each output block depends on at most one block from  $S$ .*

*Proof.* To prove this we first consider that each of the output blocks does result from at most  $(p-1) \cdot f_{in}$  bits from the previous layer, with gates of fanin equal to  $f_{in}$ . For the subsequent layers, each bit depends on at most  $f_{in}$  elements of the previous layer, except for the last layer. Here as there are  $p-1$  input bits per block, each element can depend on  $(p-1) \cdot f_{in}$  input blocks. This means that each output block has a locality equal to  $l' = (p-1)^2 \cdot f_{in}^d = (p-1)^2 \cdot l$ , respective to the input blocks.

At this point, we can turn to the intersection graph that includes all the output blocks as vertices and connects vertices with an edge if they share an input block. This graph will have  $m$  vertices. Given that each output block can depend on  $(p-1)^2 \cdot l$  input blocks, and each of these inputs can influence up to  $(p-1)^2 \cdot l$  output blocks, it follows that each vertex is connected to at most  $(p-1)^4 \cdot l^2$  other vertices. Therefore, this graph will have at most  $\mathcal{O}(m \cdot (p-1)^4 \cdot l^2)$  edges.

The final step involves applying Turán's theorem, which provides an upper bound for the number of edges  $E$  in a graph  $G$  to avoid having with certainty a complete subgraph  $K_S$ , given by the inequality  $(1 - \frac{1}{S}) \frac{n^2}{2} \leq E$ . Our goal, however, is to ascertain the minimum size of the independent set. To this end, we consider the complement graph  $\overline{G}$ , where an edge exists in  $G$  wherever it was absent in  $\overline{G}$ , and vice versa. This ensures that if the original graph contained a complete subgraph of size  $S$ , then the complement graph  $\overline{G}$  will contain an independent set of the same size. Consequently, we can establish a lower bound for the size of this independent set as  $(1 - \frac{1}{S}) \frac{n^2}{2} \geq \binom{n}{2} - E$ . By simplifying the previous expression, we find that  $S \geq \frac{n^2}{E}$ . Substituting in the number of edges we have, we obtain  $S \geq \frac{n^2}{m(p-1)^4 l^2}$ .  $\square$

Subsequently, by integrating the previous lemma with the upper bounds for the correlations of classical strategies with the Modular XOR non-local games, we demonstrate that the extent to which an  $\text{NC}^0$  circuit successfully solves the ISMR problems is directly influenced by the circuit's locality, its depth, and the length of the desired output string.

In particular, we will determine these upper bounds on the correlation for uniform input distributions over  $\mathbb{F}_2^n$  and, subsequently, for uniform distributions over  $\mathbb{F}_p^n$ .

**Lemma 4.19.** *Let  $C$  be a circuit in  $\text{NC}^0/\text{rpoly}$  with locality  $l$ . Then,  $C$  fails to solve each of the  $\mathcal{R}_p^m$  problems, with a uniform distribution  $\mathcal{D}_p$  over  $\mathbb{F}_2^n$  and Hamming weight satisfying  $(\sum_{i=1}^n x_i) \bmod p = 0$ , with a correlation larger than,*

$$\text{Corr}_{\mathcal{D}_p}(C, \mathcal{R}_p^m) = \mathcal{O} \left( \text{Re} \left( \frac{2^{1-p} e^{\frac{2\pi i}{p^2}} \left( e^{-\frac{2\pi i}{p^2}} \left( 1 + e^{\frac{2\pi i}{p^2}} \right) \right)^p}{1 + e^{\frac{2\pi i}{p^2}}} \right)^{\min(n, \frac{n^2}{m(p-1)^4 l^2})} \right). \quad (4.49)$$

In particular, for  $p = 3$  we can bind the success probability by

$$\Pr_{\substack{x \sim \mathbb{F}_2^n \\ |x| \bmod 3 = 0}} [C(x) \in R_3^m(x)] \leq \frac{1}{3} + \left( \frac{9}{10} \right)^{\min(n, \frac{n^2}{16ml^2})}. \quad (4.50)$$

*Proof.* This follows directly from the combination of [Lemma 4.18](#) with [Lemma 4.16](#) and [Lemma 4.17](#), provided that one considers all the blocks in the independent set  $S$  derived by [Lemma 4.18](#) as outcome bits producing an outcome equivalent to linear functions in  $\mathbb{F}_p$  over a set of input bits of equal size. Therefore, for this input distribution which translates as a uniform distribution over  $\mathbb{F}_2^n$  to a biased distribution over  $\mathbb{F}_p^n$  with the respective bias determined by  $\Delta_2^p$ , the efficiency cannot exceed the respective probability or correlation determined in [Lemma 4.16](#) and [Lemma 4.17](#). Thereby establishing a lower bound on the efficiency of an  $\text{NC}^0$  circuit based on its locality and size.

In addition, we can consider that a random advice string allows for the probabilistic mixture of  $\text{NC}^0$  circuits. However, since all these circuits can be reduced to the efficiency of a single classical strategy for the ISMRP at hand, and since there is no probabilistic mixture with a larger correlation with the optimal outcomes, the same applies to  $\text{NC}^0/\text{rpoly}$  circuits.  $\square$

Considering a biased binary input distribution, further reducing the respective classical correlation bound for  $\text{NC}^0$  circuits is possible.

**Corollary 4.20.** *Let  $C$  be a circuit in  $\text{NC}^0/\text{rpoly}$  with locality  $l$ . Then,  $C$  fails to solve each of the  $\mathcal{R}_p^m$  problems with a biased binary input distribution  $\mathcal{D}'_p$ , which is defined by a uniform distribution over  $\mathbb{F}_p^n$  that is converted into a binary distribution using one of the potential inverse mappings of the Hamming encoding, with an average correlation larger than,*

$$\text{Corr}_{\mathcal{D}'_p}(C, \mathcal{R}_p^n) = \mathbb{E}_{\substack{x \sim H^{-1}(\mathbb{F}_p^{n/\log(p)}) \\ |x| \bmod p = 0}} \left( \text{Re} \left( e^{i \frac{2\pi(|C(x)| - |\mathcal{R}_p^n(x)|)}{p}} \right) \right) \quad (4.51)$$

$$\leq \frac{p}{p-1} \left( \text{Re} \left( e^{\frac{2\pi i}{p^2}} \right) \right)^{\min\left(n, \frac{n^2}{m(p-1)^4 l^2}\right)}. \quad (4.52)$$

In particular, for  $p = 3$  we can with the same setting bind the success probability by

$$\Pr_{\substack{x \sim H^{-1}(\mathbb{F}_3^{n/\log(3)}) \\ |x| \bmod 3 = 0}} [C(x) \in R_3^m(x)] \leq \frac{1}{3} + \left( \frac{17}{20} \right)^{\min\left(n, \frac{n^2}{16ml^2}\right)}. \quad (4.53)$$

*Proof.* The corollary follows exactly the same steps as the proof of Lemma 4.19 with the respective use of the bias consideration of  $\Delta_p^p$  in Lemma 4.16 and Lemma 4.17.  $\square$

### bPTF<sup>0</sup>[ $k$ ] lower bounds

The last lower bound to be determined for the higher-dimensional analysis pertains to the bPTF<sup>0</sup>[ $k$ ] circuit. This will follow, once again, from the use of our switching lemma developed in Lemma A.9, in combination with the previous lower bounds for  $\text{NC}^0$  circuits to which the initial circuit is reduced. Here again one of the main points for consideration is the goal to determine super-polylogarithmic values of  $k$ , for which no polynomial-size bPTF<sup>0</sup>[ $k$ ] circuit solves any of the  $\mathcal{R}_p^m$  problems with fixed and constant correlation value.

**Lemma 4.21.** *For sufficiently large  $n$  and  $q \in \mathbb{N}_{>0}$ , any bPTF<sup>0</sup>[ $k$ ]/rpoly circuit of depth  $d \geq 4$ , size  $s \leq \exp(n^{1/(2d-2)})$  and parameter  $k \leq n^{1/(5d)}$  solves the  $\mathcal{R}_p^m$  with correlation bounded by,*

$$\text{Corr}_{\mathcal{D}_p}(|C|, |\mathcal{R}_p^m|) = \mathcal{O} \left( \text{Re} \left( \left( \frac{2^{1-p} e^{\frac{2\pi i}{p^2}} \left( e^{-\frac{2\pi i}{p^2}} \left( 1 + e^{\frac{2\pi i}{p^2}} \right) \right)^p}{1 + e^{\frac{2\pi i}{p^2}}} \right)^{\frac{n^2}{2^{2q} m^{1+2/q} \mathcal{O}(\log(s)^{2d-1}) k^{2d}}} \right) \right), \quad (4.54)$$

with  $\mathcal{D}_p$  being the uniform distribution over string in  $\mathbb{F}_2^n$  that satisfy  $|x| \bmod p = 0$ .

*Proof.* Beginning with a bPTF<sup>0</sup>[ $k$ ] circuit, we intend to reduce this object, enabling the application of appropriate lemmas to the problem at hand. The initial segment of our proof parallels the approach in Lemma 4.7, initiating with a random restriction denoted as  $\rho$ . The probability of this restriction is set to  $p = \frac{1}{m^{1/q}} \cdot \mathcal{O}(\log(s)^{d-1} \cdot k^d)$ , where  $t$  is chosen to be  $\frac{pn}{8}$ . Subsequently, a second random restriction,  $\tau$ , is applied to the  $2t$  variables within the global decision tree, which, after the initial random restriction, is reduced to  $\text{DT}(q-1)^m$ . This second restriction occurs with a probability of  $1 - \exp(-\Omega(pn))$ .

Thus, using  $p$ -random restrictions we obtained that sampling  $|x| \bmod p$  strings consistent with the restrictions does provide us with a uniform distribution over the  $|x| \bmod p$  strings, given that over any non-total subset of the input bits these are uniform distributions in  $\mathbb{F}_2$ . Exactly, the same argument does work over the restriction  $\tau$  given that the variables of the global decision tree are selected randomly in  $\{0, 1\}^{2t}$ . This



property of  $p$ -random restrictions, combined with the fact that we can reconstitute the surviving variables into a new string for which we need to solve the initial problem, allows us to apply [Lemma 4.19](#) directly without any limitations on the specific locations of the variables that remain alive. Combining this with the fact that with a high probability more  $pn/4$  variables are alive, and the circuit does have to evaluate the  $\mathcal{R}_p^m$  problem with local decision trees of depth  $q-1$ , we obtain that these depend at most on  $2^q$  of the variables alive. Consequently, we have that any  $\text{bPTF}^0[k]$  circuit does compute the ISMR problems with a correlation bounded by,

$$\begin{aligned} \text{Corr}_{\mathcal{D}_p}(|C|, |\mathcal{R}_p^m|) &\leq \text{Re} \left( \left( \frac{2^{1-p} e^{\frac{2\pi i}{p^2}} \left( e^{-\frac{2\pi i}{p^2}} \left( 1 + e^{\frac{2\pi i}{p^2}} \right) \right)^p}{1 + e^{\frac{2\pi i}{p^2}}} \right)^{\Omega\left(\frac{(pn)^2}{2^{2q}m}\right)} / (p-1) \right) \\ &= \mathcal{O} \left( \text{Re} \left( \left( \frac{2^{1-p} e^{\frac{2\pi i}{p^2}} \left( e^{-\frac{2\pi i}{p^2}} \left( 1 + e^{\frac{2\pi i}{p^2}} \right) \right)^p}{1 + e^{\frac{2\pi i}{p^2}}} \right)^{\frac{n^2}{2^{2q}m^{1+2/q} \mathcal{O}(\log(s)^{2d-1}) k^{2d}}} \right) \right), \end{aligned}$$

with  $\mathcal{D}_p$  being the uniform distribution over string in  $\mathbb{F}_2^n$  that satisfy  $|x| \bmod p = 0$ .

Finally, the same proof does hold for the case where the  $\text{bPTF}^0[k]$  circuit is given a random string as advice. Since any  $\text{bPTF}^0[k]$  reduces to the same object after the use of random restriction, and that from [Lemma 4.19](#) we do now that any probabilistic strategy defined by the random advice does fail, so do  $\text{bPTF}^0[k]/\text{rpoly}$  circuits.  $\square$

This finishes determining the classical upper bounds for the correlations achieved by the  $\text{bPTF}^0[k]$  circuit for the entire set of ISMR problems. Finally, we will also enunciate a bound for the maximum probability with which the same circuit class can solve the specific case of  $\mathcal{R}_3^m$ , as in this case, it follows directly from the correlation bound.

**Corollary 4.22.** *For sufficiently large  $n$  and  $q \in \mathbb{N}_{>0}$ , any  $\text{bPTF}^0[k]/\text{rpoly}$  circuit of depth  $d \geq 4$ , size  $s \leq \exp(n^{1/(2d-2)})$  and parameter  $k \leq n^{1/(5d)}$  solves the  $\mathcal{R}_3^m$  with a probability bounded by,*

$$\Pr_{\substack{x \sim \mathbb{F}_2^n \\ |x| \bmod 3 = 0}} [C(x) \in R_3^m(x)] \leq \frac{1}{3} + \left( \frac{9}{10} \right)^{\Omega\left(\frac{n^2}{2^{2q}m^{1+2/q} \mathcal{O}(\log(s)^{2d-1}) k^{2d}}\right)}. \quad (4.55)$$

*Proof.* The proof follows in the same manner as in [Lemma 4.21](#) by executing all the steps up to the use of the lower bound for the success probability with  $\text{NC}^0/\text{rpoly}$  circuits. In particular, at this point, we consider the upper bound determined for the success probability in the specific case of  $\mathcal{R}_3^m$  as outlined in [Lemma 4.19](#).  $\square$

### 4.2.3 Qupit upper bound

In this section, we will describe  $\text{QNC}^0$  circuits over qupits to solve probabilistically the ISMR problems. This will use the qupit generalizations of poor man's cat states from [\[BKM<sup>+</sup>24\]](#). However, we apply some slight modifications such that it simplifies the following set of proofs as it also contributes to the self-containment of the document.

**Definition 4.23** (Generalized poor-man's qudit state). *Let  $p$  be a prime and  $z^{+0} \in \mathbb{F}_p^n$ . We define a generalized poor-man's qudit state  $|\text{GPM}_p^n\rangle = \frac{1}{\sqrt{p^n}} \sum_{i \in \mathbb{F}_p} |z^{+i}\rangle$  with  $z^{+i}$  being the string that takes a initial defined string  $z^{+0}$  and applies the bitwise sum of  $i$  to each bit of the string obtaining with that,*

$$z^{+i} = ((z_1 + i) \bmod p) || ((z_2 + i) \bmod p) || \dots || ((z_n + i) \bmod p). \quad (4.56)$$

Now it will be important to prove these types of states can be created with a  $\text{QNC}^0$  circuit.

**Lemma 4.24.** For  $n \in \mathbb{N}$ ,  $|\text{GPM}_p^n\rangle$  can be prepared with  $\text{QNC}^0$  circuit based on a fully connected and without cycles graph  $G = (V, E)$  over the respective qudit prime dimension  $p$ . The respective string  $v$  defining the precise state is described by the following recurrence relation between vertex qudits and the measurement outcomes from the edge qudits,

$$v_u = \left( \sum_{e_{i,j} \in \text{Path}(u,w)} (-1)^{|\text{Path}(u,j)| + |\text{Path}(u,w)|} e_{i,j} + v_w \right) \bmod p \quad (4.57)$$

for any two vertices  $u, w \in V$ , and the shortest path  $\text{Path}(u, w)$  from  $u$  to  $w$  in the graph  $G$ .

*Proof.* We will provide proof by describing concretely the circuit that does create the  $|\text{GPM}_p^n\rangle$  states. In particular, we will describe how the various stages of the circuit illustrated in Figure 9 compute the correct state.

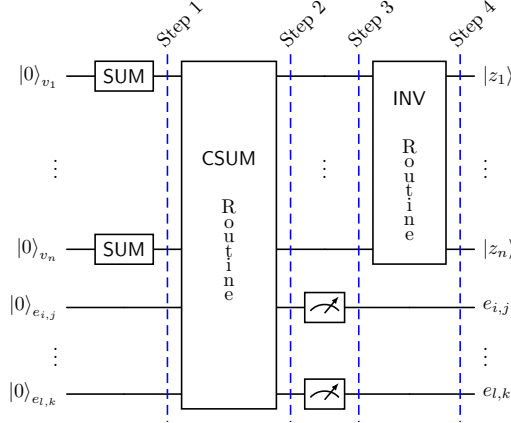


Figure 9: Illustration of a constant-depth quantum circuit for generating a generalized poor man's cat state, accompanied by the classical information needed to describe the specific instance created.

**Step 1.** The circuit does start with a qudit of prime dimension  $p$  for each vertex and edge in the graph  $G = (V, E)$ . Based on this labeling, we apply a Fourier gate or higher dimensional Hadamard gate  $F$  to each vertex qudit. This does create the state  $|\Psi_1\rangle = \frac{1}{\sqrt{p^n}} \sum_{x \in \mathbb{F}_p^n} |x\rangle |0\rangle^{\otimes l}$ .

**Step 2.** Then, the CSUM routine applies a CSUM gate between every edge  $e_i$  and vertex  $v_i$  qudit that is connected in the graph  $G$ , with the former being the target and the latter the control. Creating with that the state  $|\Psi_2\rangle = \frac{1}{\sqrt{p^n}} \sum_{x \in \mathbb{F}_p^n} |x, e_{i,j}, \dots, e_{l,k}\rangle$ , with  $e_{i,j} = v_j + v_i \bmod p$ , given that  $e_{i,j}$  is an edge between the vertexes  $v_j$  and  $v_i$  in  $G$ .

**Step 3.** Subsequently, one does measure all the qudits with the edge labeling. Previously, these were in a superposition of possible values for the sums of the computational bases of the respective vertexes. Now, these are fixed and this does fix strictly that the quantum state over the vertex qudits fulfill the following relation,

$$v_u \equiv \left( \sum_{e_{i,j} \in \text{Path}(u,w)} (-1)^{|\text{Path}(u,j)|} e_{i,j} + (-1)^{|\text{Path}(u,w)|} v_w \right) \bmod p. \quad (4.58)$$

Considering a certain vertex in the graph, we immediately obtain that we have for this vertexes the superposition  $\sum_{i \in \mathbb{F}_p} \frac{1}{\sqrt{p}} |i\rangle$ , and that for each one of this computational basis states all the other computational basis states are fixed, such that,  $|\Psi_3\rangle = \frac{1}{\sqrt{p}} \sum_{i \in \mathbb{F}_p} |x_i, e_{i,j}, \dots, e_{l,k}\rangle$ , with  $x_1, \dots, x_p \in \mathbb{F}_p^n$  and dictated by the relation described in Equation (4.58). In particular, if we select the first listed vertex  $v_0$  as our reference, and with, we can describe the previous states as

$$|\Psi_3\rangle = \frac{1}{\sqrt{p}} \sum_{i \in \mathbb{F}_p} |v_0^{+i}, \dots, v_j^{(-1)^{\text{Path}(0,j)}i}, \dots, v_n^{(-1)^{\text{Path}(0,n)}i}, e_{i,j}, \dots, e_{l,k}\rangle, \quad (4.59)$$

with  $v^{+0} \in \mathbb{F}_p^n$ .

**Step 4.** The state in the previous stage is very close to fulfilling the definition of a generalized qudit poor-mans cat state. The only issue is that for every vertex the path that is of odd size to the reference vertex, has the computational basis changing by the additive inverses of  $i$  of the reference qudit. In the final step, This can be simply solved by applying a INV gate to all these qudits in the “INV Routine”. The final state, then is of the form  $|\Psi_4\rangle = \frac{1}{\sqrt{p}} \sum_{i \in \mathbb{F}^d} |v^{+i}, \dots, v_n^{+i}, e_{i,j}, \dots, e_{l,k}\rangle$ , with  $v^{+0} \in \mathbb{F}_p^n$ . This exactly fulfills the definition of the poor-mans qudits states,  $|\text{GPM}_p^n\rangle$ . Also, the individual  $z_i$  bits fulfill the following recurrence relation,

$$v_u \equiv \left( \sum_{e_{i,j} \in \text{Path}(u,w)} (-1)^{|\text{Path}(u,j)| + |\text{Path}(u,w)|} e_{i,j} + v_w \right) \bmod p. \quad (4.60)$$

□

Now we will show that there exists a  $\text{QNC}^0$  circuit that can solve the probabilistic  $R_3^m$  ISMR problem, with a probability strictly larger than the upper bound determined for the classical solutions. We do the qutrit case first as it works as a specific instance and is easier to follow, and then we generalize for the arbitrary qudit prime dimension.

**Lemma 4.25.** *There exists a  $\text{QNC}^0$  circuit that given a  $|\text{GPM}_3^n\rangle$  state, along with the corresponding graph  $G$  and a set of measured edges  $E = \{e_{i,j}, \dots, e_{l,k}\}$ , is capable of solving the modular relation problem denoted as  $\mathcal{R}_3^m$ , over a uniform distribution of strings satisfying  $\sum_{i=1}^n x_i \bmod 3 = 0$  in  $\mathbb{F}_2^n$ , with a success probability exceeding  $1/2$  for any given input. Here,  $m = n \cdot g^2$ , the size of the outcome string, depends on the length  $g$  of the largest path in  $G$  from any vertex to a particular vertex that minimizes the maximum distance to any other vertex.*

*Proof.* For this proof, we consider the quantum circuit that archives this and is represented in Figure 10. Also, we consider the existence of a  $\text{QNC}^0$  based on Lemma 4.24 that prepares the resource state, which will be in this case the  $|\text{GPM}_3^n\rangle$  state. Also, we consider the additional access to the corresponding graph  $G$  and string  $E$  for the measured edges in the state preparation.

**Step 1.** In this step, controlled qudit  $Z$  rotations will be applied to each one of the qudits of the resource state. The control of each one of these rotations will be a bit of input string  $x$ . Obtaining with that the following state,

$$|\Psi_1\rangle = \bigotimes_{i=1}^n R_z\left(\frac{2\pi x_i}{9}\right) |\text{GPM}_3^n\rangle = \frac{1}{\sqrt{3}} \sum_{i=0}^2 e^{\frac{2\pi i \langle x, z^{+i} \rangle}{9}} |z^{+i}\rangle. \quad (4.61)$$

Although the previous expression accurately represents the resulting state, it would be beneficial to reformulate the state in a manner more conducive to further analysis. Specifically, we aim to show that the resulting phases of these states, when rewritten as follows, more effectively capture the output strings obtained after applying step 2,

$$|\Psi_1\rangle = e^{\frac{2\pi i \cdot \langle x, z \rangle}{9}} \frac{1}{\sqrt{3}} \sum_{i=0}^2 e^{\frac{2\pi i \cdot \langle x, z^{+i} \rangle - \langle x, z \rangle}{9}} |z^{+i}\rangle \quad (4.62)$$

$$= e^{\frac{2\pi i \cdot \langle x, z \rangle}{9}} \frac{1}{\sqrt{3}} \left( |z\rangle + \sum_{i=1}^2 e^{\frac{2\pi i \cdot (2\langle z^{+i}, x \rangle + \langle \sum_{j \in \{1,2\} \setminus i} \langle z^{+j}, x \rangle)}{9}} |z^{+i}\rangle \right) \quad (4.63)$$

$$= e^{\frac{2\pi i \cdot \langle x, z \rangle}{9}} \frac{1}{\sqrt{3}} \left( |z\rangle + e^{\frac{2\pi i \cdot (|x|/3 + \langle x, (z^{+1})^2 \rangle)}{3}} |z^{+1}\rangle + e^{\frac{2\pi i \cdot (2|x|/3 - \langle x, z^2 \rangle)}{3}} |z^{+2}\rangle \right). \quad (4.64)$$

We begin by highlighting the initial phase component of  $z^{+0}$ , or equivalently  $z$ , by treating it as a universal phase factor. Then, the transition to the second expression is achieved by considering that  $\sum_{i=0}^2 \langle x, z^{+i} \rangle = 3|x|$ , and rewriting the various phase terms. Likewise, given our assumption that  $|x| \bmod 3 = 0$ , the term  $\frac{3|x|}{9}$  will be matching to a multiple of  $2\pi$  and can thus be disregarded.

For the last step, we need to examine the inner products present in the phases. For simplicity, we will analyze the ideal cases where  $z$  is uniformly equal,

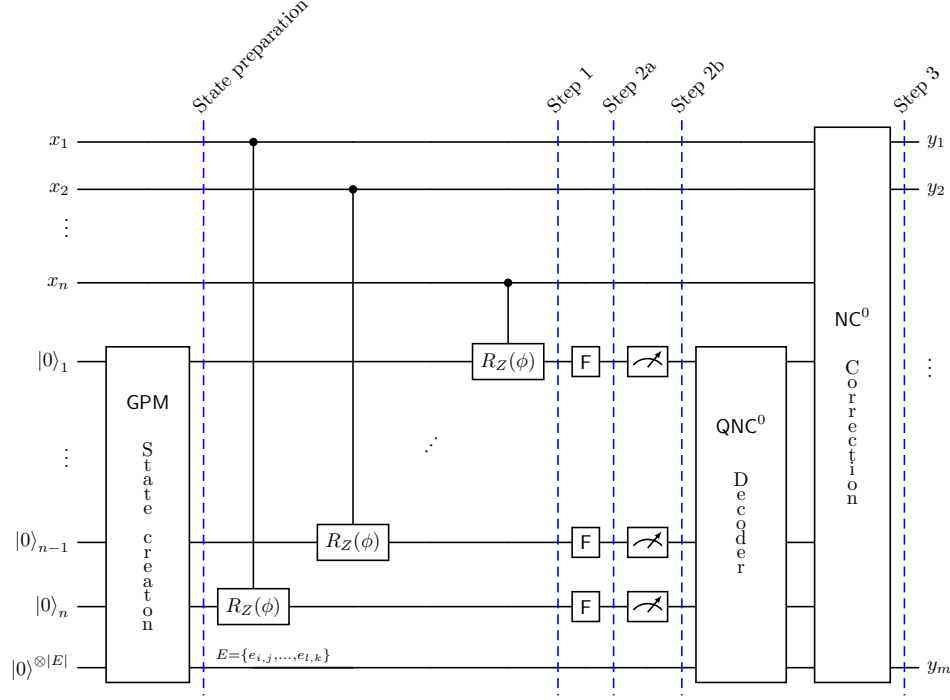


Figure 10: Illustration of a constant-depth quantum circuit solving all instances of the ISMR problems  $\mathcal{R}_p^m$  with parameter  $p$  prime.

Phases	$z = 0^{\otimes n}$	$z = 1^{\otimes n}$	$z = 2^{\otimes n}$
$2\langle z^{+1}, x \rangle + \sum_{j \in \{1,2\} \setminus 1} \langle z^{+j}, x \rangle$	$4 x $	$4 x $	$ x $
$2\langle z^{+2}, x \rangle + \sum_{j \in \{1,2\} \setminus 2} \langle z^{+j}, x \rangle$	$5 x $	$2 x $	$2 x $

Although  $z$  can assume any value in  $\mathbb{F}_3^n$ , we can divide the string into three sub-components corresponding to the aforementioned strings. Specifically, the first term contributes at least  $|x|$  and the second term with  $2|x|$ , while one can introduce additional terms that determine the correct phases based on the specific random string  $z$ . This determination is straightforward due to an additional contribution of magnitude 3 in cases where the bits  $z_i$  are either 0 or 1 for the first phase term, which can be computed using the expression  $\langle x, (z^{+1})^2 \rangle$ . The same principle applies to the second phase, with the additional contribution determinable via the expression  $\langle x, z^2 \rangle$ , resulting in the final expression.

**Step 2.** In this step, we will first apply the respective Fourier gate  $F_3$  to each one of the qudits of the state, and analyze the resulting support of the outcome state,

$$|\Psi_{2a}\rangle = \bigotimes_{l=1}^n F_3 \left( e^{\frac{2\pi i \cdot \langle x, z \rangle}{9}} \frac{1}{\sqrt{3}} \left( |z\rangle + e^{\frac{2\pi i \cdot (|x|/3 + \langle x, (z^{+1})^2 \rangle)}{3}} |z^{+1}\rangle + e^{\frac{2\pi i \cdot (2|x|/3 + \langle x, z^2 \rangle)}{3}} |z^{+2}\rangle \right) \right) \quad (4.65)$$

$$= e^{\frac{2\pi i \cdot \langle x, z \rangle}{9}} \frac{1}{\sqrt{3}} \left( \sum_{y \in \mathbb{F}_3^n} e^{\frac{2\pi i \cdot \langle y, z \rangle}{3}} |y\rangle + e^{\frac{2\pi i \cdot (|x|/3 + \langle x, (z^{+1})^2 \rangle)}{3} + \frac{2\pi i \cdot \langle y, z^{+1} \rangle}{3}} |y\rangle \right. \quad (4.66)$$

$$\left. + e^{\frac{2\pi i \cdot (2|x|/3 + \langle x, z^2 \rangle)}{3} + \frac{2\pi i \cdot \langle y, z^{+2} \rangle}{3}} |y\rangle \right) \quad (4.67)$$

$$= e^{\frac{2\pi i \cdot \langle x, z \rangle}{9} + \frac{2\pi i \cdot \langle y, z \rangle}{3}} \frac{1}{\sqrt{3}} \sum_{y \in \mathbb{F}_3^n} |y\rangle + e^{\frac{2\pi i \cdot (|x|/3 + |y| + \langle x, (z^{+1})^2 \rangle)}{3}} |y\rangle + e^{\frac{2\pi i \cdot (2(|x|/3 + |y|) + \langle x, z^2 \rangle)}{3}} |y\rangle. \quad (4.68)$$

Now, we can analyze the outcomes of the measurements after step 2b. In particular, let's consider the ideal case where the inner products  $\langle x, (z^{+1})^2 \rangle$  and  $\langle x, z^2 \rangle$  are both zero. In this scenario, we find that for

$|x|/3 + |y| \bmod p = 0$ , the three phases are equal to 1, and all the base states  $y$  meeting this criterion are measured with equal probability. Specifically, the strings  $y$ , observed after measurement, are all congruent with the additive inverse of  $|x|/p$ . Also, we do obtain that, whenever the  $|x|/3 + |y| \bmod p$  equals either 1 or 2, it generates all three roots of unity as one can see in Equation (4.68). These basis states then have a zero probability of being observed. This proves that, for these ideal values of the inner products  $\langle x, (z^{+1})^2 \rangle$  and  $\langle x, z^2 \rangle$ , we can perfectly solve the inverse strict modular relation problem  $\mathcal{R}_3^n$ .

Unfortunately, these two additional terms in the phase can take any value in  $\mathbb{F}_3$ , and therefore scramble the outcomes that we intended to observe. Forcing us to analyze all possible cases.

**Step 3.** The final step, is intended to handle the randomness resulting from the inner products in the phases of Equation (4.68). In particular, we can process the outcome such that we increase the probability of having the correct outcomes to the desired relation problem at hand. Moreover, we will list all possible values, and divide their analysis into three cases.

Case 1	$a_1$	$b_1$	$c_1$	Case 2	$a_2$	$b_2$	$c_2$	Case 3	$a_3$	$b_3$
$\langle x, (z^{+1})^2 \rangle$	1	1	0	$\langle x, (z^{+1})^2 \rangle$	2	2	0	$\langle x, (z^{+1})^2 \rangle$	2	1
$\langle x, z^2 \rangle$	2	0	2	$\langle x, z^2 \rangle$	1	0	1	$\langle x, z^2 \rangle$	2	1

**Case 1.** For the assignment of values to the inner product displayed in  $a_1$ , the measured strings  $y$  are congruent with the additive inverse of  $|x|/3 + 1$ , due to the phases being related to  $|x|/3 + |y| + 1 \bmod 3 = 0$ . Furthermore, in cases  $b_1$  and  $c_1$ , we obtain strings  $y$  that fulfill the same property with a probability of  $1/2$ .

In these scenarios, more than half of the subcases map to an incorrect string. However, more than half of the subcases also map to a string that deviates by the addition of two to its Hamming weight. This effect can be simply countered by adding the value 1 (it's additive inverse). Nevertheless, this addition must be informed by the specific cases under consideration. Therefore, we will use the term  $\langle x, (z^{+1})^2 \rangle$  for this purpose, and the method to construct this value will be described later. Ultimately, given that the probability of event  $a$  is non-zero, all these cases map to the correct string with a probability greater than  $1/2$ .

**Case 2.** For  $a_2$ , we encounter the inverse scenario of  $a_1$ . In this case, the states are projected onto strings that are equal to the additive inverse of  $(|x|/3 + 2)^{-1}$ , resulting in a shift of 1 from the correct Hamming weights. The subcases described in  $b_2$  and  $c_2$  exhibit a similar effect, mapping to the correct string half of the time, while in the other instances, the strings have their correct Hamming weights increased by one.

It's noteworthy that, by applying the same correction as in case 1, specifically the term  $\langle x, (z^{+1})^2 \rangle$ , the strings in  $a_2$  which were all previously shifted, are now corrected. Furthermore, the two subcases  $b_2$  and  $c_2$  continue to map correctly half of the time. This, following the same line of reasoning presented previously, demonstrates that for all these cases, the input strings are mapped to the correct result with a probability greater than  $1/2$ .

**Case 3.** The last two cases,  $a_3$  and  $b_3$  are instances where both map with a probability of  $1/2$  to the two incorrect strings. These strings are congruent to  $(|x|/3 + 1)^{-1}$  and  $(|x|/3 + 2)^{-1}$ . Therefore, by applying our correction term  $\langle x, (z^{+1})^2 \rangle$ , we ensure that one of them is correctly mapped in both scenarios, thus correctly solving half of these instances. Additionally, by considering the ideal case discussed initially, which is unaffected by the corrections, more than half of the outcome strings are correct.

**Correction string.** Finally, as previously demonstrated, our correction is effective in all cases, ensuring consistency across all computed probabilities. As a result, we obtain final measured strings capable of solving the problem with a probability greater than  $1/2$ , given any  $|GPM\rangle$  characterized by arbitrary  $z$  and  $G$ . However, to fully substantiate this conclusion, one must demonstrate that the term  $\langle x, (z^{+1})^2 \rangle$  can be computed using an  $NC^0$  circuit. To achieve this, we can compute this value using the following expression,

$$\langle x, (z^{+1})^2 \rangle = \sum_{i \in [n]} x_i \cdot \left( \sum_{e_{i,j} \in Path(i,c)} (-1)^{|Path(i,j)| + |Path(i,c)|} e_{i,j} + z_c + 1 \right)^2 \bmod 3. \quad (4.69)$$

The inner sum  $\sum_{e_{i,j} \in Path(i,c)} (-1)^{|Path(i,j)| + |Path(i,c)|} e_{i,j}$  can be constructed by enumerating the values of the edge measurements along the respective paths. Then, achieving the sum of the two values  $z_0$  and 1 can be straightforwardly accomplished by appending these digits to the string. To realize the square, we only

need to generate all the terms that would result from squaring this expression and perform the individual multiplication operations over  $\mathbb{F}_3$  for these elements. Subsequently, all these bits are multiplied with the respective input bit  $x_i$ , and this process is repeated for all values of  $i$  in the outer sum. The total number of sums is  $n$  while using the largest path  $g$  we have that the exponentiation creates  $g^2$  terms at most and we end up with  $ng^2$  size correction string.

We have been describing these operations over  $\mathbb{F}_3$ , but one can perform these operations over  $\mathbb{F}_2$  using an inverse of the Hamming encoding and the respective logical operations considering our encoding. This approach allows us to use an  $\text{NC}^0$  circuit for this reduction after using a  $\text{QNC}^0$  decoder to map the measured dits to bits. Finally, the binary version of the string  $\langle x, (z^{+1})^2 \rangle$  is added to the measurement outcomes from stage 3, as previously described, thereby concluding the proof.  $\square$

The generalization to arbitrary qupits does follow the same ideas as previously. However, the states generated by the randomness of the qubit poor-mans cat states are more evolved. This will be encapsulated in the following lemmas, with the added consideration that one can solve the modular inverted strict relation problems closer to the correct outcomes within the Abelian domains and with a probability that exceeds mere random guessing.

**Lemma 4.26.** *A  $\text{QNC}^0$  circuit, denoted as  $C_q$ , is given a state  $|\text{GPM}_p^n\rangle$ , the corresponding graph  $G$ , and a set of measured edges  $E = \{e_{i,j}, \dots, e_{l,k}\}$ . This circuit is capable of solving the modular relation problem, represented as  $\mathcal{R}_p^m$ , across a uniform distribution  $\mathcal{D}_p$  of strings that satisfy the condition  $\sum_{i=1}^n x_i \bmod p = 0$  within  $\mathbb{F}_2^n$ . It achieves this with a success probability of  $\frac{2p-2}{p^2}$  for any given input. Moreover, it maintains an average correlation with the correct outcome within the Abelian domain,*

$$\text{Corr}_{\mathcal{D}_p}(C, \mathcal{R}_p^m) = \frac{p-1}{p^2}. \quad (4.70)$$

In this context,  $m = n \cdot g^{p-1}$ , where  $m$  represents the size of the outcome string. This size is influenced by  $g$ , which is the length of the longest path within  $G$  from any vertex to a designated vertex that minimizes the greatest distance to all other vertices.

*Proof.* To prove this, we will once again consider the circuit that effectively achieves this. In particular, we will revisit the circuit presented in Figure 10, as it possesses the structure necessary to solve all ISMR problems by simply adapting the correct prime-dimensional Hilbert space for each stage. Starting, with the consideration that a resource state for the form of a  $|\text{GPM}_p^n\rangle$  state will be provided in addition to the corresponding graph  $G$  and string  $E$  for the measured edges in the state preparation.

**Step 1.** The first step applies controlled qudit  $Z$  rotations parameterized by the angle  $\phi = \frac{2\pi}{p^2}$  to the resource state, while the control bits of each one of these rotations will refer to the input string  $x$ . Obtaining with that the following state,

$$|\Psi_1\rangle = \bigotimes_{i=1}^n R_z\left(\frac{2\pi x_i}{p^2}\right) |\text{GPM}_p^n\rangle = \frac{1}{\sqrt{p}} \sum_{i=0}^{p-1} e^{\frac{2\pi i \langle x, z^{+i} \rangle}{p^2}} |z^{+i}\rangle \quad (4.71)$$

$$= e^{\frac{2\pi i \cdot \langle x, z \rangle}{p^2}} \frac{1}{\sqrt{p}} \left( |z\rangle + \sum_{i=1}^{p-1} e^{\frac{2\pi i \cdot (2\langle z^{+i}, x \rangle + (\sum_{j \in \{1, \dots, p-1\} \setminus i} \langle x, z^{+j} \rangle))}{p^2}} |z^{+i}\rangle \right) \quad (4.72)$$

$$= e^{\frac{2\pi i \cdot \langle x, z \rangle}{p^2}} \frac{1}{\sqrt{p}} \left( |z\rangle + \sum_{i=1}^{p-1} e^{\frac{2\pi i \cdot (i|x|/p + (\sum_{j \in \{1, \dots, i\}} \langle x, z^{+j} \rangle)^{p-1})}{p}} |z^{+i}\rangle \right). \quad (4.73)$$

All the reductions until the last transition from Equation (4.72) to Equation (4.73) follow exactly equally as the reduction from Lemma 4.25. For the last, one does need to redo the analysis of the contribution to the resulting phases by each string of the type  $z = 0^n, 1^n, \dots, (p-1)^n$ . In particular, one can determine that for these values of  $z$ , we have that,



Phases	$z = 0^{\otimes n}$	$\dots$	$z = (p-2)^{\otimes n}$	$z = (p-1)^{\otimes n}$
$2\langle z^{+1}, x \rangle + \dots$	$(p\Pi(p) - p + 1) x $	$\xleftrightarrow{r}$	$(p\Pi(p) - p + 1) x $	$(p\Pi(p) - 2p + 1) x $
$2\langle z^{+2}, x \rangle + \dots$	$(p\Pi(p) - p + 2) x $	$\xrightarrow{r}$	$(p\Pi(p) - 2p + 2) x $	$(p\Pi(p) - 2p + 2) x $
$\vdots$	$\vdots$	$\dots$	$\vdots$	$\vdots$
$2\langle z^{+(p-1)}, x \rangle + \dots$	$(p\Pi(p) - 1) x $	$\xleftarrow{r}$	$(p\Pi(p) - p - 1) x $	$(p\Pi(p) - p - 1) x $

with  $\Pi(p)$  representing the prime counting function, which determines the number of primes up to and including  $p$ . Additionally, the symbol  $\xleftrightarrow{r}$  indicates that the value on the left and right repeats for all strings  $z$  in between. In contrast,  $\xrightarrow{r}$  signifies that the value from the preceding string is repeated for all intermediate strings, while  $\xleftarrow{r}$  implies that the value from the string on the right is repeated in between.

Using these phases it is easy to account for all the terms contributions in the phase by the internal product of the input with the random string  $z$  in Equation (4.73).

**Step 2.** Subsequently, we will consider the effect of applying the respective Fourier gates  $F_p$  to the qudits of the resource state. More precisely we obtain the following states,

$$|\Psi_{2a}\rangle = \bigotimes_{l=1}^n F_p \left( e^{\frac{2\pi i \cdot \langle x, z \rangle}{p^2}} \frac{1}{\sqrt{p}} \left( |z\rangle + \sum_{i=1}^{p-1} e^{\frac{2\pi i \cdot (i|x|/p + (\sum_{j \in 1, \dots, i} \langle x, (z^{+j})^{p-1} \rangle))}{p}} |z^{+i}\rangle \right) \right) \quad (4.74)$$

$$= e^{\frac{2\pi i \cdot \langle x, z \rangle}{p^2}} \frac{1}{\sqrt{p}} \left( \sum_{y \in \mathbb{F}_p^n} e^{\frac{2\pi i \langle y, z \rangle}{p}} |y\rangle + \sum_{i=1}^{p-1} e^{\frac{2\pi i \cdot (i|x|/p + (\sum_{j \in 1, \dots, i} \langle x, (z^{+j})^{p-1} \rangle))}{p} + \frac{2\pi i \langle y, z^{+j} \rangle}{p}} |y\rangle \right) \quad (4.75)$$

$$= e^{\frac{2\pi i \cdot \langle x, z \rangle}{p^2} + \frac{2\pi i \langle y, z \rangle}{p}} \frac{1}{\sqrt{p}} \left( \sum_{y \in \mathbb{F}_p^n} e^{\frac{2\pi i \langle y, z \rangle}{p}} |y\rangle + \sum_{i=1}^{p-1} e^{\frac{2\pi i \cdot (i|x|/p + |y| + (\sum_{j \in 1, \dots, i} \langle x, (z^{+j})^{p-1} \rangle))}{p}} |y\rangle \right). \quad (4.76)$$

The resulting state from step 2a will then be measured. Once again, if all the inner products of the type  $\langle x, (z^{+i})^{p-1} \rangle$  are equal to zero, the final string  $y$  measured will fulfill  $|x|/p + |y| \bmod p = 0$ . Therefore, it would produce the correct outcome for each of the inverse strict modular relation problems.

Regrettably, the values of these terms vary across the field  $\mathbb{F}_p$ . However, they assume uniformly random values within  $\mathbb{F}_p$ , facilitating the prediction of precise outcomes. More precisely, this allows us to consider the support of the outcome strings and their respective probabilities based on these values and the input strings.

In particular, for this, we will consider all possible vectors such as  $(0, 0, \dots, 0)$  and  $(0, 1, 2, \dots, p-1)$  to  $(p-1, 0, 1, \dots, p-2)$  with a simple inline shift, which represents the values of the terms  $\langle x, (z^{+i})^{p-1} \rangle$  that induce a shift in the correct outcome by an increment of 0 and 1 to  $p-1$ , respectively. Following this representation, we can assert that it is possible to decompose any of the possible values that these terms might adopt into vectors of the form  $(a_1, a_2, \dots, a_{p-1})$ . The degree of overlap between these vectors and the aforementioned basis vectors directly determines the probability of measuring a string offset related to the corresponding basis vector. Given this description and the uniform distribution of all  $a_i$  within  $\mathbb{F}_p$ , the probability of yielding each shift relative to the accurate outcome string is uniform. This ensures that a correct string is produced with a probability of  $1/p$  and every incorrect string equally with a probability of  $1/p$ .

**Step 3.** This process now aims to use the information provided by the state's creation, which defines the random string  $z$ , to increase the probability of accurately computing the solutions to inverse strict modular relation problems.

To achieve this, we will begin by analyzing the vectorization that determines the probability of obtaining the outcome with a shift in its Hamming weight originating from the randomness in the creation of the generalized poor man's cat state. More specifically, we consider the use of a single term representative of one of the inner product terms  $\langle x, (z^{+i})^{p-1} \rangle$ . Thus, by selecting the first  $a_1$  from  $(a_1, a_2, \dots, a_n)$  and then adding the inverse shift associated with  $(a_1, a_1 + 1, a_1 + 2, \dots, a_1 + (p-1))$ , we ensure that the outcome string

is corrected for this component. In particular, we find that the outcome strings are shifted based on the inner product with a vector of the type  $(0, a_2^*, a_3^*, \dots, a_{p-1}^*)$  and all the basis vectors, with all the values  $a_2^*, a_3^*, \dots, a_{p-1}^*$  remaining uniformly random over  $\mathbb{F}_p$ .

This ensures that the overlap with a zero shift is  $\frac{2p-2}{p^2}$ , and all the other shifts from 1 to  $p-1$  have probability  $\frac{p-1}{p^2}$ . Also, the average overlap with the correct outcomes within the Abelian domains can be determined as being

$$\text{Corr}_{\mathcal{D}_p}(|C|, |\mathcal{R}_p^m|) = \frac{p}{2^n} \sum_{\substack{x \sim \mathbb{F}_2^n \\ |x| \bmod p = 0}} \text{Re} \left( e^{-i \frac{2\pi |C_q(x)|}{p}} e^{i \frac{2\pi |\mathcal{R}_p^m(x)|}{p}} \right) \quad (4.77)$$

$$= \frac{p-1}{p^2}, \quad (4.78)$$

with  $\mathcal{D}_p$  being the uniform distribution over string in  $\mathbb{F}_2^n$  that satisfy  $|x| \bmod p = 0$ .

This value can be easily obtained by dividing the probabilities of having a shift as follows: with a probability of  $\frac{p-1}{p^2}$ , there is no shift at all, and with a probability of  $1 - \frac{p-1}{p^2}$ , there is a uniform distribution of shifts. Therefore, the second fraction of shifts does not contribute to the value, as this represents a sum over all the values for the roots of unity with equal probability and equals zero. Simultaneously, a  $\frac{p-1}{p^2}$  fraction of the inputs contributes to the value 1.

**Correction string.** For the correction, we only need to guarantee that the term  $\langle x, (z^{+1})^{p-1} \rangle$  is computationally possible to produce within the considered class such that we can sum it to the outcome string  $y$ . To achieve this, we consider that we can determine this value using the following expression,

$$\langle x, (z^{+1})^{p-1} \rangle = \sum_{i \in [n]} x_i \cdot \left( \sum_{e_{i,j} \in \text{Path}(i,c)} (-1)^{|\text{Path}(i,j)| + |\text{Path}(i,c)|} e_{i,j} + z_c + 1 \right)^{p-1} \bmod p. \quad (4.79)$$

The inner sum  $\sum_{e_{i,j} \in \text{Path}(i,c)} (-1)^{|\text{Path}(i,j)| + |\text{Path}(i,c)|} e_{i,j}$  can be constructed by enumerating the edge measurement results along the respective paths. Additionally, the sum of the values  $z$  and 1 can be straightforwardly achieved by appending these values to the string. To exponentiate, it is sufficient to create all the terms that result from this sequence of products, and since the exponent is finite, each term is a product involving at most  $p-1$  terms, making them all efficiently computable. These terms are then multiplied in  $\mathbb{F}_p$  with the respective input bit  $x_i$ . The total number of sums is  $n$  while using the largest path  $g$  we have that the exponentiation creates  $g^{p-1}$  terms at most and we end up with  $ng^{p-1}$  size correction string.

Similar to the qutrit case, one can use a  $\text{QNC}^0$  decoder to map the measured dits to bits based on an inverse of the Hamming encoding. Therefore, all the previously described operations over  $\mathbb{F}_p$  can be performed over  $\mathbb{F}_2$  using the respective logical operations with an  $\text{NC}^0$  circuit. In conclusion, the string  $\langle x, (z^{+1})^{p-1} \rangle$  in bits is concatenated with the measurement outcomes from stage 3, thereby concluding the proof.  $\square$

## Quantum vs. Classical circuit separations

We will now combine the lower bounds determined for  $\text{NC}^0$  and  $\text{bPTF}^0[k]$  circuits in [Section 4.2.2](#) with the upper bounds established for  $\text{QNC}^0$  circuits in this section to derive new quantum-classical separations. We begin by stating explicit separations of qupit  $\text{QNC}^0$  circuits against  $\text{NC}^0$  circuits.

**Theorem 4.27.** *For every ISMR problem defined for a prime dimension  $p$ , denoted by  $\mathcal{R}_p^m$ , considering a uniform distribution  $\mathcal{D}_p$  over  $\mathbb{F}_2^n$  of strings with Hamming weight that satisfies  $(\sum_{i=1}^n x_i) \bmod p = 0$  as the input distribution, there exists a  $\text{QNC}^0$  circuit with all-to-all connectivity that solves the problem for  $m = n \cdot \log n^{p-1}$  archiving a correlation with the correct outcome of  $\frac{p-1}{p^2}$ . In contrast, any  $\text{NC}^0/\text{rpoly}$  circuit with locality  $l$  fails to solve this problem with a correlation larger than,*

$$\text{Corr}_{\mathcal{D}_p}(C, \mathcal{R}_p^m) = \mathcal{O} \left( \text{Re} \left( \frac{2^{1-p} e^{\frac{2\pi i}{p^2}} \left( e^{-\frac{2\pi i}{p^2}} \left( 1 + e^{\frac{2\pi i}{p^2}} \right) \right)^p}{1 + e^{\frac{2\pi i}{p^2}}} \right)^{\frac{n}{\log n(p-1)^{4l^2}}} \right). \quad (4.80)$$

In particular, for  $p = 3$  there exist a  $\text{QNC}^0$  circuit with 3D connectivity that solves this specific ISMRP instance for  $m = n^{4/3}$  with an efficiency larger the  $1/2$  on all inputs, while the success probability for any  $\text{NC}^0/\text{rpoly}$  is bound by

$$\Pr_{\substack{x \sim \mathbb{F}_2^n \\ |x| \bmod 3 = 0}} [C(x) \in R_3^m(x)] \leq \frac{1}{3} + \left(\frac{9}{10}\right)^{\frac{n^{2/3}}{16t^2}}. \quad (4.81)$$

*Proof.* We consider the upper bound determined in Lemma 4.26 to ascertain the correlation with which one can compute each of the ISMR problems using a  $\text{QNC}^0$  circuit with all-to-all connectivity. Concurrently, we refer to Lemma 4.19 for the classical lower bound of the same quantity, utilizing the values for  $m = n \cdot \log n^{p-1}$  obtained by the quantum solution and the considered input distribution.

For the specific case where  $p = 3$ , we examine the lower bound on the success probability determined in Lemma 4.25 for a qutrit  $\text{QNC}^0$  circuit with 3D connectivity, alongside the classical lower bound in Lemma 4.19 for the respective input distribution and output size of  $m = n^{4/3}$ .  $\square$

The previous separation can be extended using the techniques from the works of [Gal19; CSV21] for parallel repetitions, such that the success probability decreases exponentially fast to zero. This results in an exponential separation between the quantum and classical efficiencies, specifically for  $\text{QNC}^0$  and  $\text{NC}^0$  circuits, across the entire class of inverted strict modular relation problems. Additionally, due to our findings in Corollary 4.20, it is possible to accelerate this convergence. A different input distribution allows for larger worst-case separations. We do not explicitly determine these results, as they are not the main focus of this document, and we intend to further explore the separation against the  $\text{bPTF}^0[k]$  class.

Finally, we combine the lower bounds for  $\text{bPTF}^0[k]$  and quantum upper bounds for the same problems. We determine that one can achieve separation between  $\text{QNC}^0$  and  $\text{bPTF}^0[k]$  using any prime instance of the inverted strict modular relation problems with the asymptotically largest possible value of  $k$ .

**Proof of Theorem 4.12.** The quantum upper bound is derived by combining Lemma 4.24 and Lemma 4.26, which determines the precise correlation  $\frac{p-1}{p^2}$ . The output size  $m$ , which allows us to solve each of the problems using a  $\text{QNC}^0$  circuit over qutrits, follows from considering the all-to-all connectivity. Specifically, it is defined that the minimum-maximum path  $g$  in the graph will have a size of  $\log n$ , which in turn defines  $m$  to be  $n \cdot \log n^{p-1}$ .

Simultaneously, the classical lower bounds are derived by considering Lemma 4.21, with all parameters being defined by the quantum solution. Furthermore, all additional values for the expressions, as well as the optimal values of  $q$ , are determined in the same manner as in Theorem 4.2.  $\square$

Finally, as one can determine success probabilities for the ISMRP  $\mathcal{R}_p^m$  where  $p = 3$ , just as one can for the binary case where  $p = 2$ , we can establish a separation in the success probabilities for this problem. Additionally, this case is particularly intriguing as it demonstrates that all instances of the  $\mathcal{R}_3^m$  problem can be solved with a probability strictly greater than  $1/2$  in the quantum case, whereas any classical circuit solves the problem with at most a probability asymptotically close to random guessing, which for this problem corresponds to a success probability of  $1/3$ . This indicates that  $\text{QNC}^0$  effectively addresses the probabilistic version of  $\mathcal{R}_3^m$ , adhering to the standard definition for bounded-error probabilistic problems, while any classical circuit within the  $\text{bPTF}^0[k]$  class fails to solve the same problem. Furthermore, the quantum circuit can exhibit this advantage while maintaining geometric locality in a 3D geometry.

**Proof of Corollary 4.13.** We derive the lower bounds for the probabilities of the quantum solution using Lemma 4.25 and the parameters  $m = n^{4/3}$  from the specific 3D connectivity.

Then, we consider the lower bounds for the probability of solving the  $\mathcal{R}_3^{n^{4/3}}$  defined by Lemma 4.17. Finally, the determination of the values of  $q$  for both values of  $k$  follows equally as in Theorem 4.2.  $\square$

In conclusion, all the newly derived bounds, including those applicable to the qubit scenario, could potentially be extended with parallel repetition games, thereby enhancing the quantum advantage even further. We have not yet pursued this path, as our focus has been on expanding the problem set and tightening the bounds. Our priority is to establish unconditional separations against broader and more powerful classes of classical circuits, aiming to reduce the resources needed for a quantum advantage. This is

because parallel repetition games only become valuable once the initial problem set, which is to be repeated, has achieved a quantum advantage.

## 5 Noise-resilient quantum advantage

In this section, we demonstrate that the separations we proved against  $\text{bPTF}^0[k]$  in the preceding section can be made noise-robust. Specifically, we show that a separation can still be achieved even when our quantum circuits are noisy and classical circuits are noiseless. As before, we present the qubit and qubit cases separately.

Both separations are proven for new noise-tolerant relations  $\mathfrak{R}_p$ , defined based on the ISMR problems as follows.

**Definition 5.1.** Let  $\mathcal{R}_p : \mathbb{F}_p^n \mapsto \mathbb{F}_p^{n'}$  be the original ISMR problem (Definition 4.1). Then, the noise tolerant extension  $\mathfrak{R}_p : \mathbb{F}_p^n \times \mathbb{F}_p^{n' \cdot m} \mapsto \mathbb{F}_p^{n'}$  is defined as follows,

$$\mathfrak{R}_p(x, y) = \left( \left| \mathcal{R}_p^{n'}(x) \right| - \left| \text{DEC}^*(y) \right| \right). \quad (5.1)$$

Here  $\text{DEC}^*$  is an arbitrary functions of the form  $\text{DEC}^* : \mathbb{F}_p^{n' \cdot m} \mapsto \mathbb{F}_p^{n'}$  which must be computable by an  $\text{AC}^0$  circuit.

We begin by presenting our noise-robust separation for qubits with arbitrary prime  $p$ , which is the more intricate case. Notably, for qubits with  $p \geq 3$ , the quantum circuits solving the candidate relation problems are not Clifford circuits. This necessity arises because Bell violations with stabilizer states alone do not generalize from qubits to qubits with  $p \geq 3$  [Gro06; HBV13; MŠM<sup>+</sup>24]. This indicates that quantum strategies can not have larger winning probabilities than classical ones if only Clifford circuits are considered for general qubits. Therefore, for this separation, we require quantum advice states, specifically magic states in their logical form, with the same code distance under which the remaining quantum circuit will operate. This requirement stems from the additional conjecture that any magic state factory that creates a logical magic state with at least  $\text{poly}(\log n)$  code distance is not realizable within  $\text{QNC}^0$ . Simultaneously, we must resolve the incompatibilities between the presented quantum circuits, solving the ISMR problems from Section 4.2.3, and the quantum circuit architecture for non-Clifford circuits described and proven to be noise-resistance in Section 5.1, Section 5.1.1 and Section 5.1.2. Solving the previous incompatibility involves demonstrating that quantum circuits equipped with non-adaptive magic state injection gadgets can solve all the ISMR problems with equal effectiveness, as shown in Section 5.2.1.

**Theorem 5.2.** Let  $x$  be an input drawn uniformly at random from the subset of  $n$ -bit strings with Hamming weight satisfying  $(\sum_{i=1}^n x_i) \bmod p = 0$ . Consider the local stochastic noise  $\mathcal{E} \sim \mathcal{N}(\tau)$  with bounded probability  $\tau < \tau_{th}$ . Then, there is a  $\text{QNC}^0 / |\overline{T^{1/p}}\rangle$  circuit that solves the relation  $\mathfrak{R}_p(x, y)$  for output strings  $y = o(n^2)$  with a constant positive correlation.

Further, any circuit  $C \in \text{bPTF}^0[k]/\text{rpoly}$  with fixed depth  $d$  and size  $s$ , for large enough  $d' \in \mathbb{N}^+$  has exponentially small correlation with  $\mathfrak{R}_p$  bounded by

	$k = \mathcal{O}(1) \ (\equiv \text{AC}^0/\text{rpoly})$	$k = n^{1/(5d)}$
$\text{Corr}_{\mathcal{D}_p}(\mathfrak{R}_p(x, C(x)))$	$\exp \left( -\Omega \left( \frac{n^{1-\mathcal{O}(1)}}{(\log n)^{p-1} (\log s)^{2(d+d')-2}} \right) \right)$	$\exp \left( -\Omega \left( \frac{n^{3/5-\mathcal{O}(1)}}{(\log n)^{p-1} (\log s)^{2(d+d')-2}} \right) \right)$

We also obtain a separation for the qubit case. Later in this section, we highlight the distinctions between the two cases. However, the main difference is that the qubit case allows for an advice-free separation between the noisy  $\text{QNC}^0$  and noiseless  $\text{bPTF}^0[k]$  circuits. Therefore, we will with our qubit separation lift the previously proven noise-resilient separations from  $\text{NC}^0$  and  $\text{AC}^0$  to  $\text{bPTF}^0[k]$  for optimal  $k$  [BGK<sup>+</sup>20; CCK23].

**Corollary 5.3.** *Let  $x$  be an input drawn uniformly at random from the set of binary even strings. Consider the local stochastic noise  $\mathcal{E} \sim \mathcal{N}(\tau)$  with bounded probability  $\tau < \tau_{th}$ . Then, there is a  $\text{QNC}^0$  circuit that solves the relation  $\mathfrak{R}_2(x, y)$  for output string  $y = o(n^2)$  with a constant probability bounded away from  $1/2$ . However, any circuit  $C \in \text{bPTF}^0[k]/\text{rpoly}$  with fixed depth  $d$  and size  $s$ , for parameter  $k = 1/(5d)$  large enough  $d' \in \mathbb{N}^+$  has exponentially small correlation with  $\mathfrak{R}_2$  bounded by*

$$\Pr[\mathfrak{R}_p(x, C(x)) = 0] = \frac{1}{2} + \exp\left(-\Omega\left(\frac{n^{3/5-\mathcal{O}(1)}}{(\log s)^{2(d+d')-1}}\right)\right). \quad (5.2)$$

The correlation bounds previously described differ from the noise-free bounds in [Theorem 4.12](#), particularly in the exponent of the  $\log(s)$  term, which arises from the additional overhead for error correction. However, this does not compromise the exponential deviation between the classical and quantum correlations achieved by the respective circuit classes.

To demonstrate these separations with higher-dimensional systems, we show that the roadmap established in [\[BGK<sup>+</sup>20\]](#) for the qubit case can be adapted to extend this advantage in the presence of noise. We will proceed in several steps. First, we outline the requirements for the fault-tolerant construction in constant depth for the higher-dimensional versions of the code, including the additional state injection. Next, we introduce a new decoder for the surface code over qudits, highlighting the differences between the two cases. Then, we generalize the single-shot state preparation for the two-qudit states known as  $\text{GHZ}_2$  (generalized qudit Bell states). Finally, we identify new non-adaptive qupit circuits based on the magic state injection gadget, solving the new noise-resilient relation problems to establish our bounds against  $\text{bPTF}^0[k]$ .

## 5.1 Noise-resilient qupit Clifford circuits with quantum advice

To demonstrate our noise-robust separations, we introduce constant-depth quantum circuits that incorporate logical quantum states as advice, as illustrated in [Figure 11](#). This model adopts the structure used in standard error-corrected quantum circuits with magic state injection, presenting broader interest. It is important to note, however, that while our circuit architecture is noise-robust, it does not support the noise-resilient realization of adaptive quantum circuits that include gates controlled by prior measurement outcomes. Instead, it is limited to noise-resilient, non-adaptive constant-depth Clifford circuits with magic state injection. Thus, we restrict our analysis to a subset of  $\text{QNC}^0$  circuits for a noise-resilient version of these circuits.

The difficulty in realizing adaptive measurements in a noise-resilient manner arises because the code distance necessary for good error correction properties unfortunately also requires the execution of the decoding function, which is beyond the computational capabilities of  $\text{QNC}^0$  circuits with the considered codes and decoder. This creates a conundrum where either the noise levels render the outcome useless or the information is recoverable but not by the circuit class  $\text{QNC}^0$  itself. Therefore, we focus on non-adaptive constant-depth Clifford circuits with magic state injection, which we will show in [Section 5.2.1](#) are sufficient to obtain noise-robustness for our qupit separations.

In particular, we will consider the conditions a quantum error correcting code must satisfy, so that we may use it to obtain a noise-resilient version of circuits with this structure. We will prove that these conditions are sufficient, and subsequently demonstrate that the qupit surface code, along with the hard normalization decoder, fulfills all the requirements for a noise-resilient execution of a non-adaptive Clifford circuit with advice states.

**Definition 5.4** (noise-resilient constant-depth quantum code conditions). *A CSS-type code  $Q_m$  exhibiting the following properties gives constant depth fault tolerant circuit constructions for qudit local stochastic noise  $\mathcal{E} \sim \mathcal{N}(\varrho)$ .*

1. *Any qudit advice state  $|A\rangle$  required must be provided in its logical form  $|\overline{A}\rangle$ , while being affected by local stochastic noise  $\mathcal{E}_A \sim \mathcal{N}(\tau)$  at most as follows,*

$$|\overline{A}\rangle \propto \mathcal{E}_A \text{PREP}(|A\rangle) |0\rangle^{\otimes(|A| \cdot m)}. \quad (5.3)$$

where  $\text{PREP}(|A\rangle)$  represents the noise-free quantum circuit that prepares the logical state  $|\overline{A}\rangle$  over a code of distance  $m$ .

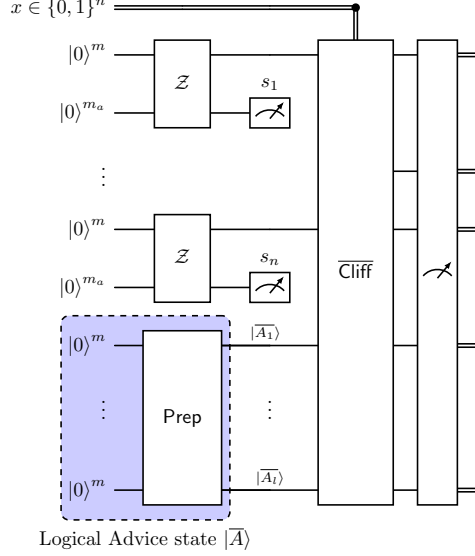


Figure 11: Constant-depth non-adaptive Clifford quantum circuit with quantum advice states.

2. The logical qudit Clifford gates can be implemented in constant depth (as defined in [Section 3.4](#)).
3. There exist recovery and repair functions

$$\begin{aligned} \text{REC} : \mathbb{F}_p^{m_a} &\mapsto \text{Pauli}(m) \\ \text{REP} : \text{Pauli}(m + m_a) &\mapsto \text{Pauli}(m) \end{aligned}$$

respectively, where  $\text{Pauli}(n)$  represents a Pauli operator over  $n$  qupits, such that the application of a constant depth Clifford circuit  $\mathcal{Z}$  on the state  $|0\rangle^{\otimes m} \otimes |0\rangle^{\otimes m_a}$  followed by the  $Z$ -measurement of its ancillary qudits, leading to an outcome  $s \in \mathbb{F}_p^{m_a}$ , can be represented by the channel

$$(|s\rangle\langle s| \otimes \text{REC}(s)) \mathcal{Z} \left( |0\rangle^{\otimes m} \otimes |0\rangle^{\otimes m_a} \right) \propto |\bar{0}\rangle \otimes |s\rangle, \quad (5.4)$$

where  $|\bar{0}\rangle$  represents the logical zero state. In the case of local stochastic noise  $\mathcal{E} \sim \mathcal{N}(\varrho)$ , this becomes

$$(|s\rangle\langle s| \otimes \text{REC}(s)) \mathcal{E} \mathcal{Z} \left( |0\rangle^{\otimes m} \otimes |0\rangle^{\otimes m_a} \right) \propto \text{REP}(\mathcal{E}) |\bar{0}\rangle \otimes |s\rangle, \quad (5.5)$$

for a local stochastic function  $\text{REP}(\mathcal{E}) \sim \mathcal{N}((c'\varrho)^{c''})$ .

4. There exists a decoding function  $\text{DEC} : \mathbb{F}_p^m \mapsto \mathbb{F}_p$  such that

$$\text{DEC}(y) := \text{Mod}_p(y), \quad (5.6)$$

for  $y \in \mathbb{F}_p^m$  such that  $y$  belongs to the space of all basis vector obeying  $Z$ -type stabilizers. When subject to noise, for error rate  $q < q_{th}$  i.e. a threshold parameter, and error string  $v \in \mathbb{F}_p^m$  it is the case that

$$\Pr[\text{DEC}(x \oplus v) = \text{Mod}_p(x)] \geq 1 - e^{-(c'm^c)}, \quad (5.7)$$

for some  $c$  and  $c' \in \mathbb{R}_{>0}$ .

We have that any error correction code that fulfills the previous condition, will allow us to realize error resilient version of the any logical quantum circuit with the structure of [Figure 11](#).



**Lemma 5.5.** Let  $\mathcal{EC}_C$  represent the error-corrected version of  $C$ , a logical classically controlled constant-depth Clifford circuit with advice states  $|A\rangle$ . Respecting the structure depicted in Figure 11 and utilizes a quantum error correction code featuring a decoding function DEC, single-shot state preparation circuit  $\mathcal{Z}$ , a recovery function REC, and a repair function REP, all of which meet the conditions specified in Definition 5.4. Then, for an arbitrary input  $x \in \mathbb{F}_2^n$  and denote the outputs of the noisy implementation  $s$  and  $y$  such that  $\mathcal{EC}_C(x) = (s, y)$ , with local stochastic noise  $\mathcal{E} \sim \mathcal{N}(\varrho)$  affecting the circuit execution and  $\mathcal{E}_A \sim \mathcal{N}(\tau)$  the advice state. Then, for  $m = \mathcal{O}(\text{poly log } n)$  and all local stochastic noise with  $\varrho_{th} = 2^{-2^{\mathcal{O}(d)}}$ , where  $d$  is a constant representing the depth of the circuit, the following holds for all  $\tau$  and  $\varrho < \varrho_{th}$ ,

$$\Pr[f(s, y) \equiv C(x)] > 0.99, \quad (5.8)$$

with  $f(s, y) = \otimes_{i=0}^{n-1} \text{DEC}(y_i \oplus w_i)$  for  $w$  such that  $\langle w | \overline{C}(x) \text{REC}(s)^\dagger \overline{C}(x)^\dagger | 0 \rangle^{\otimes n \cdot m} = 1$ .

*Proof.* We start by using the first condition of Definition 5.4, which guarantees that we can describe the advice states as  $|\overline{A}\rangle \propto \mathcal{E}_A \text{PREP}(A) |0\rangle^{\otimes |A| \cdot m}$ , with  $\mathcal{E}_A \sim \mathcal{N}(\tau)$ . Additionally, given that the remainder of the logical circuit is a classically controlled Clifford circuit of constant depth  $C(x)$ , we have, according to condition 2 of Definition 5.4, that its logical version also is a Clifford circuit of constant depth. Therefore, all the Pauli errors that can occur due to the local stochastic noise under consideration can be commuted to the end using Lemma 3.20. Thus, the distribution  $\mathcal{D}_{\mathcal{EC}_C}(x)$  over strings that result from the  $\mathcal{EC}_C(x)$  circuit can be described as follows,

$$\mathcal{D}_{\mathcal{EC}_C}(x) = \langle s, y | \mathcal{E}_t \overline{C}(x) (\mathcal{Z} \otimes I) |0\rangle^{\otimes n \cdot m} |0\rangle^{\otimes n \cdot m_{anc}} |\overline{A}\rangle. \quad (5.9)$$

with  $\mathcal{E}_t = \mathcal{N}(\tau')$  for  $\tau' = \mathcal{O}(\max(\tau^{-2^d}, \varrho^{-2}))$  and  $\varrho$  being the noise level of the local stochastic noise affecting the state preparation circuit  $\mathcal{Z}$  as well as  $C(x)$  and the measurements.

Now, we need to describe the effect of the measurements in the single-shot state preparation to define the support of the circuit's outcome more precisely. For that, we commute the total error back through the Clifford circuit  $\overline{C}(x)$ , which we describe as  $\mathcal{E}'_t = \overline{C}(x) \mathcal{E}_t \overline{C}(x)^\dagger$  and divide  $\mathcal{E}'_t = \mathcal{E}'_{t_1} \otimes \mathcal{E}'_{t_2}$  with  $\mathcal{E}'_{t_1}$  operating over the first  $n \cdot (m + m_{anc})$  qudits, while  $\mathcal{E}'_{t_2}$  operates over the last  $|A|$  qudits of the advice state. Thus, we obtain that for each logical qupit that is affected by  $\mathcal{E}'_{t_1}$  the following equality based on condition 3 of Definition 5.4,

$$(I \otimes |s\rangle \langle s|) \overline{C}(x) (\mathcal{E}'_{t_1} \otimes \mathcal{E}'_{t_2}) (\mathcal{Z} \otimes I) |0\rangle^{\otimes n \cdot m} |0\rangle^{\otimes n \cdot m_{anc}} |\overline{A}\rangle \quad (5.10)$$

$$\propto \overline{C}(x) (I \otimes \mathcal{E}'_{t_2}) \text{REC}(s)^\dagger \text{REP}(\mathcal{E}'_{t_1}) |\overline{0}\rangle^{\otimes n} |s\rangle |\overline{A}\rangle \quad (5.11)$$

$$\propto \overline{C}(x) (\mathcal{E}''_{t_1} \otimes \mathcal{E}'_{t_2}) \text{REC}(s)^\dagger |\overline{0}\rangle^{\otimes n} |s\rangle |\overline{A}\rangle \quad (5.12)$$

$$\propto \mathcal{E}'''_t \overline{C}(x) \text{REC}(s)^\dagger |\overline{0}\rangle^{\otimes n} |s\rangle |\overline{A}\rangle, \quad (5.13)$$

with  $\mathcal{E}''_{t_1} = \text{REC}(s)^\dagger \text{REP}(\mathcal{E}'_{t_1}) \text{REC}(s)$ , and consequently using the proprieties of the local stochastic noise we obtain that  $\mathcal{E}'''_t \sim \mathcal{N}(\tau'')$  with  $\tau'' = \mathcal{O}(\max((c' \tau^{-2^d} \cdot c'')^{-2^d}, (c' \varrho^{-2^d} \cdot c'')^{-2^d}))$ .

Therefore, we now are able to rewrite the distribution  $\mathcal{D}_{\mathcal{EC}_C}(x)$  as follows,

$$\mathcal{D}_{\mathcal{EC}_C}(x) = \langle s, y | \mathcal{E}'''_t \overline{C}(x) \text{REC}(s)^\dagger |\overline{0}\rangle^{\otimes n} |s\rangle |\overline{A}\rangle. \quad (5.14)$$

Subsequently, we have that  $\mathcal{E}'''_t = \omega X(a) Z(b)$ . At this point, we can use condition 4 of Definition 5.4 to define a noise threshold  $q < q_{th}$  based on our local stochastic noise to prove that for  $p < p_{th}$ , given  $p_{th} = \Omega(q_{th}^{\mathcal{O}(1)})$ , we have with exponentially high confidence,

$$\mathcal{D}_{\mathcal{EC}_C}(x) = \langle s, y \oplus a | \overline{C}(x) \text{REC}(s)^\dagger |\overline{0}\rangle^{\otimes n} |s\rangle |\overline{A}\rangle, \quad (5.15)$$

where  $a$  is the vector that defines the  $X(a)$  operator, derived solely from the Pauli  $X$  component of  $\mathcal{E}'''_t$ . The previous assumption on the error threshold then implies that after the error correction process we obtain with exponential high confidence that  $\text{DEC}(y \oplus a) = \text{DEC}(y)$  such that the resulting error corrected distribution is equal to,

$$\mathcal{D}'_{\mathcal{EC}_C}(x) = \langle s, y | \overline{C}(x) \text{REC}(s)^\dagger |\overline{0}\rangle^{\otimes n} |s\rangle |\overline{A}\rangle \quad (5.16)$$

$$= \langle s, y \oplus w | \overline{C}(x) |\overline{0}\rangle^{\otimes n} |s\rangle |\overline{A}\rangle \quad (5.17)$$

for  $w$  such that  $\overline{C}(x)\text{REC}(s)^\dagger \overline{C}(x)^\dagger |0\rangle^{\otimes n \cdot m} = |w\rangle$ .

From the last expression, after applying the function  $f$  defined previously—which corrects possible errors introduced during single-shot state preparations and decodes the error-corrected quantum circuit—we find that the outcome of our circuit  $C$  can be described by  $\langle y | C(x) | 0 \rangle^{\otimes n} | A \rangle$ . Finally, it is important to note that the bounds allow us to achieve this with a probability close to 1.  $\square$

We will demonstrate that the surface code over qupits fulfills all the necessary conditions of [Definition 5.4](#). To begin, we consider the first two conditions. The first one follows trivially, as it is possible to create any quantum state  $|A\rangle$  in its logical version within the surface code, while the local stochastic noise can be seen as a layer of errors occurring after the noise-free state preparation. For condition 2, we need to demonstrate that the Clifford operators are realizable in constant depth. Fortunately, this was shown previously for both the qubit and qudit cases in the work of [\[Mou16\]](#).

**Lemma 5.6** ([\[Mou16\]](#)). *Any qudit Clifford operators  $C$  of prime dimension can be implemented in constant depth with the surface code.*

We turn to proving conditions 3 and 4 in the next two subsections. We first introduce the new decoder under consideration and prove that, when applied to the surface code, it fulfills conditions 3 and 4. Afterwards, we will show that the generalization of single-shot state preparation for qupits, as demonstrated for qubits in [\[BGK<sup>+</sup>20\]](#), holds equally well. We have changed the order of presentation for these two conditions for clarifying the details more coherently.

### 5.1.1 Qupit error threshold

As remarked in [Definition 5.4](#), we need to show that the qupit surface code, along with the selected decoder, achieves the required noise resilience properties. In particular, the higher dimensional case requires several changes, the most important of which is the decoder used. Prior work [\[BGK<sup>+</sup>20\]](#) uses the *minimum weight perfect matching* (MWPM) decoder for the qubit case. We now discuss below why the qupit case needs a different decoder and present our choice, the hard decision renormalization group decoder.

A single physical (Pauli) error on the surface code over qubits generates two defects (i.e. X syndromes), appearing on the vertices  $v_1$  and  $v_2$  that share the edge  $(v_1, v_2)$  where the error was detected, which form the boundary of the error. If we have another error on an adjacent edge  $(v_2, v_3)$ , the defect on the common vertex  $v_2$  cancels out, leaving only the defects on  $v_1$  and  $v_3$ . Hence a succession of adjacent errors generates a path on the surface code with defects on its boundary. One method to tackle such errors is to find the most likely one and correct it. An efficient algorithm for this is to find minimum (Pauli) weight operators representing the errors that connect the defects. This problem can be mapped to a weighted graph where the goal is to find a perfect matching with minimum weight. The MWPM in this case can be solved efficiently [\[diFO<sup>+</sup>24; Edm65\]](#).

This error pattern happens because the Pauli operators in two dimensions (i.e.  $p = 2$ ) are self-inverse, leading to cancellations. However, this is not the case for generalized Pauli operators with  $p > 2$ ; these operators are in general neither self-inverse nor self-adjoint. Hence the intermediate defects do not cancel along a (edge-)path of errors, instead leaving scattered defects throughout the lattice. For  $p > 2$ , the equivalent problem would be to find the perfect matching of *hyperedges* in a  $p$ -uniform hypergraph, a well known NP-hard problem. The MWPM decoder is hence ill-suited to deal with qupits due to efficiency issues.

### Hard-Decision Renormalization Group decoder

A more suitable choice for our case is the Hard-Decision Renormalization Group (HDRG) decoder [\[BH13\]](#). This decoder operates iteratively. In each iteration or level, it considers all the defects (syndromes) in the lattice and groups them into subsets called clusters. The defects are clustered by comparing their pairwise distances with a threshold distance for each level, known as the search distance. All defects with pairwise distance below the threshold are merged into a cluster. Formally, at the  $l$ th level, the search distance is based on a function  $D(l)$ , chosen to be the Chebyshev distance  $D(l) = 2^l$  in [\[BH13\]](#). However, other choices and subsequent improvements have used different metrics or combinations thereof, such as the Manhattan distance and a linear search distance  $D(l) = l + 1$ .

In the first iteration, the decoder considers all the syndrome information and creates the first set of clusters, which then become the inputs for the second iteration. For each cluster at any level, it checks if the sum of the syndrome measurements equals zero modulo  $p$ , the dimension of the qupit system. If the sum is zero, the cluster is called neutral, indicating that a Pauli operator exists that can turn all the syndromes trivial (i.e., remove the defects). If the cluster is neutral, a valid correction operator is recorded, and the cluster is removed from the next iteration. If a cluster is charged (not neutral), it is added to the set of clusters to be grouped in the next iteration or level, where the search distance (defining which clusters are merged) will increase, and the process is repeated. If no cluster is left after the last iteration, which is defined by the largest possible value of the search distance that does not exceed the maximum distance between any two lattice points, the decoder returns the composition of all the Pauli operators determined for all levels so far. Otherwise, it returns failure.

Here, for simplicity, we use the original proposal for the HDRG due to [BH13], but the results can be improved by considering subsequent refinements [ABC<sup>+</sup>14; HLW15]. We start off with the essential definitions required to describe the operational behaviour of this decoder, which will help us prove the required error threshold.

First, we define the vertices and edges in the 2D lattice as sites, and consider the following distance measure between sites  $x = (x_1, x_2)$  and  $y = (y_1, y_2)$ :  $\text{dist}(x, y) = \max\{|x_1 - y_1|, |x_2 - y_2|\}$ . Suppose the lattice is affected by a Pauli error  $\mathcal{E}$ . Then we define the diameter of a subset of  $\mathcal{E}'$  errors (where the notion of subset means that  $\text{Supp}(\mathcal{E}') \subseteq \text{Supp}(\mathcal{E})$ ) by the maximum pairwise distance between the sites within this subset,  $\text{diam}(\mathcal{E}') = \max\{\text{dist}(a, b) \mid a, b \in \text{Supp}(\mathcal{E}')\}$ . To understand how the decoder merges error clusters, we define a notion of connectivity for subsets of errors. In particular, a subset of errors  $\mathcal{E}'$  is  $r$ -connected if there does not exist subsets  $A \in \text{Supp}(\mathcal{E}')$  and  $B = \text{Supp}(\mathcal{E}' \setminus A)$  such that the distance between  $a \in A$  and  $b \in B$  is larger than  $r$ .

Next, we recursively define a notion of level- $k$  errors in terms of subsets of a Pauli error  $\mathcal{E}$  that can occur. These are distinct from the level- $k$  clusters; the clusters over which the decoder operates are formed from the defects generated by  $\mathcal{E}$ . Level- $k$  errors ultimately determine the syndromes and influence the behavior and efficiency of the decoder, and will therefore be the object of analysis.

**Definition 5.7.** A subset  $\mathcal{E}' \subseteq \mathcal{E}$  of an error  $\mathcal{E}$  is called a level- $k$  error if it satisfies the following conditions, for a fixed integer  $l \gg 1$ .

- It contains at least two disjoint level- $(k-1)$  errors.
- The maximum distance between single Pauli errors within  $\mathcal{E}'$  is  $\frac{l^k}{2}$ .
- The level-0 errors are single Pauli errors.

The union of all level- $k$  errors of  $\mathcal{E}$  is denoted by  $\mathcal{E}_k$ .

With this definition of level- $k$  errors, any error  $\mathcal{E}$  can be partitioned into a disjoint union of indexed subsets, where each subset consists of lattice sites in the support of  $\mathcal{E}$  that appear only in errors of a level equal to the index of that subset. This implies that all subsets are mutually exclusive, denoted as  $F_i = \mathcal{E}_i \setminus \mathcal{E}_{i+1}$ . We refer to this as the decomposition of the error  $\mathcal{E}$  and write

$$\mathcal{E} = \bigsqcup_{i=0}^h F_i, \quad (5.18)$$

where the length of the decomposition  $h$  is closely related to the structure of the error  $\mathcal{E}$ . This decomposition can uniquely determine whether the decoder will succeed or fail. In particular, a decoder that runs for less than  $h$  iterations will abort.

**Lemma 5.8** ([BH13]). Let  $l \geq 10$  and  $m$  be the lattice size. For any Pauli error  $\mathcal{E}$  with a decomposition of length  $h$  that satisfies  $l^{h+1} < m$ ,  $\mathcal{E}$  is corrected by the HDRG decoder.

It is also of interest to understand the sizes of and distances between the errors in the last iteration of the decoder, which precisely determine the conditions under which the decoder fails. The following lemma addresses this issue.

**Lemma 5.9** ([BH13]). *Let  $l \geq 6$  and  $\mathcal{E}'$  be  $l^k$ -connected subset of  $F_k$ . Then  $\mathcal{E}'$  has diameter  $\leq l^k$  and is separated from the set  $\mathcal{E}_k \setminus \mathcal{E}'$  by distance  $> \frac{1}{3}l^{k+1}$ .*

Subsequently, considering the local stochastic nature of the errors, we must determine the threshold below which an error occurring according to our noise model has a sufficiently small decomposition with very high probability. Simultaneously, we obtain the error threshold below which the decoder operates with exponential accuracy. The proof follows as in [BH13], with some additional considerations for the local stochastic noise model that we use in this work.

**Lemma 5.10.** *There exists a constant threshold  $\tau_{th} > 0$  such that for any  $\tau < \tau_{th}$  the HDRG decoder over distance- $m$  qubit surface code corrects local stochastic errors  $\mathcal{E} \sim \mathcal{N}(\tau)$  with failure probability bounded by*

$$\Pr[\text{Fail}] \leq \exp(-\Omega(m^\eta)), \quad (5.19)$$

for some constant  $\eta > 0$ .

*Proof.* The HDRG decoder continues to iterate as long as the area over which it attempts to merge clusters is still within the 2D lattice of the surface code. Therefore, the decoder fails if the decomposition of the error is longer than  $h \approx \log(m)/\log(l)$  as given by Lemma 5.8. We need to bound the probability  $p$  that an error  $\mathcal{E} \sim \mathcal{N}(\tau)$  has a decomposition longer than  $h$ . This event implies the existence of at least one  $h$ -level error, which causes the decoder to fail.

The 2D lattice that defines our surface code and the associated distance measures imply that the HDRG decoder will consider squares over the lattice as the site-enclosing objects, to analyze  $k$ -level errors. For a level- $h$  error to exist, it must overlap with a square  $\square_h$  of side length  $l^h$ , which can be considered independently at any position on the 2D lattice, as the following properties are translation-invariant. Furthermore, from Lemma 5.9, we obtain that a larger square  $\square'_{h+1}$  of size  $9l^{h+1}$  centered on a box  $\square_l$  must fully contain a level- $k$  error if it overlaps with  $\square_h$ . This allows us to decompose the probability of failure as follows

$$\Pr[\text{HDRG fails}] \leq \Pr[\mathcal{E}_h \in \square'] \quad (5.20)$$

$$\leq \Pr[(\mathcal{E}_{h-1} \sqcup \mathcal{E}'_{h-1}) \in \square'] \quad (5.21)$$

Since the failure probability of the HDRG decoder is bounded by the probability of  $\square'$  containing a level- $h$  error, we can bound the same probability in terms of the probability of the same square containing two disjoint level- $(h-1)$  errors by the definition of a level- $h$  error.

Finally, the probability of having two disjoint level- $(h-1)$  errors in the same square can be further bounded. The events whose probabilities we are bounding here are known as *increasing events*, as defined in percolation theory. In simple terms, increasing events are those events that remain true when the state space leading to the event is extended or augmented. For instance, rain occurs whenever a certain threshold of water falls from the sky (precipitation rate), and it remains a true event if the precipitation rate increases and it rains more intensively. This implies that these events occur under varying conditions, as in our case. Most importantly, with that, we can apply the van den Berg and Kesten inequality [VK85] to bind the probability as follows,

$$\Pr[\mathcal{E}_{h-1} \in \square' \sqcup \mathcal{E}_{h-1} \in \square'] \leq \Pr[\mathcal{E}_{h-1} \in \square'] \cdot \Pr[\mathcal{E}_{h-1} \in \square'] \quad (5.22)$$

$$\leq \Pr[\mathcal{E}_{h-1} \in \square']^2. \quad (5.23)$$

Subsequently, we have that there are  $(3l)^2$  squares  $\square''$  of size  $l^{h-1}$  in  $\square'$ , such that with a simple union bound we can write

$$\Pr[\mathcal{E}_{h-1} \in \square'] \leq (3l)^2 \cdot \Pr[\mathcal{E}_{h-1} \in \square'']. \quad (5.24)$$

This allows us to write the probability of the failure recursively in terms of smaller squares until we reach a single site, which coincides with the probability that a single qubit is affected by noise; this in turn is definitionally equal to  $\tau$  for local stochastic errors<sup>11</sup>. Hence we have that

$$\Pr[\text{HDRG fails}] \leq (3l)^{-4} (3l^4 \tau)^{2^h} \quad (5.25)$$

$$= (3l^4 \tau)^{\Omega(m^\eta)}, \quad (5.26)$$

---

<sup>11</sup>Notice that under this reduction, the HDRG decoder has the same error correction success probability for the local stochastic error model considered in this text as for the error model considered in [BH13].

for  $\eta > 0$  using again that  $h \approx \log(m)/\log(l)$ . We thus obtain the stated asymptotic bound on the failure probability of the HDRG decoder. Conversely, it decodes correctly with high probability as required.  $\square$

The last element needed to prove the error threshold from our conditions in [Definition 5.4](#) is to define the decoding function DEC in terms of the string that the HDRG decoder outputs.

**Corollary 5.11.** *There is a decoding function DEC based on the HDRG decoder that for a distance- $m$  qupit surface code subjected to local stochastic noise  $\mathcal{E} \sim \mathcal{N}(\tau)$  with  $\tau < \tau_{th}$  satisfies*

$$\text{DEC}(x) = \text{Mod}_p(x) \quad (5.27)$$

and

$$\Pr[\text{DEC}(x \oplus v) = \text{Mod}_p(x)] \geq 1 - e^{-\Omega(m^\eta)}, \quad (5.28)$$

for every  $v \in \mathbb{F}_p^m$  defined by  $|v\rangle = \mathcal{E}_X |0\rangle^{\otimes m}$ , where  $\mathcal{E}_X$  denotes the restriction of the error  $\mathcal{E}$  to those qupits where it acts as a tensor of Pauli  $X$  operators.

*Proof.* Recall that the logical measurement operation of a logical qupit in the surface code is performed by single qupit  $Z$  measurements of the physical qupits along a diagonal of the lattice. The value of the logical measurement result is determined by the sum of the physical measurement results modulo  $p$ , with  $p$  being the dimension of the qupit system. In particular, in the noise-free case when  $\tau = 0$ , the result of this operation effectively produces the correct value for the logical qupit.

For the noisy case, we can model the error that occurs just before the measurement operation as  $\mathcal{E} = \omega^i X(a)Z(b)$ . This error introduces deviations to the measurement results through the  $X(a)$  component. For convenience, we represent these deviations from the noise-free measurement results with an additional string  $v \in \mathbb{F}_p^n$ , which follows from the  $X(a)$  component. We then use the fact that the HDRG decoder, with exponentially high probability, can guess the string  $v$  from the error syndromes based on [Lemma 5.10](#). Therefore, if we consider the decoding function DEC as the modular remainder of the measured string combined with the outcome of the HDRG decoder  $v_{\text{Guess}}$ , we have, with exponential confidence, that

$$\text{Mod}_p(x \oplus v \oplus v_{\text{Guess}}) = \text{Mod}_p(x). \quad (5.29)$$

This finishes the proof of the corollary establishing the exponential confidence for our choice of the decoding function.  $\square$

With this proof of [Corollary 5.11](#) we have completed the proof of the condition which was required to demonstrate the effectiveness of our selected decoder for the qupit surface code. We now proceed to the next crucial ingredient in our noise-resilient construction, single-shot state preparation.

### 5.1.2 Qupit single-shot state preparation

In this section, we will demonstrate how to achieve single-shot state preparation of the  $\text{GHZ}_2$  state for qupit surface codes. Considering adaptive state preparation processes, we will outline the predetermined state preparation operations and the adaptive correction mechanisms. Specifically, the latter involves a designated recovery function used to correct errors from the fixed state preparation operations in creating our logical resource state and a repair function that addresses additional noise that may occur in the preceding circuit.

We then construct a 3D cubic lattice into which the logical  $\text{GHZ}_2$  state will be encoded. To this end, we define all the required stabilizer generators on the 3D lattice and determine the measurement pattern that allows us to create our resource state. The additional Pauli operators that will be required, controlled by the measurement outcomes, define our recovery function. Lastly, we prove that there exists a valid repair function that takes as input any local stochastic error affecting single-shot state preparation and produces as output a global correction in the form of another local stochastic error. Recall that this type of correction implies that our decoder can recover the encoded information with a higher likelihood. This is achieved by demonstrating that the selected repair function satisfies the lifting property, as defined in [\[BGK<sup>+</sup>20\]](#). Similar to the qubit case, it ensures the correct behavior of the repair function across all qupit cases. By combining these two demonstrations, we achieve a single-shot state preparation that fulfills the condition specified in [Definition 5.4](#) required for fault-tolerant executions of shallow-depth quantum circuits.

## Qupit recovery and repair functions

The construction of the resource state needed to demonstrate an advantage in the qupit case involves two main stages, each comprising several steps. In the first stage, a constant-depth Clifford circuit  $\mathcal{Z}$  is applied to  $2m$  physical qupits and  $m_a$  ancilla qupits. The former qupits will be designated for the two logical qupits in the  $|\overline{\text{GHZ}}_2\rangle$  state, while the latter are uniquely employed in the state preparation process. Specifically, the correction applied to the state after the measurement process in  $\mathcal{Z}$  is described as the recovery operation  $\text{REC}(s)$ , where  $s$  is a string resulting from measuring the  $m_a$  ancilla qupits. More precisely, after executing the constant-depth circuit  $\mathcal{Z}$  and the recovery operation  $\text{REC}(s)$ , we obtain the following state,

$$(|s\rangle\langle s| \otimes \text{REC}(s)) \mathcal{Z} \left( |0\rangle^{\otimes 2m} \otimes |0\rangle^{\otimes m_a} \right) \propto |\overline{\text{GHZ}}_2\rangle \otimes |s\rangle. \quad (5.30)$$

However, when this process is subject to local stochastic errors, it changes the LHS of the above equation to

$$(|s\rangle\langle s| \otimes \text{REC}(s)) \mathcal{E} \mathcal{Z} \left( |0\rangle^{\otimes 2m} \otimes |0\rangle^{\otimes m_a} \right), \quad (5.31)$$

where  $\mathcal{E}$  accounts for all the errors occurring in the circuit  $\mathcal{Z}$ . This is possible because  $\mathcal{Z}$  is a constant-depth Clifford circuit, and we can commute the individual errors occurring in each layer to the end (using again [Lemma 3.20](#)). However, this error will be carried to the output state; hence, in the presence of noise, [Equation \(5.30\)](#) would not be valid. To obtain the valid expression we need to resort to an additional degree of freedom that it will correct for noise, this will be expressed in the form of a repair function  $\text{REP}(\mathcal{E})$ , and the updated condition for the single-shot state preparation,

$$(|s\rangle\langle s| \otimes \text{REC}(s)) \mathcal{E} \mathcal{Z} \left( |0\rangle^{\otimes 2m} \otimes |0\rangle^{\otimes m_a} \right) \propto \text{REP}(\mathcal{E}) |\overline{\text{GHZ}}_2\rangle \otimes |s\rangle. \quad (5.32)$$

Subsequently, we will describe these steps in more detail, showing how both the recovery and repair functions are going to be defined for the higher dimensional case. The arguments will follow similarly to those in the qubit cases in [\[BGK<sup>+</sup>20; RBH05\]](#).

Our process will utilize a 3D lattice, employing  $m$  qupits on two opposing faces for the logical qupits of the  $\text{GHZ}_2$  state, with all  $m_a$  qupits in the bulk of this lattice serving as ancilla qupits. Specifically, we will define stabilizers over this lattice as  $\mathcal{S}_0$  whenever they are uniquely associated with the ancilla qupits and  $\mathcal{S}_1$  when they are defined over the entire lattice. These will be detailed further in the next subsection. However, to provide a high-level description, consider that elements of  $\mathcal{S}_0$  are the qupits measured during the process of creating the  $|\overline{\text{GHZ}}_2\rangle$ . Moreover,  $S_0^i$  will correspond to a trivial stabilizer of the  $|\overline{\text{GHZ}}_2\rangle$  state. Consequently, the syndrome of the error  $\mathcal{E}$  associated with it will only depend on  $s$ . We will define this as a string  $\text{syn}_0(\mathcal{E}) \in \mathbb{F}_d^k$ , where  $k$  represents the number of  $\mathcal{S}_0$  generators. The syndrome elements will thus depend on the commutation between the stabilizer elements of  $\mathcal{S}_0$  and  $\mathcal{E}$ . Since we are using qupits, this relationship can be defined through the Mod function, analogous to the parity function in the qubit case,

$$\text{syn}_0(\mathcal{E})_i = \text{Mod}(s, \text{Supp}(S_\alpha^i)) = \sum_{u \in \text{Supp}(S_\alpha^i)} s_u \bmod p, \quad (5.33)$$

with the index  $i$  used to describe the element of the stabilizer i.e one of  $S_0^1, \dots, S_0^k$  and the lower index  $\alpha$  describes which subgroup of stabilizers we are referring to.

In contrast, elements of  $\mathcal{S}_1$ , will act with  $\mathbf{Z}$  type Paulis on the ancilla qupits, but they will also act with both  $\mathbf{Z}$  and  $\mathbf{X}$  type Paulis on the qupits that will encode our resource state. Furthermore, all elements  $\mathcal{S}_1^i$  will stabilize  $\mathcal{Z} |0\rangle^{\otimes 2m} \otimes |0\rangle^{\otimes m_a}$  such that we have,

$$\omega^{b(s)} (|s\rangle\langle s| \otimes \mathbf{1}_B) \mathcal{Z} \left( |0\rangle^{\otimes 2m} \otimes |0\rangle^{\otimes m_a} \right), \quad (5.34)$$

with  $b(s)$  depending only on the modular sum of the bulk measurements for each stabilizer. Therefore, from  $s$  alone, one can infer the error that appears on the facets of the 3D structure with the logical qupits. If not for the existence of extra errors, one could easily obtain the intended logical state from the measurements of the auxiliary qupits. However, the actual phase that appears will be

$$\omega^{b(s) \oplus \text{syn}_1(\mathcal{E})} (|s\rangle\langle s| \otimes \mathbf{1}_B) \mathcal{Z} \left( |0\rangle^{\otimes 2m} \otimes |0\rangle^{\otimes m_a} \right), \quad (5.35)$$



with  $\text{syn}_1(\mathcal{E})$  accounting for the additional error that we cannot infer from  $s$  alone, but detected through the stabilisers in the set  $\mathcal{S}_1$ . From here on, for simplicity, we will represent the phases by their powers alone. Additionally, in the ideal implementation, 0 will be considered the correct phase. Therefore, the phase accumulated, represented as  $b(s) \oplus \text{syn}_1(\mathcal{E})$ , requires a correction,  $c$ , such that  $c \oplus b(s) \oplus \text{syn}_1(\mathcal{E}) = 0$ .

Unfortunately, the syndrome of the error on the surface cannot be determined from the measurement outcomes performed on the bulk (we do not have access to the values of the stabilizers  $S_1^i$ ). This problem is addressed in [BGK<sup>+</sup>20] by defining an appropriate proxy  $P$  for the error, chosen to be a function of the syndrome measurements,  $P = f(s)$ , in such a way that it will have the same syndrome as the error on the bulk. Then, since the effects of the measurements on the bulk, which generate additional phases on the surfaces and  $b(s)$ , are known, one can consider the following correction  $c \oplus b(s) \oplus \text{syn}_1(P) = 0$ .

Recognising  $c$  as the recovery function with syndrome  $\text{syn}_1(\text{REC}(s))$  over the set  $\mathcal{S}_1$  and using the remaining degrees of freedom that we have, in the form of a repair function, we correct for the difference between the recovery employed, based on the proxy, and the actual error present on the surface, such that

$$\text{syn}_1(\text{REC}(s)) \oplus b(s) \oplus \text{syn}_1(\mathcal{E}) \oplus \text{syn}_1(\text{REP}(\mathcal{E})) = 0, \quad (5.36)$$

leading us to a recovery of the form  $\text{syn}_1(\text{REC}(s)) = -b(s) \oplus \text{syn}_1(P)$ , and a repair function of the form  $\text{syn}_1(\text{REP}(\mathcal{E})) = -\text{syn}_1(P) \oplus -\text{syn}_1(\mathcal{E})$ .

This concludes the high-level description of the repair and recovery functions. Subsequently, we will show how this high-level behavior is concretized in our 3D constructions and demonstrate that these functions fulfill the required conditions from Definition 5.4 with their precise definitions.

### Logical GHZ<sub>2</sub> states from the 3D block construction

In this section, we define the lattice used for single-shot state preparation of the logical GHZ<sub>2</sub> state. Our lattice retains the general structure described in [RBH05] but replaces qubits with qupits at each site. Due to the asymmetries observed in the qupit surface code for  $p > 2$ , which influence how plaquette and vertex stabilizers must be oriented (see Figure 3), we must carefully incorporate these asymmetries into the design of the constant-depth quantum circuit  $\mathcal{Z}$ . Specifically, we ensure the proper alignment of each stabilizer generator in the graph states produced by the quantum circuit. Moreover, we will meticulously verify the geometric placement of each stabilizer generator, ensuring that a valid measurement pattern is achieved for the preparation of a logical GHZ<sub>2</sub> state.

The three-dimensional lattice  $\mathcal{C}$ , used for the creation of the logical GHZ<sub>2</sub> states with a qupit surface code of distance  $d$ , has a side length of  $r = 2d + 1$  and is defined as follows,

$$\mathcal{C} = \{(u_1, u_2, u_3) : 0 \leq u_1, u_2 \leq r - 1, 1 \leq u_3 \leq r\}. \quad (5.37)$$

In particular, the two opposite surfaces, corresponding to  $u_3 = 1$  and  $u_3 = r$ , are defined such that their first two coordinates  $u_1$  and  $u_2$  have different parities. We will refer to this set of qupits as the surface

$$\text{Sur} = \{(e, o, u_3), (o, e, u_3) \in \mathcal{C} : u_3 \in \{1, r\}\}^{12}. \quad (5.38)$$

When we use this lattice  $\mathcal{C}$  to build the noise-resilient circuit, qupits that lie on  $\text{Sur}$  will encode the logical GHZ<sub>2</sub> state, while we regard all other qupits as ancillary, contained in the *bulk* of this 3D lattice, defined by  $\text{Bulk} = \mathcal{C} \setminus \text{Sur}$ .

Similarly to the initial proposal in [RBH05] for qubits, we will utilize four graphs—the odd graph, even graph, surface code graph, and dual surface code graph, respectively labeled  $T_o$ ,  $T_e$ ,  $T_{sc}$ , and  $T_{sc}^*$ . These graphs help us describe the measurement pattern required for preparing the logical GHZ<sub>2</sub> state. More specifically, the set of vertices of these graphs will help us in defining the stabilizers of  $\mathcal{S}_0$  and  $\mathcal{S}_1$  and are given by

$$\begin{aligned} V(T_e) &= \{(e, e, e) \in \mathcal{C}\}, & V(T_o) &= \{u = (o, o, o) \in \mathcal{C} : u_3 \notin \{1, r\}\}, \\ V(T_{sc}) &= \{u = (e, e, o) \in \mathcal{C} : u_3 \in \{1, r\}\}, & V(T_{sc}^*) &= \{u = (o, o, o) \in \mathcal{C} : u_3 \in \{1, r\}\}, \end{aligned}$$

<sup>12</sup>Throughout this section, we use the symbols  $o$  and  $e$  inside set notation to mean variables that range over all arbitrary odd and even indices respectively

while the edge sets of  $T_o$  and  $T_e$  will aid in defining the stabilizers of the resulting logical state, which are given by

$$E(T_e) = \{(e, e, o), (e, o, e), (o, e, e) \in \mathcal{C}\}, \quad E(T_o) = \{u = (o, o, e), (o, e, o), (e, o, o) \in \mathcal{C} : u_3 \notin \{1, r\}\}.$$

Now, to address the previously mentioned asymmetry and achieve the intended logical  $\text{GHZ}_2$  states, we define the constant-depth quantum circuit  $\mathcal{Z}$  over the qubits on the lattice  $\mathcal{C}$ . For simplicity, we will divide the circuit into operations over the 2D layers running along  $u_1$  and  $u_2$ , for even and odd values of  $u_3$ , designated as  $\mathcal{Z}_{\text{even}}$  and  $\mathcal{Z}_{\text{odd}}$ , respectively. Additionally, as we will discuss, we will require stabilizers with four different directionalities. To keep track, we define the following function  $\text{dir}(u) = (-u_1 + u_2 + u_3) \bmod 4$ , which will help us position each of these four elements. Having considered all these details about the circuit, we obtain the following definitions,

$$\mathcal{Z}_{\text{even}} = \left( \prod_{\text{dir}(u)=\{0,1\}} \mathbf{X}_u^\dagger \right) \mathbf{F}_u \left( \prod_{v \in n(u), \text{dir}(u)=\{2,3\}} \text{CZ}_v^{-(v_1 - u_1 + v_2 - u_2 + v_3 - u_3)} \right) \quad (5.39)$$

$$\left( \prod_{v \in n(u), \text{dir}=\{0,1\}} \text{CZ}_v^{-(v_1 - u_1 - (v_2 - u_2) + v_3 - u_3)} \right) \prod_{u \in E(T_o) \cup E(T_e) \setminus \text{Sur}} \mathbf{F}^{\otimes n} \quad (5.40)$$

for all  $u = (\cdot, \cdot, e) \in \mathcal{C}$  with the nearest neighbors of each site  $u$  given by  $n(u) = \{v \in \mathcal{C} : |u_1 - v_1| + |u_2 - v_2| + |u_3 - v_3| = 1\}$ , and respectively

$$\mathcal{Z}_{\text{odd}} = \left( \prod_{\text{dir}(u)=\{2,3\}} \mathbf{X}_u^\dagger \right) \mathbf{F}_u \left( \prod_{v \in n(u), \text{dir}(u)=\{0,1\}} \text{CZ}_v^{-(v_1 - u_1 + v_2 - u_2 + v_3 - u_3)} \right) \quad (5.41)$$

$$\left( \prod_{v \in n(u), \text{dir}=\{2,3\}} \text{CZ}_v^{-(v_1 - u_1 - (v_2 - u_2) + v_3 - u_3)} \right) \prod_{u \in E(T_o) \cup E(T_e) \setminus \text{Sur}} \mathbf{F}^{\otimes n} \quad (5.42)$$

for all  $u = (\cdot, \cdot, o) \in \mathcal{C}$ .

Then, the state  $\mathcal{Z}|0\rangle^{\otimes |\mathcal{C}|}$ , with  $\mathcal{Z} = \mathcal{Z}_{\text{even}}\mathcal{Z}_{\text{odd}}$ , resulting from our constant-depth circuit, will be measured in the  $Z$  basis on all the qubits of the lattice  $\mathcal{C}$  such that  $u \notin E(T_o) \cup E(T_e) \setminus \text{Sur}$ . These sites can be directly removed from our analysis for simplicity, as such measurements over graph states correspond to the simple removal of the vertex from the graph. Therefore, for the remaining qubits, the stabilizers of the state are transformed with the Fourier gate to the  $X$  basis, resulting in the stabilizers,

$$K_u = S_0^a = Z_u \left( \prod_{v \in n(u)} \mathbf{X}_v^{(v_1 - u_1 + v_2 - u_2 + v_3 - u_3)} \right) \text{ for } u = (\cdot, \cdot, e), \text{dir}(u) = 3 \text{ or } u = (\cdot, \cdot, o), \text{dir}(u) = 0; \quad (5.43)$$

$$= S_0^b = Z_u \left( \prod_{v \in n(u)} \mathbf{X}_v^{(v_1 - u_1 - (v_2 - u_2) + v_3 - u_3)} \right) \quad \dots \quad \text{dir}(u) = 2 \quad \dots \quad \text{dir}(u) = 1; \quad (5.44)$$

$$= (S_0^a)^\dagger \quad \dots \quad \text{dir}(u) = 1 \quad \dots \quad \text{dir}(u) = 2; \quad \dots \quad = (S_0^b)^\dagger \quad \dots \quad \text{dir}(u) = 0 \quad \dots \quad \text{dir}(u) = 3; \quad (5.45)$$

with all the vertex are of the type  $u \in E(T_o) \cup E(T_e) \setminus \text{Sur}$ . See Figure 12 for a spacial representation of the placement of the stabilisers over  $\mathcal{C}$

Having defined the stabilizer group  $\mathcal{S}$  over the remaining qubits of the lattice  $\mathcal{C}$ , which arises from the generators  $K_u$  and the graphs  $T_o$ ,  $T_e$ ,  $T_{sc}$ , and  $T_{sc}^*$ , we can now specify the two special subgroups of this stabilizer group,  $\mathcal{S}_0 < \mathcal{S}_1 < \mathcal{S}$ . As discussed in the definition of the recovery and repair functions in the previous subsection, these subgroups facilitate the retrieval of the intended outcome state following the measurements of the ancillary qubits. More concretely, within our lattice  $\mathcal{C}$ , elements of  $\mathcal{S}_0$  are designed to act trivially on  $\text{Sur}$  and to affect  $\text{Bulk}$  solely through  $Z$  operations. In contrast, elements of  $\mathcal{S}_1$  perform  $X$  or  $Z$  operations on  $\text{Sur}$  and only  $Z$  operations on  $\text{Bulk}$ . These elements are specifically required to be stabilizers

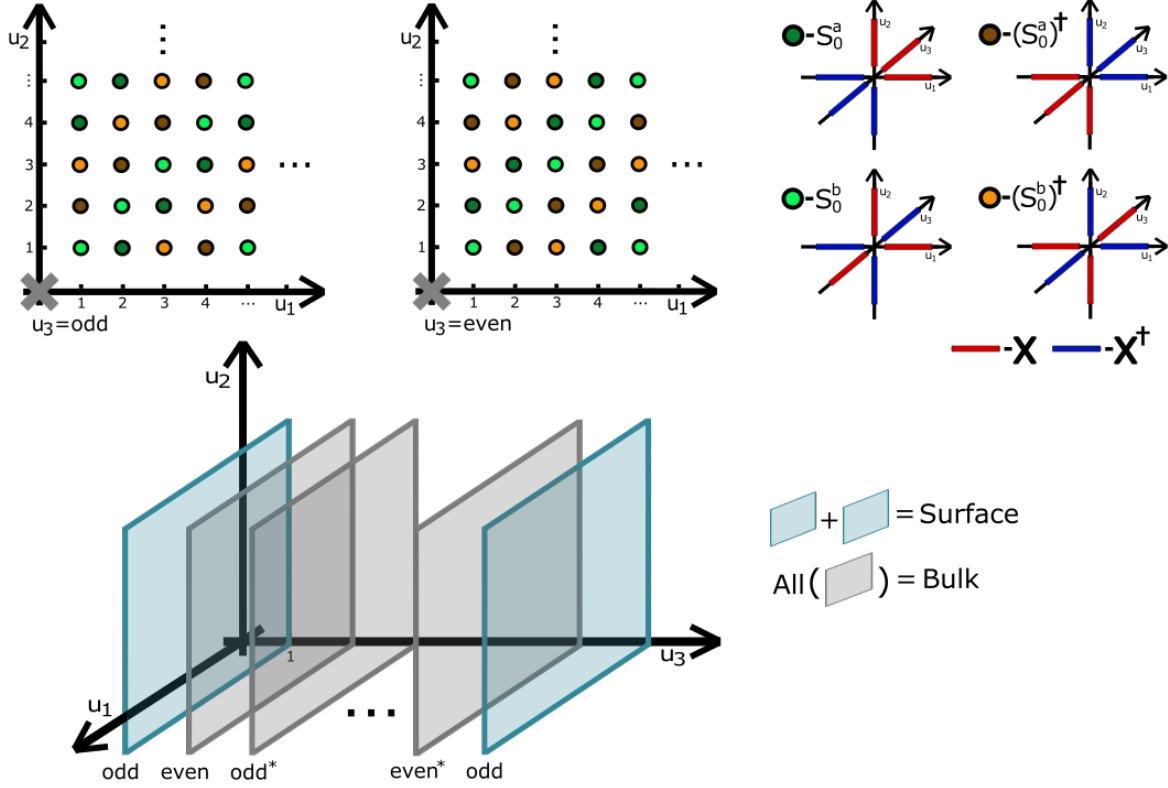


Figure 12: On the top left, we have a representation of the distribution of the stabilizer generators over layers (planes) parallel to the  $u_1$  and  $u_2$  axes, corresponding to even and odd values of  $u_3$  in the lattice  $\mathcal{C}$ . The layers termed "even\*" and "odd\*" are equivalent, having the same pattern defined by the distribution of stabilizers, to the "even" and "odd" layers, respectively, except for the translation by two units in the same plane formed by  $u_1$  and  $u_2$ . The cross ( $\times$ ) at the origin of the 2D graphs indicates that the  $u_3$  axis is inward-directed. The top right panel displays a representation of the stabilizer generators  $K_u$  from Equation (5.43) with their respective spatial orientation. At the bottom, we have a depiction of the entire lattice  $\mathcal{C}$ , indicating the layers and defining stabilizer positions after the application of the constant-depth circuit  $\mathcal{Z}$  to the lattice. Note that the first and last layers constitute the surface (Sur), where the logical qubits reside, while the remaining middle layers define the bulk (Bulk).

of the logical GHZ<sub>2</sub> state. Additionally, we intend to have a subset of the stabilizers of  $\mathcal{S}_1$ , which function as plaquette and vertex stabilizers of the surface qudit code.

Starting with the generators of  $\mathcal{S}_0$ , which are associated with the qupits corresponding to vertices of  $T_o$  and  $T_e$ , we can describe these based on our stabilizers referenced in Equation (5.43) as follows,

$$S_0^u = \prod_{v \in n(u)} K_v = \prod_{v \in n(u)} Z_v^{(v_1 - u_1 + v_2 - u_2 - (v_3 + u_3))}, \text{ with } u \in V(T_e), \quad (5.46)$$

and

$$S_0^u = \prod_{v \in n(u)} K_v = \prod_{v \in n(u)} Z_v^{(v_1 - u_1 - (v_2 - u_2) + v_3 - u_3)}, \text{ with } u \in V(T_o). \quad (5.47)$$

In both cases, all the  $X$  operators from the  $K_v$  stabilizers overlap with some other  $X^\dagger$  operators within the same stabilizer set and completely cancel out. Thus, we obtain exclusively  $Z$  operators for this stabilizer subgroup, as intended.

The second subgroup,  $\mathcal{S}_1$ , utilizes the graphs  $T_{sc}$  and  $T_{sc}^*$  to define two types of stabilizers; one functions as the vertex stabilizer and the other as the plaquette stabilizer of the qudit surface code, as we will see

subsequently demonstrate.

$$S_1^u = K_u = \prod_{v \in n(u)} Z_u^\dagger \left( \prod_{v \in n(u)} X_v^{-(v_1 - u_1 - (v_2 - u_2) + v_3 - u_3)} \right), \text{ with } \text{dir}(u) = 1, u \in V(T_{sc}), \quad (5.48)$$

$$\prod_{v \in n(u)} Z_u \left( \prod_{v \in n(u)} X_v^{(v_1 - u_1 - (v_2 - u_2) + v_3 - u_3)} \right), \text{ with } \text{dir}(u) = 3, u \in V(T_{sc}). \quad (5.49)$$

These operators act exclusively on the qubits in the planes of the logical qubits where  $u_3 = 1, r$ , since operators in adjacent layers affect qubits that have already been measured out. Additionally, the vertices  $u \in V(T_{sc})$  are not located on Sur, the 2D lattice containing the logical qubit. Consequently, these aforementioned operators precisely function as the vertex stabilizer operators within the qubit surface code for any logical states on Sur.

Subsequently, we will define the subgroup of  $\mathcal{S}_1$  generating plaquette operators stabilizers,

$$S_1^u = K_{u \pm (0,0,1)} \prod_{v \in (n(u) \cap \text{Sur})} K_v = \prod_{v \in n(u)} Z_v^{-(v_1 - u_1 + v_2 - u_2 + v_3 - u_3)}, \text{ with } \text{dir}(u) = 1, u \in V(T_{sc}^*), \quad (5.50)$$

$$\prod_{v \in n(u)} Z_v^{(v_1 - u_1 + v_2 - u_2 + v_3 - u_3)}, \text{ with } \text{dir}(u) = 3, u \in V(T_{sc}^*). \quad (5.51)$$

This equality follows because all the  $X$  operators for the selected elementary stabilizer generators  $K_u$  cancel each other out completely, leaving us with only the previously mentioned set of  $Z$  operators. In particular, these two stabilizers, each operating on half of the vertices defined by  $T_{sc}^*$ , generate the precisely the plaquette operators of the qubit surface code when restricted to Sur, with the correct orientations.

Finally, we have defined all the state-independent stabilizers for the logical qubits on the surface Sur. However, we still need to identify the final one for these states to determine the specific logical stabilizer state they represent. Therefore, given our goal to obtain the logical GHZ<sub>2</sub> state, ideally, the logical stabilizers  $\bar{X}^\dagger \otimes \bar{X}^\dagger$  and  $\bar{Z} \otimes \bar{Z}^\dagger$  would be generated from the graph state stabilizers in  $\mathcal{S}_1$ . Furthermore, the previous logical operators are defined over the lattice as follows,

$$\bar{X}^\dagger \otimes \bar{X}^\dagger = \prod_{u=(1,e,1) \in \text{Sur}} X_u^\dagger \prod_{u=(1,e,r) \in \text{Sur}} X_u^\dagger \text{ and } \bar{Z} \otimes \bar{Z}^\dagger = \prod_{u=(0,o,1) \in \text{Sur}} Z_u \prod_{u=(0,o,r) \in \text{Sur}} Z_u^\dagger. \quad (5.52)$$

We will demonstrate that our resulting logical state, up to some local Clifford operations, is equivalent to the intended GHZ<sub>2</sub> state. To begin, we obtain that for an even-dimensional code distance  $d$ , the stabilizer  $S_1^X$  is defined as follows,

$$S_1^{X^\dagger} = \prod_{(u_1, u_1-1, e) \in \mathcal{C}} K_u = \prod_{u=(u_1, u_1-1, 1) \in \mathcal{C}} X_u^\dagger \prod_{(u_1, u_1-1, r) \in \mathcal{C}} X_u^\dagger \prod_{(u_1, u_1-1, e) \in \mathcal{C}, \text{dir}(u)=3} Z_u \prod_{(u_1, u_1-1, e) \in \mathcal{C}, \text{dir}(u)=1} Z_u^\dagger \quad (5.53)$$

$$\equiv \left( \bar{X}^\dagger \otimes \bar{X}^\dagger \right)_{\text{Sur}} \prod_{(u_1, u_1-1, e) \in \mathcal{C}, \text{dir}(u)=3} Z_u \prod_{(u_1, u_1-1, e) \in \mathcal{C}, \text{dir}(u)=1} Z_u^\dagger, \quad (5.54)$$

with  $(\cdot)_{\text{Sur}}$  designating that this operator is applied on the qubits of the surface Sur, which encode our logical qubits. In particular, this ensures that the logical states we generate through our single-shot state preparation  $|\phi\rangle$  are transformed by the application of the identified stabilizers as follows  $\bar{X}^\dagger \otimes \bar{X}^\dagger$  to produce  $|\phi\rangle = \lambda_{X^\dagger X^\dagger} |\phi\rangle$ .

Similarly, we will also define another stabilizer for the resulting state,  $S_1^{Z^\dagger}$ , as described below,

$$S_1^{Z^\dagger} = \prod_{(u_1, u_1-1, o) \in \mathcal{C}} K_u = \prod_{u=(u_1, u_1-1, 1) \in \mathcal{C}} Z_u^\dagger \prod_{(u_1, u_1-1, r) \in \mathcal{C}} Z_u^\dagger \equiv \left( \bar{Z}^\dagger \otimes \bar{Z}^\dagger \right)_{\text{Sur}}. \quad (5.55)$$

This second stabilizer ensures that our state satisfies  $\bar{Z}^\dagger \otimes \bar{Z}^\dagger |\phi\rangle = \lambda_{Z^\dagger Z^\dagger} |\phi\rangle$ . Consequently, following a correction based on the measurement outcomes from elements in Bulk, the resultant state  $|\phi'\rangle$  will, up to

some known logical Clifford operations, be equivalent to the  $\text{GHZ}_2$  state for two qupits, represented as  $|\overline{\text{GHZ}}_2\rangle = \frac{1}{\sqrt{p}} \sum_{i=0}^{p-1} |\bar{i}\bar{i}\rangle$ .

We note that one could also consider the case where the code distance  $d$  is of odd dimension; however, the stabilizers would become slightly more complex. In addition, unlike the previous solutions and the qubit setting, the qupit surface code will exhibit directionality. Consequently, the copy of the surface code at  $u_3 = r$  will serve as a mirror image of the surface code at  $u_3 = 1$ .

## Properties of the Repair function

We will now show that the repair function continues to be manageable even in the higher dimensional case; in particular, it continues to output a local stochastic correction. For a local stochastic error  $\mathcal{E} = \mathcal{E}_{\text{Bulk}} \otimes \mathcal{E}_{\text{Sur}} \sim \mathcal{N}(\tau)$  with  $\tau \leq 1$  acting on our lattice  $\mathcal{C}$ , this condition translates to

$$\Pr_{\mathcal{E}}[V \subseteq \text{Supp}(\text{REP}(\mathcal{E}_{\text{Bulk}}))] \leq \tau^{|V|}. \quad (5.56)$$

This can be inherited from the analysis of the qubit cases presented in [BGK<sup>+</sup>20]. However, we must define our recovery and repair functions more concretely. Unlike previous works that use the MWPM decoder, these functions will be based on the HDRG decoder. For example, the recovery function is defined as the Pauli correction operator produced by the HDRG decoder, parameterised on a fixed distance value  $k$ , which uses as input the syndromes generated by our proxy  $P$  and the additional Pauli corrections from the bulk measurements  $b(s)$ . Therefore, the repair function will be the Pauli operator derived from the difference between the two Pauli operators obtained from the HDRG, corresponding to the concrete error  $\mathcal{E}_{\text{Bulk}}$  and our guessed proxy  $P$ ,

$$\text{syn}_1(\text{REP}(\mathcal{E}_{\text{Bulk}})) = \text{syn}_1(\mathcal{E}_{\text{Bulk}}) \oplus \text{syn}_1(P). \quad (5.57)$$

Now, more importantly, we need to demonstrate that under this precise definition, the repair function retains the property expressed in Equation (5.56). To achieve this, we can leverage two properties, collectively introduced as the *lifting property* in [BGK<sup>+</sup>20], to substantiate that Equation (5.56) holds for our  $p$ -dimensional repair function. In particular, there must be a lifting function  $f : V_K \rightarrow V_L \subseteq 2^{\mathcal{C}}$  that maps a subset  $V_K$  of the surface  $\text{Sur}$  to a set of subsets within  $\mathcal{C}$ . Then, using these functions, the first property stipulates that for each  $V_K \subseteq \text{Supp}(\text{REP}(\mathcal{E}))$  there exists a set  $V_{\mathcal{E}'} \in f(V_K)$  such that

$$|V_{\mathcal{E}'} \cap \text{Supp}(\mathcal{E})| \geq \alpha |V_{\mathcal{E}'}|. \quad (5.58)$$

Secondly, for every  $\lambda > 0$ , there must be a corresponding  $\lambda_1 > 0$  such that

$$\sum_{V_L \in f(V_K)} \lambda^{|V_L|} \leq \lambda_1^{|V_K|}. \quad (5.59)$$

Previously, these properties were demonstrated for the qubit case using a repair and lifting function based on the MWPM decoder. Next, we will demonstrate that this property applies to a repair and lifting function constructed using the HDRG decoder. The lifting function based on the MWPM decoder was defined to output an edge-disjoint union of trees (also called a forest) with boundaries at the endpoints of a subset of the Bulk. In this paper, we define the lifting function to output the set of all subsets  $V_L$ , which are  $r$ -connected components that intersect  $V_K$  at each connected component. Recall that these connected components, according to our definition of  $r$ -connectivity, are subsets of the error at a distance bounded by  $r$  between each other.

Now for the first condition in Equation (5.58), consider that errors  $\mathcal{E}_{\text{Bulk}}$  on the Bulk that anti-commute with the stabilisers of  $\mathcal{S}_1$  and therefore, activate an  $S_1^i$  syndrome, are localised single errors on one of the vertexes of  $V(T_{sc})$  or  $V(T_{sc*})$ . This follows from the fact that these stabilisers are related to single  $Z$  stabilisers when we are considering unique errors on the Bulk and, therefore, do not cause any degeneracy. Furthermore, we will observe that our repair function will have an error on the surface  $\text{Sur}$ , localised on one of the stabilisers  $S_1^i$ , to correct an error of our proxy  $P$  that generates a different syndrome from the error  $\mathcal{E}_{\text{Bulk}}$  on the same vertex.

We consider the non-trivial case where  $\text{syn}_1(\mathcal{E}_{\text{Bulk}})$  is a non-zero value for some stabilizer  $S_1^i$ , indicating the presence of an error at the corresponding vertex associated with  $S_1^i$ . If, in this situation, the Pauli operator

resulting from our repair function, defined on the sites  $V_K$ , intersects the support of  $S_1^i$ , we can conclude that the lift of  $V_K$  certainly includes an error set with the connected component containing the error on the vertices on the bulk defined by  $S_1^i$ . Moreover,  $V_K$  is defined exclusively on the surface  $\text{Sur}$  and includes only the sites where the previous case repeats with the  $S_1^i$  type stabilizers. Specifically, the Pauli operators on the sites of  $V_K$  address errors at vertices in the Bulk, which are signaled by the syndromes of  $S_1^i$  and were not accounted for by our proxy  $P$ . Therefore, the lift of  $V_K$  generates certainly a set of  $r$ -connected components of the error  $\mathcal{E}_{\text{Bulk}}$ . This and the fact that the size of the  $r$ -connected components is finite implies that the size of the set  $V_K$  correlates with the number of  $r$ -connected components of  $\mathcal{E}_{\text{Bulk}}$ , ensuring that the overlap between one of the elements in lift and the original error  $\mathcal{E}_{\text{Bulk}}$  is proportional, thereby fulfilling the condition in Equation (5.58) for some constant  $\alpha$ .

Secondly, we upper bound Equation (5.59) by upper bounding the number and size of the  $r$ -connected components that can be generated on the lattice  $\mathcal{C}$  from a specific set  $V_K$ .

**Lemma 5.12.** *There exists a lifting function  $f$  defined using the HDRG decoder such that for any subset  $V_K$  of  $\text{Sur}$  and arbitrary value of  $\lambda > 1$  we have that*

$$\sum_{V_L \in f(V_K)} \lambda^{|V_L|} \leq \lambda_1^{|V_K|}, \quad (5.60)$$

with  $\lambda_1 > 1$ .

*Proof.* We use the previously described lifting function  $f$  based on the HDRG decoder and employ two bounds to constrain the sum on the left-hand side of Equation (5.60). We start to bind the size of each connected component. To do this, we observe that at most  $|V_K|$  connected components exist in  $|V_L|$  since  $V_L$  must intersect all the vertices of  $V_K$ . Next, we bound the size of each component by taking each vertex in  $V_K$  as a root node and consider respectively the largest tree that can be spanned given the graph's connectivity  $D$ . Given that we are considering  $r$ -connected components, the maximum distance between our root element, a vertex in  $V_K$ , and the leaf nodes is  $r$ .

In the second step, we need to bind the number of possible sets  $V_L$  in the lift. Since these are simply all the possible sets one can form, we can consider the power set of the vertices in the largest set  $V_L$  previously determined. By sequentially applying these steps, we obtain that

$$\sum_{V_L \in f(V_K)} \lambda^{|V_L|} \leq \sum_{V_L \in f(V_K)} \lambda^{|V_K| \cdot D^r} \quad (5.61)$$

$$\leq \sum_{i=0}^{|V_K| \cdot D^r} \binom{|V_K| \cdot D^r}{i} \lambda^{|V_K| \cdot D^r} \leq \left( (2\lambda)^{D^r} \right)^{|V_K|} \quad (5.62)$$

taking  $(2\lambda)^{D^r}$  as  $\lambda_1$  completes the proof.  $\square$

With this, we conclude that there exists a lifting function with the necessary properties to ensure that our the repair function for single-shot state preparation satisfies the local stochastic property defined in Equation (5.56).

Finally, we obtain that with the 3D construction described in the previous section, as well as the respective recovery and repair functions, we obtain a noise-resilient single-shot GHZ<sub>2</sub> state preparation process for the qutrit surface code as required by our conditions in Definition 5.4.

**Lemma 5.13.** *Let  $\mathcal{E} \sim \mathcal{N}(\tau)$  be a local stochastic error and consider a surface code with code distance  $d$ . Then, there exists a constant-depth Clifford circuit  $\mathcal{Z}$ , along with corresponding recovery and repair functions, such that the conditions in Definition 5.4 are satisfied, ensuring noise-resilient preparation of the logical GHZ<sub>2</sub> state.*

*Proof.* This culminates with all the descriptions in the proofs of this subsection. We consider for that construction a 3D lattice composed of qutrits as described in Equation (5.37), along with the corresponding constant depth state preparation circuit  $\mathcal{Z}$ , defined by Equation (5.39) and Equation (5.41). After performing the respective measurements on the Bulk, we use the precise repair and recovery functions defined based on the stabilisers of  $\mathcal{S}_0$  and  $\mathcal{S}_1$  from Equation (5.46), Equation (5.47) and Equation (5.48), Equation (5.50),



Equation (5.53), Equation (5.55) respectively. The application of these functions, as shown previously, results in a logical GHZ<sub>2</sub> state on the qupit surface code, with a code distance of  $d$ .  $\square$

This provides the last ingredient for the noise-resilient implementation of any quantum circuit over qupits that has with the structure illustrated in Figure 11 using the qupit surface code. Next, we will discuss the specific quantum circuits that will resort to that circuit structure.

## 5.2 Noise-resilient quantum advantage with magic state injection

In this subsection, we address the incompatibilities between the logical quantum circuits proposed in section Section 4 and the circuit structure (Figure 11) required for proving noise resilience. This primarily involves managing non-Clifford operations in the quantum circuits, for which we have demonstrated computational separations for qupits with dimensions  $p \geq 3$ . These operations are essential and necessary because the separations observed with Clifford circuits using qubits do not generalize to qupits [Gro06; HBV13]. Additionally, we face the constraint that the circuit cannot be adaptive, preventing the use of standard gate teleportation gadgets. To resolve this, we introduce a new quantum circuit that can solve the ISMRP family of problems using magic states and a non-adaptive constant-depth Clifford circuit.

We start off by demonstrating the existence of such a logical quantum circuit. We will then combine all the elements from the previous sections with our new logical quantum circuit, which has the necessary structure for noise-resilient execution. Finally, we will prove our noise-robust separations as outlined at the beginning of the section.

### 5.2.1 Non-adaptive Clifford circuits with magic state injection

To simplify the design of our new quantum circuits with the structure of Figure 11, we focus exclusively on the non-Clifford operators. In particular, we will address the implementation of the Z rotations for all dimensions  $p \geq 3$ . Our first step is to replace this gate with an equivalent realization using the following qupit gate teleportation gadget [dSil21; ZCC08], allowing us to offload the resource requirement for the execution of this gate into an advice state,

$$|\psi\rangle \xrightarrow{R_Z(\phi)} \equiv \begin{array}{c} \text{Advice } |T^{1/p}\rangle \text{ state} \\ \boxed{|0\rangle \xrightarrow{F} \boxed{R_Z(\phi)} \xrightarrow{\bullet} \boxed{R_Z(\phi) (X^{c_i})^\dagger (R_Z(\phi))^\dagger} \xrightarrow{R_Z(\phi)} |\psi\rangle} \\ \boxed{|\psi\rangle \xrightarrow{F^2} \oplus \xrightarrow{\text{meter}} c_i} \end{array} \quad (5.63)$$

Obtaining advice states defined as follows,

$$|T^{1/p}\rangle := R_Z\left(\frac{2\pi}{p^2}\right) F |0\rangle = \frac{1}{\sqrt{p}} \sum_{j=0}^{p-1} e^{\frac{2\pi i \cdot j}{p^2}} |j\rangle. \quad (5.64)$$

Understanding the state  $|T^{1/p}\rangle$  in more detail is crucial, as it will define the type of corrections required in Equation (5.63). Therefore, defining the new quantum circuit we intend to execute, as well as the complexity of the advice states themselves. For instance, if  $R_Z(\phi)$  is an operation from the third level of the Clifford hierarchy, the required correction within the gadget would be a Pauli operator. This correction is particularly convenient, as we can trivially commute it to the end of the circuit without significant complications.

To build intuition, notice that in the qubit case these advice states are related to the  $T$  operator. In particular,  $|T^{1/2}\rangle = TH|0\rangle$ . These states are called  $T$  magic states and are sufficient to perform universal quantum computation when combined with Clifford gates and adaptive measurements. Additionally, when provided as resource states in their logical version encoded with a quantum error correction code capable of realizing Clifford gates transversally, these states allow for universal *fault-tolerant* quantum computation. We now show that a similar type of relationship continues to hold between  $|T^{1/p}\rangle$  states and the corresponding  $T$ -type magic states in higher dimensional qupit systems.

**Lemma 5.14.** *For all prime  $p \geq 3$ , the state  $|T^{1/p}\rangle$  is derived from the  $p$ th root operator that creates the  $T$ -type qubit magic state.*

*Proof.* For universal quantum computation, it is known that any operator at the third level of the Clifford hierarchy or above, when combined with the Clifford group, allows for universal quantum computation [CGK17]. The operation considered for implementing through-the-gate teleportation is a diagonal gate, which we intend to show is sufficient for universal computation along with Clifford operations and is related to standard magic states. As described in [HV12], the generalization of  $T$  gates for qubits, in combination with Clifford gates, allows for universal quantum computation over these higher-dimensional quantum systems. This generalization includes any operator in the family ( $\omega = e^{\frac{2\pi i}{p}}$ )

$$U(v_0, v_1, \dots, v_{p-1}) = \sum_{k=0}^{p-1} \omega^{v_k} |k\rangle \langle k|, \quad (5.65)$$

parameterized by  $\{v_0, v_1, \dots, v_{p-1}\}$  satisfying  $v_k = \frac{k}{12}(\beta + k(6\gamma + (2k+3)\beta)) + k\zeta$  for each  $k \in [p-1]$  for some  $\beta, \gamma, \zeta \in \mathbb{F}_p$ . Furthermore, our advice state is created from the  $p$ th root of the operator that yields the following state

$$|T\rangle = \frac{1}{\sqrt{p}} \sum_{k=0}^{p-1} w^k |k\rangle. \quad (5.66)$$

Now, we will prove the previously defined  $|T\rangle$  states are magic states under the given conditions for the qubit generalised  $T$  gates. For that, we need to show that there exists a solution for the values of  $\beta, \gamma$  and  $\zeta$  such that we obtain the vector  $v_k = (0, 1, \dots, p-1)$  for all primes. For instance, with  $\beta = 0, \gamma = 2$ , and  $\zeta = 0$ , we obtain the vector  $v_k = (0, 1, 2)$  for the qutrit case. For  $p = 5$ , we obtain the vector  $v_k = (0, 1, 2, 3, 4)$  with  $\beta = 5, \gamma = 5$ , and  $\zeta = 6$ . More generally, we have a computer-assisted proof<sup>13</sup>, verifying analytically, that for all primes  $p$ , the following equation has solutions.

$$\frac{k}{12}(\beta + k(6\gamma + (2k+3)\beta)) + k\zeta \equiv k \pmod{p}. \quad (5.67)$$

This condition guarantees that  $|T\rangle$  is indeed a  $T$ -magic state for all prime  $p$  as defined in [HV12; GF19; BCH<sup>+</sup>20], thus concluding the proof.  $\square$

We have characterized our advice states with respect to the  $T$ -type qubit magic state. On the other hand, we know that the latter is a magic state for a gate in the third level of the Clifford hierarchy, but any  $p$ th root of this gate must be of a higher level<sup>14</sup>. Thus we find that our advice state is not a magic state for the third level of the Clifford hierarchy, but for some gate of level  $3 + p$ . Consequently, the correction operator  $R_Z(\phi) (X^{c_i})^\dagger (R_Z(\phi))^\dagger$  for the associated gate teleportation gadget using the magic state is no longer a Pauli operator. This means we cannot simply commute it through to the end of the Clifford circuit. Since our  $p$ th root operator is in the  $p+3$ th level, this forces the correction operation to be an operator above the second level. Thus, it cannot be a Clifford operator either and cannot be implemented by any composition of the logical and transversal gates of the qubit surface code.

One potential solution is to use additional advice states to perform a cascade of gate teleportations, where each correction comes down one level in the Clifford hierarchy, ultimately making the final correction a Clifford operator [dSil21; ZCC08]. However, this approach would require a number of sequential adaptive steps which is beyond our reach in the shallow-depth QNC<sup>0</sup> model of interest to us. More precisely, we would need to decode the control qubit, which is a logical qubit, necessitating computations over a string of size  $\Omega(\log n)$ . Each output of a constant depth bounded fan-in circuit can only depend on a constant number of inputs, making such computations as required above infeasible in constant depth.

Nevertheless, whenever we intend to implement a rotation through a teleportation gadget as in Equation (5.63) but cannot realize the correction operations, we can overcome this issue by accounting for the

<sup>13</sup>We resort to Wolfram Mathematica, specifically using the "Reduce" function, to analytically verify if there exist integer solutions for the free variables in all prime dimensions.

<sup>14</sup>By the recursive nature with which the Clifford hierarchy is defined (see Definition 3.17), we obtain, for instance, that the root of any operator at level  $l$  must be an element of level  $l+1$ .

effects on the output string due to the unrealized corrections, in addition to the rotations implemented by the respective gadget. More precisely, we will show that a circuit using the gadget from Equation (5.63) *without* the correction steps can still solve the target ISMRP with an exponentially larger correlation than any classical circuit. The proof for this statement will be based mainly on a different  $\text{NC}^0$  reduction as the ones in Lemma 4.25 and Lemma 4.26, producing a different correction string from those analyzed so far. However, this is only possible if the correction operators have a specific form: they need to be a Z rotation followed by a Pauli operator. The Pauli operator can be commuted to the end and its effect inverted in a simple manner within the  $\text{NC}^0$  reduction step. At the same time, the diagonal Z rotations will be accounted for with an additional correction string in the  $\text{NC}^0$  reduction, as we will show. In the next lemma, we demonstrate that the correction operations have exactly the form that we require.

**Lemma 5.15.** *For any qubit input state  $|\psi\rangle$ , the output state in the first register of the teleportation gadget, as shown on the right-hand side of Equation (5.63), can be written based on the measurement result  $c \in \mathbb{F}_p$  in the second register as,*

$$\mathbf{X}^c GR_Z(\theta_1) GR_Z(\theta_2, S_c) R_Z(\phi)^c |\psi\rangle, \quad (5.68)$$

where  $GR_Z(\theta)$  is the diagonal matrix with all diagonal elements equal to  $\theta$  and  $\theta_1 = -(2\pi c)/p^2$ . The operator  $GR_Z(\theta, S)$  is defined as follows

$$GR_Z(\theta, S) = \sum_{x \in S} e^{i\theta} |x\rangle \langle x| + \sum_{x \notin S} |x\rangle \langle x|, \quad (5.69)$$

and we have  $\theta_2 = \frac{2\pi}{p}$  and the set  $S_c$  defined for each  $c$  as  $[p - c, \dots, p - 1]$ .

*Proof.* The output state of the teleportation gadget without applying the correction of the teleportation gadget shown in Equation (5.63), can be described based on the result of the measurement in the second register  $c \in \mathbb{F}_p$  as,

$$\left( R_Z(\phi) (\mathbf{X}^c)^\dagger (R_Z(\phi))^\dagger \right)^\dagger R_Z(\phi) |\psi\rangle. \quad (5.70)$$

Thus, we only need to show that the operator  $\left( R_Z(\phi) (\mathbf{X}^c)^\dagger (R_Z(\phi))^\dagger \right)^\dagger$  is equal to  $\mathbf{X}^c GR_Z(\theta_1) GR_Z(\theta_2, S)$ . This follows from a simple analysis of how the non-zero terms in these matrix operations are composed. First, observe that  $(\mathbf{X}^c)^\dagger = \mathbf{X}^{p-c}$  and that  $(R_Z(\phi))^\dagger = R_Z(-\phi)$ . From this, we know that if  $c_i = 0$ , then we have  $R_Z(\phi) R_Z(-\phi) = I$ . This follows simply from the fact that for all bases  $|j\rangle$  with  $j \in \mathbb{F}_p$ , the first operation introduces phase term  $j \cdot \phi$ , while the second introduced  $-j \cdot \phi$ , canceling each other out. However, if  $c \neq 0$  the operator  $\mathbf{X}^c$  is not the identity. This implies that the phases which operate are shifted according to the exponent  $p - c$ , and we get the following phases,

$$e^{j(c-j)\phi}, \text{ if } j < p - c \text{ and } e^{j(-(p-c)-j)\phi}, \text{ if } j \geq p - c. \quad (5.71)$$

Therefore, we have that  $c$  many bases state obtain a phase term with the value  $-(p - c)\phi$  and  $p - c$  many bases with a phase term having the value  $c\phi$ . The particular set of bases to which each one of these phases will be applied will be ignored for now as these follow from a simple analysis of the  $\mathbf{X}^c$  operation for any  $c \in \mathbb{F}_p \setminus 0$ . Considering now the transposed conjugated operation, we obtain  $c$  many terms with the phase parameterized by  $(p - c)\phi$  and  $p - c$  terms with the phase  $-c\phi$ . Interestingly, one can write this operator simply as  $\mathbf{X}^a$  operator with  $a \in \mathbb{F}_p \setminus 0$  multiplied with a diagonal matrix defined by the previously determined phase terms.

$$D = \text{diag} \left( \underbrace{e^{-c\phi}, e^{-c\phi}, \dots, e^{-c\phi}}_{(p-c) \text{ times}}, \underbrace{e^{(p-c)\phi}, e^{(p-c)\phi}, \dots, e^{(p-c)\phi}}_{c \text{ times}} \right). \quad (5.72)$$

Subsequently, we can factorize this diagonal matrix into two diagonal matrices as follows,

$$D_1 D_2 = \text{diag} \left( e^{-c\phi}, e^{-c\phi}, \dots, e^{-c\phi} \right) \text{diag} \left( \underbrace{1, 1, \dots, 1}_{(p-c) \text{ times}}, \underbrace{e^{p\phi}, e^{p\phi}, \dots, e^{p\phi}}_{c \text{ times}} \right). \quad (5.73)$$

We obtain that  $D_1$  is exactly  $GR_Z(\theta_1)$ , as  $-c\phi$  is equal to  $-(2\pi c)/p^2$ . Similarly,  $D_2$  is exactly equal to  $GR_Z(\theta_2, S_c)$ , since  $S_c$  corresponds to the elements over which  $D_2$  operates with the phase  $p\phi$ , which is

exactly  $2\pi/p$ . In our final step, we only need to determine the exponent of the operator  $X^a$ . Before the transposition, the phase terms were shifted by the operator  $X^{p-c}$ ; thus, we obtain that  $a = c$  after the transposition and complete the proof.  $\square$

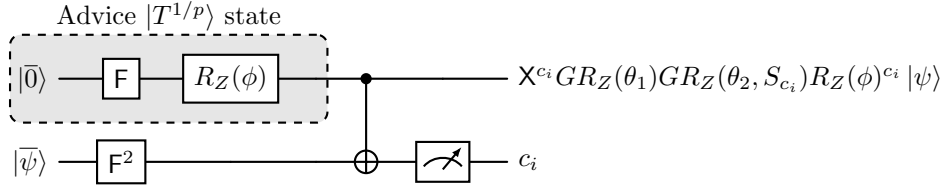
Having defined the additional rotations that result from the teleportation gadget, we will now show that there exists a Clifford circuit which when provided with the quantum advice state  $|T^{1/p}\rangle^{\otimes n}$  solves the ISMR problems with an exponentially larger correlation than  $\text{bPTF}^0[k]$  circuits with  $k = n^{1/(5d)}$ , as in [Theorem 4.12](#).

**Lemma 5.16.** *There exist a family of constant-depth Clifford circuits with the advice state  $|T^{1/p}\rangle^{\otimes n}$ , denoted as  $\text{Cliff}_{+T}$ , which can solve the ISMR problems  $\mathcal{R}_p^m$ , for a uniform distribution  $\mathcal{D}_p$  of input strings that satisfy the condition  $\sum_{i=1}^n x_i \bmod p = 0$  within  $\mathbb{F}_2^n$ . For any given input, these circuits achieve a success probability of  $\frac{2p-2}{p^2}$ . Additionally, they maintain an average correlation with the correct outcome within the Abelian domain, given by*

$$\text{Corr}_{\mathcal{D}_p}(|\text{Cliff}_{+T}|, |\mathcal{R}_p^m|) = \frac{p-1}{p^2}, \quad (5.74)$$

where  $m = \mathcal{O}(n \cdot g^{p^3})$ .

*Proof.* This circuit closely follows the quantum circuit considered in [Figure 10](#). However, we substitute the classically controlled<sup>15</sup> rotations  $R_Z$ , which are non-Clifford operators, with the teleportation gadget as represented on the right-hand side of [Equation \(5.63\)](#) without the correction operations, obtaining the following classically controlled Clifford circuit,



Furthermore, we will consider the correction string  $c \in \mathbb{F}_p^n$ , which describes the measurement outcomes in all the teleportation gadgets and determines the additional rotations applied to the states. Note that  $c_i = 0$  if  $x_i = 0$ , as no gadget is implemented for input bits, coming from the ISMR problems, with this value.

Having defined the setting, we need to redo the analysis of step 1 in [Lemma 4.26](#), as this is the first step where these two quantum circuits attempting to solve the same problems differ intrinsically. Specifically, we must describe the effect of the additional rotations resulting from the inability to perform corrections from the teleportation gadget, as detailed in [Lemma 5.15](#).

As we have three Z-rotations, they commute and we can implement these in any arbitrary order. Thus, we will consider the order most convenient for our analysis. First, we will analyze the rotations  $GR_Z(\theta, S)$ , which apply a Z rotation of magnitude  $\theta$  to all the basis states in the set  $S$ . These rotations cannot be ignored, as they alter the measurement outcomes. To better describe this operation, we first define a vectorized version of the delta function  $\vec{\delta}(x, i) : \mathbb{F}_p^n \mapsto \mathbb{F}_2^n$ , by

$$\vec{\delta}(x, i) = \delta_i(x_1), \delta_i(x_2), \dots, \delta_i(x_n), \quad (5.75)$$

with  $\delta_i(x) = 1$  if  $x = i$ , and 0 otherwise.

Now, we can analyze the effect of these rotations applied to the generalized poor-mans quipit states independently, given that these effects will add to the rotations in the ideal quantum circuit,

<sup>15</sup>Whenever we refer to a classical controlled gate, we mean that the gate will be implemented or not based on a classical binary bit defining each possible case. This contrasts with standard controlled gates that can be controlled by a qubit or quipit, which might be in a superposition

$$\bigotimes_{i=0}^{n-1} GR_Z \left( \frac{2\pi}{p}, S_{c_i} \right) |\text{GPM}_p^n\rangle = \frac{1}{\sqrt{p}} \sum_{i=0}^{p-1} e^{i \frac{2\pi \sum_{j=0}^{p-1} \sum_{k=0}^j \langle \vec{\delta}(c, j), \vec{\delta}(z^{+i}, n-k-1) \rangle}{p}} |z^{+i}\rangle \quad (5.76)$$

$$= \frac{\phi_g}{\sqrt{p}} \left( |z\rangle + \sum_{i=1}^{p-1} e^{i \frac{2\pi (\sum_{j=0}^{p-1} \sum_{k=0}^j \langle \vec{\delta}(c, j), \vec{\delta}(z^{+i}, n-k-1) \rangle - \langle \vec{\delta}(c, j), \vec{\delta}(z, n-k-1) \rangle)}{p}} |z^{+i}\rangle \right) \quad (5.77)$$

with the global phase  $\phi_g = e^{\frac{2\pi \sum_{j=0}^{p-1} \sum_{k=0}^j \langle \vec{\delta}(c, j), \vec{\delta}(z, n-k-1) \rangle}{p}}$  and  $S_{c_i} = [p - c_i, \dots, p - 1]$ . Additionally, to simplify, we will express the terms in the phases as follows,

$$\varphi(z^{+i}, c) = \sum_{j=0}^{p-1} \sum_{k=0}^j \langle \vec{\delta}(c, j), \vec{\delta}(z^{+i}, n-k-1) \rangle. \quad (5.78)$$

This will allow us to rewrite the previous states and describing the state with all the rotations applied as follows,

$$\bigotimes_{i=0}^{n-1} R_Z \left( \frac{2\pi x_i}{p^2} \right) GR_Z \left( -\frac{2\pi \cdot c_i}{p^2} \right) GR_Z \left( \frac{2\pi}{p}, S_{c_i} \right) |\text{GPM}_p^n\rangle \quad (5.79)$$

$$= \frac{e^{i \frac{2\pi \varphi(z, c)}{p}}}{\sqrt{p}} \left( \bigotimes_{i=0}^{n-1} R_Z \left( \frac{2\pi x_i}{p^2} \right) GR_Z \left( -\frac{2\pi \cdot c_i}{p^2} \right) \left( |z\rangle + \sum_{i=1}^{p-1} e^{i \frac{2\pi (\varphi(z^{+i}, c) - \varphi(z, c))}{p}} |z^{+i}\rangle \right) \right) \quad (5.80)$$

$$= \frac{\phi'_g}{\sqrt{p}} \left( |z\rangle + \sum_{i=1}^{p-1} e^{\frac{2\pi i \cdot (i|x|/p + (\sum_{j \in [i], \dots, i} \langle x, z^{+j} \rangle)^{p-1} + \varphi(z^{+i}, c) - \varphi(z, c))}{p}} |z^{+i}\rangle \right), \quad (5.81)$$

with  $\phi'_g = \exp \left( \frac{2\pi i \cdot (x, z) + p \cdot \varphi(z, c) - |c|}{p^2} \right)$ .

Subsequently, we repeat the same analysis as in [Lemma 4.26](#). We know that the measurement outcome depends on the values of  $\sum_{j \in [i]} (\langle x, z^{+j} \rangle)^{p-1} + \varphi(z^{+i}, c) - \varphi(z, c)$ , which once again are uniformly random values in  $\mathbb{F}_p$  as both strings  $z$  and  $c$  are uniformly random in  $\mathbb{F}_p^n$ . Specifically, we can use the same analysis as before, given that we can focus uniquely on the overlap with the basis states of the following form  $|\psi_p\rangle = |z\rangle + \sum_{j=1}^{p-1} e^{\frac{2\pi i \cdot (j|k|/p)}{p}} |z^{+j}\rangle$ , as these define the states that will project into strings that are congruent  $\text{mod } p$  with  $|k|$ , and thus infer the probability that our state projects into a superposition of strings congruent with the correct outcome to the respective ISMR problem.

Once again, due to the random and uniformly distributed form of the terms  $\sum_{j \in [i]} (\langle x, z^{+j} \rangle)^{p-1} + \varphi(z^{+i}, c) - \varphi(z, c)$ , the overlap with this state is equal to  $1/p$ , thus having zero correlation with ISMR problems. However, we can apply the same solution as in [Lemma 4.26](#) and concatenate a correction string to the outcome in the form of one of these terms. We then obtain a positive correlation with the correct outcome string. In particular, we obtain the same correlation if we use the first term,

$$\langle x, (z^{+1})^{p-1} \rangle + \varphi(z^{+1}, c) - \varphi(z, c). \quad (5.82)$$

The term  $\langle x, (z^{+1})^{p-1} \rangle$  we already know how to compute with a  $\text{NC}^0$  circuit, but we are missing to demonstrate that a string congruent modulo  $p$  with  $\varphi(z^{+1}, c) - \varphi(z, c)$  can be constructed with asymptotically small size using a  $\text{NC}^0$  circuit. Given the string  $c$ , the values of the terms  $\varphi(\cdot, \cdot)$  reduce to computing delta functions  $\vec{\delta}(\cdot, \cdot)$ . Moreover, the total number of such terms in the  $\vec{\delta}(\cdot, \cdot)$  function does not pose a problem, as the number of these terms needing computation is upper-bounded by  $\mathcal{O}(p^2)$ .

Now we need only to show then how the  $\vec{\delta}(a, b)$  for any input string  $a$  and dit  $b$  can be computed by an  $\text{NC}^0$  circuit. For that we show that,

$$\vec{\delta}(a, b) = \left( (a \oplus (-b)^{\otimes n})^{p-1} - 1 \right)^{p-1}. \quad (5.83)$$

Each of the terms  $(a_i \oplus -b)^{p-1} = 1$  if  $a_i \neq b$ , and equal to 0 otherwise. This means that we already have an inverse of the desired string. Now, we can subtract 1 so that all the 1s turn into 0s and the 0s to  $p-1$ . By applying the exponentiation of  $p-1$ , we ensure that all the 0s stay as zeros and the  $p-1$  indices turn 1 as desired, effectively inverting the 0s and 1s.

These terms must be efficiently computable for both the strings  $c$  and  $z^{+i}$ . For  $c$ , this is trivially true as we have access to the individual bits, and thus, each one of these operations is over a single dit and can be computed trivially with an  $\text{NC}^0$  circuit. For  $z^{+i}$ , this again is efficiently computable as the  $\oplus$  operation can be realized by adding these values to the string, and the same method can be applied for the  $-1$  operation. For the exponentiation, as described before, we can simply list all the products of terms, which are still bounded in number by  $\mathcal{O}(n \cdot g^{p^2})$  and perform these operations dit-wise. Finally, the inner product between these terms  $\langle \vec{\delta}(c, \cdot), \vec{\delta}(z^{+i}, \cdot) \rangle$  can be evaluated with the same approach as we did for  $\langle x, (z^{+1})^{p-1} \rangle$  in Lemma 4.26. With this correction string of size  $\mathcal{O}(n \cdot g^{p^3})$  computed by an  $\text{NC}^0$  circuit, we solve the respective ISMR problems with the intended correlation.

The last element to consider is that we can decompose the previously considered circuit into a constant-depth Clifford circuit if we are given the magic states  $|T^{1/p}\rangle$  (as proven in Lemma 5.14).  $\square$

With this, we have completed our construction of a family of quantum circuits over qupit gate sets composed of qupit Clifford gates with an additional  $T^{1/p}$  gate that can solve the ISMR problem for the respective prime dimension. This demonstrates that all the problems can be solved with minimal, finite, and standard universal gate sets. Additionally, we will subsequently show that the ability to rewrite these circuits as non-adaptive constant-depth Clifford circuits with access to magic states allows for error resilience while maintaining constant depth.

### 5.2.2 Noisy quantum circuits retain a computational advantage against $\text{bPTF}^0[k]$ .

Armed with all these ingredients, we are now finally ready to combine the conditions for the fault-tolerant realization of constant-depth quantum circuits with the alternative family of non-adaptive quantum circuits proposed in Section 5.2 to demonstrate that noisy qupit  $\text{QNC}^0/|T^{1/p}\rangle$  circuits can solve a family of relation problems beyond the capabilities of  $\text{bPTF}^0[k]$  circuits.

For this purpose, we use the relational problems from Definition 5.1, which are closely related to the original ISMR problems, and the noise-resilient implementation of  $\text{QNC}^0/|T^{1/p}\rangle$  circuits solving these problems from Section 5.2.1. More precisely, we will show that  $\text{QNC}^0$  circuits with  $|T^{1/p}\rangle$  provided as advice states, despite suffering from local stochastic noise, can solve a family of relational problems that are  $\text{AC}^0$ -reducible to the ISMR problems (see Figure 13). To this end, we will exploit the fact that the functions associated with the noise-resilient implementation—DEC and REC—are computable in  $\text{AC}^0$ , a necessary requirement for proving classical hardness against  $\text{bPTF}^0[k]$ .

We first prove that there exist  $\text{QNC}^0/|T^{1/p}\rangle$  circuits that solve the respective  $\mathfrak{R}_p$  problem for all prime  $p$  with a constant positive correlation, bounded away from zero.

**Lemma 5.17.** *For all primes  $p$ , there exists a family of classically controlled constant-depth Clifford circuits with all-to-all connectivity in the class  $\text{QNC}^0/|T^{1/p}\rangle$ , denoted as  $QC$ , that for any input  $x$  drawn uniformly at random from the subset of  $n$ -bit strings with Hamming weight satisfying  $(\sum_{i=1}^n x_i) \bmod p = 0$ , and affected by noise  $\mathcal{E} \sim \mathcal{N}(\tau)$  with a fixed probability  $\tau < \tau_{th}$ ,  $QC$  solves the respective relation  $\mathfrak{R}_p$  for output string of length  $y = o(n^2)$  with a constant positive correlation,*

$$\text{Corr}_{\mathcal{D}_p}(\mathfrak{R}_p(x, QC(x))) = 0.99 \cdot \left( \frac{p-1}{p^2} \right). \quad (5.84)$$

*Proof.* We will prove this claim by considering the noiseless versions of the circuit family described in Lemma 5.16, which solve the ISMR problems with a circuit architecture that can be noise-resilient based on Lemma 5.5 and Definition 5.4. Subsequently, we consider their logical version in the qudit surface code and show that the implementation of any element of this circuit family is noise-resilient with this code. Finally, we will demonstrate that decoding the logical outcome of any of these quantum circuits can be done efficiently by polynomial-size  $\text{AC}^0$  circuits, and thus their outcomes are  $\text{AC}^0$ -reducible to solutions to the ISMR problems (see Figure 13 for a representation of the described circuit).



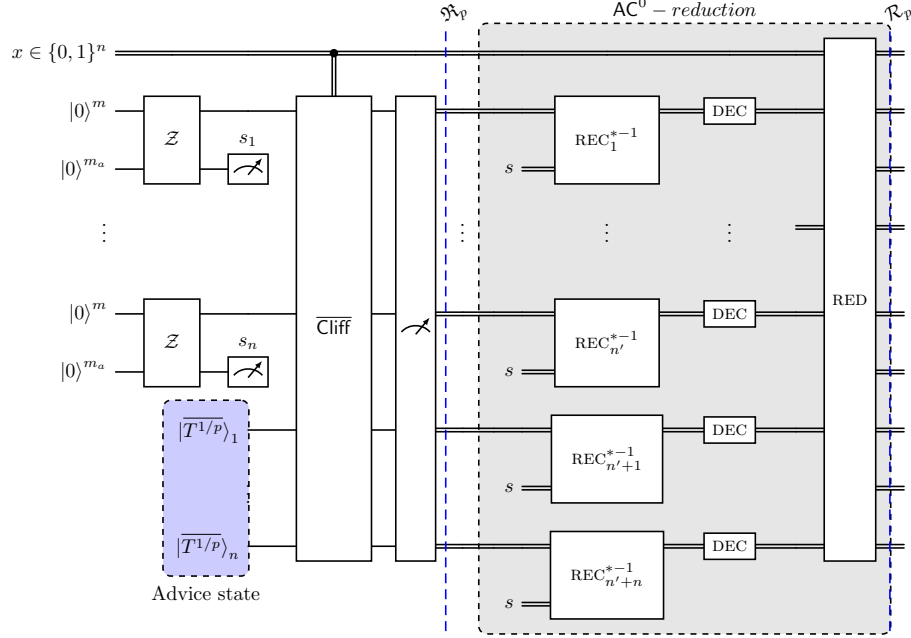


Figure 13: noise-resilient constant-depth Clifford quantum circuit with quantum advice states.

Now we will repeat the previous steps with all the necessary details. For that, we consider non-adaptive constant-depth Clifford circuits described in Lemma 5.16, and translating them into their logical version within the qubit surface code for a fixed distance  $d = \text{poly}(\log n)$ . In addition, we consider  $n$  repetitions of  $|T^{1/p}\rangle$ , the logical version of the magic state  $T^{1/p}$  in the surface code with distance  $d$ , as our advice state, which can be affected at most by local stochastic noise  $\mathcal{E} \sim \mathcal{N}(\tau)$  below a fixed threshold  $\tau_{th}$ . Simultaneously, we consider the single-shot state preparation process in Section 5.1.2 for creating the logical  $|\overline{\text{GHZ}}_2\rangle$  states within the surface code with the same distance  $d$ , without applying the recovery function REC but still producing the string  $s$ . Next, we apply the logical version of the classically controlled Clifford circuit described in Lemma 5.16, which we designate  $\overline{\text{Cliff}}(x)$ , except we omit the execution of certain logical Sum gates that are unnecessary because we start with the  $|\overline{\text{GHZ}}_2\rangle$  states and not logical  $|0\rangle$  states. The quantum circuit then concludes with a layer of Z measurements, as displayed in Figure 11.

Given the outcome of this circuit, we will consider the string  $s$  from the single-shot state preparation and the outcome of the logical circuit  $y$ . We can then define the functions  $\text{REC}_i^{*\dagger}$  (displayed in Figure 13) as the inverse of the recovery function  $\overline{\text{Cliff}}(x)\text{REC}(s)^\dagger\overline{\text{Cliff}}(x)^\dagger$ , restricted to the single logical qubit  $i$ . This undoes the effects of the errors occurring during the state preparation. Additionally, we compose to this operation the inversion of the logical X gate from the teleportation gadget introduced in Lemma 5.16, completing the definition of each  $\text{REC}_i^{*\dagger}$ . Furthermore, each one of these functions  $\text{REC}_i^{*-1}$  can be computed by an  $\text{AC}^0$  circuit using the arguments presented in [BGK+20; GJS21].

Now, given the assumption that the entire circuit is affected by local stochastic noise  $\mathcal{E} \sim \mathcal{N}(\tau)$  bounded below  $\tau_{th}$ , the noise-resilient single-shot  $\text{GHZ}_2$  state preparation from Section 5.1.2, and choosing the decoding function DEC to be a function implemented by the HDRG decoder, which can be computed by an  $\text{AC}^0$  circuit for our code distance, we derive from the combination of Lemma 5.13, Corollary 5.11, and Lemma 5.5 that after the decoding function, we have the exact outcome of the quantum circuit described in Lemma 5.16 with a probability of 0.99. By the same lemma, we have an  $\text{NC}^0$  reduction, (represented as RED in Figure 13), which provides outcome strings that correlate as described with the  $\mathfrak{R}_p$  problems, completing the proof since it is trivially computed by an  $\text{AC}^0$  circuit.  $\square$

Simultaneously, we can prove that any  $\text{bPTF}^0[k]$  circuit has close to zero correlation with the  $\mathfrak{R}_p^{n'}$  problems for the size of the outcome strings that the  $\text{QNC}^0/|T^{1/p}\rangle$  under consideration produces.

**Proof of Theorem 5.2.** From Lemma 5.17, we obtain that there exists a  $\text{QNC}^0 / |\overline{T^{1/p}}\rangle$  circuit that solves the  $\mathfrak{R}_p^{n'}$  for all prime  $p$  with the specified outcome strings. Now, we intend to demonstrate that, for the same parameters,  $\text{bPTF}^0[k]$  circuits have close to zero correlation with the same relation problems.

To link the correlation of solving  $\mathfrak{R}_p^{n'}$  with  $\mathcal{R}_p^{n'}$ , we use that by definition they are  $\text{AC}^0$ -reducible to each other. Thus, a solution with a high correlation to  $\mathfrak{R}_p^{n'}$  by a  $\text{bPTF}^0[k]$  implies the existence of a slightly larger  $\text{bPTF}^0[k]$  with the same correlation for  $\mathcal{R}_p^{n'}$ . Therefore, by considering a constant depth  $d'$  for this  $\text{AC}^0$  reduction, we obtain the bounds described in Theorem 5.2 based on the lower bound proven in Theorem 4.12, concluding the proof.  $\square$

We conclude by considering the isolated qubit case, which has two main distinguishing features compared to the previously proven qudit cases. First, it does not require magic states; unlike those for all other primes  $p \geq 3$ , the qubit circuit will be a Clifford circuit. Second, it allows for separation with a fixed probability due to the one-to-one relationship between the correlation function and the likelihood of producing a correct or incorrect outcome for the  $\mathfrak{R}_2^{n'}$  problem.

**Proof of Corollary 5.3.** This corollary follows more easily, as we consider exactly the same ideas for the qupit circuit in Lemma 5.17, but we do use as the underlying logical Clifford circuit the circuit from Lemma 4.26 for qubits, without additional advice state, nor teleportation gadgets, given that the necessary rotation is a Clifford operator.

For the  $\text{bPTF}^0[k]$  lower bound, we use the same lower bound as in Theorem 4.3, which allows us to bound the success probability of any  $\text{bPTF}^0[k]$  solving the  $\mathfrak{R}_2$  problem.  $\square$

## 6 Discussion

In this paper we have advanced the nascent line of work showing unconditional separations between the computational power of classical and quantum shallow-depth circuits. We have shown that linear-size local  $\text{QNC}^0$  circuits can solve multi-output search problems (relation problems) that polynomial-size circuits of  $k$ -bounded polynomial threshold gates fail to solve with appreciable probability even on average. We have also developed a family of non-local games over qupits of each prime dimension and used the separation in winning probabilities between classical and quantum strategies to show that the computational separation we establish for qubit  $\text{QNC}^0$  circuits extends to  $\text{QNC}^0$  circuits over higher dimensional quantum systems. This is especially significant in the light of our belief that under finite universal gate sets, the corresponding  $\text{QNC}^0$  circuit classes over  $p$  and  $q$  dimensional systems are incomparable for  $p \neq q$  (see Conjecture 1). Finally, we have also shown that the computational separations we establish are noise-robust, in that even quantum circuits affected by local stochastic noise continue to exhibit computational advantages over noiseless classical circuits, using techniques that draw on magic state injection and hard decision renormalization group decoders.

We conclude this article exploring the applicability of our results to practical developments in quantum computing and machine learning. As we rapidly progress through the NISQ era, with several noisy intermediate scale quantum devices with different underlying architectures and technologies on the horizon, precise estimates of the resource requirements for demonstrations of quantum computational advantage become increasingly relevant. Such resource estimation and optimization is of particular significance to work such as ours that focuses on shallow-depth circuits that may be within the reach of both theoretical optimization and practical implementation. In Section 6.1, we present the best known order-of-magnitude circuit width, depth and size estimates for witnessing unconditionally provable separations of computational power between  $\text{QNC}^0$  and the largest known classical circuit classes to date.

In learning theory, the expressivity of hypothesis classes such as neural network architectures commands as much attention as computational complexity. Decades of work have approached this problem with tools from circuit complexity. Proving that a forward pass through a neural network architecture can be simulated by a circuit class such as  $\text{AC}^0$  establishes upper bounds that allow us to carry over known results about circuit complexity lower bounds to understand the expressivity and generality of the neural network. In Section 6.2, we discuss some relations between our findings on circuit complexity and recent results on the simulation of popular neural network models by shallow depth classical circuits.

## 6.1 Resource estimation

In physical implementations that test the kind of unconditional separations that we present, it is key to pin down at what values of circuit depth  $d$  and input size  $n$  (i.e. number of input qubits) we observe a transition in the circuit size. That is, at what depths and input sizes do the quantum advantages kick in?

To answer this question, we can make preliminary estimates by solving for the parameter values at which the asymptotic lower bounds for the size of the best classical circuit become equal to the quantum upper bounds. Using the best estimates for the constant factors hidden in the asymptotics, we solve this equality for values of the input size  $n$  and depth  $d$  at which the quantum circuit size becomes smaller than the classical circuit size.

We can leverage our exact-case hardness bound in [Theorem 1.2](#) to derive tighter estimates compared to what is possible using prior work, bringing theoretical predictions closer to the capabilities of current quantum devices. For context, the transition point for Shor’s factoring algorithm is estimated to be  $\sim 1,700$  qubits,  $10^{36}$  Toffoli gates, and a circuit depth of  $10^{25}$  [CFS24], while for the HHL quantum matrix inversion algorithm it is roughly  $10^8$  qubits and a depth of  $10^{29}$  [SVM+17]. Recent advancements in quantum hardware favor larger devices (i.e., more qubits) over those with prolonged coherence, and so there is a push towards shallower circuits [LJV+23; BEG+23]. Thus, separations against  $\text{NC}^0$  represent a promising avenue for near-term quantum devices, requiring only hundreds to thousands of qubits to demonstrate classical non-realizability results, such as Bell violations [SMC+15; RHH+18; BGK18]. While much work in this direction has focused on such information theoretic demonstrations, a *computational* example of this is solving the 2D Hidden Linear Function problem using a noise-free quantum circuit. In this case, the classical model being compared—circuits of bounded fan-in—require a depth of at least  $d = \Omega(\log n)$  [BGK18]. This provides a demonstrable quantum advantage when the quantum circuit resolves an instance with a depth strictly smaller than the minimum possible depth for any classical circuit. In a more realistic scenario that includes noise, the depth of the quantum circuit may increase by a constant factor, but the minimal classical circuit depth will still be at least  $d = \Omega(\frac{\log n}{\log \log n})$  [BGK+20]. This adjustment, due to the presence of noise, slightly increases the previous estimates of the input sizes required for the problem to witness a quantum advantage. Additionally, imposing connectivity restrictions on the classical circuit—which are not part of the  $\text{NC}^0$  definition—the size of the input strings at which the crossover to the quantum advantage regime happens may be effectively reduced [BJ23].

Moving up the ladder of potential demonstrations of unconditional quantum advantage, the challenge is to outperform larger classical constant-depth circuit classes such as  $\text{AC}^0$ . Once again we may ask what the minimal size input size is at which which classical circuits require more gates to solve the instance than quantum circuits. As the quantum circuits for the Parity Halving Problem (PHP) have a linear number of gates  $\Theta(n)$ , our main tasks are to bound the constant factor hidden by the  $\Theta$  notation, and to determine the minimum classical circuit size. As before we equate the PHP lower bound on the size of the  $\text{AC}^0$  circuits and the upper bound on the size of the  $\text{QNC}^0$  circuits, and solve for the input size. It is crucial that we do this after fixing the minimal allowed depth, because otherwise the subexponential dependence of the classical circuit size on the depth results in astronomically large input sizes. Specifically, using the local 2D  $\text{QNC}^0$  circuit proposed in [WKS+19] that achieves a separation against  $\text{AC}^0$  under average-case scenarios, avoiding asymptotic simplifications and using the precise bounds and parameters ( $q = \sqrt{\log n}$ ) provided by the authors, and using the depth  $d = 5$  version of the circuit rewritten in the MBQC setting, we find that even with these choices we would require approximately  $10^{97}$  qubits to observe a quantum advantage.

However, by moving from local 2D circuits to all-to-all qubit connectivity and optimizing the parameters in the random restrictions technique used to lower bound the classical circuit size specifically for this connectivity, we can drop this requirement to  $10^{21}$  qubits with depth-3 quantum circuits, a considerably lower value than the previous rough estimates. Similar estimates can be obtained for increasingly larger classical circuit classes by leveraging our average-case hardness bound in [Theorem 1.2](#). For instance, for  $\text{bPTF}^0[n^{1/(5d)}]$  circuits, we obtain that one would require  $10^{40}$  qubits for a demonstration of quantum advantage, once again using suitably optimized quantum circuits and parameter values (see [Table 4](#)).

Towards this goal, with our exact-case hardness bound from [Theorem 1.2](#), without any simplification as shown in [Table 4](#), we are able to reduce by several orders of magnitude the estimated minimal quantum resources required for demonstrations of quantum advantage. Specifically, we find that depth-3 circuits with  $10^{11}$  and  $10^{22}$  qubits respectively can exhibit quantum advantages over  $\text{AC}^0$  and  $\text{bPTF}^0[n^{1/(5d)}]$  circuits. This substantial reduction in resource requirements marks a step forward in the progression of quantum advantage

$\text{bPTF}^0[k]/\text{rpoly}$	All-to-all
Exact, $k = \mathcal{O}(1)$	$\log_2(s) = \Omega \left( e^{\frac{1}{1-d}} \left( \frac{n}{\sqrt{n \log n \log(n \log n)}} \right)^{-\frac{1}{1+d}} \right)$
Exact, $k = n^{1/(5d)}$	$\log_2(s) = \Omega \left( e^{\frac{1}{1-d}} \left( \frac{n^{\frac{3}{10}}}{\sqrt{\log n \log(n \log n)}} \right)^{-\frac{1}{1+d}} \right)$
Average, $k = n^{1/(5d)}$	$\Pr[\text{Success}] \leq \frac{1}{2} + 2^{-\Omega \left( \frac{n^{8/5} (n \log n)^{-1 - \frac{2}{\sqrt{\log n + \log \log n}}}}{2(2\sqrt{\log n + \log \log n})_{(\log s)^{2d-2}}} \right)}$

Table 4: Size lower bounds for the circuit classes  $\text{bPTF}^0[k]$  without simplifications and optimal values for the parameter  $q$ .

experiment design.

To conclude, we remark that our estimates do not by any means represent lower bounds on the threshold of input size necessary to establish a quantum advantage regime, as improvements in proof methodologies and parameter optimization are still possible.

## 6.2 Neural networks as bounded polynomial threshold circuits

In this concluding section, we turn our attention to the connections between our main results and active fields of research in classical and quantum machine learning. We especially intend to (loosely) interpret how our techniques and conclusions relate to classical neural networks. We shall also identify potential implications of computational separations between shallow depth circuit classes for studying quantum over classical advantages in machine learning tasks.

### Connection to classical neural networks

The class of classical constant depth circuits  $\text{TC}^0$  was first defined in the quest for greater computational power beyond Boolean  $\text{AC}^0$  circuits [PS88]. Furthermore, it is also well motivated as a model for neural networks composed of Boolean neurons, inspired by biological neural networks [Par94]. This class notably includes the threshold function  $\text{Th}_w : x \in \{0, 1\}^n \mapsto 1$  iff  $|x| > w$  and 0 otherwise, which captures the most basic activation behavior that can be exhibited by a neuron. Interestingly, this theoretical relationship has typically been analyzed retrospectively: new neural network models first prove themselves as practically useful, and only subsequently is their standing relative to the circuit classes studied in complexity theory understood, both in terms of expressivity and computational capability. For instance, neural networks with fan-in bounded by the logarithm of the input size fall within the  $\text{AC}^0$  class [SAK92], and thus they cannot even compute the parity function. On the other hand, neural networks whose nodes can have unbounded fanout are known to be simulatable in  $\text{TC}^0$  for a wide variety of weight types associated with the neurons' activation function [Smo13]. Based on the widely held conjecture that  $\text{TC}^0 \subsetneq \text{NC}^1$ , these neural networks are therefore unlikely to be able to solve problems considered 'simple,' such as iterated matrix multiplication and solving linear equations, which are known to be solvable in  $\text{NC}^1$  and  $\text{P}$  respectively [MP00; GHR91].

More recently the transformer architectures of neural networks [VSP<sup>+</sup>17], well-known for their spectacularly successful and widespread use in large language models (LLMs) such as ChatGPT, have been analyzed through the lens of constant-depth circuit classes. For instance, depending on the type of attention function used, the expressivity of transformer models may be limited; one example is the upper bound on hard attention in terms of languages computable by  $\text{AC}^0$  circuits [Hah20]. This suggests that any such model is generally weak, as we know of various relevant and simple computational functions, such as parity and majority, that are not included in this circuit class. Nevertheless, it is also worth noting that even this potentially weak attention model still finds powerful applications in computer vision models [XBK<sup>+</sup>15], and continues to be an area of active development [EKL19]. Transformers with the less restrictive saturated attention exhibit greater

expressivity, and in a sense their power coincides with  $\text{TC}^0$  circuits [MSS22; Str23]. This matches up with our empirical understanding that transformers employing more complex attention functions demonstrate better performance. The transformer architecture can be further extended to be able to capture computations in P, and indeed even transformers restricted to hard attention are known to be Turing-complete if they are allowed to perform computations with arbitrary precision and run for an unbounded number of time-steps [PBM21]. However, this is not a realistic setting in practice, and it has been pointed out that practical cases with the precision of their internal weights and variables restricted to be logarithmic in the input length (a generous allowance) correspond exactly to uniform  $\text{TC}^0$  [MS23]. We refer the reader to [SMW<sup>+</sup>24] for a survey of studies on the expressivity of neural network models in terms of circuit complexity.

We now proceed to explore the connection between the analysis and techniques in our work and the existing literature. We will demonstrate how one can compute commonly used activation functions using  $\text{bPTF}^0[k]$  circuits, and examine how the degree-bound parameter  $k$  influences this. Notably, this shows that a substantial subclass of neural networks, including transformers with non-trivial attention functions which extend beyond  $\text{AC}^0$  circuits [MSS22] can be analyzed using our techniques and switching lemmas. Furthermore, we remark that this analysis is applicable not only to decision problems but also to relation problems. This is of significance since neural networks, especially LLMs, should primarily be considered sequence-to-sequence models, that take (bit) strings as input and produce (bit) strings as output.

Consider discretizing a function of the type  $f : \{0, 1\}^n \mapsto [0, b] \subseteq \mathbb{R}$  by choosing parameter  $w \in \mathbb{Z}$  and discretizing the range  $[0, b]$  into steps of size  $w$ , to obtain  $\hat{f} : \{0, 1\}^n \mapsto \mathbb{Z}_B$  where  $B = w \cdot \lfloor \frac{b}{w} \rfloor$ . Discretizing an activation function allows us to implement it by  $\text{bPTF}^0[k]$  circuits, generating a  $k$ -bounded function. This means that the function exhibits a ‘tail’ that always outputs 1 for inputs with a Hamming weight greater than  $k$ , akin to an AND type activation function. In Algorithm 2, we demonstrate that a discretized version of any activation function can be implemented accurately by  $\text{bPTF}^0[k]$  circuits for input bitstrings of Hamming weight less than  $k$ .

It is easy to implement the discretized version for input bitstrings with a Hamming weight greater than  $n - k$  by a related circuit. It includes an initial segment that always outputs 0 for all inputs with a Hamming weight less than  $n - k$ , resembling an OR type activation function. Specifically, our algorithm requires only a single layer of PTF gates in parallel, thereby achieving a depth-1  $\text{bPTF}^0[k]$  circuit that implements  $\hat{f}$ . Figure 14a presents a notable example of this discretization for a specific parameter  $k$  of the  $\text{bPTF}^0[k]$  circuits for the widely used ReLU activation function, which is defined as  $f(x) = \max\{0, x - c\}$  (where we have shifted the centre from 0 to  $c$ ). Our scheme considers  $\text{ReLU} : \{0, 1\}^n \rightarrow [0, n - c]$  taking  $n$ -bit strings as input and interpreting their Hamming weight as the input  $x$ .

**Remark.** Note that functions with larger activation regions (i.e., those with higher values of the degree-bound parameter  $k$ ) can be achieved by composing deeper  $\text{bPTF}^0[k]$  circuits. Also, by combining AND and OR type decompositions within a single depth-1 layer, one can obtain non-trivial activation regions for both Hamming weights smaller than  $k$  and larger than  $n - k$ . This approach results in only a central region of fixed Hamming weight rather than the entire tail as in each case, AND and OR type decompositions.

## Connection to quantum neural networks

As we have seen, our computational separations demonstrate a quantum advantage over a model that encompasses many interesting classical machine learning models. From another perspective, this contributes to the extensively studied field of quantum machine learning. In particular, several studies have identified learning tasks that might benefit from a quantum advantage. Much work has also focused on the fundamental problem of learning a robust quantum solution, with a significant discussion based on the premise that models which are easy to train tend to be classically simulatable and thus are unlikely to offer quantum advantage. Conversely, models that are very general and potentially offer a quantum advantage tend to be difficult to train, from a theoretical perspective.

It is of great interest to understand which models emerge as good candidates for quantum advantage in the first place. In this setting, some notable classical-quantum separations rely on encoding a problem known to be hard into a valid quantum solution [LAT21]. Others resort to quantum phenomena to explain enhanced expressivity and performance by explicitly pointing out where non-locality or contextuality clearly

---

**Algorithm 2** Hamming-Weight Bounded Activation Function Decomposer

---

```

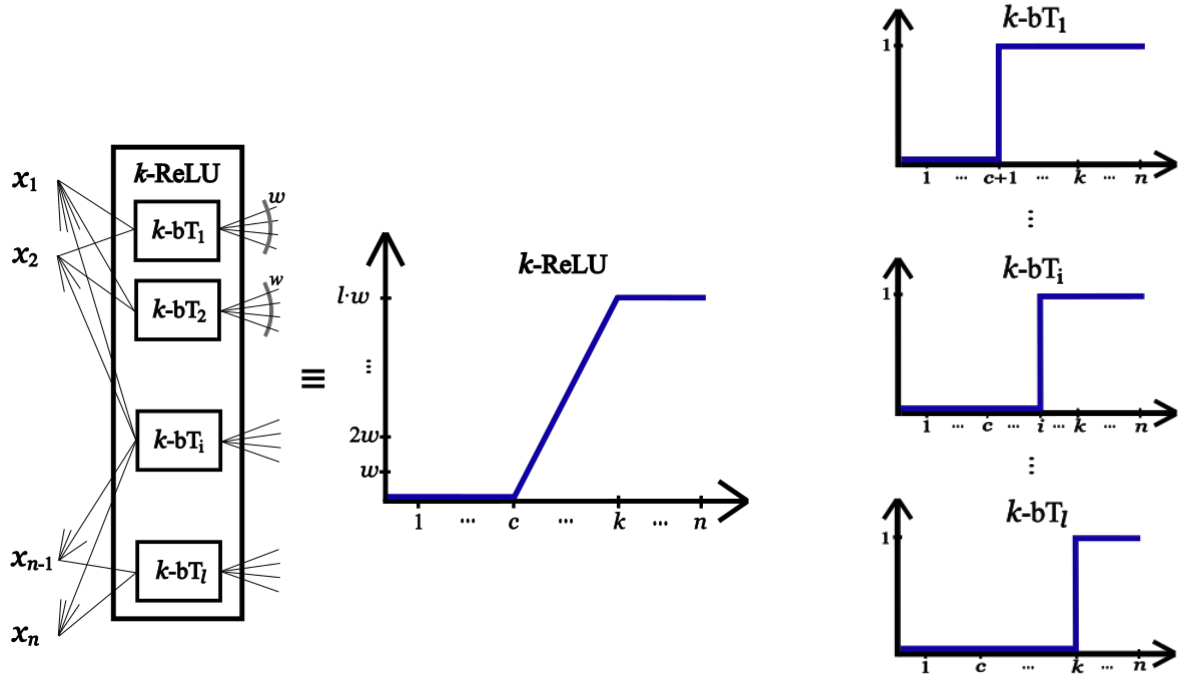
1: procedure Decomp(Degree parameter  $k$ , activation function  $f : \{0,1\}^n \mapsto \mathbb{R}$ , resolution parameter  $w \in \mathbb{N}$ )
2:    $gates \leftarrow [], i \leftarrow 0$ .
3:    $l \leftarrow \lfloor \max_x (f(x)/w) \rfloor$  for  $|x| \leq k$ . ▷ Number discrete steps/gates in the decomposition.
4:   while  $\exists x \text{ s.t. } f(x) - i \cdot w > 0$  with  $|x| \leq k$  do
5:     Find  $S_i \subseteq [n]$  s.t.  $\forall j \in S_i \lfloor (f(x_j) - i \cdot w) \rfloor = 0$ .
6:     Define
        
$$\text{bPTF}_i[k](x) = \begin{cases} 1, & \text{for all } x_j \text{ with } j \in S_i \text{ and } |x_j| \leq k \\ 0, & \text{otherwise} \end{cases}$$

7:     Concatenate  $(gates, \text{bPTF}_i(k))$ .
8:      $i = i + 1$ .
9:   end while ▷ The loop ends when  $w \cdot i > \max_x f(x)$ .
10:  return  $(l, gates)$ 
11: end procedure

```

**High-level description:** The algorithm sequentially calculates the set of points of the activation function at discrete intervals defined by  $w \cdot i$ , where  $i$  is an integer. It then groups these points into sets of indices corresponding to where the discretized function matches the value  $w \cdot i$ . This process continues iteratively until the final discretized step at  $w \cdot k'$  closely approximates the maximum value of  $f$ .

---



(a) Representation of a  $k$ -ReLU gate, which is equivalent to a ReLU gate, up to precision  $w$ , for every input string with a Hamming weight bounded by  $k$ . The  $k$ -ReLU gate is contained in  $\text{bPTF}^0[k]$ ; the precise circuit can be obtained by Algorithm 2, which defines  $k'$  the number and the particular  $\text{bPTF}[k]$  gates used in the  $k$ -ReLU layer along with the respective fan-out wires. These elements are depicted on the left side of the figure, and the composite gate, which is the outcome of the circuit, is displayed on the right.

(b) Illustration of the unbounded region of each one of the  $k'$   $\text{bPTF}[k]$  gates employed in the  $k$ -ReLU gate. These functions are obtained from Algorithm 2, based on the parameter  $k$ , the activation function  $f$  and  $w$  the size of the discretization steps.



distinguishes between quantum and classical models at the operational level [AG24; AHH<sup>+</sup>23; BWF<sup>+</sup>23; GAW<sup>+</sup>22].

Our computational separation resembles the latter, where non-classical phenomena are translated into computational complexity. Furthermore, separations like ours have been utilized in a manner that combines both of the previously mentioned ideas: they demonstrate that certain problems that intrinsically exhibit quantum phenomena can be efficiently solved by quantum models, while remaining intractable for classical models cannot handle. Interestingly, these separations enable us to explore potential quantum advantages in machine learning problems and the benefits of quantum models over classical ones. These analyses have extended to include standard figures of merit used in machine learning, such as the Kullback-Leibler divergence, which was shown to differ between classical and quantum models [ZGL<sup>+</sup>24]. This opens avenues for further research.

Finally, we note that the line of work we advance demonstrates that even simple and potentially easy-to-learn quantum circuits can outperform their classical counterparts. This supports other findings that even efficiently learnable quantum circuits could provide a quantum advantage in practical information processing tasks [AG24; HLB<sup>+</sup>24; GD17; AHH<sup>+</sup>23; ZGL<sup>+</sup>24; BWF<sup>+</sup>23; ASZ<sup>+</sup>21; DHL<sup>+</sup>21].

## Acknowledgements

We thank anonymous referees for useful comments. MdO is supported by National Funds through the FCT - Fundação para a Ciência e a Tecnologia, I.P. (Portuguese Foundation for Science and Technology) within the project IBEX, with reference PTDC/CCI-COM/4280/2021, and via CEECINST/00062/2018 (EFG). SS is supported by a Royal Commission for the Exhibition of 1851 Research Fellowship.

## References

- [Aar10] Scott Aaronson. “BQP and the polynomial hierarchy”. *Proceedings of the forty-second annual ACM symposium on Theory of computing*, pages 141–150, 2010 (page 10).
- [AA11] Scott Aaronson and Alex Arkhipov. “The computational complexity of linear optics”. *Proceedings of the forty-third annual ACM symposium on Theory of computing*, pages 333–342, 2011 (page 3).
- [Aas21] Sivert Aasnaess. *Comparing two cohomological obstructions for contextuality, and a generalised construction of quantum advantage with shallow circuits*. PhD thesis, University of Oxford, Oxford, UK, 2021 (page 5).
- [ASZ<sup>+</sup>21] Amira Abbas, David Sutter, Christa Zoufal, Aurélien Lucchi, Alessio Figalli, and Stefan Woerner. “The power of quantum neural networks”. *Nature Computational Science*, 1(6):403–409, 2021 (page 81).
- [AW93] Eric W Allender and Klaus W Wagner. “Counting hierarchies: polynomial time and constant depth circuits”, *Current trends in theoretical computer science: essays and Tutorials*, pages 469–483. World Scientific, 1993 (page 10).
- [AG24] Eric R Anschuetz and Xun Gao. “Arbitrary polynomial separations in trainable quantum machine learning”. *arXiv:2402.08606*, 2024 (page 81).
- [AHH<sup>+</sup>23] Eric R Anschuetz, Hong-Ye Hu, Jin-Long Huang, and Xun Gao. “Interpretable quantum advantage in neural sequence learning”. *PRX Quantum*, 4(2):020338, 2023 (page 81).
- [Anw14] Hussain Anwar. *Towards fault-tolerant quantum computation with higher-dimensional systems*. PhD thesis, UCL (University College London), 2014 (page 16).
- [ABC<sup>+</sup>14] Hussain Anwar, Benjamin J Brown, Earl T Campbell, and Dan E Browne. “Fast decoders for qudit topological codes”. *New Journal of Physics*, 16(6):063038, 2014 (pages 9, 59).
- [AB09] Sanjeev Arora and Boaz Barak. *Computational Complexity: A Modern Approach*. Cambridge University Press, USA, 1st edition, 2009 (page 19).

- [BV19] Pierre Baldi and Roman Vershynin. *Polynomial threshold functions, hyperplane arrangements, and random tensors*, 2019. arXiv: [1803.10868 \[math.PR\]](#) (page 3).
- [BBC<sup>+</sup>95] Adriano Barenco, Charles H. Bennett, Richard Cleve, David P. DiVincenzo, Norman Margolus, Peter Shor, Tycho Sleator, John A. Smolin, and Harald Weinfurter. “Elementary gates for quantum computation”. *Phys. Rev. A*, 52:3457–3467, 5, 1995 (page 5).
- [BCE<sup>+</sup>07] Jonathan Barrett, Carlton M. Caves, Bryan Eastin, Matthew B. Elliott, and Stefano Pironio. “Modeling pauli measurements on graph states with nearest-neighbor classical communication”. *Physical Review A*, 75(1), January 2007 (page 8).
- [Bar86] David A Barrington. “Bounded-width polynomial-size branching programs recognize exactly those languages in nc”. *Proceedings of the eighteenth annual ACM symposium on Theory of computing*, pages 1–5, 1986 (page 3).
- [BV93] Ethan Bernstein and Umesh Vazirani. “Quantum complexity theory”. *Proceedings of the twenty-fifth annual ACM symposium on Theory of computing*, pages 11–20, 1993 (page 8).
- [BP02] Alberto Bertoni and Beatrice Palano. “Structural complexity and neural networks”. *Neural Nets: 13th Italian Workshop on Neural Nets, WIRN VIETRI 2002 Vietri sul Mare, Italy, May 30–June 1, 2002 Revised Papers 13*, pages 190–216. Springer, 2002 (page 11).
- [BCH<sup>+</sup>20] Michael Beverland, Earl Campbell, Mark Howard, and Vadym Kliuchnikov. “Lower bounds on the non-clifford resources for quantum computations”. *Quantum Science and Technology*, 5(3):035009, May 2020 (page 70).
- [BMT<sup>+</sup>22] Michael E Beverland, Prakash Murali, Matthias Troyer, Krysta M Svore, Torsten Hoeffler, Vadym Kliuchnikov, Guang Hao Low, Mathias Soeken, Aarthi Sundaram, and Alexander Vaschillo. “Assessing requirements to scale to practical quantum advantage”. *arXiv:2211.07629*, 2022 (page 3).
- [BJ23] Kishor Bharti and Rahul Jain. “On the power of geometrically-local classical and quantum circuits”. *arXiv:2310.01540*, 2023 (pages 9, 77).
- [BEG<sup>+</sup>23] Dolev Bluvstein, Simon J Evered, Alexandra A Geim, Sophie H Li, Hengyun Zhou, Tom Manovitz, Sepehr Ebadi, Madelyn Cain, Marcin Kalinowski, Dominik Hangleiter, et al. “Logical quantum processor based on reconfigurable atom arrays”. *Nature*:1–3, 2023 (pages 9, 32, 77).
- [BFN<sup>+</sup>19] Adam Bouland, Bill Fefferman, Chinmay Nirkhe, and Umesh Vazirani. “On the complexity and verification of quantum random circuit sampling”. *Nature Physics*, 15(2):159–163, 2019 (page 3).
- [BWF<sup>+</sup>23] Joseph Bowles, Victoria J Wright, Máté Farkas, Nathan Killoran, and Maria Schuld. “Contextuality and inductive bias in quantum machine learning”. *arXiv:2302.01365*, 2023 (page 81).
- [BBT04] Gilles Brassard, Anne Broadbent, and Alain Tapp. “Recasting mermin’s multi-player game into the framework of pseudo-telepathy”. *arXiv preprint quant-ph/0408052*, 2004 (page 39).
- [BGK<sup>+</sup>20] Sergey Bravyi, David Gosset, Robert Koenig, and Marco Tomamichel. “Quantum advantage with noisy shallow circuits”. *Nature Physics*, 16(10):1040–1045, 2020 (pages 3, 6, 8, 9, 15–17, 24, 54, 55, 58, 61–63, 67, 75, 77).
- [BGK18] Sergey Bravyi, David Gosset, and Robert König. “Quantum advantage with shallow circuits”. *Science*, 362(6412):308–311, 2018. eprint: <https://www.science.org/doi/pdf/10.1126/science.aar3106> (pages 3, 7–10, 77).
- [BH13] Sergey Bravyi and Jeongwan Haah. “Quantum self-correction in the 3d cubic code model”. *Physical Review Letters*, 111(20), 2013 (pages 16, 24, 58–60).
- [BKM<sup>+</sup>24] Alex Bredariol Grilo, Elham Kashefi, Damian Markham, and Michael de Oliveira. “The power of shallow-depth Toffoli and qudit quantum circuits”, arXiv:2404.18104, April 2024. arXiv: [2404.18104 \[quant-ph\]](#) (pages 8, 10, 45).
- [BJS11] Michael J Bremner, Richard Jozsa, and Dan J Shepherd. “Classical simulation of commuting quantum computations implies collapse of the polynomial hierarchy”. *Proceedings of the Royal Society A: Mathematical, Physical and Engineering Sciences*, 467(2126):459–472, 2011 (page 3).

- [BBC<sup>+</sup>24] Jop Briët, Harry Buhrman, Davi Castro-Silva, and Niels M. P. Neumann. “Noisy Decoding by Shallow Circuits with Parities: Classical and Quantum (Extended Abstract)”. Venkatesan Guruswami, editor, *15th Innovations in Theoretical Computer Science Conference (ITCS 2024)*, volume 287 of *Leibniz International Proceedings in Informatics (LIPIcs)*, 21:1–21:11, Dagstuhl, Germany. Schloss Dagstuhl – Leibniz-Zentrum für Informatik, 2024. eprint: [arXiv:2302.02870](#) (pages 5, 8).
- [BCP<sup>+</sup>14] Nicolas Brunner, Daniel Cavalcanti, Stefano Pironio, Valerio Scarani, and Stephanie Wehner. “Bell nonlocality”. *Rev. Mod. Phys.*, 86:419–478, 2, 2014 (page 22).
- [CCK23] Libor Caha, Xavier Coiteux-Roy, and Robert Koenig. “A colossal advantage: 3d-local noisy shallow quantum circuits defeat unbounded fan-in classical circuits”. *arXiv:2312.09209*, 2023 (pages 3, 9, 14, 54).
- [CCK22] Libor Caha, Xavier Coiteux-Roy, and Robert Koenig. “Single-qubit gate teleportation provides a quantum advantage”. *arXiv e-prints:arXiv:2209.14158*, 2022 (page 9).
- [Che19] Lijie Chen. “Non-deterministic quasi-polynomial time is average-case hard for ACC circuits”. *2019 IEEE 60th Annual Symposium on Foundations of Computer Science (FOCS)*, pages 1281–1304, 2019 (page 3).
- [CSS16] Ruiwen Chen, Rahul Santhanam, and Srikanth Srinivasan. “Average-Case Lower Bounds and Satisfiability Algorithms for Small Threshold Circuits”. Ran Raz, editor, *31st Conference on Computational Complexity (CCC 2016)*, volume 50 of *Leibniz International Proceedings in Informatics (LIPIcs)*, 1:1–1:35, Dagstuhl, Germany. Schloss Dagstuhl – Leibniz-Zentrum für Informatik, 2016 (page 3).
- [CFS24] Clémence Chevalier, Pierre-Alain Fouque, and André Schrottenloher. “Reducing the number of qubits in quantum factoring”. *Cryptology ePrint Archive*, 2024 (page 77).
- [CGP<sup>+</sup>02] Daniel Collins, Nicolas Gisin, Sandu Popescu, David Roberts, and Valerio Scarani. “Bell-type inequalities to detect true  $n$ -body nonseparability”. *Phys. Rev. Lett.*, 88:170405, 17, 2002 (page 22).
- [CSV21] Matthew Coudron, Jalex Stark, and Thomas Vidick. “Trading locality for time: certifiable randomness from low-depth circuits”. *Communications in mathematical physics*, 382:49–86, 2021 (pages 3, 6, 53).
- [CGK17] Shawn X. Cui, Daniel Gottesman, and Anirudh Krishna. “Diagonal gates in the clifford hierarchy”. *Physical Review A*, 95(1), January 2017 (page 70).
- [diFO<sup>+</sup>24] Antonio deMartí iOliver, Patricio Fuentes, Román Orús, Pedro M. Crespo, and Josu Etxezarreta Martínez. *Decoding algorithms for surface codes*, 2024. arXiv: [2307.14989 \[quant-ph\]](#) (page 58).
- [dSil21] Nadish de Silva. “Efficient quantum gate teleportation in higher dimensions”. *Proceedings of the Royal Society A*, 477(2251):20200865, 2021 (pages 69, 70).
- [DFN<sup>+</sup>24] Yangjing Dong, Honghao Fu, Anand Natarajan, Minglong Qin, Haochen Xu, and Penghui Yao. “The Computational Advantage of MIP\* Vanishes in the Presence of Noise”. Rahul Santhanam, editor, *39th Computational Complexity Conference (CCC 2024)*, volume 300 of *Leibniz International Proceedings in Informatics (LIPIcs)*, 30:1–30:71, Dagstuhl, Germany. Schloss Dagstuhl – Leibniz-Zentrum für Informatik, 2024 (page 6).
- [Don14] Ryan O’ Donnell. *Analysis of boolean functions*. Cambridge University Press, 2014 (pages 7, 14, 22).
- [DHL<sup>+</sup>21] Yuxuan Du, Min-Hsiu Hsieh, Tongliang Liu, Shan You, and Dacheng Tao. “Learnability of quantum neural networks”. *PRX Quantum*, 2:040337, 4, 2021 (page 81).
- [Edm65] Jack Edmonds. “Paths, trees, and flowers”. *Canadian Journal of Mathematics*, 17:449–467, 1965 (page 58).
- [EKL19] Gamaleldin F. Elsayed, Simon Kornblith, and Quoc V. Le. *Saccader: improving accuracy of hard attention models for vision*. *Proceedings of the 33rd International Conference on Neural Information Processing Systems*. Curran Associates Inc., Red Hook, NY, USA, 2019 (page 78).

- [Eps87] Mark A Epstein. *Lower bounds for the size of circuits of bounded depth in basis and, xor, translation of result of aa razborov*, 1987 (page 3).
- [FGL18] Omar Fawzi, Antoine Gropellier, and Anthony Leverrier. “Constant overhead quantum fault-tolerance with quantum expander codes”. *2018 IEEE 59th Annual Symposium on Foundations of Computer Science (FOCS)*. IEEE, 2018 (page 23).
- [Gal19] François Le Gall. “Average-case quantum advantage with shallow circuits”. *34th Computational Complexity Conference (CCC 2019)*. Schloss Dagstuhl-Leibniz-Zentrum fuer Informatik, 2019 (pages 3, 8, 53).
- [GAW<sup>+</sup>22] Xun Gao, Eric R. Anschuetz, Sheng-Tao Wang, J. Ignacio Cirac, and Mikhail D. Lukin. “Enhancing generative models via quantum correlations”. *Phys. Rev. X*, 12:021037, 2, 2022 (page 81).
- [GD17] Xun Gao and Lu-Ming Duan. “Efficient representation of quantum many-body states with deep neural networks”. *Nature communications*, 8(1):662, 2017 (page 81).
- [GE21] Craig Gidney and Martin Ekerå. “How to factor 2048 bit RSA integers in 8 hours using 20 million noisy qubits”. *Quantum*, 5:433, 2021 (page 3).
- [GF19] Craig Gidney and Austin G. Fowler. “Efficient magic state factories with a catalyzed  $|CCZ\rangle$  to  $2|T\rangle$  transformation”. *Quantum*, 3:135, April 2019 (page 70).
- [GZC<sup>+</sup>22] Daniel González-Cuadra, Torsten V. Zache, Jose Carrasco, Barbara Kraus, and Peter Zoller. “Hardware efficient quantum simulation of non-abelian gauge theories with qudits on rydberg platforms”. *Phys. Rev. Lett.*, 129:160501, 16, 2022 (page 6).
- [Got14] Daniel Gottesman. *Fault-tolerant quantum computation with constant overhead*, 2014. arXiv: 1310.2984 [quant-ph] (page 23).
- [Got98] Daniel Gottesman. “Fault-tolerant quantum computation with higher-dimensional systems”. *NASA International Conference on Quantum Computing and Quantum Communications*, pages 302–313. Springer, 1998 (page 22).
- [GHM<sup>+</sup>02] Frederic Green, Steven Homer, Cristopher Moore, and Christopher Pollett. “Counting, fanout and the complexity of quantum ACC”. *Quantum Info. Comput.*, 2(1):35–65, 2002 (page 8).
- [GHR91] Raymond Greenlaw, H James Hoover, and Walter L Ruzzo. *A compendium of problems complete for P*. CiteSeer, 1991 (page 78).
- [GK24] Sabee Grewal and Vinayak M. Kumar. “Improved circuit lower bounds with applications to exponential separations between quantum and classical circuits”. -, 2024 (page 10).
- [GJS21] Daniel Grier, Nathan Ju, and Luke Schaeffer. “Interactive quantum advantage with noisy, shallow clifford circuits”. *arXiv:2102.06833*, 2021 (pages 3, 9, 16, 75).
- [GS20] Daniel Grier and Luke Schaeffer. “Interactive shallow clifford circuits: quantum advantage against NC1 and beyond”. *Proceedings of the 52nd Annual ACM SIGACT Symposium on Theory of Computing*, STOC 2020, pages 875–888, Chicago, IL, USA. Association for Computing Machinery, 2020 (pages 3, 9, 10).
- [Gro06] David Gross. “Hudson’s theorem for finite-dimensional quantum systems”. *Journal of mathematical physics*, 47(12), 2006 (pages 16, 54, 69).
- [Hah20] Michael Hahn. “Theoretical limitations of self-attention in neural sequence models”. *Transactions of the Association for Computational Linguistics*, 8:156–171, 2020. Mark Johnson, Brian Roark, and Ani Nenkova, editors (page 78).
- [HMP<sup>+</sup>93] András Hajnal, Wolfgang Maass, Pavel Pudlák, Mario Szegedy, and György Turán. “Threshold circuits of bounded depth”. *Journal of Computer and System Sciences*, 46(2):129–154, 1993 (page 9).
- [HP15] Kristoffer Arnsfelt Hansen and Vladimir V Podolskii. “Polynomial threshold functions and boolean threshold circuits”. *Information and Computation*, 240:56–73, 2015 (page 9).

- [HMS23] Prahladh Harsha, Tulasimohan Molli, and Ashutosh Shankar. “Criticality of AC0-Formulae”. Amnon Ta-Shma, editor, *38th Computational Complexity Conference (CCC 2023)*, volume 264 of *Leibniz International Proceedings in Informatics (LIPIcs)*, 19:1–19:24, Dagstuhl, Germany. Schloss Dagstuhl – Leibniz-Zentrum für Informatik, 2023 (page 3).
- [HL21] Atsuya Hasegawa and François Le Gall. “Quantum Advantage with Shallow Circuits Under Arbitrary Corruption”. Hee-Kap Ahn and Kunihiro Sadakane, editors, *32nd International Symposium on Algorithms and Computation (ISAAC 2021)*, volume 212 of *Leibniz International Proceedings in Informatics (LIPIcs)*, 74:1–74:16, Dagstuhl, Germany. Schloss Dagstuhl – Leibniz-Zentrum für Informatik, 2021 (page 10).
- [Has16] Johan Hastad. “An average-case depth hierarchy theorem for higher depth”. *2016 IEEE 57th Annual Symposium on Foundations of Computer Science (FOCS)*. IEEE, 2016 (pages 3, 18).
- [Has14] Johan Hastad. “On the correlation of parity and small-depth circuits”. *SIAM Journal on Computing*, 43(5):1699–1708, 2014 (pages 3, 88, 89, 91).
- [Hås87] Johan Håstad. *Computational limitations of small-depth circuits*, 1987 (page 10).
- [HEB04] M. Hein, J. Eisert, and H. J. Briegel. “Multiparty entanglement in graph states”. *Phys. Rev. A*, 69:062311, 6, 2004 (page 33).
- [HBV13] Mark Howard, Eoin Brennan, and Jiri Vala. “Quantum contextuality with stabilizer states”. *Entropy*, 15(6):2340–2362, 2013 (pages 16, 54, 69).
- [HV12] Mark Howard and Jiri Vala. “Qudit versions of the qubit  $\pi/8$  gate”. *Phys. Rev. A*, 86:022316, 2, August 2012 (page 70).
- [HLB<sup>+</sup>24] Hsin-Yuan Huang, Yunchao Liu, Michael Broughton, Isaac Kim, Anurag Anshu, Zeph Landau, and Jarrod R McClean. “Learning shallow quantum circuits”. *arXiv:2401.10095*, 2024 (page 81).
- [HLW15] Adrian Hutter, Daniel Loss, and James R Wootton. “Improved hrg decoders for qudit and non-abelian quantum error correction”. *New Journal of Physics*, 17(3):035017, 2015 (page 59).
- [IPS97] Russell Impagliazzo, Ramamohan Paturi, and Michael E. Saks. “Size–depth tradeoffs for threshold circuits”. *SIAM Journal on Computing*, 26(3):693–707, 1997. eprint: <https://doi.org/10.1137/S0097539792282965> (page 9).
- [KKL17] Valentine Kabanets, Daniel M Kane, and Zhenjian Lu. “A polynomial restriction lemma with applications”. *Proceedings of the 49th Annual ACM SIGACT Symposium on Theory of Computing*, pages 615–628, 2017 (page 20).
- [KW16] Daniel M. Kane and Ryan Williams. “Super-linear gate and super-quadratic wire lower bounds for depth-two and depth-three threshold circuits”. *Proceedings of the Forty-Eighth Annual ACM Symposium on Theory of Computing*, STOC ’16, pages 633–643, Cambridge, MA, USA. Association for Computing Machinery, 2016 (page 9).
- [Kro08] Anders Krogh. “What are artificial neural networks?” *Nature Biotechnology*, 26:195–197, 2008 (page 3).
- [Kum23] Vinayak M. Kumar. “Tight correlation bounds for circuits between ac0 and tc0”. *Proceedings of the Conference on Proceedings of the 38th Computational Complexity Conference*, CCC ’23, Warwick, United Kingdom. Schloss Dagstuhl–Leibniz-Zentrum fuer Informatik, 2023 (pages 1, 3–7, 10, 12, 18, 20, 21, 88–90).
- [Law17] Jay Lawrence. “Mermin inequalities for perfect correlations in many-qutrit systems”. *Physical Review A*, 95(4):042123, 2017 (page 7).
- [LAT21] Yunchao Liu, Srinivasan Arunachalam, and Kristan Temme. “A rigorous and robust quantum speed-up in supervised machine learning”. *Nature Physics*, 17(9):1013–1017, 2021 (page 79).
- [LJV<sup>+</sup>23] Thomas Lubinski, Sonika Johri, Paul Varosy, Jeremiah Coleman, Luning Zhao, Jason Nécise, Charles H Baldwin, Karl Mayer, and Timothy Proctor. “Application-oriented performance benchmarks for quantum computing”. *IEEE Transactions on Quantum Engineering*, 2023 (page 77).
- [MP00] Carlo Mereghetti and Beatrice Palano. “Threshold circuits for iterated matrix product and powering”. *RAIRO - Theoretical Informatics and Applications*, 34(1):39–46, 2000 (page 78).



- [Mer90a] N. David Mermin. “Extreme quantum entanglement in a superposition of macroscopically distinct states”. *Phys. Rev. Lett.*, 65:1838–1840, 15, 1990 (page 13).
- [Mer90b] N. David Mermin. “Simple unified form for the major no-hidden-variables theorems”. *Phys. Rev. Lett.*, 65:3373–3376, 27, 1990 (page 8).
- [MS23] William Merrill and Ashish Sabharwal. “The parallelism tradeoff: limitations of log-precision transformers”. *Transactions of the Association for Computational Linguistics*, 11:531–545, 2023 (pages 3, 11, 79).
- [MSS22] William Merrill, Ashish Sabharwal, and Noah A. Smith. “Saturated transformers are constant-depth threshold circuits”. *Transactions of the Association for Computational Linguistics*, 10:843–856, 2022 (pages 3, 11, 79).
- [MŠM<sup>+</sup>24] Uta Isabella Meyer, Ivan Šupić, Damian Markham, and Frédéric Grosshans. *Bell nonlocality from wigner negativity in qudit systems*, 2024. arXiv: 2405.14367 [quant-ph] (pages 16, 54).
- [MGD<sup>+</sup>20] Rawad Mezher, Joe Ghalbouni, Joseph Dgheim, and Damian Markham. “Fault-tolerant quantum speedup from constant depth quantum circuits”. *Phys. Rev. Res.*, 2:033444, 3, 2020 (page 9).
- [MP69] Marvin Minsky and Seymour Papert. “An introduction to computational geometry”. *Cambridge tiass.*, *HIT*, 479(480):104, 1969 (page 3).
- [Mou16] Jonathan E. Moussa. “Transversal clifford gates on folded surface codes”. *Physical Review A*, 94(4), 2016 (pages 16, 58).
- [Mur71] Saburo Muroga. “Threshold logic and its applications”, 1971 (page 3).
- [MW18] Cody Murray and Ryan Williams. “Circuit lower bounds for nondeterministic quasi-polytime: an easy witness lemma for np and nqp”. *Proceedings of the 50th Annual ACM SIGACT Symposium on Theory of Computing*, STOC 2018, pages 890–901, Los Angeles, CA, USA. Association for Computing Machinery, 2018 (page 3).
- [OS03] Ryan O’Donnell and Rocco A Servedio. “New degree bounds for polynomial threshold functions”. *Proceedings of the thirty-fifth annual ACM symposium on Theory of computing*, pages 325–334, 2003 (page 20).
- [OBG24] Michael de Oliveira, Luís S. Barbosa, and Ernesto F. Galvão. “Quantum advantage in temporally flat measurement-based quantum computation”. *Quantum*, 8:1312, April 2024 (page 27).
- [PLS<sup>+</sup>24] Louis Paletta, Anthony Leverrier, Alain Sarlette, Mazyar Mirrahimi, and Christophe Vuillot. “Robust sparse IQP sampling in constant depth”. *Quantum*, 8:1337, May 2024 (page 9).
- [Par94] Ian Parberry. *Circuit Complexity and Neural Networks*. en. Foundations of Computing. MIT Press, London, England, 1994 (page 78).
- [PS88] Ian Parberry and Georg Schnitger. “Parallel computation with threshold functions”. *Journal of Computer and System Sciences*, 36(3):278–302, June 1988 (pages 3, 78).
- [PPJ<sup>+</sup>18] Ojas Parekh, Cynthia A Phillips, Conrad D James, and James B Aimone. “Constant-depth and subcubic-size threshold circuits for matrix multiplication”. *Proceedings of the 30th on Symposium on Parallelism in Algorithms and Architectures*, pages 67–76, 2018 (page 11).
- [Per90] Asher Peres. “Incompatible results of quantum measurements”. *Physics Letters A*, 151(3):107–108, 1990 (page 8).
- [PBM21] Jorge Pérez, Pablo Barceló, and Javier Marinkovic. “Attention is turing-complete”. *Journal of Machine Learning Research*, 22(75):1–35, 2021 (page 79).
- [PP22] Vladimir Podolskii and Nikolay V. Proskurin. “Polynomial Threshold Functions for Decision Lists”. Sang Won Bae and Heejin Park, editors, *33rd International Symposium on Algorithms and Computation (ISAAC 2022)*, volume 248 of *Leibniz International Proceedings in Informatics (LIPIcs)*, 52:1–52:12, Dagstuhl, Germany. Schloss Dagstuhl – Leibniz-Zentrum für Informatik, 2022 (page 20).



- [RHH<sup>+</sup>18] Dominik Rauch, Johannes Handsteiner, Armin Hochrainer, Jason Gallicchio, Andrew S. Friedman, Calvin Leung, Bo Liu, Lukas Bulla, Sebastian Ecker, Fabian Steinlechner, Rupert Ursin, Beili Hu, David Leon, Chris Benn, Adriano Ghedina, Massimo Cecconi, Alan H. Guth, David I. Kaiser, Thomas Scheidl, and Anton Zeilinger. “Cosmic bell test using random measurement settings from high-redshift quasars”. *Phys. Rev. Lett.*, 121:080403, 8, 2018 (page 77).
- [RBH05] Robert Raussendorf, Sergey Bravyi, and Jim Harrington. “Long-range quantum entanglement in noisy cluster states”. *Physical Review A*, 71(6), 2005 (pages 7, 17, 62, 63).
- [RT22] Ran Raz and Avishay Tal. “Oracle separation of bqp and ph”. *ACM Journal of the ACM (JACM)*, 69(4):1–21, 2022 (page 10).
- [RZB<sup>+</sup>94] Michael Reck, Anton Zeilinger, Herbert J. Bernstein, and Philip Bertani. “Experimental realization of any discrete unitary operator”. *Phys. Rev. Lett.*, 73:58–61, 1, 1994 (page 5).
- [RMP<sup>+</sup>22] Martin Ringbauer, Michael Meth, Lukas Postler, Roman Stricker, Rainer Blatt, Philipp Schindler, and Thomas Monz. “A universal qudit quantum processor with trapped ions”. *Nature Physics*, 18(9):1053–1057, 2022 (page 6).
- [Ros17] Benjamin Rossman. *An entropy proof of the switching lemma and tight bounds on the decision-tree size of  $ac0$* , 2017 (pages 17, 18, 20, 92).
- [RST15] Benjamin Rossman, Rocco A. Servedio, and Li-Yang Tan. “An average-case depth hierarchy theorem for boolean circuits”. *2015 IEEE 56th Annual Symposium on Foundations of Computer Science*, pages 1030–1048, 2015 (page 3).
- [SVM<sup>+</sup>17] Artur Scherer, Benoit Valiron, Siun-Chuon Mau, Scott Alexander, Eric Van den Berg, and Thomas E Chapuran. “Concrete resource analysis of the quantum linear-system algorithm used to compute the electromagnetic scattering cross section of a 2d target”. *Quantum Information Processing*, 16:1–65, 2017 (pages 3, 77).
- [SMC<sup>+</sup>15] Lynden K. Shalm et al. “Strong loophole-free test of local realism”. *Phys. Rev. Lett.*, 115:250402, 25, 2015 (page 77).
- [SAK92] John S. Shawe-Taylor, Martin H.G. Anthony, and Walter Kern. “Classes of feedforward neural networks and their circuit complexity”. *Neural Networks*, 5(6):971–977, 1992 (page 78).
- [ŠO03] Jiří Šíma and Pekka Orponen. “General-purpose computation with neural networks: a survey of complexity theoretic results”. *Neural Computation*, 15(12):2727–2778, 2003 (page 11).
- [SB91] Kai-Yeung Siu and Jehoshua Bruck. “On the power of threshold circuits with small weights”. *SIAM Journal on Discrete Mathematics*, 4(3):423–435, 1991 (pages 3, 11).
- [Smo13] Paul Smolensky. *Mathematical Perspectives on Neural Networks*. Psychology Press, 2013 (page 78).
- [Smo87] R. Smolensky. “Algebraic methods in the theory of lower bounds for boolean circuit complexity”. *Proceedings of the Nineteenth Annual ACM Symposium on Theory of Computing, STOC ’87*, pages 77–82, New York, New York, USA. Association for Computing Machinery, 1987 (pages 3, 10).
- [Str23] Lena Strobl. *Average-hard attention transformers are constant-depth uniform threshold circuits*, 2023. arXiv: [2308.03212 \[cs.CL\]](#) (page 79).
- [SMW<sup>+</sup>24] Lena Strobl, William Merrill, Gail Weiss, David Chiang, and Dana Angluin. “What formal languages can transformers express? a survey”. *Transactions of the Association for Computational Linguistics*, 12:543–561, 2024. arXiv: [2311.00208 \[cs.LG\]](#) (pages 11, 79).
- [TT16] Yasuhiro Takahashi and Seiichiro Tani. “Collapse of the hierarchy of constant-depth exact quantum circuits”. *computational complexity*, 25:849–881, 2016 (pages 5, 8).
- [VK85] Jacob Van Den Berg and Harry Kesten. “Inequalities with applications to percolation and reliability”. *Journal of applied probability*, 22(3):556–569, 1985 (page 60).
- [VSP<sup>+</sup>17] Ashish Vaswani, Noam Shazeer, Niki Parmar, Jakob Uszkoreit, Llion Jones, Aidan N Gomez, Lukasz Kaiser, and Illia Polosukhin. “Attention is all you need”. I. Guyon, U. Von Luxburg, S. Bengio, H. Wallach, R. Fergus, S. Vishwanathan, and R. Garnett, editors, *Advances in Neural Information Processing Systems*, volume 30. Curran Associates, Inc., 2017 (page 78).

- [Vol98] Heribert Vollmer. “Relating polynomial time to constant depth”. *Theoretical Computer Science*, 207(1):159–170, 1998 (page 10).
- [WAB15] Fern H. E. Watson, Hussain Anwar, and Dan E. Browne. “Fast fault-tolerant decoder for qubit and qudit surface codes”. *Phys. Rev. A*, 92:032309, 3, 2015 (page 16).
- [WKS<sup>+</sup>19] Adam Bene Watts, Robin Kothari, Luke Schaeffer, and Avishay Tal. “Exponential separation between shallow quantum circuits and unbounded fan-in shallow classical circuits”. *Proceedings of the 51st Annual ACM SIGACT Symposium on Theory of Computing*, pages 515–526. Association for Computing Machinery, 2019 (pages 1, 3, 4, 6–11, 13, 15, 17, 25, 31, 77).
- [WP23] Adam Bene Watts and Natalie Parham. “Unconditional quantum advantage for sampling with shallow circuits”. *arXiv:2301.00995*, 2023 (pages 3, 5, 9).
- [Wil21] R. Ryan Williams. “Complexity lower bounds from algorithm design”. *2021 36th Annual ACM/IEEE Symposium on Logic in Computer Science (LICS)*, 2021 (page 3).
- [Wil14] Ryan Williams. “Nonuniform acc circuit lower bounds”. *J. ACM*, 61(1), 2014 (page 3).
- [XBK<sup>+</sup>15] Kelvin Xu, Jimmy Ba, Ryan Kiros, Kyunghyun Cho, Aaron Courville, Ruslan Salakhudinov, Rich Zemel, and Yoshua Bengio. “Show, attend and tell: neural image caption generation with visual attention”. Francis Bach and David Blei, editors, *Proceedings of the 32nd International Conference on Machine Learning*, volume 37 of *Proceedings of Machine Learning Research*, pages 2048–2057, Lille, France. PMLR, July 2015 (page 78).
- [Yao85] Andrew Chi-Chih Yao. “Separating the polynomial-time hierarchy by oracles”. *26th Annual Symposium on Foundations of Computer Science (sfcs 1985)*, pages 1–10. IEEE, 1985 (pages 3, 10).
- [YJS19] Mithuna Yoganathan, Richard Jozsa, and Sergii Strelchuk. “Quantum advantage of unitary clifford circuits with magic state inputs”. *Proceedings of the Royal Society A*, 475(2225):20180427, 2019 (page 9).
- [ZGS16] Ehsan Zahedinejad, Joydip Ghosh, and Barry C. Sanders. “Designing high-fidelity single-shot three-qubit gates: a machine-learning approach”. *Phys. Rev. Appl.*, 6:054005, 5, 2016 (page 32).
- [ZCC08] Bei Zeng, Xie Chen, and Isaac L. Chuang. “Semi-clifford operations, structure of  $\mathcal{C}_k$  hierarchy, and gate complexity for fault-tolerant quantum computation”. *Phys. Rev. A*, 77:042313, 4, April 2008 (pages 69, 70).
- [ZGL<sup>+</sup>24] Zhihan Zhang, Weiyuan Gong, Weikang Li, and Dong-Ling Deng. “Quantum-classical separations in shallow-circuit-based learning with and without noises”. *arXiv:2405.00770*, 2024 (page 81).

## A Proof of the tight multi-switching lemma for bounded PTF circuits

In this appendix we state and prove our multi-switching lemma and depth-reduction lemma for  $\text{bPTF}^0[k]$  circuits. We begin by proving Lemma 2.2, and then proceed to proving Lemma 2.3.

### A.1 Tight multi-switching lemma

The first lemma of this type will be a multi-switching lemma that reduces a finite set of depth-2  $\text{bPTF}^0[k] \circ \text{AND}_w$  circuits, which are defined by  $\text{bPTF}[k]$  gate with AND gates of bounded fan-in  $w$  as input, to a  $\text{DT}(w)^m \rightrightarrows \text{DT}(t)$  decision forest. It is worth noting that Theorem 3.12 serves as a multi-switching lemma of this type. However, a higher probability of success is required to reduce the initial circuit to a tree-like object, enabling the subsequent proof of quantum advantage with respect to the  $\text{QNC}^0$  circuit class.

In particular, better parameters can be obtained with additional assumptions on the decision trees to which the initial circuit will be reduced. This is demonstrated in the subsequent lemma, where we combine the inductive technique of [Has14] with the canonical decision trees proposed by [Kum23] for  $\text{bPTF}^0[k]$  circuits restricted by a random restriction  $\rho$ .

**Lemma A.1.** Let  $\mathcal{F} = \{F_1, F_2, F_3, \dots, F_m\}$  be a list of  $\text{bPTF}[k] \circ \text{AND}_w$  circuits on  $\{0, 1\}^n$ ,  $t > 0$ ,  $l \geq \log(m) + k + 2$  and  $p < \frac{1}{40w}$ , then,

$$\Pr_{\rho \in R_p} [\mathcal{F} \upharpoonright_{\rho} \text{DT}(l)^m \not\Rightarrow \text{DT}(t)] \leq m \cdot 2^k (80wp)^t. \quad (\text{A.1})$$

*Proof.* Our proof employs an inductive approach similar to the one used by [Has14] for his multi-switching lemma. However, this necessitates the use of downward closed random restrictions. This attribute ensures that the size of the canonical decision tree does not expand when additional variables from the initial random restriction are restricted. It guarantees the monotonicity of the canonical decision tree's size under random restriction, which is crucial for the inductive reasoning process. Therefore, we will first establish some properties of the random restrictions and then utilize them in the proof of the new multi-switching lemma using inductive techniques.

**Downward closedness.** We start with defining the downward closeness of random restrictions.

**Definition A.2.** Let  $\mathcal{P}$  be a set of downward closed restrictions, and consider any  $\rho \in \mathcal{P}$ . Then for any other restriction  $\rho'$  which satisfies  $\rho'(x_i) = \rho(x_i)$  for all  $i \in I = \{i \mid \rho(x_i) \in \{0, 1\} \wedge \rho'(x_i) \in \{0, 1\}\}$ , we have that  $\rho' \in \mathcal{P}$ .

Building on this definition, our interest lies in combining restrictions, necessitating the set of restrictions used in this process to be downwards closed. This requirement can be ensured with the following lemma.

**Lemma A.3.** Let  $\mathcal{P}$  and  $\mathcal{P}'$  be two downward-closed sets, then  $\mathcal{P} \cap \mathcal{P}'$  is also a downward-closed set.

*Proof.* This follows directly by the definition of the downward-closed set.  $\square$

Now, we need to demonstrate that the random restrictions chosen to bind the entire probability for the multi-switching lemmas are also downwards closed. To achieve this, we must analyze the canonical decision trees generated from  $F \upharpoonright_{\rho}$ , where  $F$  is an initial circuit of the type  $\text{bPTF}[k] \circ \{\text{AND}, \text{OR}\}_w$ , and  $\rho$  represents the random restrictions of interest. We will consider two objects defined in [Kum23]. The first is the algorithmic process that constructs the canonical decision tree from  $F$  and  $\rho$ , while the other is the resulting description of the canonical decision tree in a non-standard format as considered by the author.

---

**Algorithm 3** Canonical Decision Tree

---

```

1: procedure  $CDT_F(F = G(C_1, \dots, C_n) + \text{black-box access to a string } x \in \{0, 1\}^n.)$ 
2:    $j^* \leftarrow 0; x \leftarrow (*)^n; ctr \leftarrow 0$ 
3:   while  $j^* \leq m$  do
4:     Find  $j \geq j^*$  such that  $C_j \not\equiv 0$ . If no such  $j$  exists, exit the loop.
5:      $B_j \leftarrow$  the set of variables not used by  $C_j(x)$ 
6:     Query  $\alpha_{x_{B_j}}$ 
7:     Set  $x_{B_j} \leftarrow \alpha_{B_j}$ .
8:     if  $C_j(x) = 1$  then
9:        $ctr \leftarrow ctr + 1$ 
10:      if  $ctr = k$  then
11:        return  $G(1^m)$ 
12:      end if
13:    end if
14:     $j^* \leftarrow j$ 
15:  end while
16:  return  $F(x \circ 0^n)$ 
17: end procedure

```

---

Given Algorithm 3 that produces the canonical decision tree  $T_{F \upharpoonright_{\rho}}$  for  $F \upharpoonright_{\rho}$ , we can define the following object known as an  $s$ -witness. At an information-theoretical level, an  $s$ -witness describes the depth  $s$  subtree of the canonical decision tree of  $F \upharpoonright_{\rho}$ .

**Definition A.4** (t-witness [Kum23]). Let  $F$  be a  $\text{bPTF}[k] \circ \text{AND}_w$  circuit and  $\rho$  a restriction. Let  $t \geq 1$ . Consider the tuple  $(r, l_i, s_i, B_i, \alpha_i)$  where

- $r \in [1, t + k]$  is an integer;
- $(l_1, \dots, l_r) \in [m]^r$  is an increasing list of indices;
- $(s_1, \dots, s_r)$  is a list of non-negative integers, at most  $k$  of which are allowed to be 0, such that  $s := \sum_{i=1}^r s_i \in [t, t + w - 1]$ ;
- $(B_1, \dots, B_r)$  is a list of subsets of  $[w]$  satisfying  $|B_i| = s_i$ ;
- $(\alpha_1, \dots, \alpha_r)$  is a list of potential bit strings satisfying  $|\alpha_i| = s_i$ .
- $(r, l_i, s_i, B_i, \alpha_i)$  is called a  $t$ -witness for  $\rho$  if there exists an  $\alpha \in \{0, 1\}^n$  such that
  - When we run  $T_{F|_\rho}$  on a  $\alpha$ ,  $C_{l_i}$  is the  $i$ -th term queried by  $T_{F|_\rho}$ .
  - $T_{F|_\rho}$  queries  $s_i$  variables in  $C_{l_i}$ , and the relative location of those variables within  $C_{l_i}$  are specified by set  $B_i$ .
  - $T_{F|_\rho}$  receives  $\alpha_i$  in response to its  $i$ -th batch query.

The size of the witness  $(r, l_i, s_i, B_i, \alpha_i)$  is defined to be  $s := \sum_{i=1}^r s_i$ . We may denote the size of a witness  $W$  as  $\text{size}(W)$ .

Given Algorithm 3 and a  $t$ -witness as defined in Definition A.4, the previous statements can be made precise with the following fact.

**Fact 1.** [Kum23] For every  $\rho$  such that  $F|_\rho \geq \text{DT}(t)$ , there exists a  $t$ -witness for  $\rho$ .

Now, we can begin to establish precise statements about the random restriction of interest. Our first property is as follows, which will aid in establishing downward closedness for two types of random restrictions.

**Lemma A.5.** For all random restrictions  $\rho$  and  $F = \text{bPTF} \circ \{\text{AND}, \text{OR}\}_w$ , for which  $F|_\rho$  has an  $l$ -witness, let  $L$  be the set of variables in the canonical decision tree  $\text{DT}(l)$ . If  $\rho'$  is a random restriction such that  $\rho'(x_i) = \rho(x_i) \forall i \notin T$ , where  $T = \{*\}^t$  and  $L \cap T = \emptyset$ , then  $F|_{\rho'}$  has the same  $l$ -witness.

*Proof.* If a variable within  $T$  is assigned a Boolean value, it implies that all clauses preceding the first non-fixed clause, denoted by  $l_1$  in the  $l$ -witness, retain their assigned values. Crucially, any ‘alive’ variables that could influence the outcome of this clause are encompassed within  $B_1$ , which are, by definition, elements of  $L$ . This assertion is supported by the ‘Canonical Decision Tree’ algorithm and the definition of an  $s$ -witness. Thus, altering any variable in  $T$  leaves the initial segment of the  $l$ -witness unchanged. By inductively applying this reasoning to each element of the  $l$ -witness, we establish that variable assignments within  $T$  do not alter the overall structure of the  $l$ -witness. Therefore,  $F|_{\rho'}$  has exactly the same  $l$ -witness as  $F|_\rho$ .  $\square$

Now we will prove that a particular set of random restrictions is downward closed.

**Lemma A.6.** The set of restrictions  $\rho$  for which a circuit  $F = \text{bPTF} \circ \{\text{AND}, \text{OR}\}_w$  reduces to a decision tree of the type  $\text{DT}(l)$ , with  $l \in \mathbb{N}$ , is downward closed.

*Proof.* We will demonstrate the lemma by considering a general scenario where any restriction  $\rho$  satisfies the condition  $F|_\rho \in \text{DT}(l)$ . For such a restriction  $\rho$ , we observe that it designates  $*$  to all variables within the decision tree  $\text{DT}(l)$ , which we will refer to as the set  $L$ . Additionally, there exists a distinct set  $T$  of variables also assigned  $*$  that do not intersect with  $L$ , i.e.,  $T \cap L = \emptyset$ .

When a variable in  $L$  is set to a Boolean value, the downward closedness property is maintained. This is because the application of the ‘Canonical Decision Tree’ algorithm would yield an identical tree, albeit with the fixed variables omitted or potentially with further reductions. Such reductions occur if the fixed variables directly satisfy a complete clause  $C_{l_i}$ , with  $l_i$  being an index of the  $l$ -witness. Consequently, the new  $s$ -witness encompasses at most a subset of the elements from the previous  $l$ -witness.

Now, by Lemma A.5, we can conclude that assigning a value to any variable in  $T$  generates a new random restriction that does not change the  $s$ -witness of the initial function under this new restriction. Therefore, the resulting canonical decision tree is the same as for  $\rho$ .

We can hence deduce that the set of restrictions for which  $F|_\rho \in \text{DT}(l)$  is indeed downward closed.  $\square$

**Induction.** As mentioned previously, the precise proof of the multi-switching lemma will follow the inductive idea of the initial multi-switching theorem by [Has14]. Specifically, we will apply induction to the circuits  $\text{REC}_i^{*-1}$  and the input size. Whenever we encounter a circuit that does not reduce to a decision tree of the type  $\text{DT}(l)$ , we make a query on the variables that are alive to reduce this circuit and use these as variables of the global decision tree  $\text{DT}(t)$ .

The theorem trivially holds when  $m = 0$  and  $n = 0$ , where  $m$  represents the number of  $\text{bPTF}[k] \circ \{\text{AND}, \text{OR}\}_w$  circuits considered, and  $n$  denotes the input size. Now, we can divide the required induction step into two cases: one where the first  $F_1[\rho]$  does have a decision tree of depth  $l$ , and another where it does not.

$$\Pr[\mathcal{F}[\rho \notin \text{DT}(l)^m \not\Rightarrow \text{DT}(t)] = \Pr[\mathcal{F}[\rho \notin \text{DT}(l)^m \not\Rightarrow \text{DT}(t) \mid F_1[\rho \notin \text{DT}(l)] \cdot \Pr[F_1[\rho \notin \text{DT}(l)] \quad (\text{A.2})$$

$$+ \Pr[\mathcal{F}[\rho \notin \text{DT}(l)^m \not\Rightarrow \text{DT}(t) \mid F_1[\rho \in \text{DT}(l)] \cdot \Pr[F_1[\rho \in \text{DT}(l)]]. \quad (\text{A.3})$$

For  $F_1[\rho \in \text{DT}(l)]$ , we obtain that we can simply induct on the  $\mathcal{F} \setminus F_1$ . By doing that we obtain the following probability,

$$\begin{aligned} \Pr[\mathcal{F}[\rho \notin \text{DT}(l)^m \not\Rightarrow \text{DT}(t) \mid F_1[\rho \in \text{DT}(l)]] &= \Pr[(\mathcal{F} \setminus F_1)[\rho \notin \text{DT}(l)^m \not\Rightarrow \text{DT}(t) \mid F_1[\rho \in \text{DT}(l)]] \\ &\leq (m-1) \cdot 2^k (80wp)^t. \end{aligned}$$

To completely establish Equation (A.3), we would need to bound  $\Pr[F_1[\rho \in \text{DT}(l)]]$ . However, this is unnecessary as we will observe when determining the conditional probability in Equation (A.2). In addition to the previous argument, we need to ensure that the random restrictions guaranteeing  $F_1$  to reduce to a decision tree of depth  $l$  are downward closed, i.e.,  $F_1[\rho \in \text{DT}(l)] \wedge \rho \in \mathcal{F}$ . This has already been proven in Lemma A.6, thus ensuring Lemma A.3 that the same property holds for all random restrictions used in the inductive step of Equation (A.3).

Now, we need to analyze the case where the first circuit does not have a reduction to a small decision tree. For that, we will use the following fact.

**Fact 2.** *For every  $\rho$  such that  $\text{DT}(F[\rho]) \geq t$  there exists a  $t' > t$ , such that  $\text{DT}(F[\rho]) = t'$ .*

This allows us to rewrite the expression which facilitates the application of the intended inductive step.

$$\begin{aligned} \Pr[\mathcal{F}[\rho \notin \text{DT}(l)^m \not\Rightarrow \text{DT}(t) \mid F_1[\rho \notin \text{DT}(l)]] \cdot \Pr[F_1[\rho \notin \text{DT}(l)]] &\leq \\ \sum_{l' > l} \Pr[\mathcal{F}[\rho \notin \text{DT}(l)^m \not\Rightarrow \text{DT}(t) \mid F_1[\rho \in \text{DT}(l')]] \cdot \Pr[F_1[\rho \in \text{DT}(l')]]. \end{aligned}$$

Now, we will use precisely the size of the canonical decision tree resulting from the restriction on the first circuit  $F_1[\rho]$  to provide us with a second restriction  $\tau$ . The idea is that we can rewrite the same probability  $\Pr[\mathcal{F}[\rho \notin \text{DT}(t) \circ \text{DT}(l)^m \mid F_1[\rho \in \text{DT}(l')]]$  as  $\Pr[\mathcal{F}[\rho \circ \tau \notin \text{DT}(t-l') \circ \text{DT}(l)^m \mid F_1[\rho \in \text{DT}(l')]]$  when  $l' < t$ , where  $\tau$  is the assignment of the  $l'$  variables of the canonical decision tree resulting from  $F_1[\rho]$ .

$$\sum_{l' > l} \Pr[\mathcal{F}[\rho \notin \text{DT}(l)^m \not\Rightarrow \text{DT}(t) \mid F_1[\rho \in \text{DT}(l')]] \cdot \Pr[F_1[\rho \in \text{DT}(l')]] = \quad (\text{A.4})$$

$$\sum_{l' > l} \sum_{\tau \in \{0,1\}^{l'}} \Pr[\mathcal{F}[\rho \circ \tau \notin \text{DT}(l)^m \not\Rightarrow \text{DT}(t-l') \mid F_1[\rho \in \text{DT}(l')]] \cdot \Pr[F_1[\rho \in \text{DT}(l')]]. \quad (\text{A.5})$$

In particular, when  $l' < t$  we can bind the first term of Equation (A.5) inductively, while the second can be very largely bound by the probability that  $F_1[\rho \notin \text{DT}(l')]$ ,

$$\begin{aligned} \sum_{l' > l} \sum_{\tau \in \{0,1\}^{l'}} \Pr[\mathcal{F}[\rho \circ \tau \notin \text{DT}(t-l') \circ \text{DT}(l)^m \mid F_1[\rho \in \text{DT}(l')]] \cdot \Pr[F_1[\rho \in \text{DT}(l')]] \\ \leq \sum_{l' > l} (20pw)^{l'} 2^k 2^{l'} (m \cdot (80wp)^{t-l'} 2^k) \\ \leq (80wp)^{t-1} \sum_{l' > l} 2^{k+1} 2^{-l'} m. \end{aligned}$$

Using our initial assumption that  $l \geq \log(m) + k + 2$  yields that,

$$\sum_{l' > l} 2^{-l'} \cdot m \cdot 2^k \leq 1. \quad (\text{A.6})$$

Therefore, the second term in Equation (A.2) in our initial division is inductively bounded above by  $(80wp)^t 2^{k-1}$  for cases where  $l' < t$ . When we consider this first case for the second term in Equation (A.2), it's imperative to ensure that the random restrictions in question maintain the property of downward closedness. To this end, we invoke Lemma A.3 inductively, but we must also affirm the same property for the composition of restrictions  $\rho \circ \tau$  when  $F_1 \upharpoonright_{\rho \in \text{DT}(l')}$ .

Since  $\tau$  assigns definitive values to all variables within  $\text{DT}(l')$ , our task simplifies to confirming that all variables not specifically assigned by the composition  $\rho \circ \tau$  do not alter the conditional probability that our induction is predicated upon. This condition is indeed satisfied, as established by Equation (A.5), thus ensuring the downward closedness of the random restrictions we are considering. With this confirmation, our inductive argument remains robust and consistent.

Now, to show that an equal bound holds for the case that  $l' \geq t$ , we obtain that the first conditional probability of Equation (A.2) is fixed and equal to 1, while second, we bound again with  $F_1 \upharpoonright_{\rho \notin \text{DT}(l')}$ .

$$\begin{aligned} \sum_{l' > t} \Pr [F \upharpoonright_{\rho \notin \text{DT}(t) \circ \text{DT}(l)^m} \mid F_1 \upharpoonright_{\rho \in \text{DT}(l')}] \cdot \Pr [F_1 \upharpoonright_{\rho \in \text{DT}(l')}] &\leq 2^k \sum_{l' > t} (20pw)^{l'} \\ &\leq 2^k \cdot 2(20pw)^t = 2^k \cdot 2^{2t-1} (80pw)^t. \end{aligned}$$

For any  $t > 0$  we obtain that this case is smaller or equal to  $2^{k-1}(80pw)^t$ . Thus, if we use the two values that build up Equation (A.2) and the value for Equation (A.3) obtained, we obtain that,

$$\begin{aligned} \Pr[F \upharpoonright_{\rho \notin \text{DT}(t) \circ \text{DT}(l)^m}] &\leq (m-1)2^k(80pw)^t + 2^k(80pw)^t \\ &\leq m \cdot 2^k(80pw)^t, \end{aligned}$$

completing the proof.  $\square$

## A.2 Depth reduction lemmas

Provided with the previous multi-switching lemma we can construct a new depth reduction lemma for  $\text{bPTF}^0[k]$  circuits. This follows the proof technique from [Ros17].

**Lemma A.7.** *If  $d, t \geq 1$  and  $F \in \text{bPTF}[k; d; s_1, s_2, \dots, s_d] \circ \text{DT}(w) \succcurlyeq \text{DT}(t-1)$ ,  $l \geq \log s_1 + k + 2$  and  $p < \frac{1}{40w}$ , then*

$$\Pr[F \upharpoonright_{\rho \notin \text{bPTF}[k; d-1; s_2, \dots, s_d] \circ \text{DT}(l)} \succcurlyeq \text{DT}(t-1)] \leq s_1 \cdot 2^k (400wp)^{t/2}. \quad (\text{A.7})$$

*Proof.* Suppose that  $F$  is computed by a depth  $t-1$  decision tree  $T$ , each of whose leaves  $\lambda$  is labelled by a circuit  $C_\lambda \in \text{bPTF}[k; d; s_1, s_2, \dots, s_d] \circ \text{DT}(w)$ , we will assume the following two events,

$$\mathcal{A} \iff T \upharpoonright_p \text{ has depth } \leq t/2 - 1 \quad (\text{A.8})$$

$$\mathcal{B} \iff C_\lambda \upharpoonright_p \in \text{bPTF}[k; d-1; s_2, \dots, s_d] \circ \text{DT}(l) \succcurlyeq \text{DT}(t/2-1) \text{ for every leaf } \lambda \text{ of } T \quad (\text{A.9})$$

such that,

$$\mathcal{A} \wedge \mathcal{B} \implies F \upharpoonright_{\rho \in \text{bPTF}[k; d-1; s_2, \dots, s_d] \circ \text{DT}(l)} \succcurlyeq \text{DT}(t-1). \quad (\text{A.10})$$

Now, the probability that neither of the events occurs will be considered. For the first event, we obtain the value this event to be

$$\Pr[\neg \mathcal{A}] = \Pr[T \upharpoonright_p \text{ has depth } \geq t/2] \leq (4ep)^{t/2}. \quad (\text{A.11})$$



For the second, we sort to [Lemma 3.13](#) to translate  $\text{bPTF}[k; d; s_1, s_2, \dots, s_d] \circ \text{DT}(w)$  to  $\text{bPTF}[k; d; s_1, s_2, \dots, s_d] \circ \text{AND}_w$ , and with [Lemma A.1](#) we obtain

$$\begin{aligned} \Pr[\neg \mathcal{B}] &\leq \sum_{\lambda} \Pr[C_{\lambda} \not\in \text{bPTF}[k; d-1; s_2, \dots, s_d] \circ \text{DT}(l) \not\Rightarrow \text{DT}(t/2-1)]. \\ &\leq \sum_{\lambda} s_1 \cdot 2^k (80wp)^{t/2} \end{aligned} \quad (\text{A.12})$$

$$\leq 2^{t-1} (s_1 \cdot 2^k (80wp)^{t/2}). \quad (\text{A.13})$$

Combining both, we obtain,

$$\begin{aligned} \Pr[F|_{R_p} \not\in \text{bPTF}[k; d; s_2, \dots, s_d] \circ \text{DT}(l) \not\Rightarrow \text{DT}(t-1)] &\leq \Pr[\neg \mathcal{A}] + \Pr[\neg \mathcal{B}] \\ &\leq (4ep)^{t/2} + 2^{t-1} (s_1 \cdot 2^k (80wp)^{t/2}) \end{aligned} \quad (\text{A.14})$$

$$\leq (4ep)^{t/2} + (s_1 \cdot 2^{k-1} (400wp)^{t/2}) \quad (\text{A.15})$$

$$\leq s_1 \cdot 2^k (400wp)^{t/2}. \quad (\text{A.16})$$

□

The previous lemma allows one to reduce the depth of a  $\text{bPTF}^0[k]$  circuit. Now, this lemma can be employed sequentially to reduce the entire circuit.

**Lemma A.8.** *Let  $d, t, k, q, m, s_1, l_1, \dots, s_{d-1}, l_{d-1} \in \mathbb{N}$ ;  $d, t > 0$ ;  $l_i \geq \log s_i + k + 2$ ;  $p_1, \dots, p_d \in (0, 1)$ ;  $p_i < \frac{1}{40l_i}$ . Let  $F \in \text{bPTF}^0[k; d; s_1, \dots, s_{d-1}, m]$  with  $n$  inputs and  $m$  outputs. Let  $s = s_1 + \dots + s_{d-1} + m$ . Let  $p = p_1 \cdot p_2 \cdot \dots \cdot p_d$ . Then,*

$$\begin{aligned} \Pr_{\rho \sim R_p} [F|_{\rho} \not\in \text{DT}(q-1)^m \not\Rightarrow \text{DT}(2t-2)] &\leq s_1 \cdot 2^k \mathcal{O}(p_1)^{t/2} \\ &\quad + \left( \sum_{i=2}^{d-1} s_i \cdot 2^k \mathcal{O}(p_i l_i)^{t/2} \right) + 2^k m^{1/q} \mathcal{O}(p_d \cdot l_d)^t. \end{aligned}$$

*Proof.* The first step is to consider our function  $f$  as a  $\text{bPTF}^0[k; d; s_1, \dots, s_{d-1}, m] \circ \text{DT}(1) \not\Rightarrow \text{DT}(t-1)$  circuit. Then, to reduce this object sequentially through random restrictions we use [Lemma A.7](#) and  $p_1$ , such that

$$\begin{aligned} \Pr[F|_{\rho} \not\in \text{bPTF}_{d-1}^0(k; d-1; s_2, \dots, s_n) \circ \text{DT}(l_1) \not\Rightarrow \text{DT}(t-1)] &\leq s_1 \cdot 2^k (400p_1)^{t/2} \\ &\leq s_1 \cdot 2^k \mathcal{O}(p_1)^{t/2}. \end{aligned}$$

We will denote  $F|_{\rho} \not\in \text{bPTF}_{d-1}^0(k; d-1; s_2, \dots, s_n) \circ \text{DT}(l_1) \not\Rightarrow \text{DT}(t-1)$  as event  $E_1$ , and subsequent depth reductions equally for  $E_i$ . Building on this and based on the same [Lemma A.7](#), we obtain that,

$$\Pr[\neg E_i | E_1 \wedge \dots \wedge E_{i-1}] \leq s_i \cdot 2^k (400l_i p_i)^{t/2} \quad (\text{A.17})$$

$$\leq s_i \cdot 2^k \mathcal{O}(p_i \cdot l_i)^{t/2}. \quad (\text{A.18})$$

Now after applying  $d-1$  times [Lemma A.7](#) we obtain that  $G$  defined as  $G = F|_{p_1 \circ \dots \circ p_{d-1}}$  is

$$G \in (\text{bPTF}[k] \circ \text{DT}(l_{d-1}))^m \not\Rightarrow \text{DT}(t-1), \quad (\text{A.19})$$

with a probability equal to the probability with the following sequence of event  $E_1 \wedge E_2 \wedge \dots \wedge E_{d-1}$  hold. Now, to the leaves of each of the global decision tree  $\text{DT}(t-1)$ , we apply [Theorem 3.12](#), such that for each leave, we have that,

$$\Pr[G_{\lambda|_{\rho_d}} \not\in \text{DT}(q-1)^m \not\Rightarrow \text{DT}(t-1)] \leq 4 \left( 64(2^k m)^{1/q} p_d \cdot l_d \right)^t \quad (\text{A.20})$$

$$\leq 2^k m^{1/q} \mathcal{O}(p_d \cdot l_d)^t. \quad (\text{A.21})$$

Then, we apply the union bound to all the leaves, which multiplies these values by  $2^{t-1}$ . However, this value will be upper bounded by the same value previously defined. Thus, we obtain that,

$$\Pr [\neg E_1 \wedge \neg E_2 \wedge \dots \wedge E_d] = \sum_{i=1}^d \Pr[\neg E_i | E_1 \wedge \dots \wedge E_{i-1}] \quad (\text{A.22})$$

$$\leq s_1 \cdot 2^k \mathcal{O}(p_1)^{t/2} + \left( \sum_{i=2}^{d-1} s_i * 2^k \mathcal{O}(p_i \cdot l_i)^{t/2} \right) + 2^k m^{1/q} \mathcal{O}(p_d \cdot l_d)^t. \quad (\text{A.23})$$

□

In the final step, we provide a value for the probabilities of the various random restrictions and dimensions for the local decision trees to derive a new lemma. This describes based on the previous values, and the size of the global decision tree  $t$ , the size of the initial circuit  $s$ , and the type of circuit parametrized by  $k$  the probability of the success of reducing the circuit to decision tree of the type  $\text{DT}(q-1)^m \gg \text{DT}(2t-2)$ .

**Lemma A.9.** *Let  $F : \{0,1\}^n \mapsto \{0,1\}^m$  be an  $\text{bPTF}^0[k]$  circuit of size  $s$ , depth  $d$ . Let  $p = 1/(s_d^{1/q} \cdot \mathcal{O}(\log(s)^{d-1} \cdot k^{d-1}))$ . Then,*

$$\Pr_{\rho \sim R_p} [F|_{\rho} \notin \text{DT}(q-1)^m \gg \text{DT}(2t-2)] \leq s \cdot 2^{-t+k}. \quad (\text{A.24})$$

*Proof.* This follows by applying [Lemma A.8](#) with  $p_1 = 1/\mathcal{O}(1)$  and  $p_2 = \dots = p_{d-1} = 1/\mathcal{O}(\log(s) + k)$  and  $p_d = 1/\mathcal{O}(s_d^{1/q} \cdot (\log(s) + k))$ . □